



1-1-2012

# Pilot-Scale Evaluation Of Advanced Solvents For CO<sub>2</sub> Capture From Coal-Fired Utilities

Brandon Michael Pavlish

Follow this and additional works at: <https://commons.und.edu/theses>

---

## Recommended Citation

Pavlish, Brandon Michael, "Pilot-Scale Evaluation Of Advanced Solvents For CO<sub>2</sub> Capture From Coal-Fired Utilities" (2012). *Theses and Dissertations*. 1369.

<https://commons.und.edu/theses/1369>

This Thesis is brought to you for free and open access by the Theses, Dissertations, and Senior Projects at UND Scholarly Commons. It has been accepted for inclusion in Theses and Dissertations by an authorized administrator of UND Scholarly Commons. For more information, please contact [zeinebyousif@library.und.edu](mailto:zeinebyousif@library.und.edu).

PILOT-SCALE EVALUATION OF ADVANCED SOLVENTS FOR CO<sub>2</sub> CAPTURE  
FROM COAL-FIRED UTILITIES

by

Brandon Michael Pavlish  
Bachelor of Science, University of North Dakota, 2006

A Thesis

Submitted to the Graduate Faculty

of the

University of North Dakota

in partial fulfillment of the requirements

for the degree of

Master of Science

Grand Forks, North Dakota

December

2012



Copyright 2012 Brandon Pavlish

This thesis, submitted by Brandon M. Pavlish in partial fulfillment of the requirements for the Degree of Master of Science from the University of North Dakota, has been read by the Faculty Advisory Committee under whom the work has been done and is hereby approved.

---

Steven Benson

---

Michael Mann

---

Brian Tande

This thesis meets the standards for appearance, conforms to the style and format requirements of the Graduate School of the University of North Dakota, and is hereby approved.

---

Wayne Swisher  
Interim Dean of the Graduate School

---

Date

Title	Pilot-Scale Evaluation of Advanced Solvents for CO <sub>2</sub> Capture from Coal-Fired Utilities
Department	Chemical Engineering
Degree	Master of Science

In presenting this thesis in partial fulfillment of the requirements for a graduate degree from the University of North Dakota, I agree that the library of this University shall make it freely available for inspection. I further agree that permission for extensive copying for scholarly purposes may be granted by the professor who supervised my thesis work or, in his absence, by the chairperson of the department or the dean of the Graduate School. It is understood that any copying or publication or other use of this thesis or part thereof for financial gain shall not be allowed without my written permission. It is also understood that due recognition shall be given to me and to the University of North Dakota in any scholarly use which may be made of any material in my thesis.

Brandon Pavlish  
December 2012

TABLE OF CONTENTS

LIST OF FIGURES .....x

LIST OF TABLES .....xiv

ACKNOWLEDGMENTS .....xvi

ABSTRACT .....xvii

CHAPTER

    I. INTRODUCTION ..... 1

    II. BACKGROUND .....3

        Global Climate Change Explained.....3

        CO<sub>2</sub> Regulatory Background..... 10

            Federal Legislation..... 10

            EPA Regulations..... 11

            Regional Climate Initiatives ..... 14

            Regional Greenhouse Gas Initiative ..... 14

            Individual State Actions ..... 16

        Existing Market for CO<sub>2</sub> Capture: Existing Power Plant Fleet ..... 19

        CO<sub>2</sub> Capture Review Summarized.....24

            Precombustion .....25

            During Combustion.....26

            Postcombustion.....28

III. ADVANCED SOLVENTS .....	39
Production of Amines .....	39
Implementation of Amine Scrubbing.....	41
Process Chemistry.....	42
Process Description.....	44
Flue Gas Pretreatment .....	45
Absorber .....	46
Stripping (Regeneration) .....	47
CO <sub>2</sub> Compression and Drying Unit .....	48
Amine Process Concerns.....	49
Loss of Solvent .....	49
Energy Penalty.....	49
Corrosion .....	50
Environmental Impacts .....	50
Advanced Amines.....	51
IV. ADVANCED SOLVENTS SCIENTIFIC DISCUSSION.....	53
Chemistry of Carbon Dioxide.....	54
Carbon Dioxide Scavengers .....	56
Thermodynamics and Kinetics .....	57
Thermodynamics .....	57
Kinetics.....	58
Unwanted Chemical Reactions.....	58
General Properties.....	60



V.	EXPERIMENTAL DESIGN AND APPARATUS .....	61
	Description of the CTF.....	61
	Solvent Absorption Test System and Protocol.....	64
	Description of the Solvent Scrubbing System.....	67
	Test Plan and Methods .....	76
	Fresh Amine Solvents .....	78
	Calculations .....	80
	Shakedown Testing.....	80
VI.	PILOT SCALE TEST RESULTS .....	85
	Monoethanolamine – Base Case.....	86
	System Performance .....	87
	Effects of Flue Gas Flow Rate.....	88
	MEA Sample Analysis.....	98
	Solvent Results & Comparison.....	108
	Effects of Reboiler Duty .....	108
	Effect of Liquid to Gas Ratio .....	112
	Free Amine Comparison .....	112
	HSSs.....	113
	Corrosion Products.....	117
	CO <sub>2</sub> Loading .....	120
	Solvent Summary.....	122
	Overall CO <sub>2</sub> Capture Performance .....	123
	Overall Solvent Sample Analysis .....	124

VII. SOLVENT SYSTEM MODELING AND ECONOMIC EVALUATION .....	127
Introduction .....	127
Aspen Plus Model Description .....	129
Coal Combustion .....	129
CO <sub>2</sub> Capture.....	130
CO <sub>2</sub> Compression and Liquefaction .....	134
Aspen Process Economic Analyzer .....	135
Results .....	137
Summary .....	144
VIII. CONCLUSIONS .....	147
APPENDICES.....	150
REFERENCES.....	211

## LIST OF FIGURES

Figure	Page
Figure 1. Incoming and outgoing light wavelengths (Environmental Chemistry, Baird and Cann, Freeman and Co., NY, 2005). .....	4
Figure 2. Incoming and outgoing light energy balance. ....	5
Figure 3. Greenhouse gases showing the “greenhouse” effect. ....	5
Figure 4. Land air temperature anomalies for the period of 1850 to 2007 (File: HadCRUT3, Hadley Centre, 2009) (6).....	8
Figure 5. Annual global temperature anomalies (Hadley Centre, 2007) and CO <sub>2</sub> concentration data from the Law Dome in Antarctica and the atmospheric O <sub>2</sub> -concentrations derived from air samples collected at the South Pole (6).....	9
Figure 6. Global temperatures 4500 years showing the longer term trends on earth. ....	9
Figure 7. Breakdown of CO <sub>2</sub> emissions produced from energy generating systems in the united States. ....	21
Figure 8. Amount of energy produced by fuel type in the United States. ....	21
Figure 9. CO <sub>2</sub> emissions from plants emitting more than 1 Mt of CO <sub>2</sub> annually. ....	23
Figure 10. Simple schematic for the production of amines. ....	40
Figure 11. Simple block flow diagram of a coal-fired utility with an amine-based CO <sub>2</sub> capture system. ....	45
Figure 12. 3-D representation of the CTF and SASC systems. ....	65
Figure 13. Picture of the CTF. ....	65
Figure 14. P&ID of the SASC system. ....	68
Figure 15. SASC system as tested during shakedown.....	69
Figure 16. Koch–Glitsch IMTP 25 random packing sample. ....	69

Figure 17. 3-D representation of the SASC system with Water and Energy Sustainability Technology (WEST) system shown on the far right. ....	74
Figure 18. CO <sub>2</sub> capture from coal combustion flue gas – January 6, 2010. ....	82
Figure 19. CO <sub>2</sub> removal from coal combustion flue gas and absorber inlet properties – February 2, 2010.....	83
Figure 20. MEA CO <sub>2</sub> capture and absorber inlet properties observed during testing on March 17, 2010.....	89
Figure 21. MEA CO <sub>2</sub> capture, reboiler duty, and absorber inlet properties observed during testing on March 17, 2010. ....	90
Figure 22. Effect of MEA lean solvent flow rate on CO <sub>2</sub> capture. ....	91
Figure 23. Effect of stripper pressure on MEA CO <sub>2</sub> capture performance.....	92
Figure 24. Variation of CO <sub>2</sub> capture with MEA solvent regeneration energy requirements. ....	94
Figure 25. Impact of absorber inlet solvent temperature on CO <sub>2</sub> capture. ....	95
Figure 26. Effects of absorber inlet solvent temperature and regeneration energy on CO <sub>2</sub> capture for MEA.....	96
Figure 27. Sulfate and thiosulfate concentration at various SO <sub>2</sub> injection levels. ....	97
Figure 28. Concentration of free amine in lean MEA solutions. ....	98
Figure 29. Concentration of inorganic anions in lean MEA solutions. ....	101
Figure 30. Concentration of sulfate and thiosulfate salts in lean MEA solutions during SO <sub>2</sub> injection tests.....	102
Figure 31. Concentration of organic anions in lean MEA solutions. ....	103
Figure 32. Concentration of trace metals in lean MEA solutions. ....	104
Figure 33. Concentration of major elements in lean MEA solutions. ....	106
Figure 34. CO <sub>2</sub> loading in lean MEA samples. ....	107

Figure 35. Regeneration energy required to meet 90% CO <sub>2</sub> capture for H3-1, MDEA+PZ, and 30 wt% MEA at 4–6 psig static pressure. ....	109
Figure 36. Regeneration energy required to meet 90% CO <sub>2</sub> capture for H3-1 and 30 wt% MEA at 12 psig static pressure.....	111
Figure 37. Effects of liquid flow rate on CO <sub>2</sub> capture for H3-1, MDEA+PZ, and MEA. ....	113
Figure 38. Free amine comparisons for H3-1, MEA, Huntsman additive, and MDEA+PZ. ....	114
Figure 39. Comparative analysis of sulfate concentrations for MEA, H3-1, Huntsman additive, and MDEA+PZ. ....	115
Figure 40. Comparative analysis of thiosulfate concentration for MEA, H3-1, Huntsman additive, and MDEA+PZ. ....	115
Figure 41. Comparative analysis of chloride concentrations for MEA, H3-1, Huntsman additive, and MDEA+PZ. ....	116
Figure 42. Comparative plot of nickel concentrations for MEA, H3-1, Huntsman additive, and MDEA+PZ. ....	117
Figure 43. Comparative plot of iron concentrations for MEA, H3-1, Huntsman additive, and MDEA+PZ. ....	118
Figure 44. Comparative plot of chromium concentrations for MEA, H3-1, Huntsman additive, and MDEA+PZ. ....	118
Figure 45. Comparative plot of manganese concentration for MEA, H3-1, Huntsman additive, and MDEA+PZ. ....	119
Figure 46. Comparative plot of molybdenum concentration for MEA, H3-1, Huntsman additive, and MDEA+PZ. ....	119
Figure 47. Plot of CO <sub>2</sub> loading for MEA, H3-1, Huntsman additive, and MDEA+PZ. .	121
Figure 48. Aspen Plus process model for coal combustion and flue gas cleaning. ....	130
Figure 49. Aspen Plus process model for CO <sub>2</sub> capture system.....	131
Figure 50. CO <sub>2</sub> compression and liquefaction. ....	135

Figure 51. Breakdown of levelized capital and operating expenses per ton of CO <sub>2</sub> captured.....	141
Figure 52. Breakdown of levelized capital and operating expenses per ton of CO <sub>2</sub> avoided.....	141
Figure 53. Breakdown of individual contributions for direct equipment costs.....	142
Figure 54. Energy penalty, or parasitic load. ....	143
Figure 55. Sensitivity analysis of the cost to produce electricity on CO <sub>2</sub> capture costs. ....	145
Figure 56. Sensitivity analysis of the cost to produce electricity on electricity rate increase. ....	145
Figure 57. Sensitivity analysis of the cost of CO <sub>2</sub> avoidance on electricity rate increase. ....	146
Figure 58. Acid titration curve of MEA Sample No. 95.....	156
Figure 59. Acid titration curve of Solvent A Sample No. 48.....	157
Figure 60. Base titration curve of MEA Sample No. 95.....	157
Figure 61. Base titration curve of Solvent A Sample No. 48.....	158
Figure 62. Chromatogram of 10 ppm analyte standard solutions. ....	161
Figure 63. CO <sub>2</sub> capture for various inlet flows using H3-1.....	171
Figure 64. Comparison of H3-1 reboiler duty at varying conditions. ....	172
Figure 65. Effect of stripper pressure on H3-1 performance. ....	173
Figure 66. Effect of absorber inlet solvent temperature on CO <sub>2</sub> capture for H3-1. ....	173
Figure 67. Gas flow rate and liquid-to-gas ratio effects on CO <sub>2</sub> capture. ....	174
Figure 68. Concentration of free amine in lean H3-1 solutions.....	176
Figure 69. Concentration of inorganic anions in lean H3-1 solutions.....	178
Figure 70. Concentration of trace metals in lean H3-1 solutions.....	181
Figure 71. Concentration of major elements in lean H3-1 solutions.....	181

Figure 72. CO <sub>2</sub> loading in lean H3-1 solutions. ....	183
Figure 73. Concentration of sulfate and thiosulfate salts in lean Huntsman additive solutions during SO <sub>2</sub> injection tests. ....	186
Figure 74. Concentration of nitrite and nitrate salts in lean Huntsman additive solutions during NO <sub>x</sub> injection tests. ....	187
Figure 75. Concentration of free amine in lean Huntsman additive solutions. ....	189
Figure 76. Concentration of inorganic anions in lean Huntsman additive solutions. ....	190
Figure 77. Concentration of organic anions in lean Huntsman additive solutions. ....	191
Figure 78. Concentration of trace metals in lean Huntsman additive solutions. ....	192
Figure 79. Concentration of major elements in lean Huntsman additive solutions. ....	193
Figure 80. CO <sub>2</sub> loading in lean solutions of Huntsman additive. ....	194
Figure 81. MDEA+PZ solvent performance based on flue gas flow rate and liquid-to-gas ratio. ....	197
Figure 82. Effect of stripper pressure on CO <sub>2</sub> capture for MDEA+PZ. ....	199
Figure 83. CO <sub>2</sub> capture for various inlet gas flows for MDEA+PZ. ....	200
Figure 84. MDEA+PZ solvent regeneration energy requirements. ....	200
Figure 85. Concentration of free amine in lean MDEA+PZ solutions. ....	202
Figure 86. Concentration of organic and inorganic anions in lean MDEA+PZ solution samples. ....	204
Figure 87. Concentration of trace metals in lean MDEA+PZ solution samples. ....	205
Figure 88. Concentration of major elements in lean MDEA+PZ solution samples. ....	206
Figure 89. CO <sub>2</sub> loading in lean solutions of MDEA+PZ. ....	207

## LIST OF TABLES

Table	Page
Table 1. Summary of some greenhouse gasses and their relative global warming potential. (Environmental Chemistry, Baird and Cann, Freeman and Co., NY, 2005).....	6
Table 2. States with greenhouse gas emissions targets (20).....	17
Table 3. Emission Discharge from the Manufacture of Ethanolamines by the Ammonolysis of Ethylene Oxide. ....	40
Table 4. Removal Efficiencies of Acid Gases in an Amine Absorber. ....	59
Table 5. Comparison Between Aspen Model Data and Pilot-Scale Demonstration Unit Data.....	74
Table 6. SASC Variable Test Parameters. ....	75
Table 7. Example of a Portion of a Typical Test Plan Matrix. ....	77
Table 8. Summary of Methods and Analytical Techniques.....	79
Table 9. Concentration of Fresh Amine Solvents. ....	79
Table 10. Test Parameter Ranges. ....	88
Table 11. Bound Amine in Lean MEA.....	100
Table 12. Factors developed based on pilot scale data to modify the MEA based model. ....	125
Table 13. Chemical Equilibrium Reactions for General MEA Sorbent and CO <sub>2</sub> Absorption.....	132
Table 14. Summary of CO <sub>2</sub> Capture Costs, US\$ .....	138
Table 15. Operating Parameters of the ICS 3000 System .....	160



Table 16. Gradient Conditions Used for Standards and Samples .....	161
Table 17. Proximate/Ulimate Analysis of Antelope Coal used for testing.....	168
Table 18. Typical flue gas composition from the combustion of coal. ....	168
Table 19. Bound Amine in Lean H3-1 .....	177
Table 20. Bound Amine in Lean Huntsman Additive .....	189
Table 21. Bound Amine in Lean MDEA+PZ .....	202

## ACKNOWLEDGMENTS

I wish to express my sincere appreciation to the members of my advisory committee, Steven Benson, Brian Tande, and Michael Mann, for their guidance and support during my time in the Master of Science program at the University of North Dakota.

I would also like to acknowledge the companies who supported this work which include: U.S. Department of Energy National Energy Technology Laboratory Cooperative, North Dakota Industrial Commission, ATCO Power Canada Ltd., Baker Petrolite, Black & Veatch Corporation, C-Quest Technologies, Constellation Energy, Hitachi Power Systems America Ltd., Huntsman Corporation, Lignite Energy Council, Metso Power, Midwest Generation EME LLC, Minnesota Power, Nebraska Public Power District, PPL Montana, Saskatchewan Power, and TransAlta Corporation, and the Energy & Environmental Research Center.

I would like to give a special thanks to the Energy and Environmental Research Center for allowing me to use the Partnership for CO<sub>2</sub> Capture program to complete this thesis. I would also like to thank all the researchers from the EERC who helped me in completed Phase one of that work of which much of this thesis is based on: Tony Snyder, John Kay, Nathan Fiala, Angie Morgan, and Josh Stanislawski.

## ABSTRACT

In 1992, international concern about climate change (a change to Earth's climate, especially those produced by global warming) led to the United Nations Framework Convention on Climate Change (UNFCCC). The ultimate objective of that convention was the "stabilization of greenhouse gas concentrations in the atmosphere at a level that mitigates anthropogenic interference with the climate system" (1). There has been a growing concern about global climate change which scientists believe is (arguably) caused mainly by anthropogenic emission of greenhouse gases (GHGs) into the atmosphere. The overall goal of this work was to evaluate next generation solvents at a pilot scale level to determine the advantages and disadvantages these advanced solvent have over the current industry standard. To accomplish this goal a pilot scale system was designed and fabricated on the back end of the Energy and Environmental Research Center's Combustion Test Facility. The system was used to evaluate six solvents which included Hitachi's H3-1, MDEA/Piperazine, Huntsman's Jeff Treat XP, MEA and two others. Because of the proprietary nature of these solvents not all information can be shared.

It was determined that advanced solvents are the best available technology for implementing CO<sub>2</sub> capture at the large scale. Advanced solvents will be the technology that will make it to the market place sooner than other technologies due to the long time use of amine solvents in the oil and gas industry for their removal of CO<sub>2</sub>. For the case of

postcombustion capture, the main conclusions are that 90% CO<sub>2</sub> capture can be met with MEA and advanced solvents. The EERC system was able to capture at least 90% of the CO<sub>2</sub> present in the flue gas for each advanced solvent and the baseline MEA. Results of the testing indicate that the use of advanced solvents, such as H3-1, can reduce the cost of capture considerably.

Data from the advanced solvents and MEA tests conducted show that for similar test conditions, MEA required about 10–40% more regeneration energy input to achieve 90% CO<sub>2</sub> capture than the advanced amine-based solvents. H3-1 required the lowest heat input (~1475 Btu/lb CO<sub>2</sub>), and the reboiler duty for MDEA+PZ was ~1600 Btu/lb CO<sub>2</sub>. The regeneration energy requirement for MEA was estimated to be in the range of 1775–1940 Btu/lb CO<sub>2</sub> captured. The MEA case required a 30% to 50% higher solvent flow rate than H3-1 to attain 90% CO<sub>2</sub> capture for a given amount of treated flue gas. Conversely, tests on MDEA+PZ showed a solvent usage about 135% higher than MEA to reach 90% capture. Consequently, use of H3-1 for a large-scale process could lead to significant economic benefits over MEA and MDEA+PZ. Lower solvent flow rates require smaller pumps and less energy to pump the solvent through the columns.

Advanced solvents show promise, but improvements will still need to be made to reduce capital and operating costs to make the technology economically feasible for today's market. Advanced contactors and solvent promoters will be technologies that may enable these solvent to become more economically favorable.

## CHAPTER I

### INTRODUCTION

In 1992, international concern about climate change (a change to Earth's climate, especially those produced by global warming) led to the United Nations Framework Convention on Climate Change (UNFCCC). The ultimate objective of that convention was the "stabilization of greenhouse gas concentrations in the atmosphere at a level that mitigates anthropogenic interference with the climate system" (1). There has been a growing concern about global climate change which scientists believe is (arguably) caused mainly by anthropogenic emission of greenhouse gases (GHGs) into the atmosphere. Global warming is defined as an increase in the Earth's temperature widely predicted to occur due to an increase in the greenhouse effect resulting especially from pollution.

The predominant sources are utilities that meet energy demands through combustion of fossil fuels like coal, petroleum and natural gas as well as transportation. Despite concerns about GHGs, fossil fuels currently contribute over 85% of the energy needs for the United States (1) and similar percentages elsewhere (2,3). This trend in the consumption of fossil fuels is likely to continue for at least a decade or more because fossil fuels have certain advantages, such as high energy density, low cost, availability and existing reliable technology for energy production. Research by the U.S. Department

of Energy (DOE) and the International Energy Agency (IEA) has suggested that carbon separation and sequestration can play an important role in reducing CO<sub>2</sub> in the atmosphere in the first part of the twenty-first century (2). Development of an economically feasible CO<sub>2</sub> capture technology presents one of the biggest challenges to the fossil energy industry in the 21st century. Many existing technologies are capable of capturing carbon from coal-fired power plants, but most come at a high cost and high energy penalty. Development and evaluation of new technologies are critical steps toward economical carbon capture. Currently advanced solvents are one of the most promising technologies for full scale deployment for the capture of CO<sub>2</sub> from large sources. This thesis is focused on a pilot-scale evaluation of advanced solvents. The current industry standard for chemically capturing CO<sub>2</sub> from a gas stream is the use of a monoethanolamine (MEA) solvent. Because this solvent is considered the current state of the art (due to its long time use in the oil and gas industry) it was chosen as the baseline case for comparison to all other technologies evaluated.

The overall goal of this work was to evaluate next generation solvents at a pilot scale level to determine the advantages and disadvantages these advanced solvent have over the current industry standard. To accomplish this goal a pilot scale system was designed and fabricated on the back end of the Energy and Environmental Research Center's Combustion Test Facility. The system was used to evaluate six solvents which included Hitachi's H3-1, MDEA/Piperazine, Huntsman's Jeff Treat XP, MEA and two others. Because of the proprietary nature of these solvents not all information can be shared. The solvents will be given a random letter assignment to keep the sensitive information confidential to the solvent providers.

## CHAPTER II

### BACKGROUND

#### Global Climate Change Explained

Before we can discuss the details of how to capture CO<sub>2</sub> from large point sources, global warming must be understood. There are several researchers who have proven theories for cases that show global warming is occurring and they try to predict the effects of such temperature rises. Other researchers claim that the models that are being used to predict global warming grossly over estimate the amount of warming that is and will occur in the future, while some researchers are predicting a period of global cooling.

The existence of the greenhouse effect was first postulated by ARRHENIUS in 1896 (4). According to his hypothesis, specific gases in the atmosphere of the earth, in the first place water vapor, but also carbon dioxide, methane, di-nitrogen oxide, ozone, and halogenated hydrocarbons, permit the transmission of the sun's radiation (short wavelengths), but not that of the long wavelength infrared radiation reflected by the surface of the earth. Figure 1 shows the wavelength range at which solar light is incoming to the earth and the range at which light exits from the Earth's surface. Greenhouse gases allow the incoming solar light to pass through to the earth's surface where some is absorbed by the surface and air, while a portion is reflected by the atmosphere and surface. The Earth's surface emits light energy constantly as well, the fraction of the

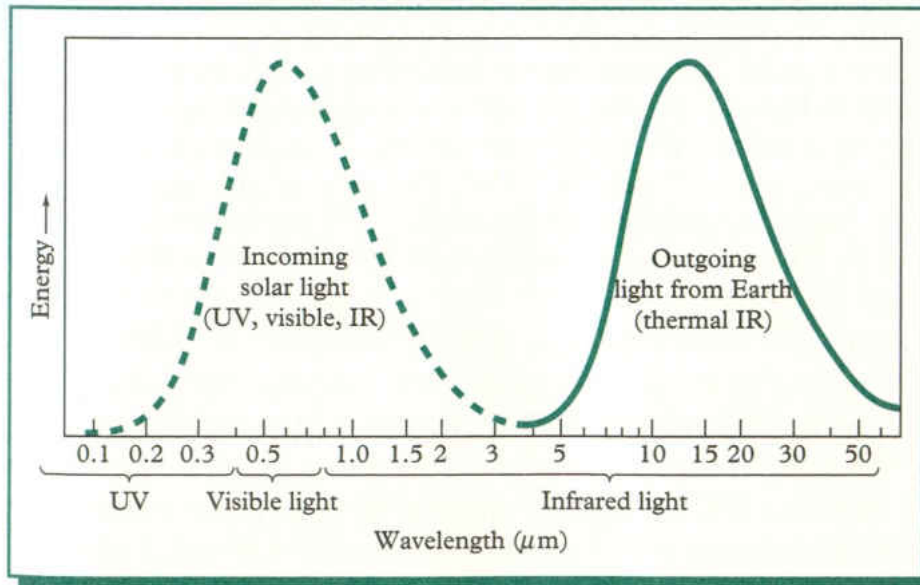


Figure 1. Incoming and outgoing light wavelengths (Environmental Chemistry, Baird and Cann, Freeman and Co., NY, 2005).

energy that is diverted back to the Earth's surface as well as the total amount of energy absorbed by gases is the net gain which causes global warming. This can be seen in Figures 2 and 3. CO<sub>2</sub> will absorb light in two regions, its maximum at the thermal IR region of 15 μm and at 4.26 μm.

Without this naturally occurring effect, the average temperature of the earth's surface would be - 18°C as compared to its real value of 15°C. This natural greenhouse effect is beneficial, since it forms the basis for the great variety of plant and animal life on earth. Where it is too strong or too weak, life cannot exist. Examples exist in our planetary system: The Martian atmosphere contains too little carbon dioxide which results in a temperature of about -60 °C. The atmosphere of Venus contains too much carbon dioxide contributing to a temperature of about + 430 °C. The questions is not



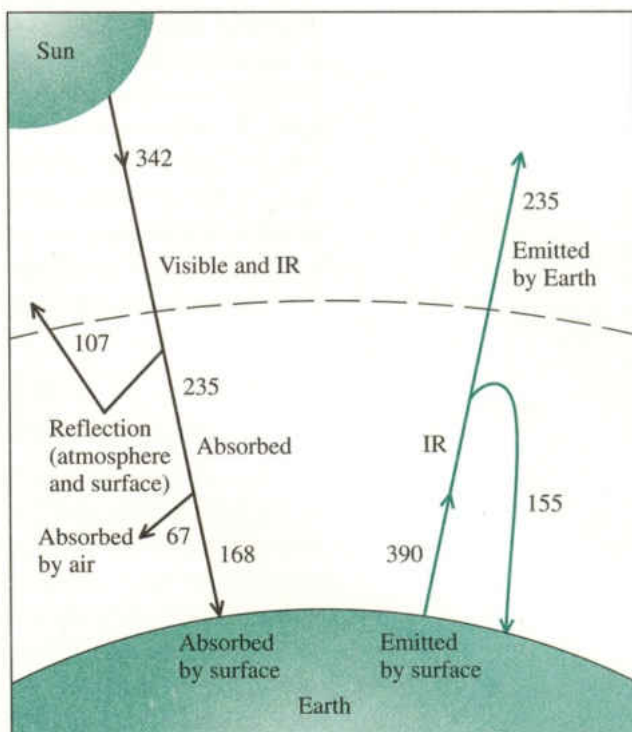


Figure 2. Incoming and outgoing light energy balance. (Environmental Chemistry, Baird and Cann, Freeman and Co., NY, 2005).

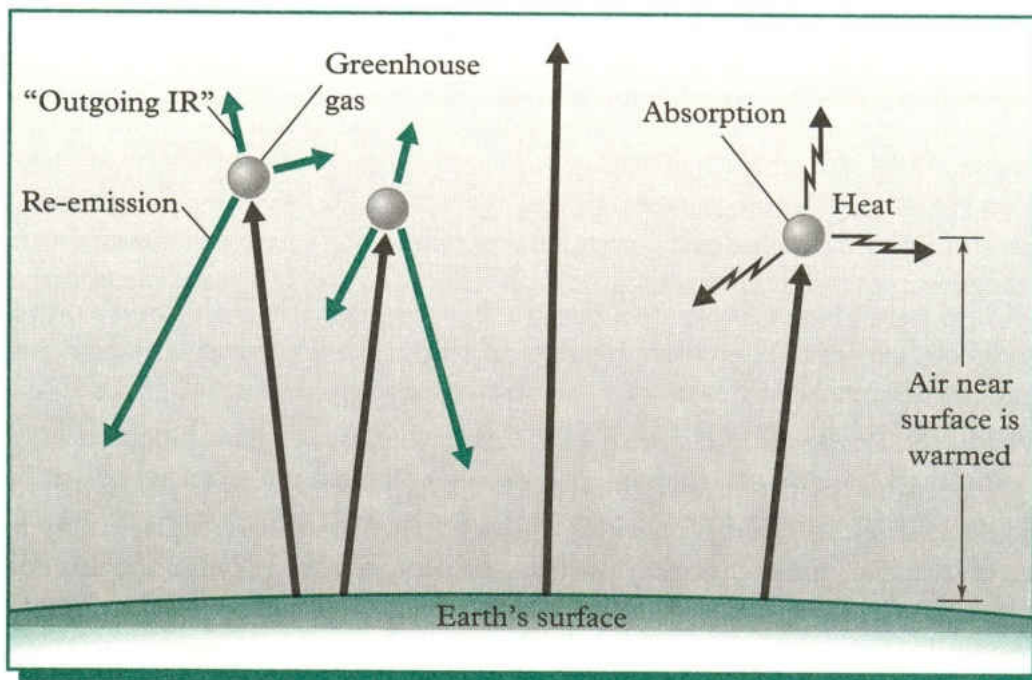


Figure 3. Greenhouse gases showing the “greenhouse” effect. (Environmental Chemistry, Baird and Cann, Freeman and Co., NY, 2005).

whether the greenhouse effect is causing global warming, but rather is man contributing to the greenhouse effect in a way that will cause global warming to reach higher levels than it would naturally achieve. (4)

CO<sub>2</sub> in the atmosphere is being considered by many scientists and engineers to be the crucial factor contributing to global warming. The intergovernmental panel on Climate Change (IPCC) has put together several reports pulling together the information from lead scientists proclaiming that CO<sub>2</sub> is causing global warming. According to the IPCC CO<sub>2</sub> is the principle anthropogenic gas that is thought to affect the Earth's radioactive balance. Table 1 lists summary information for the main greenhouse gases (neglecting water) showing their relative global warming potentials and current concentrations in the atmosphere. Although the relative potential is lower than the other gases shown, the concentration and life in the atmosphere is considerably higher. Because of this, it is thought that there is a close relationship between CO<sub>2</sub> and the change in the Earth's temperature.

Table 1. Summary of some greenhouse gasses and their relative global warming potential. (Environmental Chemistry, Baird and Cann, Freeman and Co., NY, 2005).

Gas	Current Concentration	Residence time, years	Relative global warming potential
CO <sub>2</sub>	392 ppm	50-200	1
CH <sub>4</sub>	1.77 ppm	12	23
N <sub>2</sub> O	316 ppb	120	296
CFC-11	0.26 ppb	45	4600
HCFC-22	0.15 ppb	12	1700
HFC-134a	0.01 ppb	14	1300
Halon-1301	0.003 ppb	65	6900

From the years 1850 to 1980 there is little to no change in the temperature increase. Based on data from Hadley Centre (5) the temperature appears to increase from the year 1980 to present. This can be seen in Figure 4. By plotting this temperature data with the amount of CO<sub>2</sub> present in the atmosphere versus time shows what appears to be a correlation demonstrating an average global temperature rise as CO<sub>2</sub> concentrations increase, this is demonstrated in Figure 5. The CO<sub>2</sub> concentration data comes from both ice core data (1850-1978) and direct air sample measurements (1957-2008). Many scientists argue that CO<sub>2</sub> concentrations derived from ice core data is unreliable due to several issues, sampling and analytical methods are based on ice/gas difference assumptions that are not supported experimentally and formation of solid CO<sub>2</sub> clathrates is neglected are the two main issues.(5)

Several other issues arise when this data is looked at more closely:

1. A simple statistical average of temperatures from around the globe is not an adequate measurement in which to summarize climate change.
2. Temperature measurements are not located in random locations, and are biased such especially when located in large cities.
3. The presumed global warming might merely be a urban phenomenon based on weather stations that were once located in rural locations, now located in urban areas with large paved areas acting as heat sinks.(5)

The data shown in Figure 5 seems to show a correlation in temperature rise and CO<sub>2</sub> concentration, however keep in mind this is a relatively short time frame to considered atmospheric data. Harris and Mann have shown similar data, but include a much longer time frame. Figure 6 shows the global temperatures from 2500 B.C. to 2040

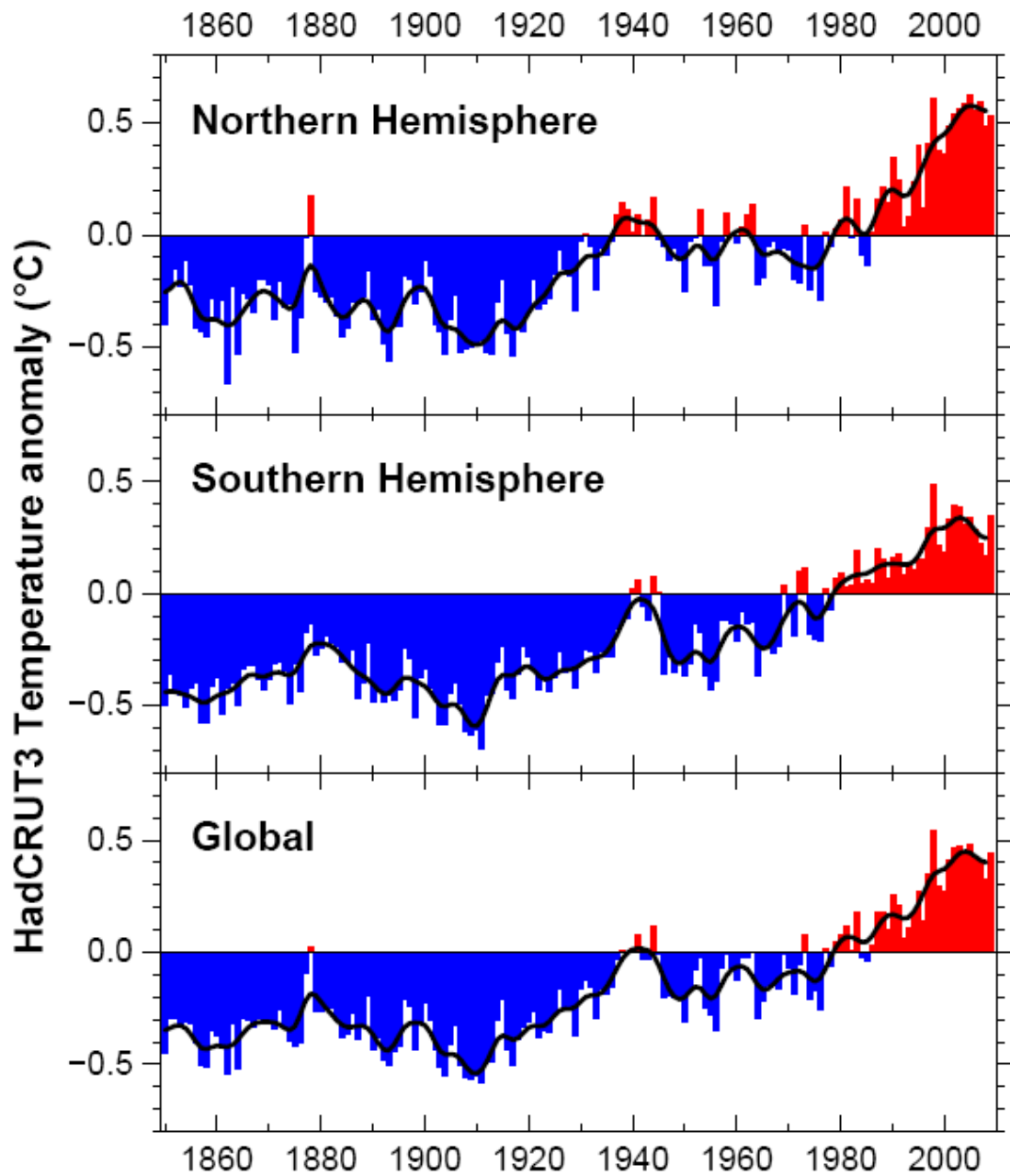


Figure 4. Land air temperature anomalies for the period of 1850 to 2007 (File: HadCRUT3, Hadley Centre, 2009) (6).

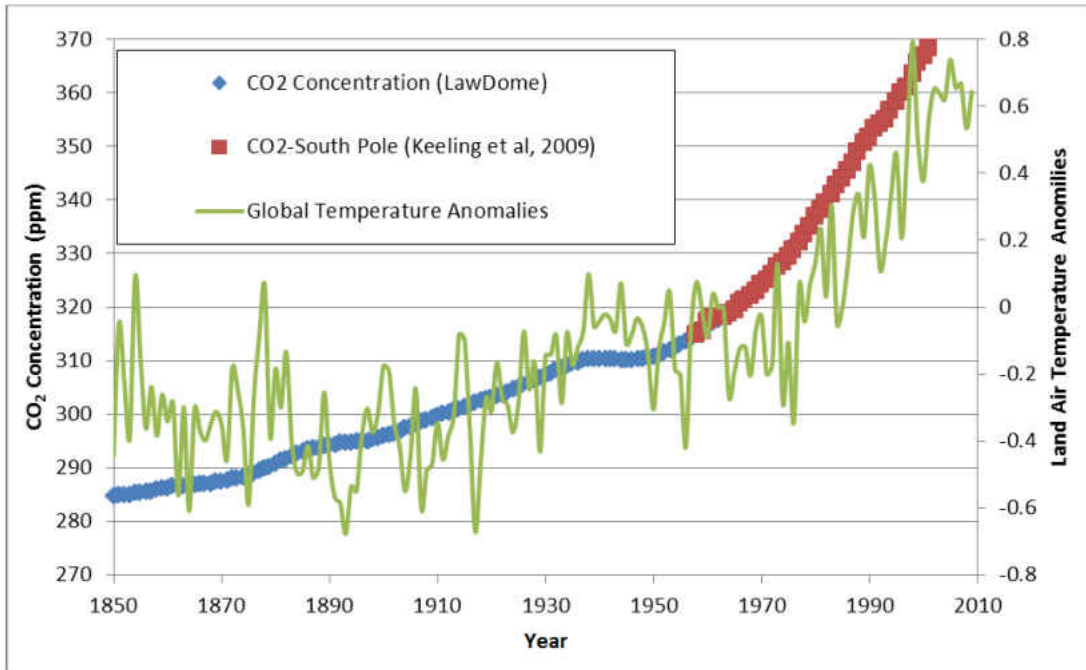


Figure 5. Annual global temperature anomalies (Hadley Centre, 2007) and CO<sub>2</sub> concentration data from the Law Dome (<http://cdiac.ornl.gov/trends/co2/lawdome.html>) in Antarctica and the atmospheric O<sub>2</sub>-concentrations derived from air samples collected at the South Pole (6).

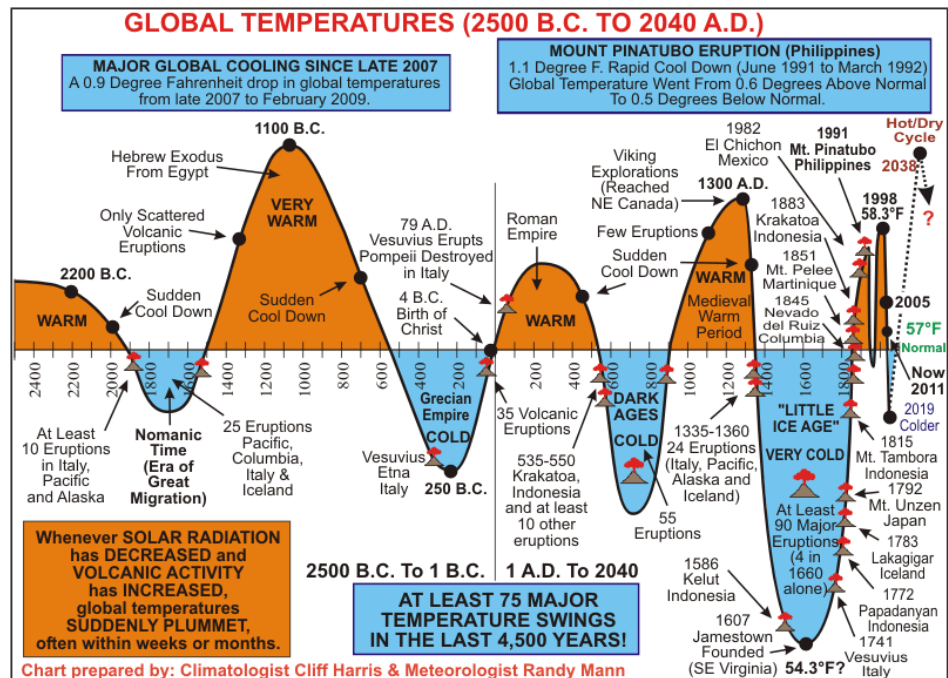


Figure 6. Global temperatures 4500 years showing the longer term trends on earth.

A.D., demonstrating that on a longer term the temperatures we are currently experiencing are not increased, but would fall within the natural swings of the earth. There is great debate whether or not global climate change is occurring, and if it is truly caused by rising CO<sub>2</sub> concentrations. In any case the costs of not acting to prevent this phenomenon may be greater than standing by and doing nothing. Therefore there has been much attention put towards capturing and sequestering CO<sub>2</sub> from large point sources, and leads us to the focus of this thesis.

## CO<sub>2</sub> Regulatory Background

### *Federal Legislation*

The regulation of greenhouse gases at the federal level has been pursued by both house and senate bills over the last decade. There has been bipartisan support for efforts to reduce the use of fossil fuels through energy efficiency incentives, incentives for renewable fuels, and research funding for low-carbon energy sources and carbon capture and sequestration. Regulation of greenhouse gases through either a carbon tax or a cap-and-trade system has been proposed in several bills. The American Clean Energy and Security Act of 2009 (H.R. 2454), also known as the Waxman-Markey bill, was passed by the U.S. House of Representatives in June 2009 but was not considered in the Senate. It included a cap-and-trade system for the entire United States (7).

In the U.S. Senate the American Power Act, known as the Kerry-Lieberman bill, was introduced in May 2010. It includes a cap-and-trade system for dealing with greenhouse gas emissions as well as incentives for increasing domestic energy production and energy efficiency (8). The bill has not passed the Senate.

Recent efforts in the U.S. Congress have focused on limiting the ability of the EPA and the federal government to regulate greenhouse gas emissions. Bills have been introduced in both the House and Senate to prevent the EPA from regulating greenhouse gases under the Clean Air Act. One of the most prominent of these is H.R. 910, also introduced in the Senate as S. 482, the Energy Tax Prevention Act of 2011, proposed by Reps. Upton and Whitfield along with Senator Inhofe. The main thrust of this bill is to prevent the regulation of greenhouse gases at the federal level. It would amend the Clean Air Act to prohibit the EPA from regulating greenhouse gases, and would repeal eleven rules issued by the EPA. H.R. 910 would not affect state rules as long as they are not part of Federal law (9). S. 228 was introduced in the Senate by Senator Barrasso of Wyoming in May 2010. Its contents are similar to those of H.R. 910 and S. 482 with the main goal of the bill being to prevent federal regulation of greenhouse gases by the President or any federal agency (10). Many bills with similar content to H.R. 910 and S. 228 have been introduced in both the House and Senate but none have passed through either chamber.

Due to the partisan nature of the debate concerning global climate change and the effect of greenhouse gases on the environment, along with the split in control of the Senate and the House, it is unlikely that legislation on this issue will pass in the near future.

### *EPA Regulations*

The EPA has been developing rules to regulate greenhouse gas emissions under the Clean Air Act. In 2010 the Mandatory Greenhouse Gas Reporting Rule was put in place due to a Congressional mandate (11). This rule requires all large emitters of greenhouse gases to collect data on the type and amount of greenhouse gases emitted and

report this data to the EPA. This rule is part of a response to a 2007 Supreme Court ruling.

In the spring of 2007 the Supreme Court issued its ruling in the case of the State of Massachusetts vs. the EPA. The State of Massachusetts along with other states and local governments had sued the EPA for not regulating four greenhouse gases in the transportation sector. The Supreme Court decided in favor of the State of Massachusetts and stated that the EPA has the authority to regulate greenhouse gases under the Clean Air Act (12). After this court ruling the EPA reviewed scientific research and issued an Endangerment Finding regarding greenhouse gases in 2009 (13). In the Endangerment Finding the EPA listed six greenhouse gases which when emitted from vehicles contribute to climate change and therefore endanger public health. This finding meant that the EPA had to regulate greenhouse gas emissions from vehicles.

In 2009 the EPA, along with the Department of Transportation (DOT) and several states, created the Corporate Average Fuel Efficiency (CAFE) standards along with GHG emissions standards for cars and light duty vehicles (11, 14). This was followed by GHG regulations and fuel efficiency requirements for heavy duty vehicles in 2010. The regulation of greenhouse gases for vehicles automatically triggered the regulation of greenhouse gases from other sources, such as refineries and power plants, under the Clean Air Act.

One consequence of this is that large projects, either new projects or major modifications to existing facilities that will result in the emission of GHGs will eventually fall underneath the Prevention of Significant Deterioration (PSD) program and the Title V Greenhouse Gas Tailoring Rule (15). The first phase of this rule went into



effect from January 2, 2011 to June 30, 2011 and will only affect sources that require permitting for non-GHG emissions under PSD and Title V. It will require projects which increase GHG emissions by 75,000 tons per year or more, based on CO<sub>2</sub> equivalents, to determine the Best Available Control Technology (BACT) for these emissions (15). During this first phase no sources will be required to obtain permits under the Clean Air Act based only on GHG emissions.

Phase II of the process began on July 1, 2011 and will last until June 30, 2013. During this phase PSD permitting requirements will cover new projects that emit at least 100,000 tons per year of GHGs even if they do not exceed permitting requirements for other pollutants covered by the Clean Air Act (15). The EPA estimates that 550 sources will need to get Title V permits for the first time during this phase and that 900 additional PSD permits will be needed each year from increases in GHG emissions (15).

The EPA is expected to release a proposal for New Source Performance Standards (NSPS) for GHG emissions from new and existing power plants and refineries on December 15, 2011. This deadline has been extended several times due to negotiations with these industries and court settlements. As a result of court settlements, the regulations need to be finalized in 2012. The power plant NSPS is due on May 26, 2012 with the refinery NSPS following on November 15, 2012 (11).

As it currently stands, the EPA will have regulations in place for large GHG emitters in the power and refining industries beginning in 2012. This timeline may change as there have already been several delays regarding the NSPS standards. Congressional action may affect the ability of the EPA to regulate GHGs as there have

been several bills proposed in both the House and Senate to prevent the EPA from regulating them under the Clean Air Act.

### *Regional Climate Initiatives*

Regional climate initiatives have been formed by groups of states to address greenhouse gas emissions and other energy related issues. Some of these include regional cap-and-trade programs while others are more focused on developing non-fossil fuel based energy resources.

### *Regional Greenhouse Gas Initiative*

The Regional Greenhouse Gas Initiative (RGGI) was formed in 2005 by states in the Northeastern U.S. Included in the initiative are Connecticut, Delaware, Maine, Maryland, Massachusetts, New Hampshire, New Jersey, New York, Rhode Island, and Vermont. The goal of the initiative is to reduce power sector CO<sub>2</sub> emissions 10 percent by 2018. Each of the ten states has its own CO<sub>2</sub> Budget Trading Program based on the RGGI model rule. These trading programs issue CO<sub>2</sub> allowances to electric power plants and administer regional CO<sub>2</sub> allowance auctions. Power plants in the RGGI can use CO<sub>2</sub> allowances from any of the state trading programs to comply with their own state programs. The trading program began in January of 2009 and includes all fossil fuel-fired power plants with a capacity of 25 megawatts or greater (16).

### *Western Climate Initiative*

The Western Climate Initiative (WCI) includes Arizona, California, Montana, Oregon, Utah, and Washington in the U.S. and British Columbia, Manitoba, Ontario, and Quebec in Canada. The WCI was originally formed in 2007 when Governors from five of the states (Arizona, California, New Mexico, Oregon, and Washington) signed an

agreement directing their states to develop a target from greenhouse gas emissions reductions (17). Since then the other states and Canadian provinces have joined the initiative. The main goal of the WCI strategy is to implement a regional cap-and-trade program by 2015. Elements that the WCI hopes to include in its cap-and-trade program include limiting emissions from major sources of global warming, include electricity related emissions under the cap from electricity that is imported from outside WCI partner jurisdictions, ensure all regulated entities use a consistent reporting methodology, and mitigate economic impacts on consumers and regulated entities (17). The Design for the WCI Regional Program was released in 2010. This document serves as a guide to WCI partners as they implement the cap-and-trade program. The first phase of the cap-and-trade program will begin in January, 2012 with a three year compliance period. In 2015 the program will expand to cover transportation fuels and other fuels not covered in phase I (17).

#### *Midwestern Greenhouse Gas Reduction Accord*

The Midwestern Greenhouse Gas Reduction Accord includes the states of Illinois, Iowa, Kansas, Michigan, Minnesota, and Wisconsin as well as the Canadian province Manitoba. The main focus of the accord is the design of a cap-and-trade style system to reduce greenhouse gas emissions in the Midwest (18). Draft recommendations for the cap-and-trade program were released in January, 2009 (18). These include a reduction of greenhouse gas emissions to 80 percent below 2005 levels by 2050 (18).

#### *Energy Security and Climate Stewardship Platform for the Midwest*

The Energy Security and Climate Stewardship Platform was released in 2007 at a meeting of twelve Midwestern governors and the Premier of Manitoba in Wisconsin. The

main goals of the platform are to increase energy efficiency, advance low carbon transportation fuels, increase the amount of electricity produced from renewable sources, implement a regional regulatory framework for carbon capture and storage (CCS), and encourage the creation of infrastructure to accommodate CCS (19).

### *Individual State Actions*

Many states have created specific climate action plans with goals to reduce greenhouse gas emissions. These climate action plans are focused on ways that states can reduce emissions through tax incentives, efficiency improvements, and development of low-carbon energy sources. Some states have also implemented state greenhouse gas emission reduction targets. Table 2 lists the states with greenhouse gas emissions targets (20). These state rules may affect the ability of utilities to sell electricity generated from coal between states. One example is an ongoing lawsuit between the states of North Dakota and Minnesota over a Minnesota law passed in 2007. The Minnesota law put restrictions on coal fired electricity generated in North Dakota and sold in Minnesota. North Dakota is arguing that this law is unconstitutional because it regulates trade between states, something that only Congress is authorized to do (21).

### *Greenhouse Gas Regulations in Other Countries*

#### *Australia*

In 2007 Australia ratified the Kyoto Protocol and agreed to limit CO<sub>2</sub> emissions to 108 percent of 1990 levels during 2008-2012 (22). In addition to this, Australia has committed to reducing GHG emissions to 5 percent below 2000 levels by 2020 with possible additional reductions of 15 percent and 25 percent below 2000 levels by 2020 depending on the extent of international actions (22). Since 2008 Australia has been

Table 2. States with greenhouse gas emissions targets (20).

State	GHG Emissions Target
Arizona	2000 levels by 2020
California	1990 levels by 2020
Colorado	20% below 2005 levels by 2020
Connecticut	10% below 1990 levels by 2020
Florida	1990 levels by 2025
Hawaii	1990 levels by 2020
Illinois	1990 levels by 2020
Maine	10% below 1990 levels by 2020
Maryland	25% below 2006 levels by 2020
Massachusetts	10% below 1990 levels by 2020
Michigan	20% below 2005 levels by 2025
Minnesota	15% below 2005 levels by 2015
Montana	1990 levels by 2020
New Hampshire	10% below 1990 levels by 2020
New Jersey	1990 levels by 2020
New Mexico	10% below 2000 levels by 2020
Oregon	10% below 1990 levels by 2020
Rhode Island	10% below 1990 levels by 2020
Utah	2005 levels by 2020
Vermont	25% below 1990 levels by 2012
Virginia	30% below BAU by 2025
Washington	Reduction to 1990 levels by 2020

working towards the establishment of the Carbon Pollution Reduction Scheme (CPRS)

which is a cap-and-trade emissions trading scheme for greenhouse gas emissions (23).

The scheme was rejected twice by parliament. In July 2011 the Australian Government

released its Clean Energy Plan which contains a carbon pricing mechanism and a Clean

Energy Legislative Package was passed by the Senate in November 2011 (24). The

carbon pricing mechanism contained in this package is being implemented and will start

in July 2012.

### *Canada*

Canada has a national target of reducing their total GHG emissions to 17 percent below 2005 levels by 2020. To achieve this goal Canada is working towards the regulation of greenhouse gas emissions for both the transportation and electricity generation sectors. Regulations for the electricity sector have been proposed and are currently being reviewed for comments with final regulations expected in 2012 (25). Several Canadian provinces are also members of regional initiatives with U.S. states as previously mentioned.

### *China*

China has committed to voluntary actions to reduce the intensity of its carbon dioxide emissions per unit of GDP. Their goal is to cut emissions by 40 to 45 percent per unit of GDP by 2020 when compared to 2005 levels (26). However, due to the rapid economic growth in China, some analysts predict that these goals will result in CO<sub>2</sub> emissions being approximately the same as they are now (26).

### *European Union*

Member states in the European Union have adopted binding GHG emissions and renewable energy targets as well as a commitment to carbon capture and storage development. By 2020 all EU member states have committed to reducing GHG emissions to 20 percent below 1990 levels as well as using 20 percent renewable energy sources (27). In addition to this, the EU has committed to investing in construction of up to 12 full scale power plants with carbon capture and storage technology integrated into the plants (27).

In order to meet emissions targets and spur innovation in renewable energy the EU created the mandatory Emissions Trading Scheme (ETS) in 2005. The ETS is currently in phase II of a multiphase program and it covers CO<sub>2</sub> emissions from power plants and five major industrial sectors (27).

### *Japan*

In a 2009 speech to the United Nations, Prime Minister Yukio Hatoyama of Japan announced his country's goal to reduce its GHG emissions to 25 percent below 1990 levels by 2020 (28). In his speech the Prime Minister includes a domestic emissions trading scheme, carbon taxes, and feed in tariffs for renewable energy as ways to meet these goals (28). Japan has also committed to assisting developing countries, especially in East Asia, to establish low-carbon economic growth models (29). In addition to these goals, Japan is cooperating with other countries on CO<sub>2</sub> mitigation and technology developments (29).

### Existing Market for CO<sub>2</sub> Capture: Existing Power Plant Fleet

Widespread deployment of CO<sub>2</sub> capture will require more than one capture technology because of the variety of fossil fuel power plants. Older and smaller plants are less efficient and more difficult to retrofit with new technologies, which make them better candidates for retirement as opposed to retrofitting them with a CO<sub>2</sub> capture technology if CO<sub>2</sub> regulations are implemented. The power generated from these plants may be replaced with new, more efficient plants or with renewable power generation, such as solar or wind power. Larger and newer plants are good candidates for the addition of postcombustion capture technologies. If CO<sub>2</sub> capture was implemented today, amine-based (advanced solvents) capture systems would be the primary technology installed due

to the matureness of the technology. Because amine-based (advanced solvents) capture has been used for many years in the gas-treating industry, the core of the technology has much less risk than more novel approaches currently being developed at small scale. Although there are still many challenges not yet proven with amine-based capture at this large of a scale, it is still years ahead of the other technologies under development. Ultimately, which postcombustion technology is chosen will depend on many variables, such as the fuel type and the existing air pollution control equipment currently in place at the plant.

In addition to these considerations, the number of fossil fuel power plants needs to be taken into consideration. In the United States, 71% of the electricity comes from fossil fuel power plants, with approximately 37% of the U.S. total (natural and anthropogenic) CO<sub>2</sub> emissions coming from coal-fired power plants, or 82% of all CO<sub>2</sub> emissions produced from the generation of electricity, as shown in Figure 7 (30, 31). However, coal also produces over 49% of total electricity generation of the United States. Figure 8 shows a breakdown of the fuel sources used in the United States to produce electricity. If CO<sub>2</sub> regulations are implemented, a large number of these plants will initiate projects to capture CO<sub>2</sub> from their flue gas or syngas streams. Currently in the United States, approximately 5172 plants burn a fuel source to produce energy either for a process or to produce electricity. These include small boilers to large coal- and gas-fired power plants. The feasibility of implementing one technology for all of these plants needs to be taken into consideration.



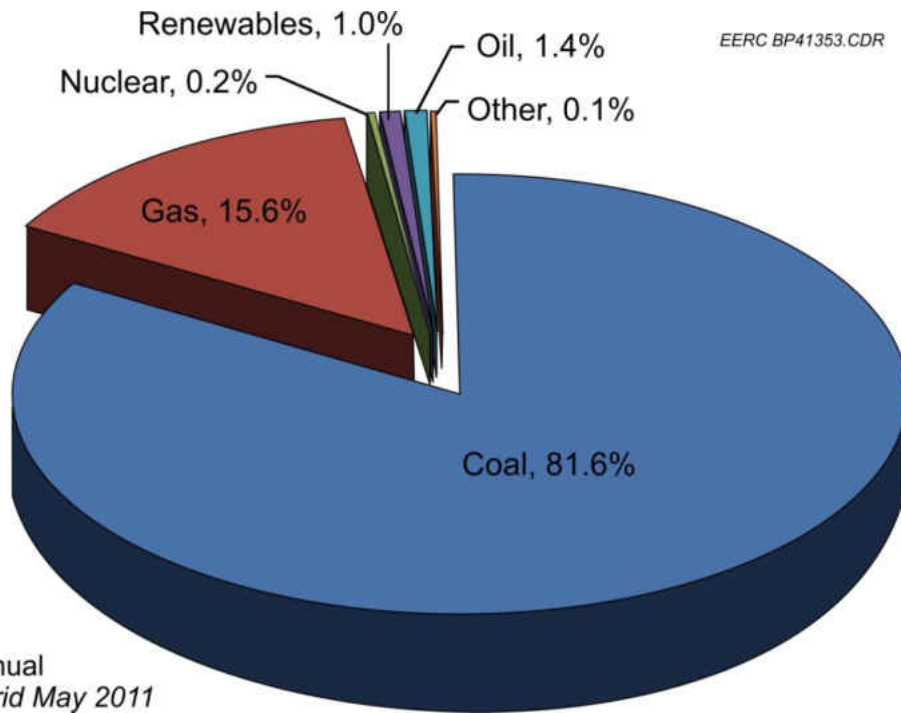


Figure 7. Breakdown of CO<sub>2</sub> emissions produced from energy generating systems in the United States.

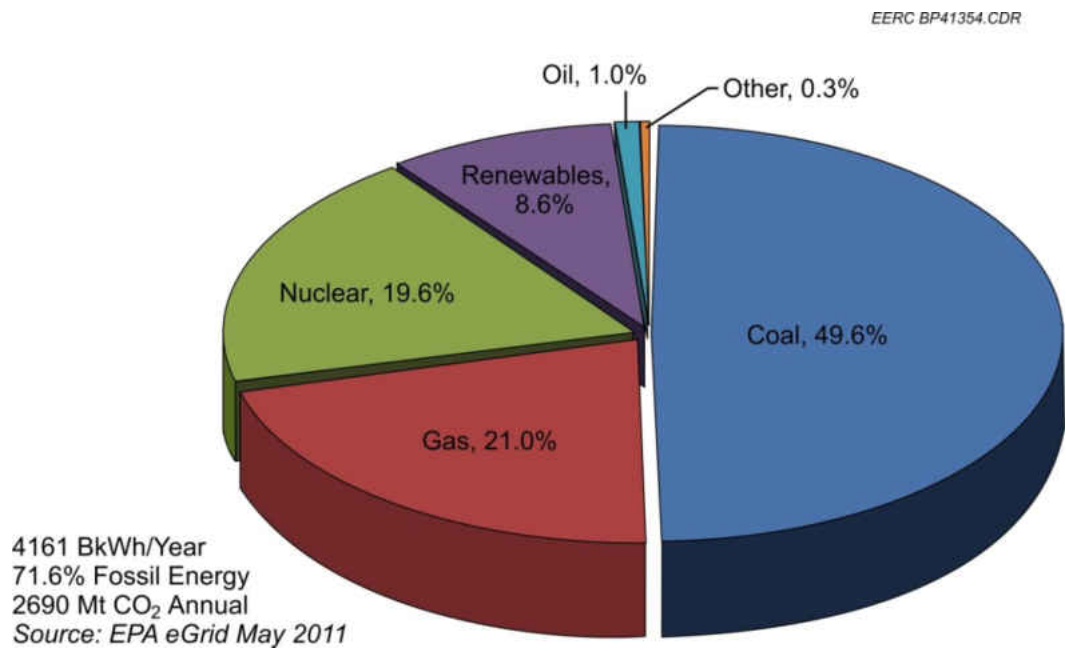


Figure 8. Amount of energy produced by fuel type in the United States.

It is unrealistic to expect that small boilers will be able to invest in the capital necessary to capture relatively small amounts of CO<sub>2</sub> emissions. In order to gain a better understanding of how much CO<sub>2</sub> could be captured, a basis needs to be chosen. Many studies claim that plants smaller than 250 MW and older than 1980 will not be viable candidates for capture. This may be true, however, in most cases, they will not be grandfathered but rather forced to retire and be replaced with something else. Therefore, these emission sources should not be ignored as the replacement plant in most cases will emit a similar amount of CO<sub>2</sub> (the new plant will be higher in efficiency initially, but the current 25%–30% energy penalty associated with CO<sub>2</sub> capture will bring the efficiencies closer together to today's operation without capture). Taking this into consideration, one could assume that emission sources generating 1 Mt (million tons) of CO<sub>2</sub> annually today would be large enough to support the infrastructure needed. In reality, some plant owners may choose to shut these plants down and build new ones, but these plants will still need to capture the same amount of CO<sub>2</sub>. When considering the current plants that emit greater than 1 Mt of CO<sub>2</sub>, a list of 497 plants is produced, which emit a total of 2401 Mt of CO<sub>2</sub> annually. Figure 9 shows the size of these units in nameplate capacity versus their 2007 CO<sub>2</sub> emissions.

It would be difficult for all of these plants to install an amine-based capture system in a short period of time. An estimate of the amount of amine needed for postcombustion capture in the United States can better illustrate why different CO<sub>2</sub> capture technologies will be needed in order for utilities and others to comply with

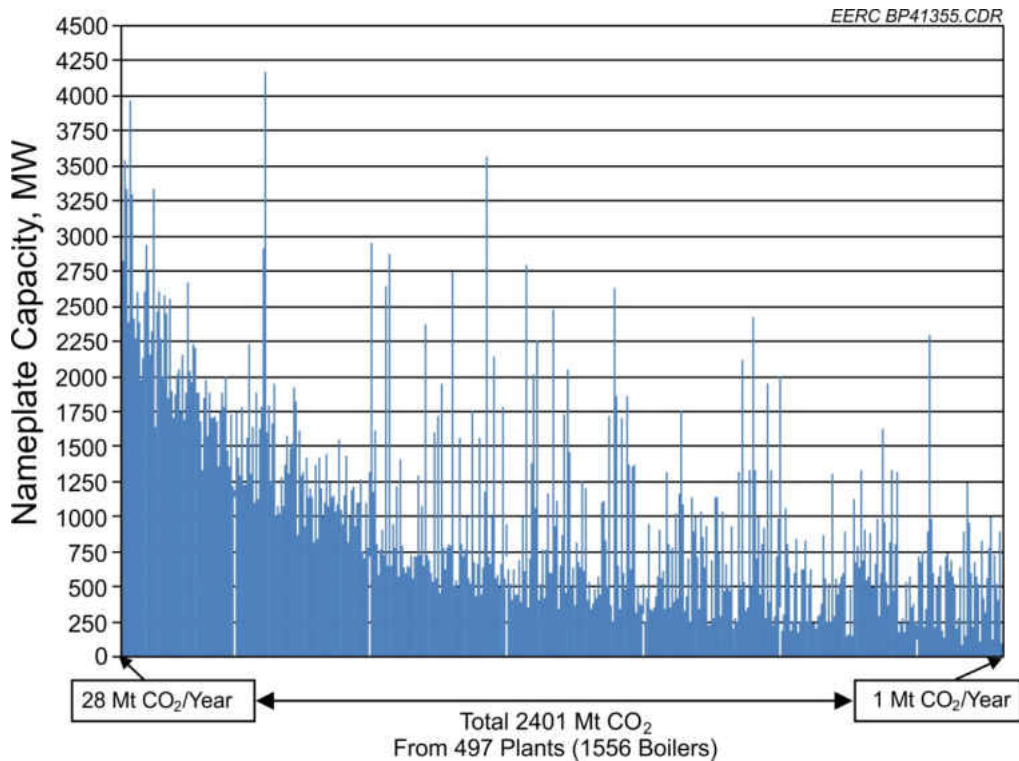


Figure 9. CO<sub>2</sub> emissions from plants emitting more than 1 Mt of CO<sub>2</sub> annually.

possible CO<sub>2</sub> regulations. The amount of MEA needed to resupply a postcombustion capture plant annually is anywhere from 0.5 to 3.1 kg of MEA per metric ton of CO<sub>2</sub> captured (32). The International Energy Agency (IEA) used a figure of 1.6 kg MEA per metric ton of CO<sub>2</sub> captured in its life cycle analysis study, which is right in the middle of the 0.5 to 3.1 kg MEA per metric ton of CO<sub>2</sub> range (33). If all of the 497 plants employed postcombustion capture using MEA, at a 90% capture rate, 2161 Mt of CO<sub>2</sub> could be captured.

Assuming a MEA replacement rate of 1.6 kg MEA per metric ton of CO<sub>2</sub> captured, the total amount of MEA needed would be approximately 3.5 million metric tons of MEA a year. In 2004, the worldwide production capacity of all ethanolamines,

including MEA, diethanolamine (DEA), and triethylamine (TEA), was approximately 1.507 million metric tons per year (34). The consumption of ethanolamines in the United States in 2004 was 450,000 tons. This illustrates that in order to supply enough MEA to meet the demand for postcombustion-based capture using MEA, production of amines will need to be greatly increased. MEA will probably not be the solvent of choice for postcombustion capture due to the fact that advanced solvents, which have greater efficiency and lower degradation rates, are now being developed. However, many of these advanced solvents are made with MEA or other amines as a base, so a large increase in amine production will still be needed if these advanced solvents are employed.

As the above discussion illustrates, more than one CO<sub>2</sub> capture technology will need to be deployed (whether it is several advanced solvents, or a combination of solvents, sorbents, and membranes) if CO<sub>2</sub> capture and sequestration are going to become widespread in the power industry in the near future. It is important to understand as many of the issues surrounding a technology as possible to ensure that the appropriate technology is deployed for each plant type. This thesis addresses issues from environmental concerns to performance and energy efficiency of several advanced solvents.

#### CO<sub>2</sub> Capture Review Summarized

As concerns are raised about the effects of GHG (primarily CO<sub>2</sub>) emission, industries around the world are investigating ways to decrease their carbon footprint. These methods include improving process efficiencies so that less carbon-based fuel is used, switching to fuels with lower fossil carbon content (e.g., biomass or biomass

blends, augmentation by wind or solar power), and capture of the CO<sub>2</sub> produced for either beneficial reuse or for permanent storage. Because CO<sub>2</sub> capture is currently an expensive process, considerable effort is being focused on the development of more efficient, cost-effective capture techniques.

There are three opportunities to capture CO<sub>2</sub> from a fossil fuel combustion system: before, during (through combustion modification), and after combustion. This review is as comprehensive as possible but, because of the proprietary and dynamic nature of technology development, it is not realistic to assume that every CO<sub>2</sub> capture technology currently under development has been included. The following overview summarizes many of the technologies (35).

#### *Precombustion*

Precombustion removal refers to near-complete capture of the CO<sub>2</sub> prior to fuel combustion and is usually implemented in conjunction with gasification (of coal, coke, waste, or residual oil) or steam reforming/partial oxidation of natural gas to produce syngas, which contains CO and H<sub>2</sub>. Subsequent conversion via the water–gas shift (WGS) reaction produces CO<sub>2</sub> from the CO, resulting in H<sub>2</sub>-rich syngas. This syngas (often with N<sub>2</sub> added for temperature control) can be combusted in gas turbines, boilers, or furnaces. Typical CO<sub>2</sub> stream concentrations before capture are 25 to 40 vol% at pressures of about 360 to 725 psia. The high partial pressure of CO<sub>2</sub>, relative to that of combustion flue gas, enables separation through physical solvent scrubbing. A physical solvent utilizes the pressure-dependent solubility of CO<sub>2</sub> in the solvent (as opposed to a chemical reaction with the solvent) to separate the CO<sub>2</sub> from the mixed-gas stream. Commercially available physical solvents that have been applied to precombustion CO<sub>2</sub>

capture include UOP's Selexol™ process, the Rectisol® process (developed independently by Linde and Lurgi), and Lurgi's Purisol® process. In these processes, the gas flows through a packed tower where it contacts the physical solvent and acid gases such as CO<sub>2</sub> and H<sub>2</sub>S dissolve into the solvent. The acid gas-rich solvent flows to a second tower where the CO<sub>2</sub> is released and the solvent is regenerated, usually by reducing the pressure.

Significant additional research efforts are being made in the area of membrane separations for precombustion gas separation. The most common approach is the use of a membrane that is permeable to hydrogen.

#### *During Combustion*

With process modifications, CO<sub>2</sub> can be captured during combustion in a process called oxygen combustion, or oxycombustion. Substitution of oxygen for the combustion air produces a CO<sub>2</sub>-rich flue gas that requires minimum separation before use or permanent storage. Conventional air combustion processes in boilers or gas turbines produce flue gas that contains predominantly N<sub>2</sub> (>80 vol%) and excess O<sub>2</sub> in addition to CO<sub>2</sub> and water; CO<sub>2</sub> must be separated from these other components. If the air is replaced by oxygen, the nitrogen content of the flue gas approaches zero (assuming minimal air leakage into the system), and the flue gas contains predominantly CO<sub>2</sub> along with small amounts of excess oxygen and water produced during the combustion process. The CO<sub>2</sub> can be recovered by compressing, cooling, and dehydrating the gas stream. The concentration of CO<sub>2</sub> can be targeted to a specific intended end-use application such as fuel production or permanent storage. When the end use requires it, noncondensable contaminants such as N<sub>2</sub>, NO<sub>x</sub>, O<sub>2</sub>, and Ar can be removed by flashing in a gas-liquid

separator. Oxygen combustion can take place in a typical combustor (albeit one retrofitted to accommodate the higher temperatures that occur during combustion in an oxygen-rich environment) or in circulating fluidized- or moving-bed boilers, which are under development by Alstom, ABB, Praxair, and Parsons Energy. These units are being tested at the large pilot scale.

Relative to coal gasification, combustion requires up to three times the amount of oxygen because all of the carbon is converted to CO<sub>2</sub>. The air separation unit (ASU) capacity (and parasitic power load) likewise will be commensurately larger. Separation of oxygen from air is expensive and is currently performed at very large scale by cryogenic distillation. Other methods of separating oxygen for use during oxycombustion are being developed, most notably oxygen or ion transport membranes. These membranes operate at temperatures of roughly 500°C, meaning that oxygen separation can be integrated with the combustion process, providing a theoretically significant reduction in parasitic power loss and O<sub>2</sub> production cost. Oxygen transport membranes are under development by Praxair and Alstom Power, while ion transport membranes are being developed by Air Products and Chemicals.

Other processes that feature combustion in oxygen include:

- Advanced Zero Emission Power (AZEP) process. This process, being developed by Alstom Power, replaces the combustion chamber of an ordinary gas turbine with a mixed conducting membrane (MCM) reactor that includes a combustor, a low-temperature heat exchanger, an MCM, and a high-temperature heat exchanger. The MCM reactor separates O<sub>2</sub> from the air for combustion with a fuel (natural gas).

- ThermoEnergy Integrated Power System (TIPS). This process, under development by ThermoEnergy Corporation, utilizes high-pressure combustion (700 to 1300 psi) and facilitates the condensation of exhaust components such as water and CO<sub>2</sub> in a condensing heat exchanger.
- Chemical looping. In chemical looping, there is no direct contact between air and fuel. The process utilizes oxygen provided by metal oxide oxygen carriers to combust the fuel, producing CO<sub>2</sub> and water. Once the steam is condensed, a relatively pure stream of CO<sub>2</sub> is produced, ready for beneficial reuse or permanent storage. Chemical looping development work is being performed by many groups and includes application to combustion of coal, petroleum coke, natural gas, and syngas as well as use in syngas and hydrogen production and incorporation into integrated gasification combined cycles (IGCC). Alstom has run a successful pilot-scale, 10-lb/hr chemical looping coal combustion system and is currently involved in scaling this to 1000 lb/hr.

#### *Postcombustion*

The most common CO<sub>2</sub> separation platform is postcombustion, where the CO<sub>2</sub> is removed from low-pressure, low-CO<sub>2</sub>-concentration flue gas following the pollution control devices. Several types of postcombustion processes have been and are being developed to separate and remove the CO<sub>2</sub> from a flue gas stream. These include absorption, adsorption, membrane, and cryogenic processes and “other” methods that include mineralization for either disposal or to produce a mineral product.



## *Absorption*

Absorption systems that are used to capture CO<sub>2</sub> after combustion typically rely on chemical reaction between the CO<sub>2</sub> and a solvent to convert the CO<sub>2</sub> into another species. In these cases, flue gas containing CO<sub>2</sub> is contacted with a solvent that reacts with the CO<sub>2</sub>. The CO<sub>2</sub>-rich solvent is regenerated by heating, which reverses the reaction and releases the CO<sub>2</sub>. The CO<sub>2</sub>-lean solvent is then recirculated for reuse. Amines are the most commonly used chemical absorbent for CO<sub>2</sub> separation from mixed-gas streams. The “baseline” amine is MEA. Commercial providers of MEA technology include CB&I/Lummus Technology/Randall Gas Technologies, Inc., and Daniel Fluor (the Econamine FG and Econamine FG Plus™ processes). Mitsubishi Heavy Industries (MHI) offers a commercial process that utilizes sterically hindered amines (KS-1) tailored to enhance their reactivity with CO<sub>2</sub>. The commercially available Catacarb® and Benfield™ processes (developed by Eickmeyer & Associates and UOP, respectively) feature activated hot potassium carbonate as the solvent.

Other chemical absorption systems are being developed to improve the cost-effectiveness of CO<sub>2</sub> capture through higher CO<sub>2</sub> absorption capacities, faster CO<sub>2</sub> absorption rates, reduced solvent degradation, reduced solvent corrosiveness, and lower regeneration energy requirements. Development efforts for these technologies range from bench to pilot scale. The technologies under development include:

- ECO<sub>2</sub>™ process, developed by DOE’s National Energy Technology Laboratory (NETL) and Powerspan, originally began with an electrocatalytic oxidation (ECO) barrier discharge reactor that oxidized flue gas pollutants. The flue gas and oxidized pollutants entered a wet scrubber in which the

oxidized pollutants reacted with ammonia. Powerspan recently discontinued the use of ammonia in the ECO<sub>2</sub> Process and separated it from the ECO process that was used to remove NO<sub>x</sub> and SO<sub>x</sub> from the flue gas. The solvent replacing the ammonia is proprietary; most likely this solvent is an amine but information confirming this supposition has not been made available publicly.

- The chilled ammonia process was developed by Nexant and Alstom. The flue gas is cooled and contacts ammonium carbonate. The CO<sub>2</sub> reacts with the ammonium carbonate to form ammonium bicarbonate. During solvent regeneration, the CO<sub>2</sub> is driven off, converting the ammonium bicarbonate back to ammonium carbonate.
- Advanced amine process (AAP) using UCARSOL™ amines is being developed by Alstom and the Dow Chemical Company. Dow had developed proprietary amines for use in process equipment developed by Alstom.
- Cansolv CO<sub>2</sub> capture process. This process is under development by Cansolv Technologies Inc. and features a staged, multipollutant scrubbing scheme in which SO<sub>2</sub> is removed, followed by CO<sub>2</sub>, then NO<sub>x</sub>, and finally mercury. A proprietary amine/amine mixture is used for the CO<sub>2</sub> removal step.
- Potassium carbonate/piperazine complex process, developed at the University of Texas at Austin, uses potassium carbonate promoted with piperazine, a cyclic diamine. The addition of piperazine speeds the rate of the CO<sub>2</sub>-potassium carbonate reaction.
- HTC Pureenergy uses proprietary amines and/or amine mixtures developed at the University of Regina, Canada, that are said to provide lower energy costs

and longer absorption solution lifetimes than are offered by MEA. The company also indicates that it makes use of preengineered, modularly constructed absorber–stripper systems.

- CORAL solvent family. The CORAL family of absorption solvents, which is under development by TNO, is based on amino acid salts.
- Vortex contactor for amine scrubbing, developed by Idaho National Engineering and Environmental Laboratory, achieves higher CO<sub>2</sub> transfer rates to the liquid absorbent by increasing turbulent mixing between CO<sub>2</sub> and the absorbent.
- Sargas carbonate process, developed by Sargas AS, is a pressurized combustion, combined-cycle power generation system with CO<sub>2</sub> capture. A modified Benfield CO<sub>2</sub> process is used to capture the CO<sub>2</sub>.
- Several organizations are continuing to work on the use of the enzyme carbonic anhydrase. The idea is to use the enzyme as a catalyst in association with amine and/or carbonate solutions in order to increase the rate of absorption and/or stripping or to enhance CO<sub>2</sub> transport across membranes. The organizations currently involved in these efforts include Akermin, Carbozyme Inc., and CO<sub>2</sub> Solution Inc. with Codexis Inc.
- Another group is working on development of synthetic catalysts designed to provide the carbonic anhydrase active site in a smaller molecule. The current work involves a partnership between United Technologies Research Center, Lawrence Livermore National Laboratory, the University of Illinois, and Babcock & Wilcox.

- Integrated vacuum carbonate absorption process (IVCAP) employs a potassium carbonate solution to capture the CO<sub>2</sub>. While the absorption takes place at atmospheric pressure, the stripper is operated at a vacuum. This process is being developed by the Illinois State Geological Survey and the University of Illinois at Urbana–Champaign.
- The Siemens postcombustion capture process is based on the reaction of CO<sub>2</sub> with amino acid salt solutions. The process was developed by Siemens and E.ON and uses conventional absorber–stripper technology.
- NeuStream™–C. Neumann Systems Group, Inc., has developed a unique horizontal-flow absorber that promises very high mass-transfer rates while reducing the overall footprint and energy consumption. The system was originally developed for SO<sub>2</sub> control for coal-fired boilers and is called NeuStream™–S. Information about the specific solvent(s) that will be used in the NeuStream™–C process for CO<sub>2</sub> capture is not publicly available.

### *Adsorption*

Adsorption CO<sub>2</sub> capture technologies remove CO<sub>2</sub> from mixed-gas streams onto the surface of solid sorbents. These sorbents generally have very high porosity; therefore, high surface areas are available per unit mass and per unit volume. As is the case with absorption, adsorption can be a simple phase-partitioning physical adsorption or it can involve a chemical reaction between the sorbent and the CO<sub>2</sub>. Some solid sorbents contain trapped or strongly attached liquid phases. In these situations, the CO<sub>2</sub> actually absorbs into the liquid phase so the capacity is not dependent on surface area but rather on the amount of liquid absorbent trapped on or in the solid support.

Solid sorbents can be applied in pressure- and temperature-swing beds where the flue gas is transported through fixed beds of sorbent material until the sorption capacity is exhausted. The flue gas is then routed to a different sorbent bed while the exhausted one is regenerated either by heating (temperature swing) or by reducing the pressure (pressure swing). This works well for smaller systems but is felt to be prohibitive for application at power plant scale.

Some research groups have been working on electrical-swing adsorption processes. In addition, much development work is being done in the area of moving-bed and fluidized-bed solid sorbent contact systems and the solid sorbents that can be applied in them. In these systems, the solid is transported into the vessel in which carbon capture takes place and moved to the regeneration vessel. A significant issue with respect to sorbent that has to be managed in order for the material to be acceptable for use in these systems is physical attrition/breakdown of the solid.

Some examples of solid adsorbent CO<sub>2</sub> capture technologies include:

- Carbonaceous materials and zeolite. Pressure swing absorption/desorption processes are typically used to remove the CO<sub>2</sub> from these typically used sorbents.
- The electrical-swing adsorption process is being developed by Oak Ridge National Laboratory and the University of Porto, Portugal. In this process, a carbon fiber composite molecular sieve serves as the solid sorbent. A low-voltage current is used to remove the adsorbed CO<sub>2</sub>.
- In the sorption-enhanced WGS process, CO<sub>2</sub>-selective hydrotalcite adsorbent is combined with WGS catalyst. The process would be applied to syngas

production during natural gas reforming. The technology developers are Air Products and Chemicals, BP, and the Energy Research Centre of the Netherlands.

- C-Quest chemical sorbent system makes use of widely available sorbent ingredients that, when reacted with CO<sub>2</sub>, form recyclable solids that can be safely disposed of. The system is being developed by C-Quest Technologies.
- Magnesium oxide regenerable adsorption, developed by the Illinois Institute of Technology and Gas Technology Institute, uses a magnesium-based sorbent to remove CO<sub>2</sub> from flue gas at the temperatures and pressures typically encountered in IGCC systems.
- Hyperbranched aluminosilica (HAS) is a laboratory-scale technology in which the sorbent consists of amine polymer groups on a silica substrate. HAS material is reusable, works in the presence of moisture, and has the potential to adsorb up to 5 times as much as other reusable materials. It is being developed by the Georgia Institute of Technology.
- RTI's dry sorbent-based capture process begins with combustion in a circulating moving-bed boiler that is temperature-controlled to 1090°C. The CO<sub>2</sub> is captured by reaction with lime to form calcium carbonate. The calcium carbonate is regenerated in a calciner, which releases the CO<sub>2</sub>. A nearly pure CO<sub>2</sub> stream is produced after the water is removed. Other candidate sorbents include sodium bicarbonate, trona, and potassium carbonate. RTI International and NETL are the developers of this technology.

- CSMG recyclable CO<sub>2</sub> adsorbent is based on surface-modified nanoporous silicas. The materials can be reused repeatedly and can capture CO<sub>2</sub> in both wet and dry environments. Carbon Capture Technologies Inc., a branch of CSMG Technologies, holds a worldwide exclusive license to the method and the sorbent composition.
- TDA dry solid sorbent captures CO<sub>2</sub> at intermediate temperatures and near-ambient pressure using an alkalized alumina sorbent. The sorbent is regenerated using steam. The technology is being developed by TDA Technologies, Babcock & Wilcox, Louisiana State University, and Western Research Institute.
- SRI novel carbon sorbent is being developed by SRI International. It is a novel carbon-based sorbent that requires moderate temperatures of 80° to 100°C for regeneration.

#### *Mixed Absorption/Adsorption*

Mixed adsorption/absorption processes are those that employ a liquid absorbent (typically a chemical absorbent) trapped in or on the solid support. These are often classified with adsorption processes because they employ similar gas–solid contact arrangements (fixed-bed, fluid-bed, or moving-bed reactors), but the actual capture process occurs in a liquid layer or liquid droplet contained on or in the support. Most commonly, the chemical sorbent is an amine, although ionic liquids are likely candidates for this type of use. Examples of mixed absorption/adsorption processes include:

- Metal organic frameworks (MOFs) are large molecules with engineered macromolecular cavities that can adsorb CO<sub>2</sub>. These nanoporous materials

consist of metal or metal oxides interconnected by rigid organic molecules. Functional groups such as tertiary amines can be added to enhance chemisorption of the CO<sub>2</sub>. The CO<sub>2</sub> is removed from the MOFs using a vacuum pressure-swing technique. Developers of MOFs are UOP, the University of California at Los Angeles, the University of Michigan, Northwestern University, Vanderbilt University, the University of Edinburgh, and many others.

- Metal monolithic amine-grafted zeolites sorbent features the novel integration of a metal monolith with amine-grafted zeolites. It is under development by University of Akron and NETL.
- Novel amine-enriched solid sorbents consist of a carbon material with amine compounds fixed upon it. The CO<sub>2</sub> reacts at the amine sites. Temperature swing is used to regenerate the sorbent.

### *Membrane Processes*

Membranes employ a permeable barrier between two fluid-phase zones. This permeable barrier provides selective transport of CO<sub>2</sub> or another gas component. The selective behavior of membranes derives from differences in permeability between different gas stream components. Permeability is the product of solubility and diffusivity. Selectivity depends on permeability driving force and membrane thickness. Desirable membranes have high selectivity and high permeability for the molecule to be transported. Membrane processes under development for CO<sub>2</sub> capture include:

- CO<sub>2</sub>-selective ceramic membrane for WGS. This technology employs a tubular ceramic membrane that is permeable only to CO<sub>2</sub> inside a WGS



reactor and would apply to separation of CO<sub>2</sub> from syngas produced from coal gasification. Developers of the technology are Membrane Technology and Process Technology, the University of Southern California, and NETL.

- MTR postcombustion CO<sub>2</sub> membrane, developed by Membrane Technology Research, Inc. (MTR), is based on MTR's commercial Polaris™ membrane.
- Dense inorganic membrane for WGS reaction is a bench-scale technology that uses oxygen transport membrane technology to facilitate in situ partial oxidation reforming. The process produces nearly pure CO<sub>2</sub> at a high pressure. The technology developer is Eltron Research/SOFCO.
- Hydrogen membrane reformer is a precombustion capture technology. The core of the technology is a syngas reactor based on a hydrogen-selective membrane. The reactor combines steam reforming, WGS reaction, and H<sub>2</sub> separation. It is under development by StatoilHydro.
- Palladium membrane reactor. This system was developed by NETL and combines a palladium-based membrane with the WGS reaction to produce a high-pressure CO<sub>2</sub> stream.
- Thermally optimized polymer membrane. In collaboration with Los Alamos National Laboratory, Idaho National Energy and Engineering Laboratory is developing a high-temperature polymer membrane made of a polybenzimidazole selective layer coated on a porous stainless steel substrate.
- Inorganic nanoporous membrane. This process was developed by Oak Ridge National Laboratory to remove H<sub>2</sub> from syngas streams (leaving CO<sub>2</sub> as the primary remaining species).

- Molecular gate membrane. This membrane, developed by the Research Institute of Innovative Technology for the Earth (RITE) in Japan, consists of a cardo-polyimide membrane. It only allows CO<sub>2</sub> molecules to permeate the membrane, blocking N<sub>2</sub> and H<sub>2</sub> and producing a CO<sub>2</sub>-rich stream.
- Kvaerner hybrid membrane–liquid absorption system. This pilot-scale process is being developed by Kvaerner and MHI. A gas–liquid membrane contactor replaces a traditional absorber in this system. CO<sub>2</sub> in the flue gas diffuses through a microporous, hydrophobic solid membrane and into the liquid, which provides the selectivity rather than the membrane.
- High-temperature polymer hydrogen/CO<sub>2</sub> membranes. This laboratory-scale process applies only to gasification–based systems. The ceramic or polymer membrane selectively allows H<sub>2</sub> to permeate through it, leaving a concentrated stream of CO<sub>2</sub> in the retentate. The process can deliver CO<sub>2</sub> at high pressures. The technology is under development by Los Alamos National Laboratory.
- Polyvinylidene fluoride-based (PVDF) polymer process is being developed by RTI International. The PVDF polymer has a specific affinity for CO<sub>2</sub>.

## CHAPTER III

### ADVANCED SOLVENTS

As discussed previously, amine-based CO<sub>2</sub> capture is the most mature technology that is currently under development for capturing CO<sub>2</sub> from large point sources. Because this technology has been used for many years in the gas-processing industry, a lot is known about the production and implementation of amines. This thesis focuses on the use of advanced solvents, in particular advanced amines. Most of what is known today is based on the large scale use of a more conventional amine, MEA. The advanced solvents that are currently under development will behave very similar to MEA, but will differ in performance. This section discusses the use of amine solvents in a general sense. More discussion on advanced amines is discussed further down.

#### Production of Amines

The primary method for producing amines is known as the amination by ammonolysis process. This process is essentially the reaction of ammonia with ethylene oxide at elevated temperature and pressure. When doing this, three main products are formed: MEA, DEA, and TEA. The formation of MEA, DEA, or TEA depends on whether an ammonia molecule reacts with 1, 2, or 3 ethylene oxide molecules. Figure 10 shows a simple schematic of the amine production process. Several other by-products and waste streams are produced during this process and are shown in Table 3.

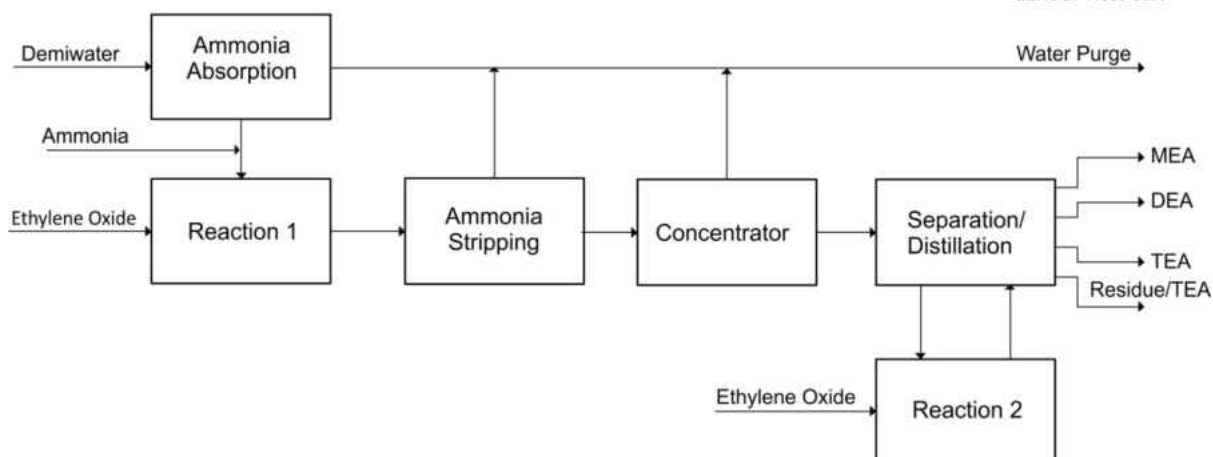


Figure 10. Simple schematic for the production of amines.

Table 3. Emission Discharge from the Manufacture of Ethanolamines by the Ammonolysis of Ethylene Oxide.

Emission	Source	Type of Discharge
Ethylene Oxide	Feedstock	Air, Water
Ammonia	Feedstock	Air, Water
Monoethanolamine	Product	Air, Water
Diethanolamine	Product	Air, Water
Triethanolamine	Product	Air, Water
Morpholine	Side reaction	Air, Water
Piperazine	Side reaction	Air, Water
Ethylene glycol	Side reaction	Air, Water
Diethalyne glycol	Side reaction	Air, Water
N-Hydroxyethyl-piperazine	Side reaction	Air, Water
N-Hydroxyethyl-morpholine	Side reaction	Air, Water
N-Ethylpiperazine	Side reaction	Air, Water
N-Ethylmorpholine	Side reaction	Air, Water
N-Ethylethanolamine	Side reaction	Air, Water
High-Molecular-Weight Condensation Products	Side reaction	Solid

In this process, ammonia and ethylene oxide are the two feedstocks that are required for the production of the amines. Ethylene oxide is produced from ethylene, which is produced commercially by the steam cracking of a wide range of hydrocarbon feedstocks (mainly naphtha, fuel oil, and condensates). Ammonia is produced basically from water, air, and energy. The energy source is usually hydrocarbons, thus providing hydrogen as well, but may also be coal or electricity. Steam reforming of light hydrocarbons (natural gas) is the most efficient route and consists of about 77% of the world's ammonia production. The production of these two feedstocks would also be in higher demand as amine production was scaled up to supply large point systems with enough amine to maintain efficient capture systems.

#### Implementation of Amine Scrubbing

Amine-based CO<sub>2</sub> absorption has been studied in the past and identified as one of the most suitable means for removing CO<sub>2</sub> from combustion-based power plants for the following reasons:

- The systems are effective for dilute CO<sub>2</sub> streams, such as are typically found in “Post-Combustion” facilities.
- The technology is proven and commercially available.
- The units are operated at standard temperatures and pressures similar to other pollution control devices currently employed at power plants.
- A current worldwide effort is being undertaken to improve amine systems because of their potential role for wide-scale CO<sub>2</sub> capture; therefore, future benefits from technology advances are anticipated.

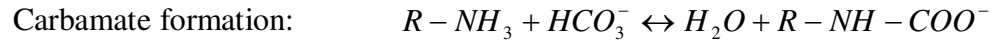
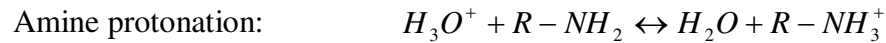
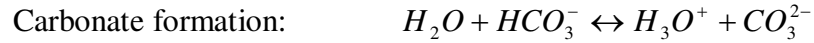
Amine-based absorption/stripping has been around for several decades as a commercial technology for CO<sub>2</sub> removal from natural gas and hydrogen. The amine process was first patented by R.R. Bottom in 1930 for acidic gas treatment. Throughout the years, the amine-based gas treatment process has remained relatively unchanged. The concept of removing or capturing CO<sub>2</sub> from flue gas streams started back in the 1970s as a possible economical source of CO<sub>2</sub>, mainly for enhanced oil recovery (EOR) operations. Today, about 80% of CO<sub>2</sub> production is used for EOR applications, most of which is obtained from natural CO<sub>2</sub> domes (36). CO<sub>2</sub> is also produced for several other industrial applications, including carbonation of brine, dry ice production, urea production, and in beverages.

Several commercial CO<sub>2</sub> plants were constructed in the late 1970s and early 1980s in the United States (37, 38). Although some of these plants are still in operation today, all of them are much smaller than a typical power plant in terms of tonnage of CO<sub>2</sub> handled or produced. Once the CO<sub>2</sub> is captured, it has to be securely stored (sequestered) to prevent it from entering the atmosphere unless an application is identified for the captured CO<sub>2</sub>.

#### Process Chemistry

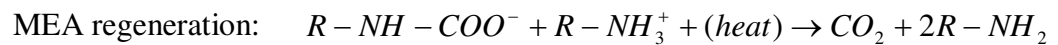
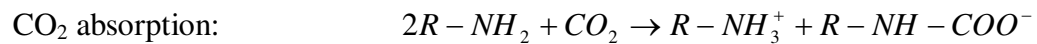
CO<sub>2</sub>, MEA, and water (H<sub>2</sub>O) are the three main compounds that are active in an amine scrubbing system. The following equilibrium reactions occur in the bulk of the liquid (39):





where MEA is represented by R-NH<sub>2</sub> and “R” stands for HO-CH<sub>2</sub>-CH<sub>2</sub>.

The process chemistry is complex, but the following are the main reactions taking place (40):



Pure MEA is an unhindered amine that forms a weakly bonded intermediate ion called carbamate, which is fairly stable. For every mole of amine, one-half mole of CO<sub>2</sub> is absorbed (for MEA), as shown in the above CO<sub>2</sub> absorption equation. Upon the application of heat, the carbamate dissociates to give back CO<sub>2</sub> and amine sorbent, as shown in the MEA regeneration equation above. Since the carbamate is fairly stable, it takes a substantial amount of energy to break the bonds and regenerate the sorbent. The theoretical minimum heat requirement to regenerate the MEA is about 1900 kJ/kg CO<sub>2</sub>. The actual heat requirement is greater than double this theoretical minimum.

Despite the use of inhibitors and dilution with water, a small quantity of MEA is lost through various unwanted reactions. Two main side reactions occur: the polymerization reaction that forms long-chained compounds and the oxidation reaction forming organic acids and liberating ammonia. Appropriate measures must be taken to avoid accumulation of the unwanted chemical species in the circulating sorbent. Flue gas impurities (acid gases) are another potential source of sorbent loss, especially for coal-

fired flue gases. Therefore, very low concentrations of these gases, on the order of 10 ppm, are desirable to avoid excessive loss of sorbent. The problem is especially acute for SO<sub>2</sub> because its concentration in flue gas is typically 700 to 2500 ppm at coal-fired plants. NO<sub>x</sub> is less of a problem because only NO<sub>2</sub> (which makes up only about 5% of the total NO<sub>x</sub>) reacts with most amines.

### Process Description

The amine scrubbing unit would be installed downstream of any existing pollution control device, such as those used for particulate, NO<sub>x</sub>, and SO<sub>x</sub> removal. It must be noted that in order for this system to operate with minimum solvent degradation, SO<sub>2</sub> control is a must. Although an SO<sub>2</sub> control device is necessary for amine scrubbing, upcoming regulations will probably require the installation of these devices prior to installing a CO<sub>2</sub> capture technology to meet SO<sub>2</sub> emission requirements. The maximum allowable amount of SO<sub>2</sub> that can be present in the flue gas is 10 ppmv, which may require several plants to upgrade their existing SO<sub>2</sub> control devices. A basic block flow diagram demonstrating the installation of an amine scrubbing system to an existing power plant can be seen in Figure 11.

The CO<sub>2</sub> capture plant, including the amine scrubbing unit, consists of four process modules: flue gas pretreatment, absorption, stripping, and CO<sub>2</sub> compression and drying. In the flue gas pretreatment section, the flue gas is cooled and conditioned before it enters the absorber; CO<sub>2</sub> is removed in the absorber by contacting the flue gas counter currently with an MEA solution. Once the CO<sub>2</sub> is absorbed in the MEA, the CO<sub>2</sub>-rich



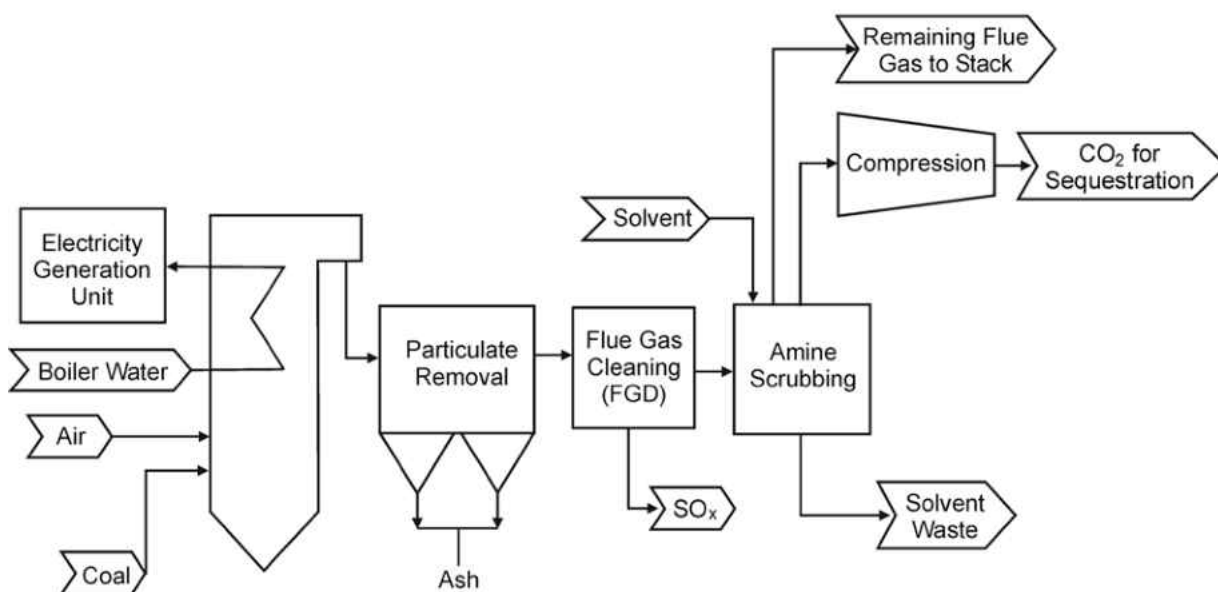


Figure 11. Simple block flow diagram of a coal-fired utility with an amine-based CO<sub>2</sub> capture system.

rich solvent is sent to the stripping section where the CO<sub>2</sub> is removed from the solvent by the addition of heat. The regenerated solvent is sent back to the absorber, while the purified CO<sub>2</sub> stream is sent to the compression and liquefaction unit. Here, the CO<sub>2</sub> is compressed and then dried in the final step, at which point it is ready to transport.

The amine-based CO<sub>2</sub> capture facility may need to consist of several trains to handle the large flow rates from the power plant.

#### *Flue Gas Pretreatment*

Flue gas from the desulfurization unit flows through a motor-driven fan in order to increase the pressure to 1.5 psig, enough to overcome the pressure drop through the direct cooler and absorber. The flue gases coming from the power plant can be very hot and may range from as low as 60°C (140°F) in the case of coal-fired plants with wet scrubbers to more than 550°C (1022°F) in the case of a natural gas-fired, simple-cycle

power plant. Typical coal-fired power plants without scrubbers have flue gas temperatures of 150°–200°C (300°–400°F). The amine system requires flue gas temperatures of about 45°–50°C (104°–122°F) in order to improve the absorption of CO<sub>2</sub> into the amine sorbent, to minimize the sorbent loss, and to avoid an excessive loss of moisture with the exhaust gases. The absorption process is exothermic and is, therefore, favored by low temperatures. In cases where coal-fired plants are equipped with a wet scrubber, an additional cooler may not be necessary as the scrubber helps in reducing the temperatures.

### *Absorber*

Cooled flue gas enters the bottom of the CO<sub>2</sub> absorber and flows upward counter currently to a stream of 30 wt% MEA solution (or other advanced solvent). The lean MEA enters the top of the column and heats up gradually as it absorbs more and more CO<sub>2</sub> and gains about –6°–21°C (20°–30°F) with 90%–95% capture. Typical CO<sub>2</sub> loading for lean MEA is 0.2–0.22 mol CO<sub>2</sub>/mol MEA. The CO<sub>2</sub>-rich MEA leaving the bottom of the column has a CO<sub>2</sub> loading of approximately 0.44 mol CO<sub>2</sub>/mol MEA. The CO<sub>2</sub> absorber can be a plate-type column or a packed tower that contains two beds of structured packing and a third bed, usually called the wash zone, at the top of the column. Most of the CO<sub>2</sub> absorbers are packed columns using some kind of polymer-based packing to provide a large interfacial area.

The CO<sub>2</sub>-rich solvent exits the bottom of the absorber column and flows through a rich/lean cross heat exchanger. The rich solvent must be heated in order to strip off the CO<sub>2</sub> and regenerate the solvent. The regenerated, or lean, solvent coming from the stripper must be cooled down before it can be circulated back to the absorber column.

Therefore, these two streams are passed through a cross heat exchanger where the rich sorbent is heated and the lean sorbent is cooled. This helps to recover some of the energy used to strip the CO<sub>2</sub> from the solvent, thus minimizing the stripper energy requirements.

In this process module, a sorbent-processing area is necessary. The regenerated sorbent needs to be further cooled to an acceptable level of about 40°C after passing through the rich/lean heat exchanger. To make up for solvent losses, a small quantity of fresh MEA must be added to the sorbent stream. The sorbent-processing area, therefore, essentially consists of a sorbent cooler, an MEA storage tank, and a mixer.

#### *Stripping (Regeneration)*

The stripping process module contains all of the equipment necessary for regenerating the sorbent and stripping the CO<sub>2</sub> and consists of a stripping column, reboiler and condenser, reflux drum, steam extractor, and MEA reclaimer. This portion of the process begins as the rich solvent enters near the top of the column. Once in the column, the weak intermediate compound that is formed between the MEA-based sorbent and the dissolved CO<sub>2</sub> (i.e., carbamate) is broken down by the addition of heat, separating the CO<sub>2</sub> from the sorbent. As the solvent flows downward, the hot vapors from the bottom reboiler strip the CO<sub>2</sub> from the solution. Stripping is completed in the reboiler with the addition of more heat. The main drawback of using MEA is that the stability of the carbamate ion requires more heat for the regeneration of the sorbent.

The hot vapors that exit the top of the stripper contain CO<sub>2</sub>, water, and solvent. The overhead vapors are cooled in a cold-water condenser where most of the water and solvent vapors condense, but the CO<sub>2</sub> does not. The condensed liquid and gaseous CO<sub>2</sub>

are separated in a reflux drum. The CO<sub>2</sub> stream continues on to the CO<sub>2</sub> purification system, while the liquid is returned to the top bed of the stripper.

In coal-fired power plant retrofit cases, a part of the low-pressure/intermediate-pressure steam has to be diverted for use in the reboiler for sorbent regeneration. This steam is obtained from the steam turbines by steam extractors.

Acid gases such as SO<sub>2</sub>, SO<sub>3</sub>, NO<sub>2</sub>, and HCl in the flue gas form compounds with the MEA solvent solution that cannot be removed by the addition of heat in the reboiler. These materials are referred to as heat-stable salts (HSSs). In order to avoid accumulation of HSS, a small slipstream of the lean solvent from the bottom of the stripper is fed to the MEA reclaimer. The MEA reclaimer is a heat exchanger that vaporizes the free MEA, leaving the high-boiling nonvolatile impurities. The reclaimer restores the MEA's usefulness by removing the impurities such as HSS, suspended solids, acids, and iron products from the solvent solution. Caustic is also added to the MEA reclaimer, freeing the MEA from its bonds with sulfur oxides because of its stronger basic attraction, minimizing MEA loss by allowing more MEA to be vaporized back into the circulating mixture. The reclaimer waste is sent for proper disposal.

#### *CO<sub>2</sub> Compression and Drying Unit*

The high-purity CO<sub>2</sub> stream from the stripper needs to be prepared for its final use. In order to easily handle the captured CO<sub>2</sub>, it must be compressed into liquid form. This is done by using a multistage compressor with interstage cooling. Most of the water is knocked out during compression and removed with intermediate suction drums. A CO<sub>2</sub> dryer is located after the last stage of compression to meet the water specifications for the CO<sub>2</sub> product. CO<sub>2</sub> is liquefied at about 194 psig and further pumped to the required

pressure. The compression unit yields a final CO<sub>2</sub> product at the specified pressure (typically 2200 psig) that contains acceptable levels of moisture and impurities.

### Amine Process Concerns

Although the amine-based absorption process is the most suitable technology currently available for postcombustion CO<sub>2</sub> capture from coal-fired power plant flue gases, several concerns exist: loss of sorbent, energy penalty, corrosion, space constraints, and environmental emissions. These problems are discussed in more detail below.

#### *Loss of Solvent*

Sorbent loss can occur throughout the process for a variety of reasons, including degradation, entrainment, vaporization, and mechanical losses (41, 42). Because of flue gas impurities, all of the sorbent that enters the stripper (regenerator) is not regenerated. Sorbent losses due to impurities have already been discussed in detail in previous sections. The MEA reclaimer is the current method used to minimize sorbent losses. Technologies such as electrodialysis are also being proposed for this purpose (43).

#### *Energy Penalty*

Separation processes in general are very energy-intensive, and amine scrubbing is no exception. Significant energy is required to regenerate the sorbent because of the stability of the carbamate ion and the large quantity of water from dilution of the amine. Substantial energy is also needed to compress the captured CO<sub>2</sub> to its final product and to meet the transportation requirements. If steam and electricity are extracted internally from a power plant, which is expected for retrofit cases, the large heat and electricity requirement will reduce the net efficiency by derating the plant. In cases of new power

plant construction, a bigger power plant will need to be built to produce the energy required by the CO<sub>2</sub> capture facility. If an existing power plant needed or wanted to maintain its power output, an auxiliary boiler and steam turbine would need to be added, thus raising the capital investment necessary for CO<sub>2</sub> capture.

### *Corrosion*

Corrosion in an amine-based CO<sub>2</sub> capture system can be a major problem. Most amines are reactive compounds. When in solution with water in the presence of oxygen and CO<sub>2</sub>, it creates a highly corrosive system. Irreversible side reactions with CO<sub>2</sub> and other flue gas components lead to the formation of various degradation by-products that are associated with increased corrosion in the system. Therefore, controlling corrosion is very important in an amine system where oxygen is present. Several things can be done to limit the rate of corrosion in the system, including reducing the concentrations of amine and by using appropriate materials of construction, corrosion inhibitors, and milder operating conditions (i.e., low temperatures and pressures) (44).

### *Environmental Impacts*

Environmental issues may arise from the use of MEA-based CO<sub>2</sub> capture systems, primarily from the spent sorbent slurry, or MEA reclaimer waste, and the emissions of MEA and ammonia carried by the treated flue gas. The amine reclaimer waste is considered to be a hazardous waste (5). This was further proven by a study performed by the U.S. Department of Energy National Energy Technology Laboratory, Pittsburgh, which identified chemical species (MEA, ammonia, 3-hydroxyethylamino-N-hydroxyethyl propanamide, 4-hydroxyethyl-2-piperizinone, 2-hydroxyethylamino-N-hydroxyethyl acetamide, and N-acetyletylethanolamine) in the reclaimer waste that are

considered to be hazardous (45, 46). Entrainment of amine with the treated flue gas will be at most a few parts per million and is minimized with the addition of a wash section in the top portion of the absorber column. Other emissions may occur such as nitrosamines and other by-products formed by decomposition reactions. The significance of these environmental impacts is not clear at this time and will need to be considered before the technology can be widely applied (46).

#### Advanced Amines

Hybrid solvents combine the best characteristics of both chemical and physical solvents and are usually composed of a number of complementary solvents. Work is under way to develop tailor-made complementary solvents where the proportions are varied to suit the application. Recent advances in chemical solvents have included the commercial introduction of the KS-family of sterically hindered amines by Mitsubishi Heavy Industries (MHI). Their molecular structure is tailored to enhance reactivity toward a specific gas component, in this instance CO<sub>2</sub>. Benefits relative to MEA include higher absorption capacity (only 1 mol of hindered amine is required to react with 1 mol CO<sub>2</sub> compared with 2 mol MEA), 90% less solvent degradation, 20% lower regeneration energy, 15% less power, 40% lower solvent recirculation rates due to higher net absorption capacity, lower regeneration temperature, less corrosion in the presence of dissolved oxygen, and lower chemical additive cost.

Other advanced liquid solvent systems being developed include:

1. Advanced amine scrubbing (Cansolv Technologies, Inc.), in which a proprietary tertiary amine is utilized. The main advantages claimed are

low salt formation, low amine degradation, and low heat of regeneration.

2. HTC Pure Energy offers a Mixture of amines with focus on a modular system design capable of capturing up to 3000+ tons per day of CO<sub>2</sub>
3. DOW teamed with Alstom Power to form a partnership where Alstom designs and installs the equipment while DOW offers a unique solvent Based on Dow's UCARSOL™ FGC3000 solvent. A pilot plant has been constructed at Dow's sprawling petrochemical complex in South Charleston, West Virginia, that Alstom will design, build, and operate. Operation began September 2009. Uses approximately 20% to 30% less energy than the method currently used to remove CO<sub>2</sub> from flue gas emissions, using traditional amine solution. A 20-megawatt pilot plant is planned in Poland to optimize the technology and enable scaling it up to operate at an 800-megawatt plant.
4. Hitachi is currently researching a proprietary mixture of amines. They have several pilot scale activities scheduled.
5. Huntsman Chemical is working on two proprietary mixtures of amines and has bench- and small-pilot-scale data to support the activity.
6. Aker Clean Carbon.



## CHAPTER IV

### ADVANCED SOLVENTS SCIENTIFIC DISCUSSION

Several technologies exist that are currently under development for the capture of CO<sub>2</sub>, many of which have been discussed above. Of these technologies advanced solvents currently are the most attractive for near term implementation. The main reasons for this is the maturity of the technology. CO<sub>2</sub> absorption with solvents is not a new technology, and many of the advanced solvents are relying on the same equipment (packed columns) that has been used in industry (oil and gas processing) for many years. Still challenges in equipment design and implementation still exist such as footprint, integration, corrosion, and unintended consequences. On the chemical side several companies are designing advanced solvent which typically will contain a mixture of several amine (primary, secondary, and tertiary amines) each providing a unique advantage to the mixture. When designing a solvent three main factors must be considered and are listed as follows:

The selection of a suitable solvent should be based on the following three factors:

- Thermodynamics and kinetics
  - Low regeneration energy
  - High CO<sub>2</sub> loading and large window of solubility
  - High absorption rate constant
  - Low vapor pressure

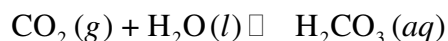
- Unwanted chemical reactions
  - Corrosion
  - Solvent degradation
- General properties
  - Toxicity
  - Biodegradability
  - Solvent cost

This section is going to attempt to explain the importance of these factors when selecting an advanced solvent.

#### Chemistry of Carbon Dioxide

The physical and chemical properties of CO<sub>2</sub> play an essential role in the development of any capture technologies. In its natural state, CO<sub>2</sub> is colorless, odorless at lower concentrations, but may smell acidic, with a sour mouth taste at much higher concentrations especially in moist environments where a weak acid might be formed. At room temperature and pressure, CO<sub>2</sub> exists as a gas and at –78.5°C and 1 atm pressure it is a solid (47). The triple point where all three phases (solid, liquid and gas) co-exist is at 5.2 atm and –57°C, which means that CO<sub>2</sub> can exist as a liquid at room temperature only if the pressure is elevated to much higher than 5.2 atm.

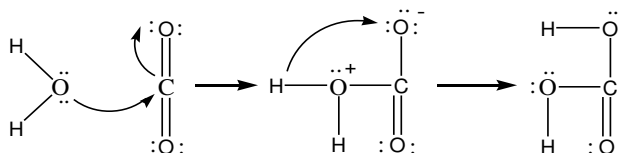
Carbon dioxide is an acid anhydride because it dissolves in water to yield a weakly acidic solution called carbonic acid,



which itself is unstable relative to dissociation into its constituent ions,



The mechanism of the hydration reaction can be understood in the Lewis acid-base framework, where water acts as a Lewis base and  $\text{CO}_2$  as a Lewis acid. The first step involves donation of a lone pair of electrons on the oxygen atom in the water molecule to the carbon atom in  $\text{CO}_2$ . An orbital is then vacated on the carbon atom to accommodate the lone pair by removal of the electron pair in one of the  $\text{C}=\text{O}$  double bonds. The final step involves a proton transfer onto the oxygen atom carrying a negative charge to form carbonic acid ( $\text{H}_2\text{CO}_3$ ) as shown in the scheme below, mechanism of the hydration of  $\text{CO}_2$  to form carbonic acid. The shifts in electrons are indicated by the curved arrows.



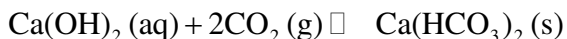
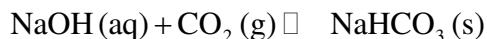
This mechanism forms the basis for understanding how the chemical reactions involved in  $\text{CO}_2$  capture solvent-base technologies work. For example in the case of amines, the amine molecule replaces the water molecule in the scheme above.

As shown in the reactions and mechanistic scheme above, the acid-base property of  $\text{CO}_2$  plays a critical role in the development of all solvent-based  $\text{CO}_2$  capture technologies. Other technologies have exploited the physical properties as well, e.g., the chilled ammonia process developed by Alstom Power Corporation is based on subjecting the gas stream to low temperatures at elevated pressures in an ammonia/ammonium carbonate solution (48). All solvent  $\text{CO}_2$  capture approaches rely on good, if not, excellent  $\text{CO}_2$  solubilities in the given solvent as well as a sound understanding of the factors that affect its reaction in an aqueous environment. Solubility data are important in

determining the extent of CO<sub>2</sub> loading in these solvents. Unfortunately, reactions under real flue gas conditions are much more complex and an understanding of the chemistry of other side reactions in the target solvent becomes also critical in developing an efficient solvent-based capture technology.

### Carbon Dioxide Scavengers

Currently, primary aliphatic amines have been used heavily in CO<sub>2</sub> capture technologies, e.g., monoethanolamine (MEA) [49,50,51], diethanolamine (DEA) [52,53], methyl-diethanolamine (MDEA) [54,55] and mixtures thereof [18]. Primary aliphatic amines, in particular, have good reaction kinetics but tend to bind too strongly to CO<sub>2</sub> causing the magnitude of the regeneration energy to become a challenge in the power industry, since it gets transferred into the cost of electricity. Consequently, other developers have resorted to sterically hindered amines, which do not have as good of kinetics, but have lower energy of regeneration [56,57,58]. Based on the acidic property of CO<sub>2</sub>, most basic substances such as aqueous solutions of the oxides of alkali and alkaline earth metals and their hydroxides or some amphoteric oxides may be useful candidates as CO<sub>2</sub> scavengers. For example, aqueous solutions of Na or Ca oxides are essentially their hydroxides, which react with CO<sub>2</sub> reversibly to yield sodium and calcium hydrogen carbonates, respectively, shown in the equations below:



Some of these will have undesirable side reactions with other flue gas components, such as reaction with SO<sub>2</sub> and NO<sub>2</sub>, but a careful investigation that includes

use of suitable additives could lead to a viable option that may be economically more feasible.

### Thermodynamics and Kinetics

The kinetics and thermodynamic properties of a solvent are very important in achieving a low cost highly efficient process. The kinetics of the solvent control equipment sizing, which can lead to reduced capital equipment expense. Kinetics can also control the total amount of solvent required in the system leading to reduced O&M costs. Thermodynamics of a solvent is the determining factor for the costs required to regenerate the solvent, which equates to higher or lower energy penalties (costs).

#### *Thermodynamics*

The energy required to regenerate an advanced chemical solvent comes from several process areas, but is primarily due to the energy required to regenerate the solvent. The energy used in the regeneration step is consumed by:

- Reversing the exothermic reaction, including the heat of condensation of CO<sub>2</sub> from the gas phase into solution in the liquid phase.
- Generating the stripping steam to carry off CO<sub>2</sub> stripped out of the liquid phase.
- Heating the CO<sub>2</sub> rich absorbent to regeneration temperature.
- Heat to make up for heat loss in the system.

This energy is typically supplied by low quality steam taken from the steam cycle of a power plant, thereby reducing the net generation of the plant (energy penalty). The first two bullets make up the majority of the total heat required and are both related to the heat of reaction between the solvent and CO<sub>2</sub>. The energy required to regenerate the

solvent is typically equal to the heat of reaction in the absorption step. In general stronger bases will yield higher heats of reaction, in turn requiring more heat for regeneration. It has been found that solvents with pKa in the range of ~ 6.5 to 8.5 result in a process with the least energy usage.

### *Kinetics*

When looking at designing a solvent for CO<sub>2</sub> capture it is important for an advanced solvent to have high CO<sub>2</sub> loading capacity and fast reaction constants. Typical amines such as MEA require 2 moles of MEA for every mole of CO<sub>2</sub> reacted. In advanced solvents tertiary amines are commonly used which react at a 1:1 mole ratio with CO<sub>2</sub>. This leads to half the amount of required solvent in the system, reducing the O&M costs. Unfortunately tertiary amines have a relatively slow mass transfer rate and therefore are not good candidates by themselves. Many groups pair tertiary amine with activators (catalysts) to help speed up the reaction rate. Secondary amines are typically used as the catalysts in these systems. Sterically unhindered secondary and primary amines react rapidly with CO<sub>2</sub> by the formation of carbamates. Secondary amines form unstably and will hydrolyze easily to bicarbonate and the protonated amine. If a tertiary amine is present in the solution, the protonated secondary and tertiary amine equilibrates with each other, yielding a net result of catalysis. Because the use of secondary amines leads to very fast mass transfer equipment sizes can be reduced, thus leading to lower capital costs.

### Unwanted Chemical Reactions

Several unwanted reactions can occur that will degrade the solvent to a point where it will need to be wasted and replaced, which increases the cost of operation dramatically.

When designing a solvent, the most important reactions to design around are avoiding the creation of heat stable salts that are formed when amines react with SO<sub>x</sub>, NO<sub>x</sub>, O<sub>2</sub>, and HCl. A small quantity of solvent is lost through various unwanted reactions in spite of dilution with water and the use of inhibitors. Long-chained compounds, formed through polymerization reactions and the oxidation reactions forming organic acids and liberating ammonia are the two main unwanted reactions that occur in the system. In general, the loss of MEA can be estimated as 3 lb MEA/ton CO<sub>2</sub>, with 50% coming from the polymerization reaction and the remaining 50% from the oxidation reaction. Other sources of amine based solvent loss exist in the creation of HSS and NH<sub>3</sub> generation; a reclaimer can be used to regenerate some of this loss. This can be expensive and if it can be avoided it is the preferred method. The acid gases present in the flue gas (i.e., SO<sub>x</sub>, NO, and HCl) are much more reactive towards the solvent than is CO<sub>2</sub>. When the gases react with the solvent, they form HSS that cannot be broken down. This causes a permanent loss of solvent that can be estimated according to the stoichiometry of their reaction with solvent. Removal efficiencies for these gases for a conventional solvent (MEA) are shown in Table 4. Advanced solvent designers have attempted to eliminate side reactions, but to date this is still one of the biggest contributions to O&M costs for a solvent based system. This is an area that research is needed in order to reduce side reaction, therefore reducing the cost of operating these systems.

Table 4. Removal Efficiencies of Acid Gases in an Amine Absorber.

Acid Gas	Removal Efficiency %	MEA Loss, mole MEA/mole acid gas
SO <sub>2</sub>	99.5	2
SO <sub>3</sub>	99.5	2
NO <sub>2</sub>	25	2
NO	0	0
HCl	95	1

## General Properties

The general properties of the solvent are important when considering how these solvents are manufactured. A great solvent may be identified, but in order to produce it may yield a large amount of unusable by-products that will need to be disposed of. In some instances for every million tons of solvent produced may yield 10 million tons of an unusable by-product. This must be considered when choosing the solvents to be used to capture CO<sub>2</sub>. Large quantities of these materials will need to be produced which will require chemical producers to scale up production rapidly. Therefore the more readily available the raw materials are the easier production will be.



## CHAPTER V

### EXPERIMENTAL DESIGN AND APPARATUS

Four advanced solvents were chosen for evaluation to determine the benefits of using an advanced amine solvent vs. the more traditionally used MEA solvent. In order to evaluate these solvents a solvent absorption and stripping system was designed and fabricated. The goal of the work was to evaluate these solvent for their ability to capture CO<sub>2</sub> from a coal derived flue gas that would mimic large scale deployment of this technology. To accomplish this, the EERC's CTF system was used to generate the coal derived flue gas. This chapter will describe the CTF test system as well as the design and fabrication of the solvent absorption and stripping system.

#### Description of the CTF

Research programs have been under way at the EERC for more than 30 years to study ash fouling of boiler heat-transfer surfaces in coal-fired utility boilers. A 550,000-Btu/hr pulverized coal (pc) pilot plant test furnace was constructed in 1967 to evaluate the influence of variables, including ash composition, excess air, gas temperature, and tube wall temperatures on ash fouling. Results from this work have shown a strong correlation between ash characteristics, boiler operating parameters, and degree of fouling.

The research capabilities of the CTF have been enhanced over the years and expanded to provide information on a wide range of combustion-related issues. To

achieve a wide range of operating conditions, the refractory-lined furnace may be fired at a rate sufficient to achieve a furnace exit gas temperature (FEGT) as high as 2500°F.

Most tests are performed with the FEGT maintained at approximately 2000°–2200°F.

Research applications of this pilot-scale combustion equipment have included the following:

- Determine ash-fouling rates and the strength, composition, and structure of fouling deposits for coals of all rank.
- Determine the effectiveness of ash-fouling additives.
- Apply sophisticated analytical methods to characterize input coal, ash, and deposits.
- Correlate coal and ash properties with deposit growth rates and strength development.
- Evaluate the combustion characteristics of coal–water fuels, biomass fuels, municipal solid waste, and petroleum coke.
- Determine fly ash collection properties of various fuels by electrostatic precipitation or fabric filtration using a pulse-jet baghouse, including high-temperature applications.
- Evaluate the slagging potential and slag corrosion in a simulated wet-bottom firing mode.
- Perform flame stability tests for comparing a particular fuel at full load and under turndown conditions.
- Evaluate fouling, slagging, and electrostatic precipitator (ESP) performance for blends of bituminous and subbituminous coals.

- Evaluate the combustion properties of petroleum coke alone and in blends with subbituminous and lignite coals.
- Evaluate sorbent injection for SO<sub>x</sub> control, and assess integrated particulate and SO<sub>x</sub>-NO<sub>x</sub> control.
- Evaluate several CO<sub>2</sub> capture technologies.

The CTF is fully instrumented to provide online analysis of the flue gas. Three flue gas-sampling ports are available. Flue gas concentrations of O<sub>2</sub>, CO<sub>2</sub>, and SO<sub>2</sub> are obtained simultaneously at the furnace exit and stack. Emissions of CO and NO<sub>x</sub> are obtained at the furnace exit. System O<sub>2</sub>, CO, and CO<sub>2</sub> analyzers are manufactured by Rosemount; the SO<sub>2</sub> analyzers are manufactured by DuPont and Ametek; and NO<sub>x</sub> is measured with a Thermo Electron chemiluminescent analyzer. All system temperatures, pressures, and flue gas analyses are recorded continuously to chart recorders and the system's computer-controlled data acquisition system.

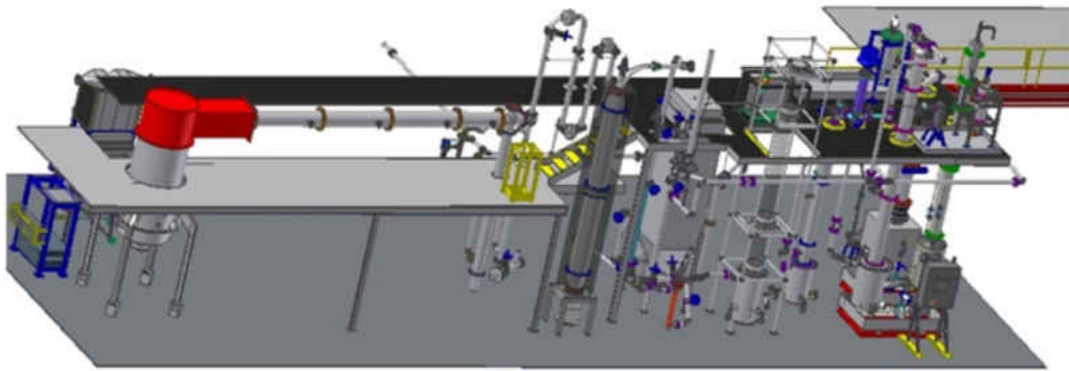
Coal is pulverized remotely in a hammer mill pulverizer to a size of 70% less than 200 mesh (75 μm). The coal is then charged to a microprocessor-controlled weight loss feeder from a transport hopper. Combustion air is preheated by an electric air heater. The pc is screw-fed by the gravimetric feeder into the throat of a venturi section in the primary air line to the burner. Heated secondary air is introduced through an annular section surrounding the burner. Heated tertiary air is added through two tangential ports located in the furnace wall about 1 ft above the burner cone. The percentages of the total air used as primary, secondary, and tertiary air are usually 10%, 30%, and 60%, respectively. An adjustable-swirl burner, which uses only primary and secondary air with a distribution of approximately 15% and 85%, respectively, is used during flame stability

testing. Flue gas passes out of the furnace into a 10-in.-square duct that is also refractory-lined. Located in the duct is a vertical probe bank designed to simulate superheater surfaces in a commercial boiler. The fouling probes are constructed of 1.66-in.-o.d. Type 304 stainless steel pipe cooled to a surface metal temperature of 1000°F (or other specified temperature) with steam. Deposit strength can be assessed by laboratory determinations using a drop impactor technique and by scanning electron microscopy (SEM). The drop impactor technique provides a calculated measurement of deposit strength, taking into account the conditions under which the test was performed. SEM point count provides a point-by-point analysis of the deposit. These data can be used to calculate the viscosity of each data point that can be related to deposit strength.

After leaving the probe bank duct, the flue gas passes through a series of water-cooled heat exchangers before being discharged through either an ESP or pulse-jet baghouse. Wet flue gas desulfurization (WFGD), spray dryer (SD), and selective catalytic reduction (SCR) systems are available and can also be installed as back-end controls on the unit. The test furnace has numerous ports that permit observation of the probes and the furnace burner zone during the test run. These ports can also be used for installation of additional test probes, auxiliary measurements, photography, or injection of additives. Figure 12 shows a schematic of the unit. Figure 13 is a photograph to give an idea of scale.

### Solvent Absorption Test System and Protocol

Four different solvent technologies were selected for testing for this thesis, including a standard 30 wt% MEA as the base case solvent and proprietary solvent H3-1 supplied by Hitachi Corporation, mixture of MEA and Huntsman's additive, and a



EERC BP37508.CDR

Figure 12. 3-D representation of the CTF and SASC systems.



EERC BP34573.CDR

Figure 13. Picture of the CTF.

mixture of MDEA (methyldiethanolamine) and piperazine (PZ). Each of these technologies was tested for about 5 days continuously on flue gas generated by burning Antelope PRB subbituminous coal on the EERC's 75-lb/hr pilot-scale modified CTF. The configuration of the CTF used in all tests includes a combustion furnace and various downstream pollution control devices: an ESP for ash and particulate control, a wet flue gas desulfurization (FGD) scrubber for SO<sub>2</sub> control, and a hot-side SCR for NO<sub>x</sub> control. In order to maintain a solvent water balance in the system, the temperatures of the inlet and outlet absorber gas were controlled to 110 °F. At these conditions the gas will be fully saturated with water.

The effects of several parameters on the CO<sub>2</sub> capture performance were investigated during these tests, including solvent regeneration energy (reboiler duty), solvent flow rate (liquid to gas ratio), stripper column pressure, and absorber inlet temperature. The level of CO<sub>2</sub> capture performance that was targeted in these tests was 90% capture, and the parameters mentioned above were varied to determine the conditions needed to achieve the CO<sub>2</sub> capture target for each technology. In addition, samples were also collected during testing and analyzed at the EERC's Analytical Research Laboratory (ARL) to determine the levels of free amine, bound amine, heat-stable salts (HSS), trace metal corrosion products, major elements, and solvent CO<sub>2</sub> loading to assist in evaluating the impact of flue gas components such as NO<sub>x</sub>, SO<sub>x</sub>, and O<sub>2</sub> on the integrity of these solvents.

The amount of "fresh" amine present in the absorber at any time after flue gas flow has been started is a measure of the ability of the resultant lean solvent to effectively absorb CO<sub>2</sub> from the flue gas. This portion of the amine is called free amine in lean

alkanolamine solutions and is often measured using acid-base titration techniques. By monitoring the free amine concentration, it is possible to determine when to add makeup solvent to maintain an optimum CO<sub>2</sub> capture level. Also, bound amine has been determined in this study as the amount of amine that is no longer available for CO<sub>2</sub> capture; i.e., it is essentially tied up with HSS anions. These explanations of free and bound amine apply to all occurrences of these terms in this report, unless otherwise specified.

This section of the report is structured as follows. The different components of the solvent absorption and scrubbing system are described in “Description of the Solvent Scrubbing System,” and a test plan and methods are described in “Test Plan and Methods.” The results from pilot plant tests and laboratory analyses are presented in “Results and Discussion,” together with appropriate discussions. In “Solvent Comparison,” the different solvent technologies are compared, and an overall summary of postcombustion tests and results is given in “Solvent Summary.”

#### *Description of the Solvent Scrubbing System*

The solvent absorption system was designed by first creating a process flow diagram and finally a modified P&ID. Aspen Tech was used to determine the overall sizing of the columns necessary to capture 90 % of the CO<sub>2</sub> using a MEA solvent. In designing the system, design review was provided from Huntsman, a global manufacturer and marketer of differentiated chemicals. This process was crucial to the design phase as Huntsman has vast experience in the gas-treating industry using similar solvents to those that were evaluated during this project. Figure 14 shows the final P&ID of the SASC system developed through the work with Huntsman.

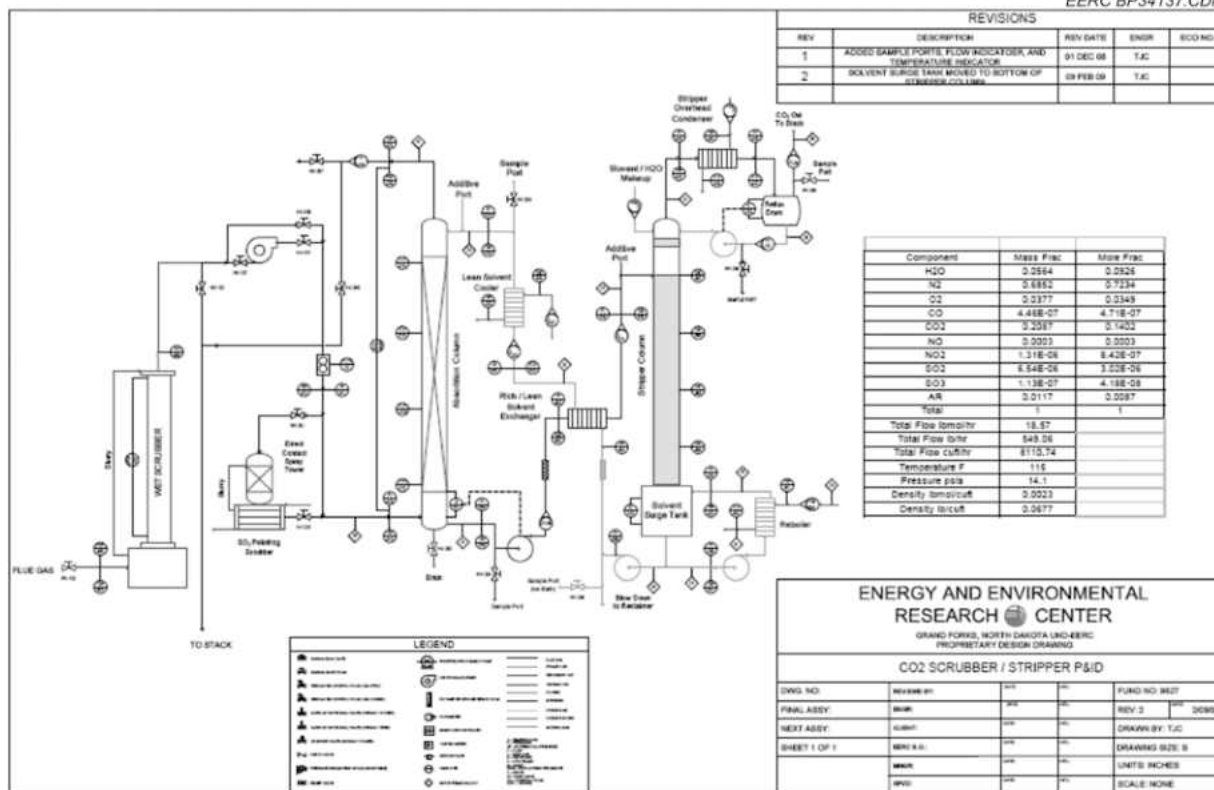


Figure 14. P&ID of the SASC system.

The fabricated unit shown in Figure 15 consists of two main columns, each constructed from 10-in.-i.d. stainless steel column sections of varying lengths bolted together to achieve a desired total height. Koch–Glitsch IMTP 25 316L stainless steel random packing was loaded in each column to enhance the liquid–gas contact area and promote better CO<sub>2</sub> absorption and regeneration.

Figure 16 shows the random packing used in the columns. Packing height, size, and type can easily be modified to accommodate different solvents and test conditions. The columns were designed to handle up to 130 scfm of flue gas generated in the CTF. A demister was installed near the top of the absorber column to keep the flue gas from





Figure 15. SASC system as tested during shakedown.



Figure 16. Koch-Glitsch IMTP 25 random packing sample.

carrying solvent through with the gas exhaust stream. A flooding model was created in Excel to determine the point at which the system will flood. A 75 % flooding capacity factor was chosen for the calculations. It was determined with this model that the system can handle ~200 scfm before flooding will occur. Because the column has a relatively static height different gas flow rates can be testing to determine the effect of residence time needed for a particular solvent. This type of test will tell us the kinetic rate of the solvent in relative terms to MEA.

A solvent collection tank, approximately 2 feet in diameter by 3 feet tall, was located at the base of both columns. During operation, rich solvent from the absorber collection tank was pumped through a lean-rich crossflow heat exchanger to heat the solvent before it reached the top of the stripper column. The solvent then flowed down through the packing in the stripper column and was pumped from the stripper collection tank through the lean-rich crossflow heat exchanger as well as a lean solvent cooler in order to cool the solvent before it reaches the top of the absorber column. In addition to the two pumps used to cycle the solvent through the columns, a third pump was used to cycle lean solvent in the stripper tank through a steam reboiler heat exchanger. This partial reboiler system added the necessary regeneration energy to heat the inventory and separate the CO<sub>2</sub> from the solvent. The reboiler system is equipped to be able to set the quality of the steam (pressure and temperature) by the use of a steam trap and an automated valve. This allows for consistent steam quality to allow for a way to compare regeneration energy requirements. A fourth pump moved condensate collected in a reflux drum back into the stripper column. Each pump was controlled with a variable-frequency

drive through the LabVIEW interface. Solvent was typically pumped at about 3–8 gallons per minute.

The absorber column was designed to operate at or around atmospheric pressure. The stripper column, however, was designed to operate at a positive static pressure. The top and bottom of the solvent collection tank of the stripper column were domed to facilitate operation as a pressure vessel. Similarly, the top section of the column was also domed. The stripper column was operated between 3 and 12 psig during shakedown and testing. Pressure in the stripper column was regulated by a back-pressure control valve on the exhaust line downstream of the reflux drum.

Filter housings were placed in both the rich and lean solvent lines to clean the solvents of any contaminants. A third filter housing was mounted in-line for the lean solvent going to the reboiler heat exchanger. All wetted parts in the system were constructed from stainless steel 316L, with the exception of the columns themselves, which were made from a duplex 2205 stainless steel alloy. Duplex 2205 stainless steel alloy was chosen as the column material for its added corrosion resistance. Sample ports were located near the base and top of each column to take solvent samples needed for analysis.

Along with the physical construction, instrumentation was a key component of the final fabricated unit. Heaters were wrapped around each column and collection tank to provide auxiliary heat in addition to the heat generated within the system. These heaters are necessary on this relatively small scale system to ensure that the results were not impacted by the large heat loss per unit area of the system. Make up heat is added to the system minimize the interference of unrealistic heat loss of the system. The stripper column was

typically run around 200°–250°F. Auxiliary heaters and insulation helped maintain those temperatures. The heaters were controlled with Watlow controllers located on a panel adjacent to the system. Each solvent collection tank, including the reflux tank, was instrumented with both a level sensor and a visual level sight glass. Early level indicators were a differential pressure style. These were later replaced in the absorber and reflux tanks with guided wave radar level indicators. Initially, vortex flow indicator/recorders were installed on rich and lean solvent lines to determine flow rate. These were later replaced with magnetic flow sensors in order to provide more reliable data. Level indicators and flowmeters were used in the LabVIEW program to control the pumps in the system. Numerous thermocouples and pressure gauges were installed on the system to closely monitor temperature and pressure at key points throughout the process. In addition to the laptop-based LabVIEW interface, a touch screen indicator was installed on the system to allow a second operator quick access to flow rates, temperatures, pressures, and other system information.

With fabrication of the system complete, a series of shakedown tests was performed on the SASC system to ensure reliable operation. The shakedown procedures allowed system operators to identify and correct problems with the design. Some design changes included moving placements of level indicators and thermocouples, adding vibration damping, and improving the usability of the LabVIEW control interface. The shakedown runs also allowed the PCO<sub>2</sub>C research group to find pump and level set points that would allow for controlled operation of the system. The first five shakedown tests were carried out using natural gas as a fuel for the CTF, and the final two tests used coal.

The Aspen computer model of the SASC system was consulted during shakedown testing to compare physical results with theoretical results. The model was calibrated to closely match the performance of the physical system. Table 5 compares Aspen model parameters with data collected from the demonstration unit after model calibration. The data generated by the model were validated by comparing them with data collected on the postcombustion system. The makeup rate shown in Table 5 for the pilot plant data is zero. During actual testing, makeup rate varied from zero to 500 mL/min. Shakedown runs used for model calibration were short in duration and did not require makeup to maintain solvent inventory levels. More discussion of Aspen modeling of the solvent system can be found in “Solvent System Modeling and Economic Analysis.”

The model was referenced when parameters such as makeup rate and packing depth were examined. 3-D computer drawings also assisted during fabrication and shakedown in helping determine placement of piping, tubing, and system components. Views of the 3-D drawing are shown in Figure 17. In a typical test run with the SASC system, many parameters were monitored to determine any resultant impact on CO<sub>2</sub> absorption. Table 6 presents the main system parameters that were manipulated in optimizing the system to maximize CO<sub>2</sub> removal. During any single test run, these parameters were manipulated to pursue an optimal CO<sub>2</sub> capture efficiency, solvent degradation rate, or other desired performance characteristic.

Operation of the CTF was the driver for a few of the variable parameters. Inlet gas flow rate was controlled by the CTF’s induced-draft fan and the CO<sub>2</sub> booster blower. Some

Table 5. Comparison Between Aspen Model Data and Pilot-Scale Demonstration Unit Data.

Parameter	Model	Pilot Plant Data
CO <sub>2</sub> Capture	69.5%	~70%
Reboiler Duty	150,000 Btu/hr	140,000 Btu/hr
MEA Flow into Absorber	6 gpm	3–6 gpm
Makeup Rate	0.6 gph	None

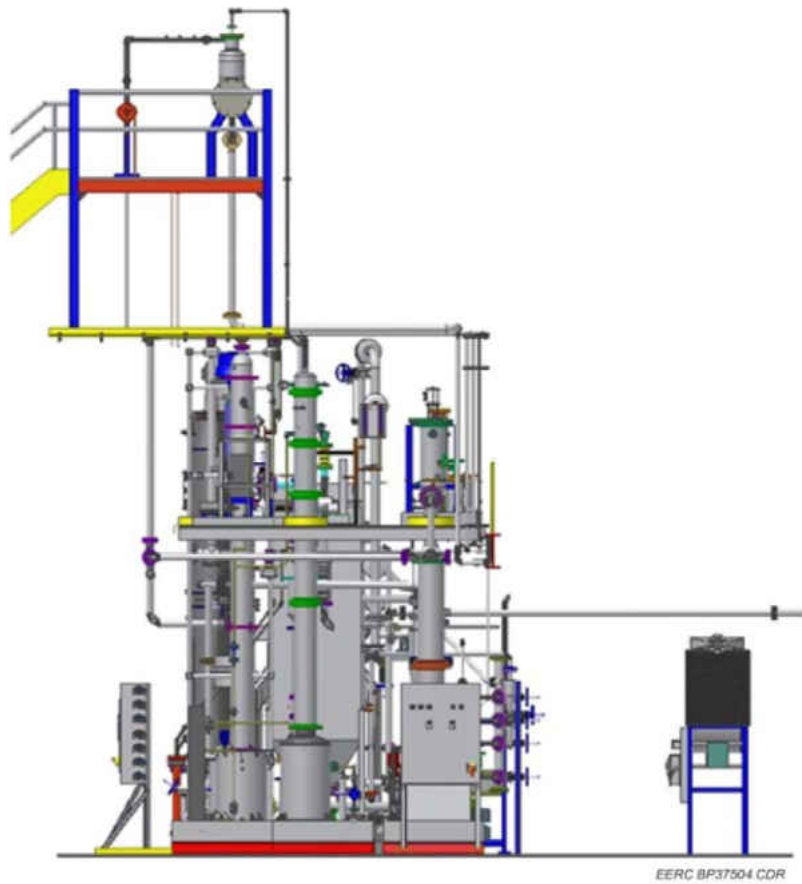


Figure 17. 3-D representation of the SASC system with Water and Energy Sustainability Technology (WEST) system shown on the far right.

Table 6. SASC Variable Test Parameters.

	Typical Range
<i>CTF System Variations</i>	
Inlet Gas Flow Rate	60–130 scfm
Inlet Gas Temperature	90–120°F
NO <sub>x</sub> to Columns	0 to 600 ppm
SO <sub>2</sub> to Columns	0 to 600 ppm
<i>SASC System Variations</i>	
Solvent Flow Rate Through Absorber	2–10 gpm
Condenser Cooling Water Flow Rate	1–6 gpm
Lean Solvent to Absorber Temperature	80–150°F
Stripper Static Pressure	3–14 psig
Steam Reboiler Pressure	10–55 psig
Solvent Concentration	As requested
Solvent Makeup Rate	0–500 mL/min

parameters, such as SO<sub>2</sub> concentration of the flue gas entering the column, are fuel-dependent. SO<sub>2</sub> concentration at the absorber inlet was manipulated in two manners: either bypassing the wet scrubber or reducing the amount of slurry used to scrub SO<sub>2</sub>, allowing some SO<sub>2</sub> through to the absorber. In other cases, all SO<sub>2</sub> from the flue gas was scrubbed out in the wet scrubber, and a known amount was added before the gas stream entered the absorber just upstream of the CO<sub>2</sub> booster blower. Specific concentrations of SO<sub>2</sub> were added by metering the gas with a glass tube-cube rotameter and verifying the level with one of the EERC's analyzer banks.

One critical test parameter was inlet gas temperature. To regulate inlet temperature, the DCC was installed just upstream of the absorber column. The DCC column was designed and fabricated to function as a spray dryer and humidity control device. Water that passed through the DCC cooled and dried the flue gas before the absorber. Inlet gas temperature was controlled by increasing or decreasing water flow through the DCC with a valved rotometer.

On the SASC operation side, the LabVIEW control interface allowed the operator to vary solvent flow rate by increasing or decreasing rich and lean pump speeds. Also, the stripper column static pressure was increased or decreased with the LabVIEW control interface. Other parameters were altered manually. Makeup rate was changed by the user by increasing or decreasing the rate at which additional solvent or water was pumped into the absorber tank.

### Test Plan and Methods

The test plan for each technology was developed and then refined based on information obtained from shakedown runs. Initial system conditions, test variables, and procedures were formulated, which were then verified during shakedown runs to ensure that the different pieces of equipment were working properly. The frequency of sample collection and location were also established. Samples were collected from the absorber (rich solvent) and stripper (lean solvent) every 2–3 hours and after any major change in the pilot plant's system variables. The conditions that were varied on the CTF include flue gas flow rate, solvent flow rate, reboiler duty, absorber inlet temperature, and stripper column pressure. When any process condition was being varied, all others were maintained as relatively steady as possible and the test run until the CO<sub>2</sub> capture rate was more or less constant. Table 7 gives an example of a test matrix showing desired values for these variables. The target CO<sub>2</sub> capture value at steady-state conditions was 90%. Several columns of the test matrix were left blank for the operators to fill in the exact values based on actual runs. In some cases where flue gas components such as NO<sub>x</sub> or SO<sub>x</sub> were also varied, target values were explicitly indicated and included in the test



Table 7. Example of a Portion of a Typical Test Plan Matrix.

Date , Time	CO <sub>2</sub> Out, %	Steam Press.,	Inlet Temp.,	Absorber Inlet Flow,			Stripper Static Press.,			Lean Solvent Flow,		
		psig	°F	scfm			psig			gpm		
		15–30	105–110	60	75	100	4	8	12	low	mid	high
				X			X			X		
				X			X				X	
				X			X					X
					X				X	X		
					X				X		X	
					X				X			X
					X			X			X	
					X			X				X
					X			X			X	

matrix prior to actual test run. For other system variables like steam pressure and absorber inlet temperature, a range of desired values was indicated.

Tests on the four technologies reported were carried out in the course of about 4 months, from February to June 2010. During the tests, several samples were collected from the absorber and the stripper periodically, usually every 2–3 hours or just before or after any major system changes. H3-1 solvent was tested on February 8–12, 2010, and during these tests, about 70 samples were collected. Next, MEA solvent was tested on March 16–22, 2010, and about 34 samples were collected. Tests on Huntsman additive were carried out on May 10–14, 2010, and about 54 samples were collected. Tests on MDEA+PZ were performed on June 14–18, 2010, and 60 samples were collected for analysis. During each test period for a given technology, the samples collected were immersed in an ice water bath immediately after collection to quench elevated temperature reactions and, thereafter, stored in airtight glass sample bottles prior to

analyses. Because of the large number of samples collected, about 35 samples were selected for analyses from the H3-1 batch of samples, 25 from the 34 MEA samples, 18 of 54 Huntsman additive, and about 50 of 60 MDEA+PZ samples. The rest of the samples from each technology were analyzed as needed to obtain sufficient data for specific test points within each test matrix.

The methods and/or procedures for analysis of the samples collected are based on standard operating procedures at the EERC's ARL. A variety of instruments both in the lab and on the CTF were utilized in order to provide a complete data set for each sample selected for analysis. Table 8 summarizes the different methods and analytical techniques used for sample analysis, along with the measured analytes for each procedure. A detail description of each method/procedure and the analytical equipment used is given in Appendix A1.

#### *Fresh Amine Solvents*

The concentration of MEA bulk solvent supplied by Huntsman Petrochemical Corporation was 85 wt%. This was diluted to obtain a 30 wt% solution that is commonly used for CO<sub>2</sub> scrubbing applications by adding deionized water. Other solvents supplied by commercial partners include H3-1, Huntsman additive, and MDEA+PZ. Bulk H3-1 was supplied as a 40–50 wt% solution and was used as-received without further dilution, while Huntsman additive and MDEA+PZ were mixtures of amines. The initial concentration of Huntsman additive and MDEA+PZ at the start of the tests, shown in Table 9, was obtained from as-supplied bulk concentrations by dilution with deionized water. In order to provide a basis for comparison with concentrations of lean amine

Table 8. Summary of Methods and Analytical Techniques.

Analyte/Procedure	Equipment and/or Analytical Method
Fresh Amine	Fischer Scientific Accumet <sup>®</sup> 950 pH meter
Free and “Bound” Amine	Fischer Scientific Accumet <sup>®</sup> 950 pH meter
Inorganic Anions	Dionex ICS 3000 ion chromatography (IC) system
Organic Anions	Dionex ICS 3000 ion chromatography (IC) system
Trace Metals and Major Elements	Leeman Labs PS1000 sequential inductively coupled plasma atomic emission spectroscopy (ICP–AES)
Furnace Exit Gas Analysis	Rosemount gas analyzers
Absorber Inlet/Outlet Gas Analysis	Rosemount gas analyzers
SO <sub>2</sub>	Ametek gas analyzers and meters
Injection/Analysis/Measurement	
O <sub>2</sub> Analysis/Measurement	Rosemount gas analyzers
CO <sub>2</sub> Loading	Shimadzu TOC-VCSN total organic carbon (TOC) analyzer

Table 9. Concentration of Fresh Amine Solvents.

Amine Type	As-Received, wt%	As-Determined, wt%
MEA	30 <sup>a</sup>	29.7
H3-1	40–50	48.2
Huntsman additive	32 <sup>b</sup>	31.7
MDEA+PZ	40–40–20 <sup>c</sup>	39.9–39.8–20.3

<sup>a</sup> Obtained by dilution with deionized water from company-supplied 85 wt% solution.

<sup>b</sup> Obtained by dilution from bulk solvent.

<sup>c</sup> This mixture comprises 40 wt% MDEA, 40 wt% PZ, and 20 wt% water.

solutions determined using a potentiometric titration method at the EERC’s ARL, the concentration of the initial amines were redetermined. The resultant as-determined concentrations presented in Table 9 show good agreement with the corresponding initial values for all solvents.

Because of an anticipated loss of amine solvent by amine slip from the columns to the stack, which could lead to a gradual drop in solvent level in the columns and/or a

concentration change over time, samples were extracted periodically from the absorber and titrated off-line. To ensure the concentrations were maintained relatively steady at the as-determined values indicated in Table 9, water and/or small amounts of amine solvent were added as needed using a small makeup pump.

### *Calculations*

Two main types of calculations were performed besides normal data reduction steps, including determination of CO<sub>2</sub> capture and stripper reboiler duty. The CO<sub>2</sub> capture was calculated using data obtained from gas analyzers installed at the furnace exit, absorber inlet and/or absorber outlet, and the stack. The raw data were then corrected for oxygen and air leakage into the system to obtain refined CO<sub>2</sub> capture performance for each technology tested.

Calculations of the reboiler duty were made by collecting data on the reboiler inlet and outlet parameters, such as steam flow rate, steam temperature, condensate temperature, and steam pressure. A key assumption made in the calculations was that the steam coming into the reboiler and condensate leaving the reboiler were saturated vapor and liquid streams, respectively. Hence, with the temperature of both streams known, enthalpy values were looked up in a standard steam table to find the heat of vaporization. The enthalpy difference between the steam and condensate streams was multiplied by the steam flow rate to produce a value for the reboiler duty. Detailed explanations of the calculations are given in Appendix A2.

### *Shakedown Testing*

MEA was chosen as a baseline solvent for testing on PCO<sub>2</sub>C's postcombustion CO<sub>2</sub> capture system because it is currently used in industry and would provide a reliable

means of comparison. MEA was diluted with deionized (DI) water to approximately 30% MEA by weight for testing. Initial shakedown of the system was performed between November 11, 2009, and January 6, 2010, with a more structured shakedown between January 26 and February 2, 2010. Initial shakedown runs of the system used natural gas as the combustion fuel to eliminate the variability inherent in coal combustion flue gas. CO<sub>2</sub> capture data for the first few shakedown runs was inconclusive in assessing the performance of the solvent. For the initial shakedown runs, some subsystems were not at full functionality, and flue gas was bypassed around the absorber column for significant lengths of time. There were sustained periods of steady CO<sub>2</sub> capture during the third shakedown run. The system captured approximately 70% to 80% of the CO<sub>2</sub> in the flue gas flowing through the absorber for two distinct half-hour intervals.

Upon completion of the natural gas shakedown runs, a standard procedure for starting up, running, and shutting down the system was developed. A shakedown run with coal as the combustion fuel assessed the developed operational procedures and changes before the planned test runs were started. The first test run using coal for the postcombustion CO<sub>2</sub> capture system occurred on January 6, 2010. The coal was Antelope PRB. Gas analyzers were maintained at the furnace outlet and the stack, with a third alternating between the absorber inlet and outlet. CO<sub>2</sub> capture was noted to be approximately 75% for a majority of the test. Figure 18 shows data collected over the coal combustion portion of the test, corrected for 3% oxygen. Attempts at optimizing the CO<sub>2</sub> capture were carried out near the end of the test. This was done by decreasing total gas flow, increasing pressure in the stripper column, and both increasing and decreasing lean solvent flow. CO<sub>2</sub> capture increased during the end of the test to nearly 83%. It was

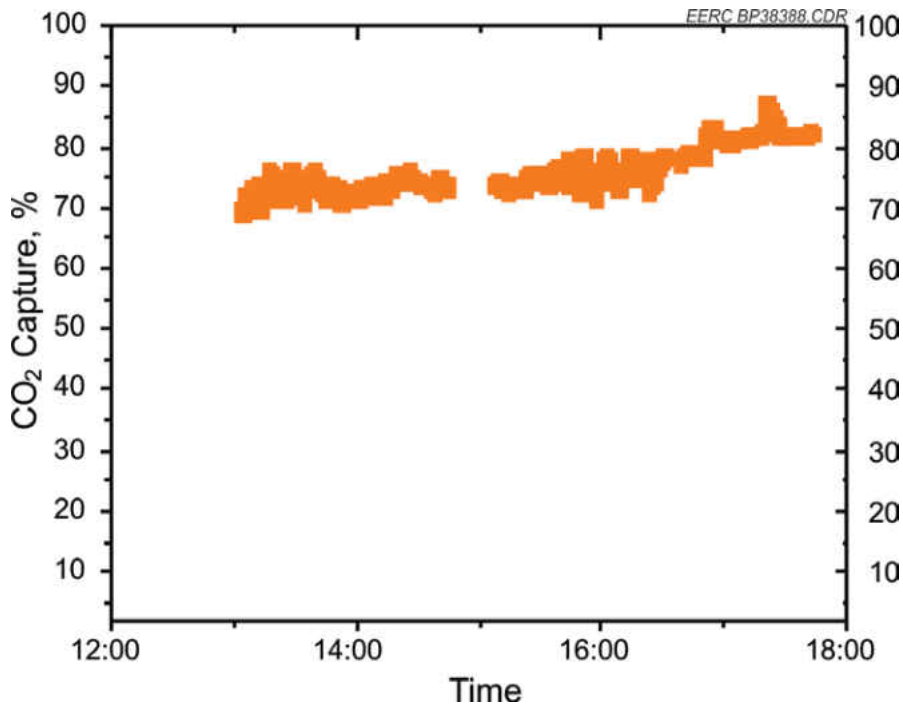


Figure 18. CO<sub>2</sub> capture from coal combustion flue gas – January 6, 2010.

difficult to conclude from the data whether any single parameter change resulted in the increased CO<sub>2</sub> capture rate. A longer period of more controlled conditions would have been necessary to make such a conclusion.

Following the initial shakedown runs, a series of five single-day tests were completed between January 26 and February 2, 2010. Each of these shakedown runs was performed with Antelope PRB coal with the same CTF configuration used during the initial shakedown period.

The first 3 days of the structured shakedown testing saw highly variable data in terms of steam flow, inlet temperature and, ultimately, CO<sub>2</sub> removal. By the final 2 days of the test, most of the operational concerns were addressed, and a mostly steady run state was achieved. Near 85% CO<sub>2</sub> capture was achieved on February 2, 2010, which is close

to the goal of over 90% CO<sub>2</sub> capture. Figure 19 presents the calculated corrected CO<sub>2</sub> capture from the system as well as properties for the inlet gas stream and solvent flow rate. One correlation that was apparent from the data was the direct relationship shown between CO<sub>2</sub> capture and absorber inlet temperature.

Several issues with the system were identified and fixed during shakedown. These included the installation of a valved water flowmeter on the DCC upstream of the absorber to better regulate temperature of the incoming flue gas, orifice assemblies

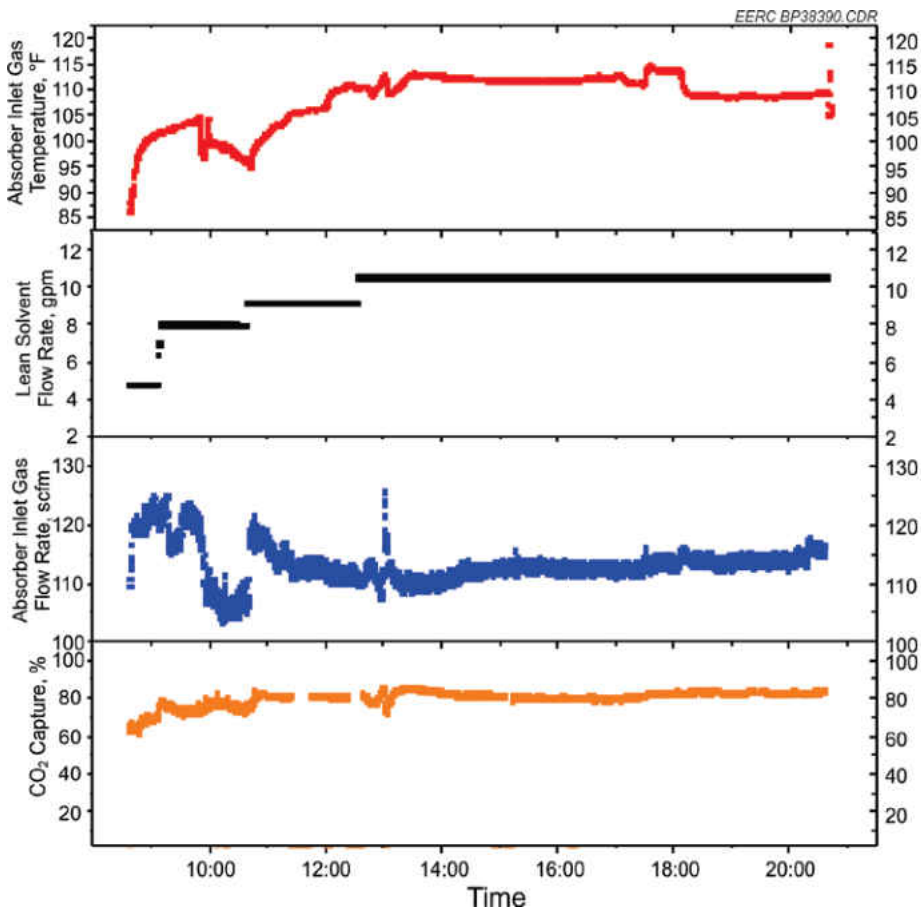


Figure 19. CO<sub>2</sub> removal from coal combustion flue gas and absorber inlet properties – February 2, 2010.

installed at absorber inlet and product gas outlet, insulation of all system piping and column sections to closely control temperature, and fixing any and all significant solvent system leaks. Instrumentation, physical systems, and run methods and operation were improved and developed during shakedown to facilitate the long-term test runs.



## CHAPTER VI

### PILOT SCALE TEST RESULTS

The results of pilot-scale postcombustion tests conducted on four main amine solvent technologies during Phase I of the PCO<sub>2</sub>C project are presented and discussed based on interpretation of the data obtained. The solvent technologies that were tested include standard 30 wt% MEA used as the base case and H3-1 (40–50 wt%), Huntsman additive, and MDEA+PZ supplied by commercial partners. The effects of several parameters on the CO<sub>2</sub> capture performance were investigated during these tests, including solvent regeneration energy (reboiler duty), solvent flow rate, stripper column static pressure, and absorber inlet temperature. In addition, samples were also collected during testing and analyzed at the EERC's ARL to determine the levels of free amine; bound amine; HSS; trace metal corrosion products; and major elements and solvent CO<sub>2</sub> loading to determine the impact of flue gas components such as NO<sub>x</sub>, SO<sub>x</sub>, and O<sub>2</sub> on the integrity of these solvents. The overall goal of this testing was to be able to gather enough information to develop factor to input into the models being generated in the Aspen plus software package. Because it is very expensive to accurately model advanced solvents (due to lack of fundamental data) these factors are used to modify a very robust MEA model that was developed through this program. The results obtained from pilot plant tests as well as those obtained from laboratory analysis of the collected samples are

described below in detail for MEA the base case and summarized in a comparison for the other solvents. Full details for the three advanced solvents can be found in Appendix B. Because MEA was used as the bench mark for the modeling as well as an overall comparison more discussion is given in the main body of the report. Typical flue gas compositions and a fuel analysis of the coal used can also be found in Appendix B.

#### Monoethanolamine – Base Case

A standard 30 wt% MEA solution was used as the state-of-the-art baseline solvent with which other recently developed advanced and/or mixtures of amines were compared. The selection of MEA as the baseline technology was based on its use in acid gas scrubbing applications for a long time at the commercial scale and benchmark data available for verification. Although the data obtained at a smaller pilot-scale facility like the EERC's CTF cannot be directly compared to full-scale facilities, trends and optimum operating conditions/variables are well known and provide a good guide for what might be expected. The coal fired during this test was Antelope PRB subbituminous coal. The CTF was operated in an air-fired mode, with the SCR, ESP and wet FGD as downstream pollution control devices. Various gas analyzers and thermocouples were installed at different locations on the CTF to monitor the flue gas properties as it enters the CO<sub>2</sub> scrubbing system. Typical locations included furnace exit, stack, and another location that was moveable from reflux offgas to upstream and/or downstream of the absorber column. NO<sub>x</sub> levels were maintained at baseline values of about 2 ppm for Antelope PRB coal. The SO<sub>2</sub> level was raised from baseline amount (~1 ppm or less) toward the end of MEA testing to about 20–50 ppm by tuning the operating conditions on the wet FGD

scrubber. This allowed the possibility to investigate the effects of SO<sub>x</sub> on solvent and the amount of SO<sub>x</sub>-related HSS such as sulfates and thiosulfates.

### *System Performance*

Several goals for testing the postcombustion system with MEA and other amine-based solvents were established prior to testing. The overall goal was to introduce coal combustion flue gas to the solvent continuously for over 100 hours. During testing, the team examined the effects of multiple test parameters. These parameters included static pressure in the stripper column, reboiler duty, solvent flow rate, flue gas flow rate and temperature, and flue gas SO<sub>2</sub> levels. A portion of each test was a long-term steady-state run where variables would be kept as static as operationally possible. The test plan involved manipulating the variables described in Table 10 to develop CO<sub>2</sub> removal values for a wide range of run conditions.

The system variables typically had a high, low, and midrange setting. For a lean solvent flow rate, low and high values were defined, but a midrange value is not given because the flow rate spectrum was continuous. Similarly, a midrange setting was not defined for the steam input rate because the steam was operated between high and low values on a continuous spectrum.

For each test run, CO<sub>2</sub> capture levels of 90% were not reached until late in the first 24 hours of testing. Many of the system parameters needed to be ramped up before reaching operating conditions. Stripper pressure, solvent temperature, and column temperatures all took time to reach their operating levels. Once proper temperatures and pressures were able to be maintained, optimization parameters such as solvent flow rate and reboiler duty were

Table 10. Test Parameter Ranges.

	Stripper Static Pressure, psig	Absorber Inlet Flow Rate, scfm	Lean Solvent Flow Rate, gpm	Steam Input Rate, kBtu/hr
Low	4	60	3	90
Mid	8	75	–	–
High	12	100	8	150

manipulated to reach 90% capture. Changes to the system were done gradually to avoid drastically upsetting the system equilibrium.

#### *Effects of Flue Gas Flow Rate*

Flue gas flow rate to the absorber is one of the key variables in determining CO<sub>2</sub> removal rate. Baseline testing was run at flow rates of 60, 75, and 100 scfm. Figure 20 shows corrected results for the end of testing Day 1 and all of Day 2. Within Figure 20, all three flow rates tested are presented. The most significant change in CO<sub>2</sub> removal rate occurred when the absorber inlet flow rate was dropped from 100 to 75 scfm at around 23:40 on March 16, 2010. This drop corresponded with an increase in CO<sub>2</sub> removal rate from about 85% to nearly 95%. Figure 21, however, shows that the drop in flow rate also corresponded with a decrease in the mass of CO<sub>2</sub> removed from the system. With 25% less flue gas to treat, there was substantially less total CO<sub>2</sub> in the flue gas, so even though the percentage of CO<sub>2</sub> captured increases with the decrease in flow rate, the overall mass of CO<sub>2</sub> absorbed by the solvent decreases because of less CO<sub>2</sub> mass entering the absorber.

Absorber inlet flow rate is presented for all flow rates tested under multiple test conditions in Figures 20 and 21. Figure 20 shows the CO<sub>2</sub> capture as a function of lean pump flow for flue gas flow rates of 60, 75, and 100 scfm with the stripper column

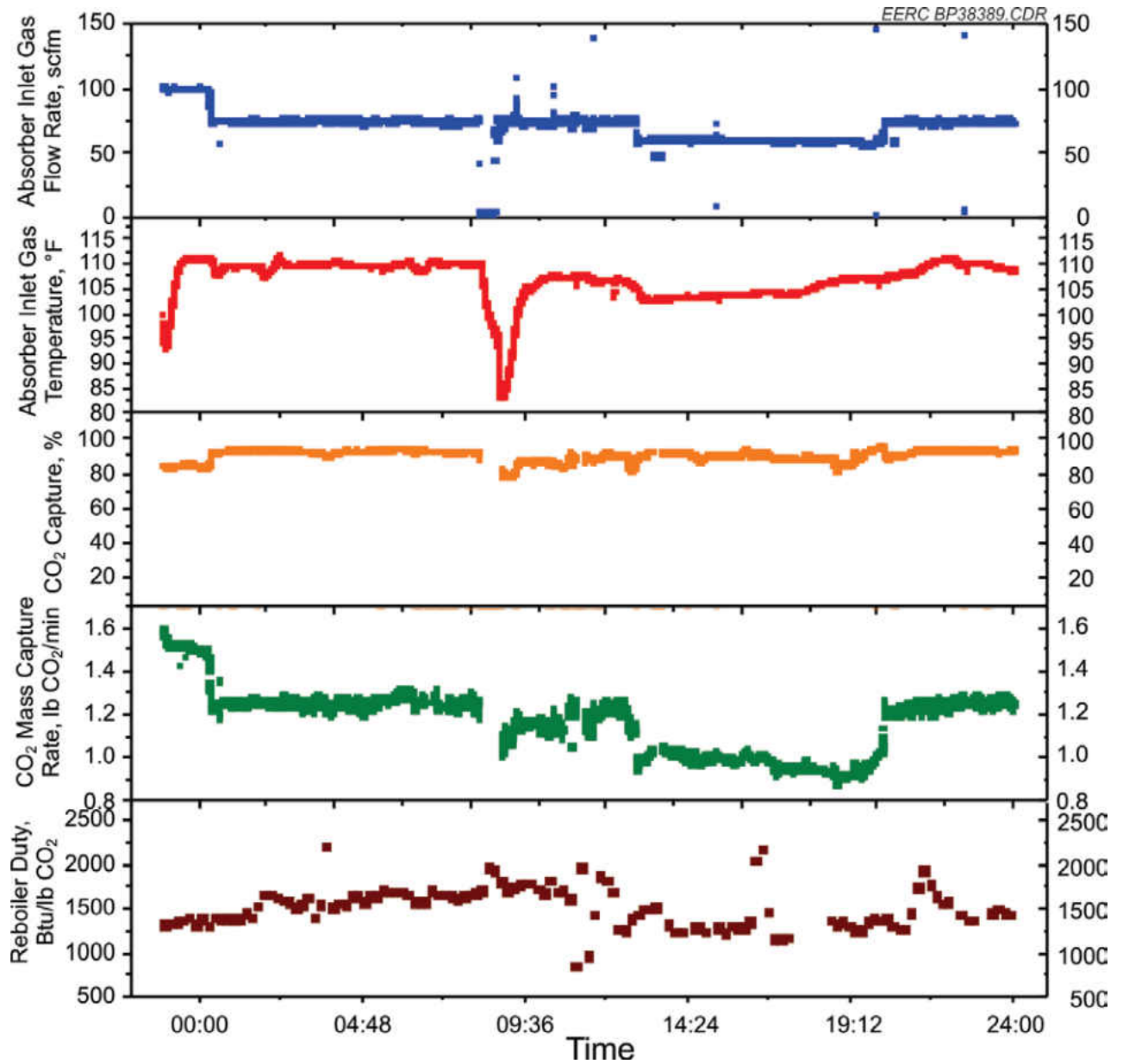


Figure 20. MEA CO<sub>2</sub> capture and absorber inlet properties observed during testing on March 17, 2010.

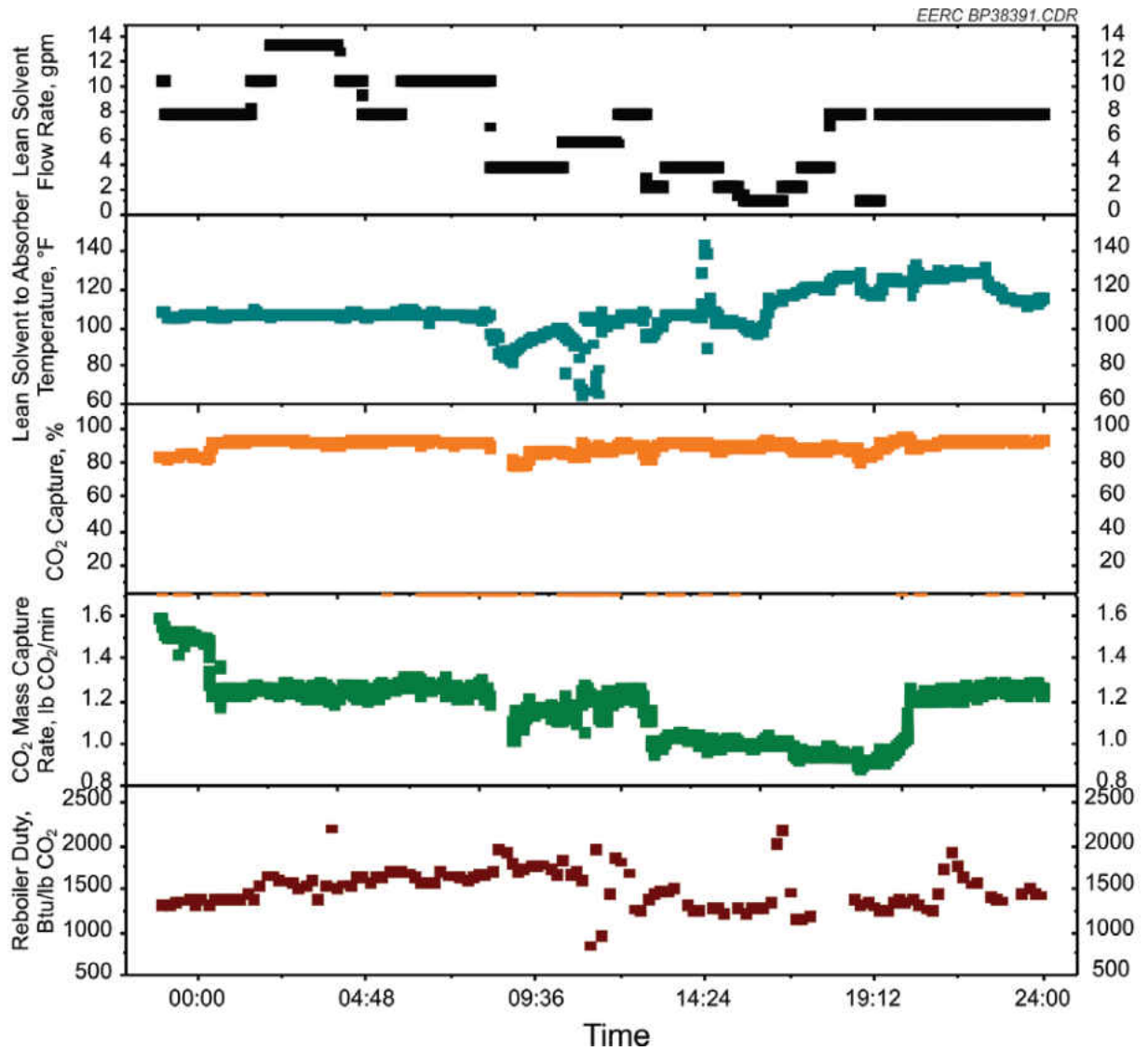


Figure 21. MEA CO<sub>2</sub> capture, reboiler duty, and absorber inlet properties observed during testing on March 17, 2010.

operating at 8 psig static pressure. CO<sub>2</sub> percent removal rates fall between 80% and 94% for all flow rates, with the lowest values corresponding to a flow rate of 100 scfm. At each flow rate, the CO<sub>2</sub> capture trends upward with increasing lean solvent flow. At higher flue gas flow rates, additional lean pump flow was required in order to capture additional CO<sub>2</sub> molecules entering the absorber column. Flue gas flow rate did have an

effect on CO<sub>2</sub> capture, as shown in Figure 22. Several test periods have been condensed to show the flow rate effect in Figure 22. With the system treating less flue gas, typically a smaller amount of solvent flow is required to capture 90% of the incoming CO<sub>2</sub>. At 60 scfm, the lowest absorber flow rate, about 2.6 gpm lean solvent flow was required to meet 90% CO<sub>2</sub> capture. For 75 scfm, about 4 gpm lean solvent flow was required for 90% capture, and for 100 scfm test periods, Figure 22 indicates more than 8 gpm would be required to meet the 90% capture goal. The increase in solvent flow rates was expected because of more CO<sub>2</sub> molecules entering the SASC at higher flue gas flow rates.

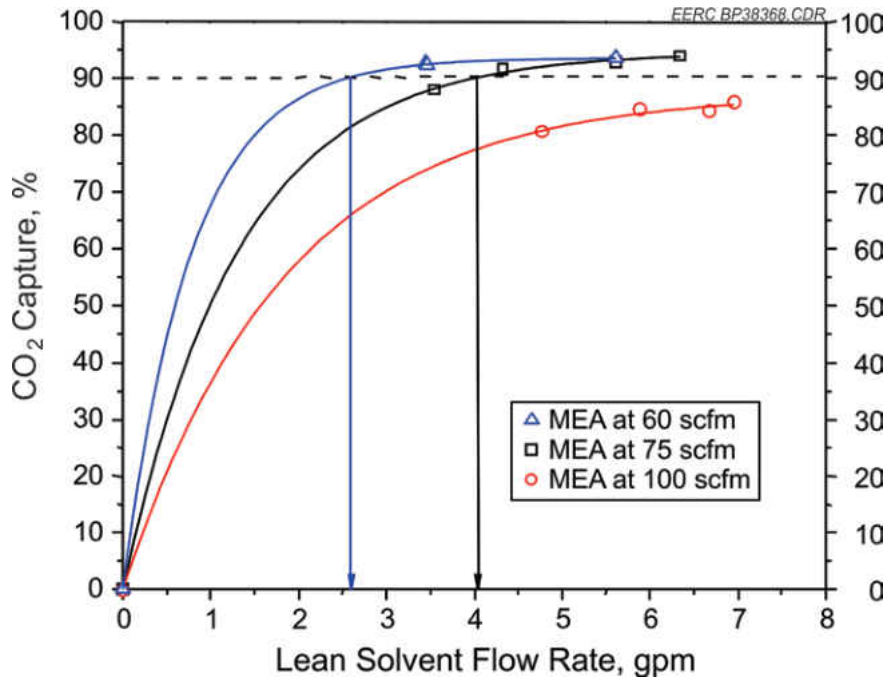


Figure 22. Effect of MEA lean solvent flow rate on CO<sub>2</sub> capture.

### Effects of Stripper Column Pressure

Figure 23 shows the CO<sub>2</sub> capture rate and corresponding liquid-to-gas ratio of the system for the average test period at each stripper column pressure tested. Tests were run with stripper column static pressures of 4, 8, and 12 psig. As pressure on the column was increased, the CO<sub>2</sub> capture rate appeared to increase from 85% up to about 90%. Liquid-to-gas ratio was, on average, higher for tests run at 12 psig than for those run at 4 psig. In commercial operation, it would be advantageous to operate at as high of a pressure as possible to meet sequestration specifications, but because of thermal degradation of solvents, there is a maximum pressure for each formulation.

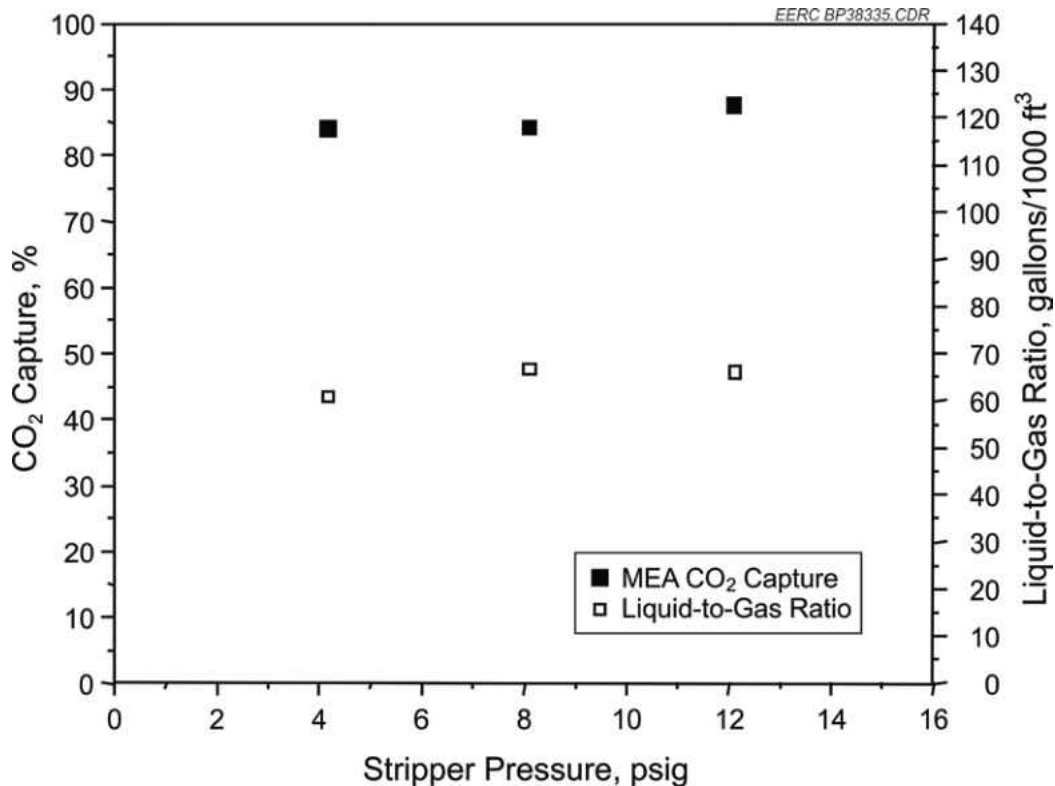


Figure 23. Effect of stripper pressure on MEA CO<sub>2</sub> capture performance.



The observed effect of stripper column pressure has some implications for CO<sub>2</sub> storage equipment energy and size needs. It appears that the stripper column can be run at 12 psig with capture properties similar to tests run at 4 psig. Running at higher pressure in the stripper column could lead to lower compression needs for CO<sub>2</sub> storage, resulting in more favorable economics.

#### *Solvent Regeneration Energy Requirement*

Reboiler duty, as explained in the previous section, is essentially the energy required to regenerate the CO<sub>2</sub> absorption qualities of the solvent in the stripper column. Reboiler duty was recorded for each test period. Regeneration energy required to reach 90% CO<sub>2</sub> capture was dependent upon a number of variables, including the temperature of the solvent entering the column and lean solvent pumping rate. Figure 24 shows that the regeneration energy input requirement for 90% capture at low stripper column pressures generally ranged between 1680 and 1800 Btu/lb CO<sub>2</sub> captured. At 12 psig on the stripper column, the baseline energy input for solvent regeneration to a 90% capture level was between 1775 and 1940 Btu/lb CO<sub>2</sub>. For both high and low pressure on the stripper column, an increase in reboiler duty generally corresponded to an increase in CO<sub>2</sub> capture. This trend appeared to hold for all test periods examined.

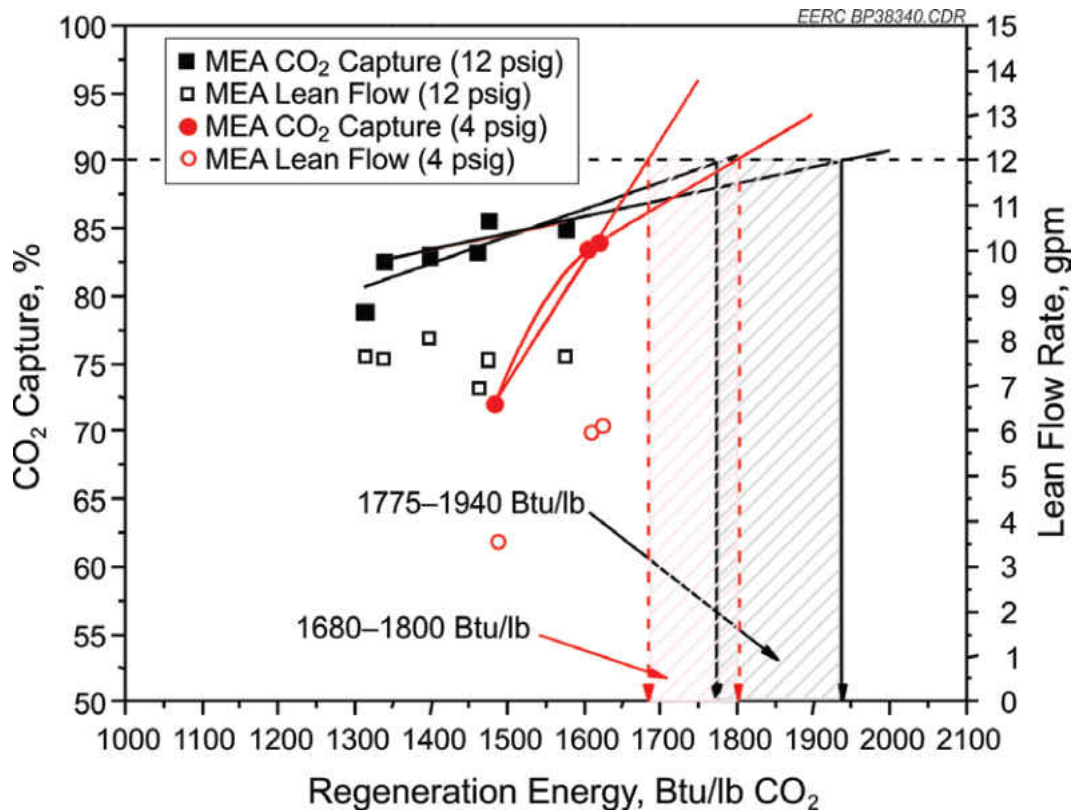


Figure 24. Variation of CO<sub>2</sub> capture with MEA solvent regeneration energy requirements.

#### *Effects of Absorber Inlet Temperature*

Temperature profiles in the stripper and absorber columns are critical in determining CO<sub>2</sub> capture rates. One of the key temperatures in the system was the temperature of the lean solvent entering the absorber. Figure 25 shows the CO<sub>2</sub> capture impact of temperature of the solvent at the absorber inlet. CO<sub>2</sub> capture appears to decrease gradually as the temperature of MEA entering the absorber increases, until it reaches a point where the capture rate drops rapidly. With MEA flowing at 5 gpm, CO<sub>2</sub> capture dropped off around 110°F. A second case, shown with a 20% higher solvent flow rate, appears to have a higher drop-off point in CO<sub>2</sub> capture. The two cases show not only

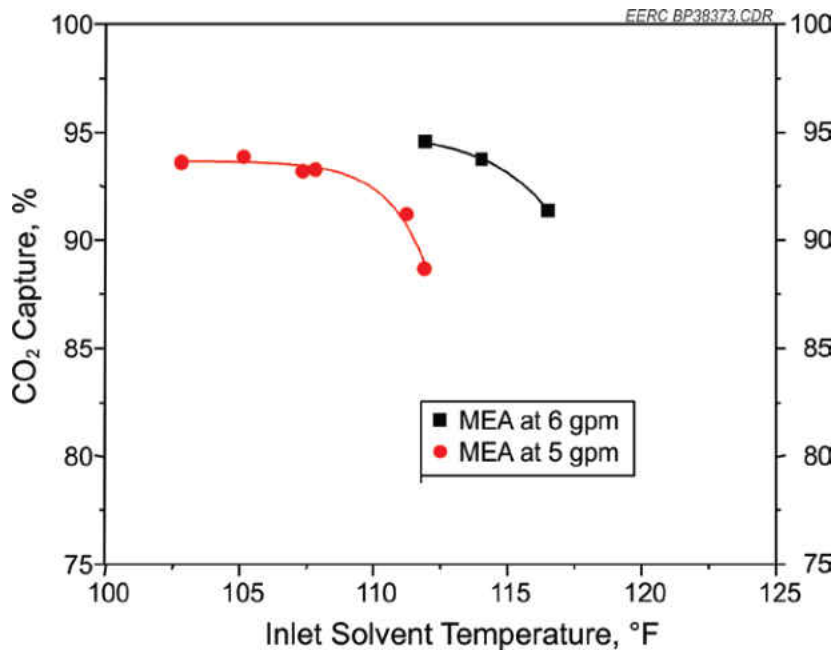


Figure 25. Impact of absorber inlet solvent temperature on CO<sub>2</sub> capture.

that CO<sub>2</sub> capture was dependent upon solvent inlet temperature, but that solvent inlet temperature may have been dependent upon solvent flow rate.

Figure 26 shows the effect of solvent inlet temperature on both CO<sub>2</sub> capture rate and the regeneration energy requirement to reach the 90% capture goal. Test periods for solvent inlet temperatures of 100° and 115°F were plotted. Solvent flow for the two cases presented was relatively consistent, with both lying between 6 and 8 gpm. The high-temperature case was closer to 8 gpm, and the lower inlet temperature case was around 6 gpm.

With both solvent flow rate and regeneration energy input being relatively constant between the two cases, it appeared that solvent inlet temperature was a significant factor in achieving the desired results. The high-temperature case required about 33% more

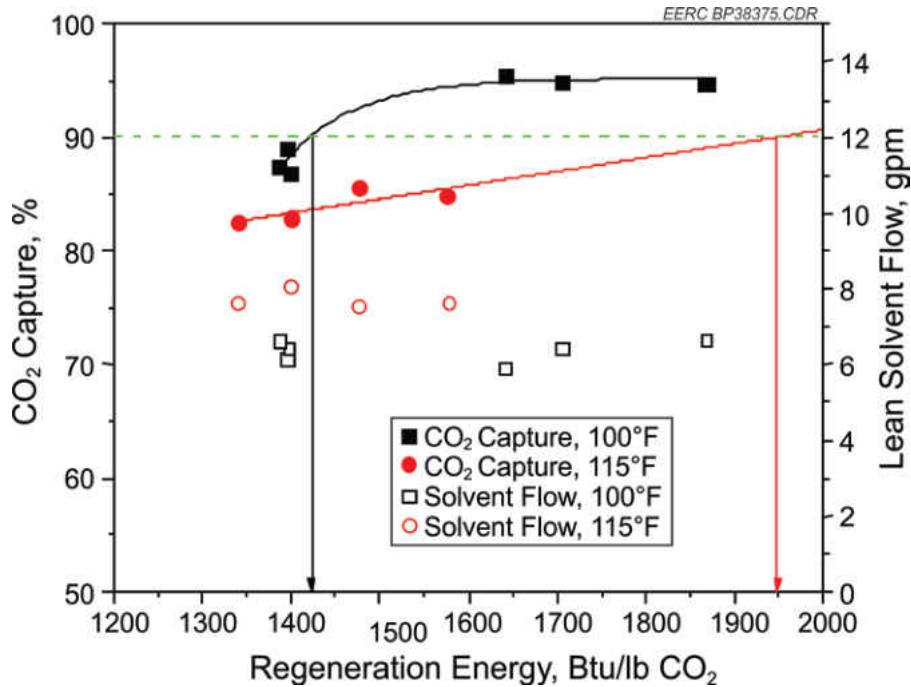


Figure 26. Effects of absorber inlet solvent temperature and regeneration energy on CO<sub>2</sub> capture for MEA.

regeneration energy input to reach 90% capture compared to the low-temperature case. This represents a potentially substantial cost-saving opportunity for the end user in the area of steam use. This is due to achieving higher CO<sub>2</sub> loading capacity at lower temperatures in the absorber.

### *SO<sub>2</sub> Injection Test*

For the first 2 days of testing, the wet scrubber on the CTF removed nearly all SO<sub>2</sub> from the flue gas entering the absorber. SO<sub>2</sub> levels at the absorber inlet were assumed to be about 1 ppm. On the final 2 days of baseline testing, SO<sub>2</sub> was added to the flue gas through a spiking system. The amount of SO<sub>2</sub> added to the absorber was regulated using a Matheson Tri-Gas tube-cube-style flowmeter. SO<sub>2</sub> levels of 10, 20, and 50 ppm were introduced to the absorber column. Figure 27 shows the SO<sub>2</sub> injection levels

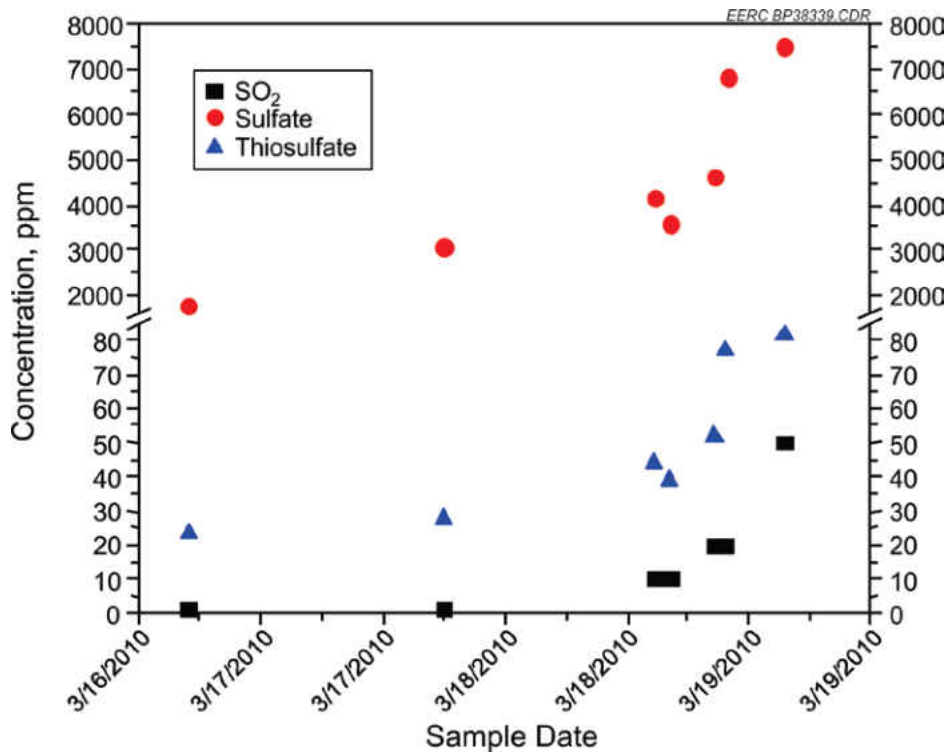


Figure 27. Sulfate and thiosulfate concentration at various SO<sub>2</sub> injection levels.

for the metered tube cube readings and the SO<sub>2</sub> analyzer readings as well as the absorber inlet analyzer. The data show a direct correlation between the SO<sub>2</sub> concentration and the sulfur-based HSS present in the absorber and stripper columns. The trends of the data are similar in slope and emphasize the need to keep flue gas SO<sub>2</sub> concentrations as low as possible. Low SO<sub>2</sub> concentrations allow more of the solvent in the SASC to interact with the CO<sub>2</sub> instead of forming a sulfur-based HSS which improves CO<sub>2</sub> capture and reduces the amount of lean amine that needs to be added to the solution.

## MEA Sample Analysis

### Free Amine in Lean MEA Solutions

The concentration of free amine in lean MEA solutions was determined using an acid-base titration method using aqueous HCl as titrant. A summary of the results is shown in Figure 28, and the full results of the 25 samples that were selected and analyzed are presented in Table A3-1 in Appendix A3. The results show that the concentration of free amine in the absorber ranged from about 17 to 20 wt% and that in the stripper ranged from about 20 to 24 wt%; the initial concentration was determined to be 29.7 wt%. The sharp drop between the initial amine concentration and Day 1 of the test is a reflection of the fact that fresh amine solvent without any flue gas exposure contains no absorbed CO<sub>2</sub> and other compounds, but after Day 1 of the test, the solution becomes lean (i.e., loaded with CO<sub>2</sub>), and so the concentration of free amine in lean solution is much lower than for

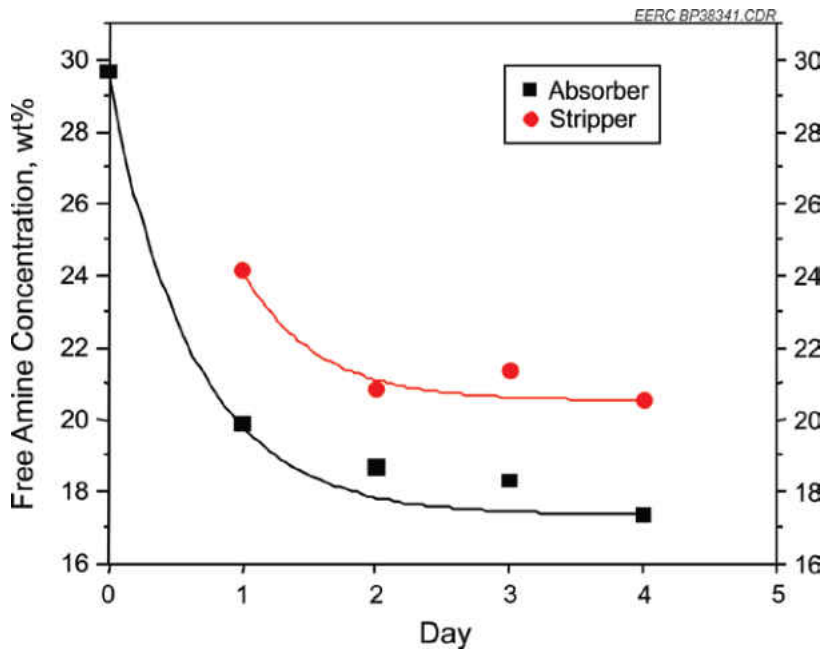


Figure 28. Concentration of free amine in lean MEA solutions.

fresh amine solution. These results indicate that our titration protocol was reasonable and relatively accurate for these samples, given that similar approaches reported previously by Cummings et al. (20) have shown overestimates as much as 100% for free amine in lean amine solution samples. Our relatively accurate results are not surprising since aqueous sodium hydroxide solution was not used in our study to combat HSS as was the case in the Cummings et al. study and as commonly practiced in some power plants. By not using NaOH, the interference of  $\text{OH}^-$  on the free amine endpoint in a potentiometric titration is removed. However, weak acid anions such as formate, acetate, and carbonates and bicarbonates also consume some of the HCl during titration and, thus, present some difficulty. These weak acid anions have lower basicity than free amines, and as such, they have a lower endpoint than the free amine; hence, the two endpoints can be detected separately. Also discernible from Figure 28 is the fact that the concentration of free amine in the absorber was lower than that in the stripper, which is expected, since free amine is regenerated in the stripper. An important trend observed from the plots is the exponential decrease in the free amine concentration with time, which correlates well with increasing trends observed for HSS formation in solution.

#### *Bound Amine in Lean MEA Solutions*

The concentration of bound amine in lean MEA solutions was also determined by titration using aqueous NaOH solution as the titrant. The endpoints in these base titrations were difficult to detect because they were not sharp; hence pH curves were used to obtain the reference pH at the endpoint of 11.5. Using this reference pH to mark the endpoint, the concentrations of bound amine in the sample solutions were determined. Because the titration quantifies all amine cation species in solution, the

amount of amine cation obtained for the first day of the test was used as baseline and subtracted from values of subsequent days to obtain what is truly bound and not regenerable. The results are summarized in Table 11 for the absorber and stripper; a complete set of results for the 25 samples that were selected and analyzed is shown in Table A2-2 of Appendix A3. It appears that the concentration of bound amine in both the absorber and the stripper decreases roughly exponentially with time, similar to the trends observed for free amine. The data show that the base titration is a poor indicator for bound amine during this test and is not consistent with the HSS data.

*Inorganic Anions in Lean MEA Solutions*

The results of inorganic anion determinations, including sulfates, thiosulfates, chlorides, nitrites, and nitrates, are shown graphically in Figure 29. The complete results are provided in Table A3-3 of Appendix A3. In all the samples collected during MEA testing, very low concentrations of nitrite and nitrate ions were observed, which is consistent with the low NO<sub>x</sub> levels in the flue gas (~ 2 ppm on average) during the test. It is also possible that the 5-day test period was not long enough to have observed significant accumulations of these ions because

Table 11. Bound Amine in Lean MEA.

Day	Absorber Bound Amine, wt%	Stripper Bound Amine, wt%
1	0.00	0.00
2	-1.66	-1.10
3	-2.10	-2.00
4	-4.54	-2.93



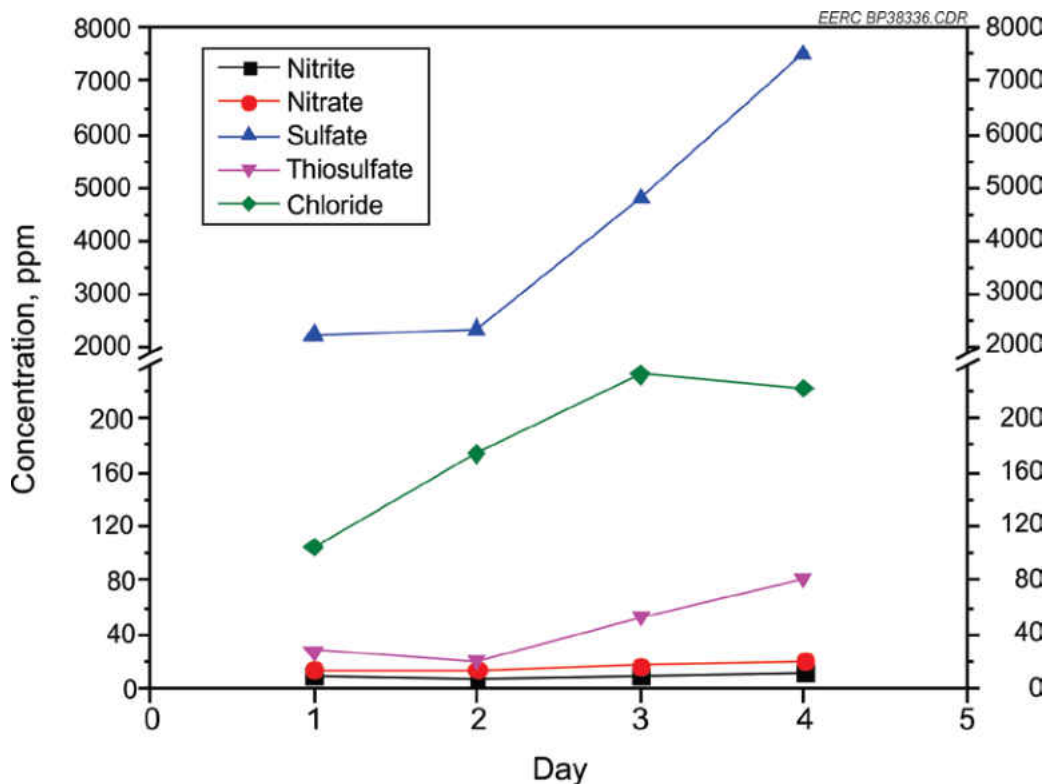


Figure 29. Concentration of inorganic anions in lean MEA solutions.

of baseline  $\text{NO}_x$  concentration. Over the 5 days of testing, the amounts of sulfates, thiosulfates, and chlorides slowly accumulated in the system, with the amounts in the absorber and stripper remaining similar. The increase in the amounts of sulfates and thiosulfates on the third and fourth day of testing correspond to the injection of about 10–50 ppm of  $\text{SO}_2$  in the flue gas as shown in Figure 30. At the beginning of the tests,  $\text{SO}_2$  levels were maintained at baseline ( $\sim 1$  ppm), and only minimal amounts of these HSS were observed. Although the chloride ion level was not directly measured in the flue gas entering the absorber, chloride levels can be compared with coal chlorine level, which is

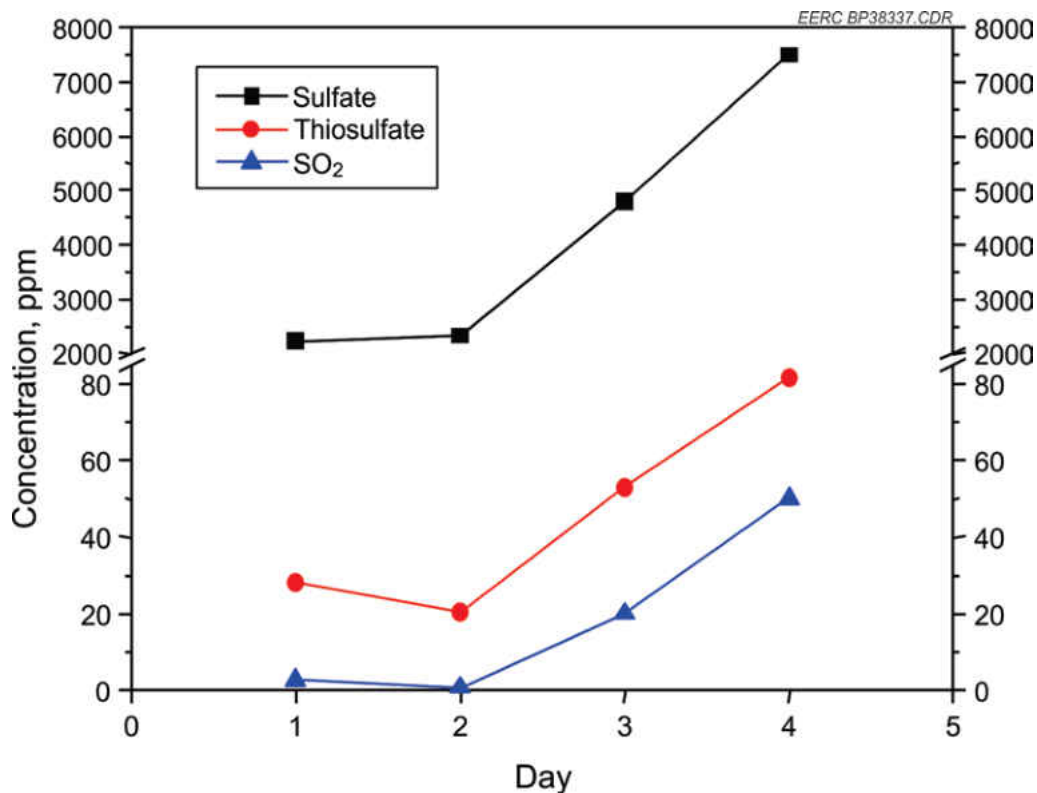


Figure 30. Concentration of sulfate and thiosulfate salts in lean MEA solutions during SO<sub>2</sub> injection tests.

typically about 20 ppm for the Antelope PRB subbituminous coal used in this test. The amount of chloride ion in solution was in the range about 100–220 ppm during the test period which suggests that a significant amount of the chloride in the flue gas formed a HSS and remained in the SASC system.

#### *Organic Anions in Lean MEA Solutions*

Formate, acetate, and oxalate ions were the three organic anions detected in MEA samples. The results are summarized in Figure 31, together with flue gas O<sub>2</sub> concentrations. A complete table of the data is provided in Table 3-4 in Appendix A3. These anions were present in rather small amounts, and the amounts in the stripper and

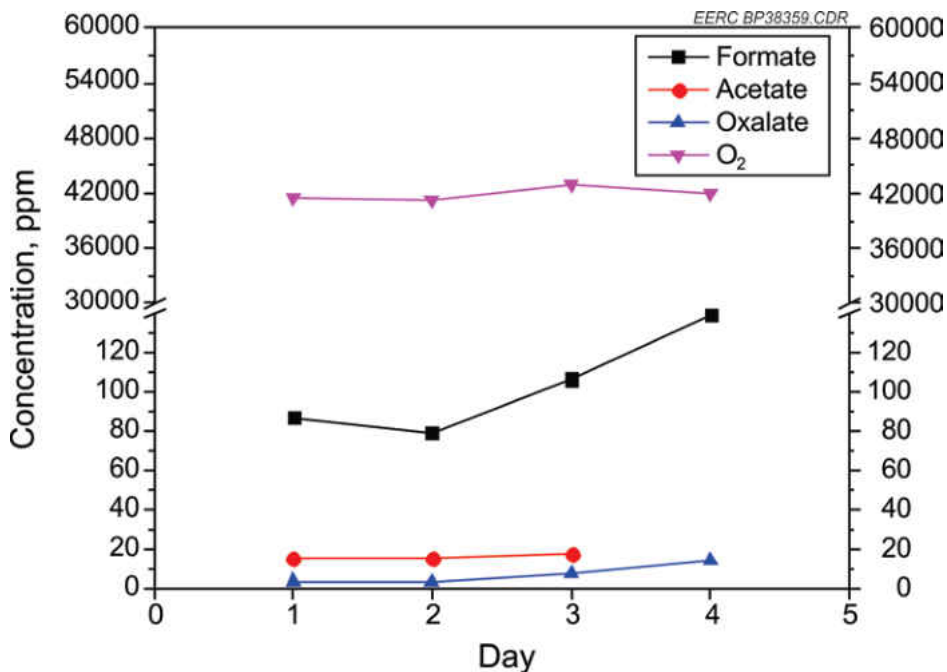


Figure 31. Concentration of organic anions in lean MEA solutions.

absorber were similar. In general, the concentrations increase with time which indicates a gradual buildup of HSS of these anions. Formate anions appeared in the largest concentration, ranging from about 80 to 130 ppm, while the amounts of acetate and oxalate were each less than 20 ppm. It is not surprising to find larger amounts of formate compared to acetate and oxalate because formate anions are the first compounds formed from oxidative degradation of MEA; acetate and oxalate are formed from subsequent degradation steps after formate anions are formed.

#### *Trace Metals in Lean MEA Solutions*

Trace metal concentrations observed in lean MEA solutions were generally low. These results are presented in Figure 32 for the samples that were selected and analyzed. The full data set is presented in Appendix A3 (Table A3-5). The trace metals that were

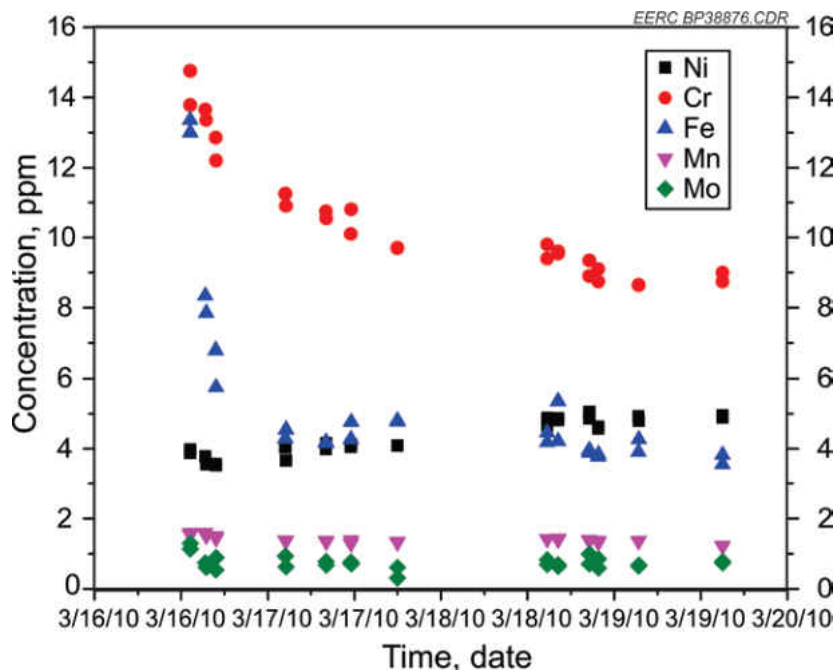


Figure 32. Concentration of trace metals in lean MEA solutions.

analyzed include typical stainless steel components like Ni, Cr, Fe, Mn, and Mo. Of these, only Cr and Fe had concentrations that ranged from about 8 to 15 ppm and 4 to 8.5 ppm, respectively; both decrease exponentially with time. The nickel concentration was much lower, ranging from about 3 to 5 ppm and increasing linearly with time. The concentration of Mn and Mo were each less than 2 ppm and appeared to be relatively constant throughout the test period. The amounts of Mn and Mo are consistent with the fact these elements are only minor components of stainless steels, with Ni, Fe, and Cr being the major constituents. The concentrations in the absorber were similar to those seen in the stripper. It is unclear why the amounts of Cr and Fe decrease with time in this study. Decreasing trends observed for Cr and Fe are rather surprising because it was expected that the longer the process equipment was exposed to HSS building up in

solution, the greater the amount of corrosion products to be observed. Although some studies have shown that the formation of high amounts of sulfates, thiosulfates, and other inorganic anions may inhibit corrosion rate for carbon steel (21), the steel used in the process equipment for this study was stainless steel. Given this previous study, the trends observed for Fe and Cr may be consistent with the relatively high sulfate concentrations observed as discussed in the previous section. Also, such low levels of corrosion possibly reflect the relatively short testing time and, hence, the low amounts of corrosive HSS in solution that make it difficult to observe significant effects. The low amounts of HSS observed are also due to the fact that the flue gas composition had relatively low amounts of  $\text{NO}_x$  and  $\text{SO}_x$ .

#### *Major Elements in Lean MEA Solutions*

Lean MEA solutions were also screened for other elements such as Al, Ca, K, Mg, and Na using ICP–AES. Figure 33 displays a summary of the results, and complete data are presented in Appendix A (Table A3-6). These are the alkali and alkaline-earth elements typically found in low-rank coals such as lignite; aluminum is often part of the silicate minerals. If these are released into solution as ions, they may impact the solution chemistry. These results indicate that, as expected, Na was present in the highest concentration, averaging about 100 ppm, followed by Al with an average concentration of about 24 ppm. Ca, K, and Mg were present in much smaller concentrations, which were less than 20 ppm. As in the case of trace metals, levels of these metals in absorber were similar to those in the stripper. These concentrations are still very low to have any significant impact on the chemistry and/or the integrity of the amine solvent. Such results are to be expected since the ESP used to control particulates has a removal efficiency of

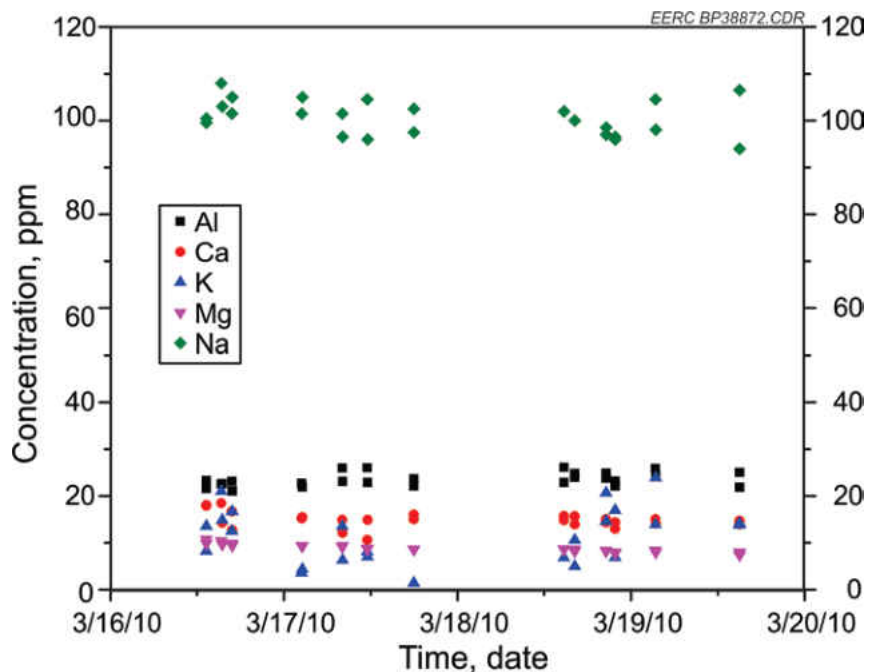


Figure 33. Concentration of major elements in lean MEA solutions.

>99.9%. As a result, residual amounts of particulates bearing some of these elements that contact the solution are very low. However, given prolonged exposure time such as in the real power plant, levels of such elements could build up and become problematic to the scrubbing system.

#### *CO<sub>2</sub> Loading in Lean MEA Solutions*

The results of CO<sub>2</sub> loading in lean MEA solutions are presented in Figure 34 for absorber and stripper samples collected during the test period. The full results are provided in Appendix A3, Table A3-7. These results were obtained by determining the total inorganic carbon (TIC) content of the samples using a TOC analyzer. This analysis gives data on the total carbon (TC) and TIC, and the TOC is obtained by difference. For the purpose of this study, only the TIC data are of relevance, which is made up of

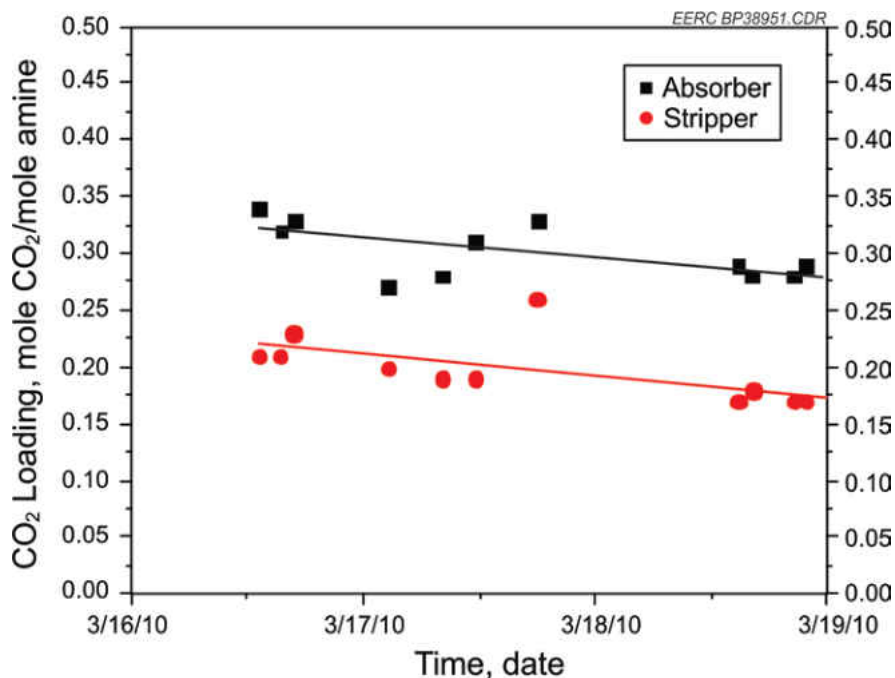


Figure 34. CO<sub>2</sub> loading in lean MEA samples.

carbonates, bicarbonates, and the -COO moiety of the carbamate complexes formed between CO<sub>2</sub> and the amine.

To determine the total amine in the solution, a potentiometric titration technique was used. The total free amine and total amine cations were determined and added together to get the total amine in the sample. The total amine from the titrations and the total CO<sub>2</sub> from TOC analysis were then used to calculate the CO<sub>2</sub> loading for the sample as the ratio of the total amount of CO<sub>2</sub> to that of amine. The average CO<sub>2</sub> loading in the absorber was in the range of about 0.28–0.32, while the average loading in the stripper was in the range 0.16–0.22. These results are consistent with the fact that CO<sub>2</sub> is absorbed by the solution in the absorber and released from solution in the stripper. The plots also indicate that the CO<sub>2</sub> loading for the absorber and the stripper show a decreasing trend

with time, which is consistent with the gradual buildup of HSS in solution that takes up some of the free amine that would otherwise absorb more CO<sub>2</sub>.

### Solvent Results & Comparison

Three advanced amine solvents and 30 wt% MEA used as baseline were tested in the EERC's pilot-scale postcombustion CO<sub>2</sub> capture system. Data collected during tests were reduced and analyzed to draw comparisons about the differences in performance among the solvents. Several test parameters, including reboiler duty, solvent flow rate, stripper column static pressure, absorber inlet temperature, and flue gas flow rate were used in making direct comparisons across solvents.

#### *Effects of Reboiler Duty*

The reboiler duty is a measure of the heat input required to regenerate the rich solvent by driving off the absorbed CO<sub>2</sub>. Reboiler duty (regeneration energy) had a significant effect on the CO<sub>2</sub> capture performance of each solvent. Figure 35 displays the differences in performance for two advanced solvents, H3-1 and MDEA+PZ, and MEA. Each data point shown in the plots represents a test period where variables were kept relatively constant until a steady CO<sub>2</sub> capture rate was reached. Each case was run at a relatively low stripper column static pressure of about 4–6 psig.

Generally, the data show that an increase in regeneration energy corresponds to an increase in CO<sub>2</sub> capture for all solvents. The maximum CO<sub>2</sub> capture achieved for MEA and MDEA+PZ was 85% and about 88%, respectively, which corresponds to regeneration energy of about 1600 Btu/lb for MEA and about 1450 Btu/lb for MDEA+PZ; H3-1 solvent attained the 90% CO<sub>2</sub> capture target with regeneration energy



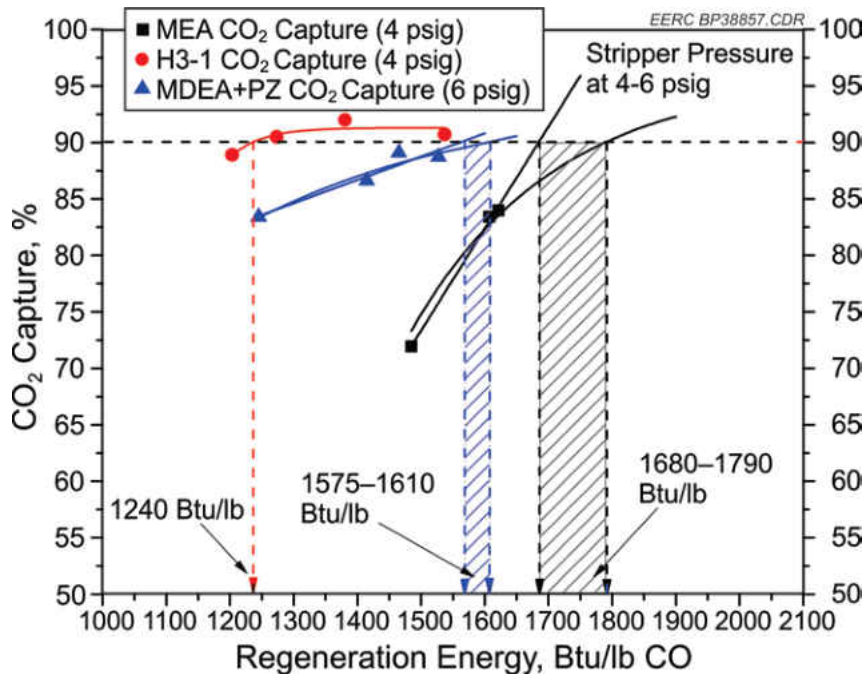


Figure 35. Regeneration energy required to meet 90% CO<sub>2</sub> capture for H3-1, MDEA+PZ, and 30 wt% MEA at 4–6 psig static pressure.

of about 1240 Btu/lb. The regeneration energy required to reach 90% CO<sub>2</sub> capture target for MEA and MDEA+PZ was estimated by extrapolating the curves to the 90% level. The values obtained were in the ranges of 1680–1790 Btu/lb CO<sub>2</sub> for MEA and 1575–1610 Btu/lb for MDEA+PZ. These results indicate that based on the 90% CO<sub>2</sub> capture target, H3-1 solvent has the lowest regeneration energy demands compared to MDEA+PZ and MEA; MDEA+PZ’s energy input requirement is, in turn, lower than that of MEA. Specifically, H3-1 solvent appears to require about 35%–45% less energy than MEA, and MDEA+PZ requires about 5%–12% less energy than MEA. At low stripper column static pressures, H3-1 solvent appeared to require substantially less energy input to regenerate the rich solvent stream than both MDEA+PZ and MEA. Huntsman additive

solvent was not tested following the same protocol as for H3-1 and MDEA+PZ, so a direct comparison of the effects of reboiler duty among all three advanced solvents was not possible.

The estimation approach used to obtain the reboiler duty ranges for MEA is based on linear and exponential extrapolation schemes to the 90% mark, since corrected data from the pilot plant tests showed less than 90% CO<sub>2</sub> capture as opposed to the uncorrected raw data. Two trend lines were used to obtain the lower and upper limits, where the linear trend line afforded the lower limit value and an exponential trend line, with a linear extrapolation, gave the upper limit value. However, for MDEA+PZ, the trend lines extended across the 90% mark, and no additional extrapolation was needed to estimate the reboiler duty range for 90% CO<sub>2</sub> capture.

Comparisons at a higher stripper column pressure of 12 psig for the same CO<sub>2</sub> capture target of 90% are shown in Figure 36, where the regeneration energy for MEA was monitored at a solvent flow rate of about 7.5 gpm and variation in H3-1's regeneration energy was obtained at two solvent flow rates: 3.5 and 5 gpm. The results also show that, similar to the case of the 4–6 psig static pressure, H3-1 attains 90% CO<sub>2</sub> capture at much lower regeneration energy input of about 1475 Btu/lb with a solvent flow rate of 3.5 gpm compared to a 30 wt% MEA solution with a regeneration energy of about 1775–1940 Btu/lb (estimated by extrapolation) at 7.5 gpm. H3-1 essentially reaches ~95% CO<sub>2</sub> capture maximum at 5 gpm flow rate, 12 psig static pressure, and a regeneration energy of about 1500 Btu/lb; any further increase in regeneration energy did not have any significant effect on CO<sub>2</sub> capture.

As with the 4 psig stripper column cases, data from the MEA test run were assumed to continue one of two possible linear trends through 90% capture. A probable regeneration energy requirement window for 90% CO<sub>2</sub> capture for MEA was found by extrapolating the data points between 80% and 85% CO<sub>2</sub> capture. This gave an estimated range of 1775 to 1940 Btu/lb CO<sub>2</sub> captured.

Figure 36 also presents a series of test periods illustrating the CO<sub>2</sub> capture for H3-1 at two different solvent flow rates. The high flow case had solvent flow rates ranging from 4.5 to 6 gpm, and the low lean flow case had flow rates in the range of 3.5 to 4 gpm. The data suggest that the reboiler duty rate was much higher than necessary to reach the

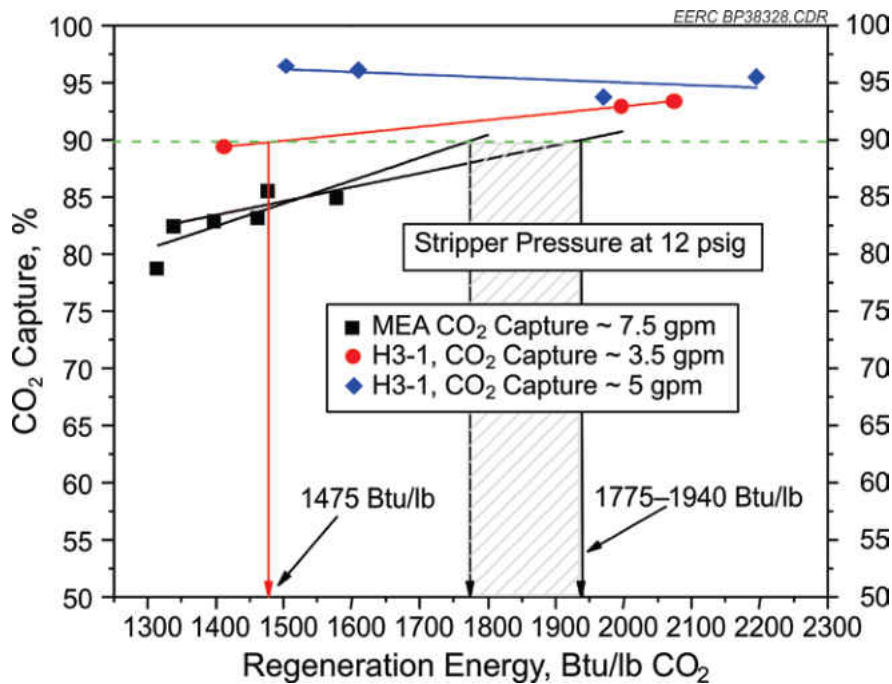


Figure 36. Regeneration energy required to meet 90% CO<sub>2</sub> capture for H3-1 and 30 wt% MEA at 12 psig static pressure.

90% capture benchmark for the high flow rate at a stripper column static pressure of 12 psig. Comparing with the low lean flow case for H3-1, the regeneration energy requirement of 1475 Btu/lb CO<sub>2</sub> to reach 90% CO<sub>2</sub> capture at low flow rates showed a CO<sub>2</sub> capture rate of nearly 97% at high lean flow. The MEA case presented in Figure 36 had a solvent flow rate of about 8–9 gpm, higher than either H3-1 case shown, yet still required about 20%–30% more regeneration energy input to reach the 90% capture goal.

#### *Effect of Liquid to Gas Ratio*

The effect of solvent flow rate on CO<sub>2</sub> capture was investigated by calculating the liquid-to-gas ratios, i.e., amount of solvent in gallons per 1000 cubic feet of flue gas, and determining the capture capacity for a given liquid-to-gas ratio. The results are plotted in Figure 37. As shown in the plot, H3-1 has the smallest liquid-to-gas ratio needed to attain 90% CO<sub>2</sub> capture (i.e., ~29 gallons/1000 ft<sup>3</sup>), followed by MEA (~55 gallons/1000 ft<sup>3</sup>); MDEA+PZ has the highest solvent demands (~129 gallons/1000 ft<sup>3</sup>) to reach 90% CO<sub>2</sub> capture. Thus H3-1 uses about 47% less solvent than MEA while MDEA+PZ uses more than double the amount of solvent than MEA to achieve 90% CO<sub>2</sub> capture. Based on these results and depending on the cost of the amine solvents, this could have a significant impact on the overall process economics.

#### *Free Amine Comparison*

The concentrations of free amine in lean solvent solutions were determined for all solvents during testing. Although the initial fresh amine concentrations were different for the different solvents, trends in the free amine contents with time were determined for

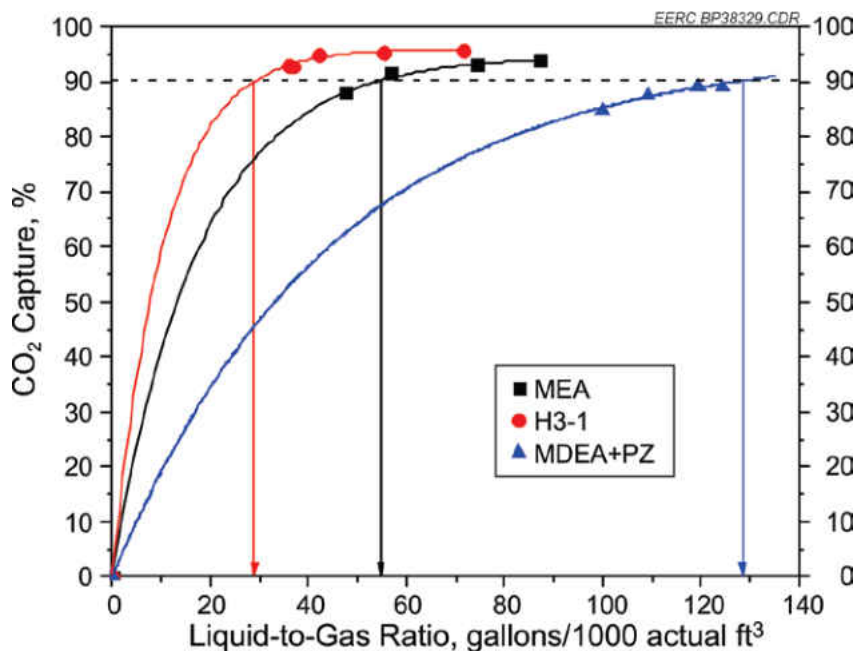


Figure 37. Effects of liquid flow rate on CO<sub>2</sub> capture for H3-1, MDEA+PZ, and MEA.

each solvent and are shown in Figure 38. These plots indicate that the free amine content in each solvent was decreasing roughly exponentially from the start to the end of each test period, except for the MDEA+PZ solvent which showed a slight increase. Because of the difficulty in the titration of MDEA+PZ solution, more accurate methods will be developed in Phase II to improve confidence in the trend. MEA which had similar starting fresh amine concentrations as Huntsman additive showed lower free amine content in lean solutions than Huntsman additive.

### *HSSs*

HSSs are characterized in terms of the amount of the corresponding organic and inorganic anions formed in solution. The inorganic anions result from reactions of NO<sub>x</sub>, SO<sub>x</sub>,

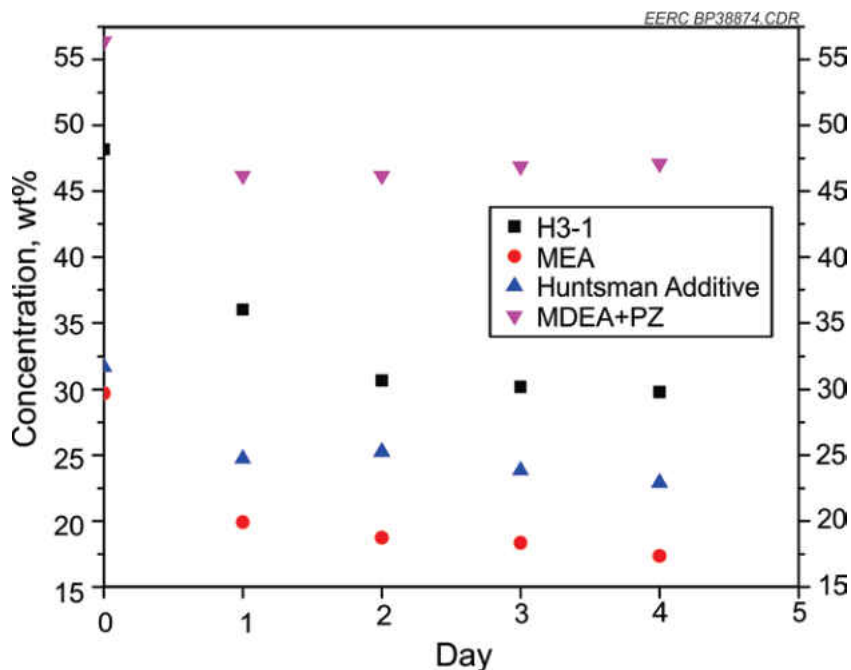


Figure 38. Free amine comparisons for H3-1, MEA, Huntsman additive, and MDEA+PZ.

chlorides and, possibly, cyanides in the flue gas, while organic anions are the result of oxidative degradation products that are often in the form of organic carboxylic acids.

Sulfate, thiosulfate, and chloride anions were present in each of the solvents tested and provide a data set to compare the performance of each solvent tested. Figures 39–41 display the concentrations of each anion for the three different solvents. For each of the anions, the MEA solvent had much higher anion concentrations and was typically 3 times higher than H3-1 anion concentrations. The sulfate and thiosulfate curves increased sharply on the last days of testing, which indicates an exponential increase in anion concentration. These sharp increases for all solvents were due to additional amounts of  $\text{SO}_2$  injected into the flue gas upstream to the absorber. In order to maintain the scrubbing

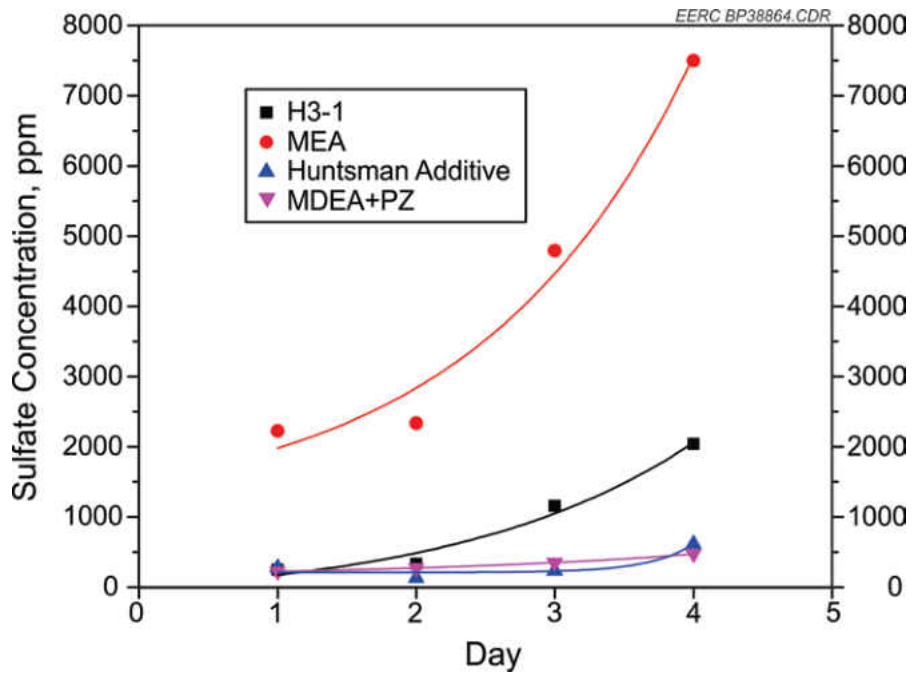


Figure 39. Comparative analysis of sulfate concentrations for MEA, H3-1, Huntsman additive, and MDEA+PZ.

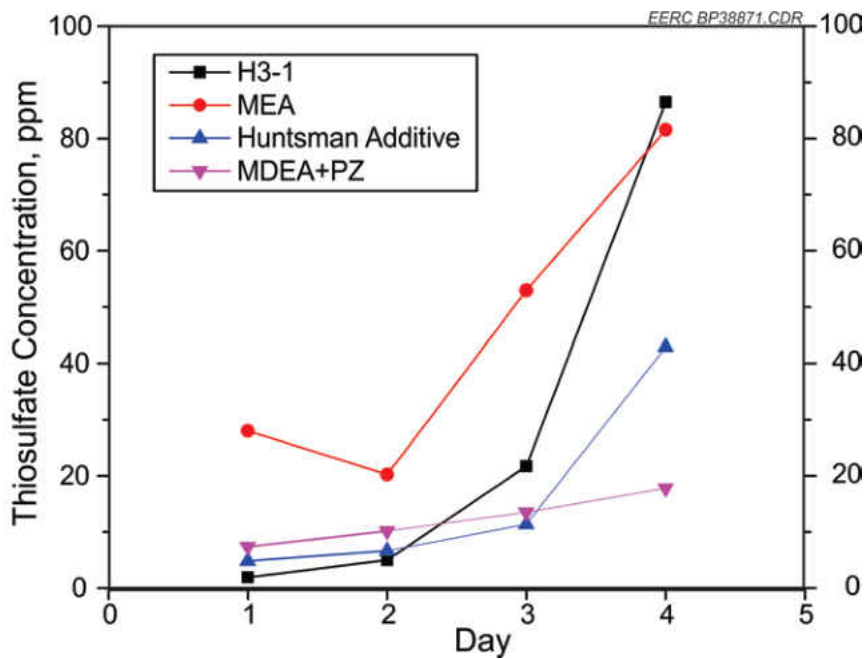


Figure 40. Comparative analysis of thiosulfate concentration for MEA, H3-1, Huntsman additive, and MDEA+PZ.

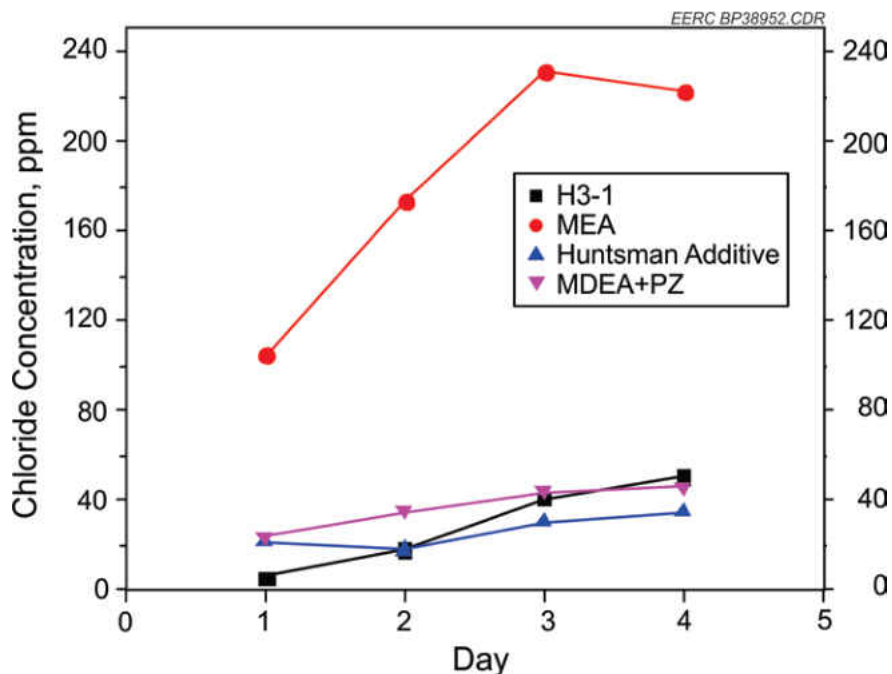


Figure 41. Comparative analysis of chloride concentrations for MEA, H3-1, Huntsman additive, and MDEA+PZ.

capacity of the solvent, additional fresh MEA would need to be added to the system as well as the amine solutions reclaimed, which would result in increased operational costs.

H3-1 appears to have performed much better than MEA, with anion concentrations approximately 50% lower than the MEA solvent. The thiosulfate trend for H3-1 increased much faster than either MEA or Huntsman additive. This is likely due to differences in the solution chemistry which leads to an increase in sulfate oxidation to thiosulfate.

Huntsman additive performed best with respect to HSS formation. The slopes of the curves for Huntsman additive were also shallower, which suggests that longer run times are possible with a given batch of solvent, thereby reducing the amount of fresh



solvent that must be added to the system. This offers a significant cost savings because MDEA+PZ is one of the most expensive variables in the CO<sub>2</sub> capture process.

MDEA+PZ solvent behaves similarly to Huntsman additive in terms of HSS levels and trends.

### Corrosion Products

Corrosion was monitored in this study by analyzing the test sample solutions for typical trace metals found in stainless steel such as Ni, Cr, Fe, Mn, and Mo. Figures 42–46 show the level of trace metals obtained for the four solvents tested. As shown in these

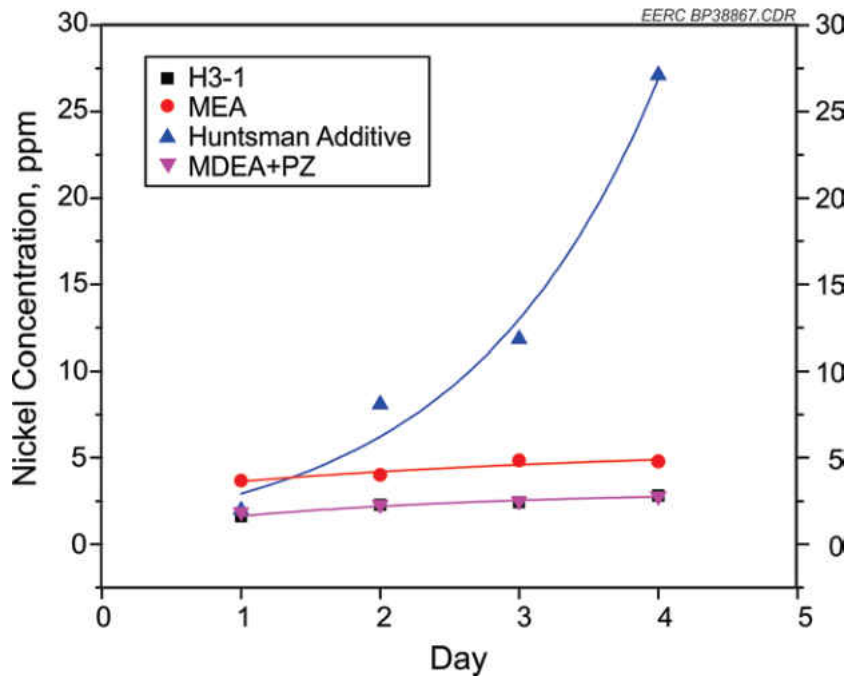


Figure 42. Comparative plot of nickel concentrations for MEA, H3-1, Huntsman additive, and MDEA+PZ.

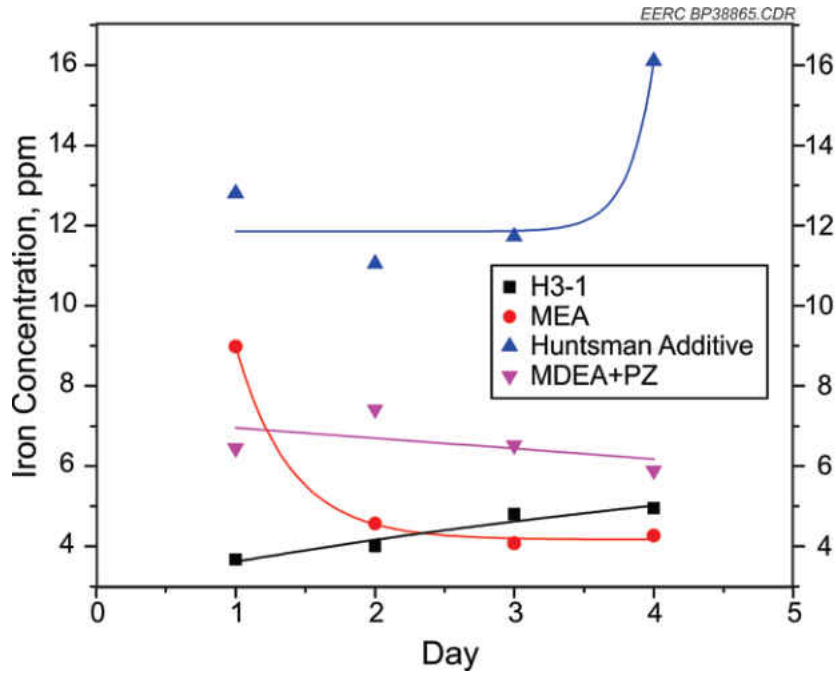


Figure 43. Comparative plot of iron concentrations for MEA, H3-1, Huntsman additive, and MDEA+PZ.

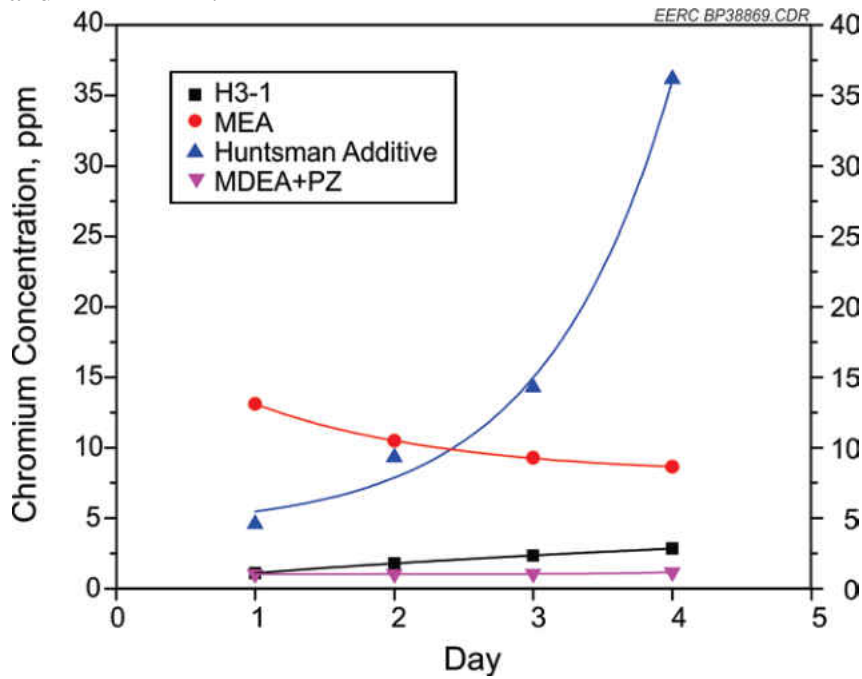


Figure 44. Comparative plot of chromium concentrations for MEA, H3-1, Huntsman additive, and MDEA+PZ.

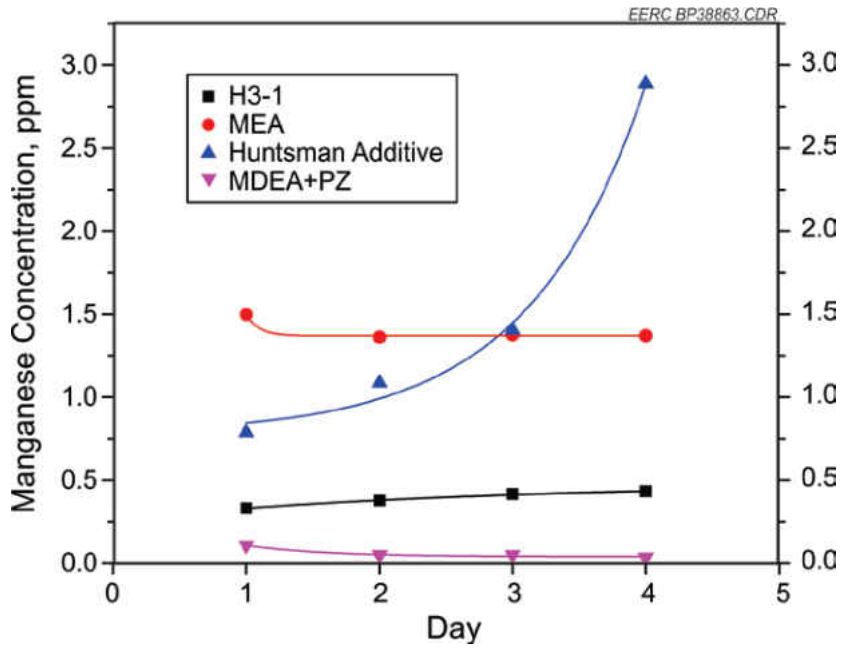


Figure 45. Comparative plot of manganese concentration for MEA, H3-1, Huntsman additive, and MDEA+PZ.

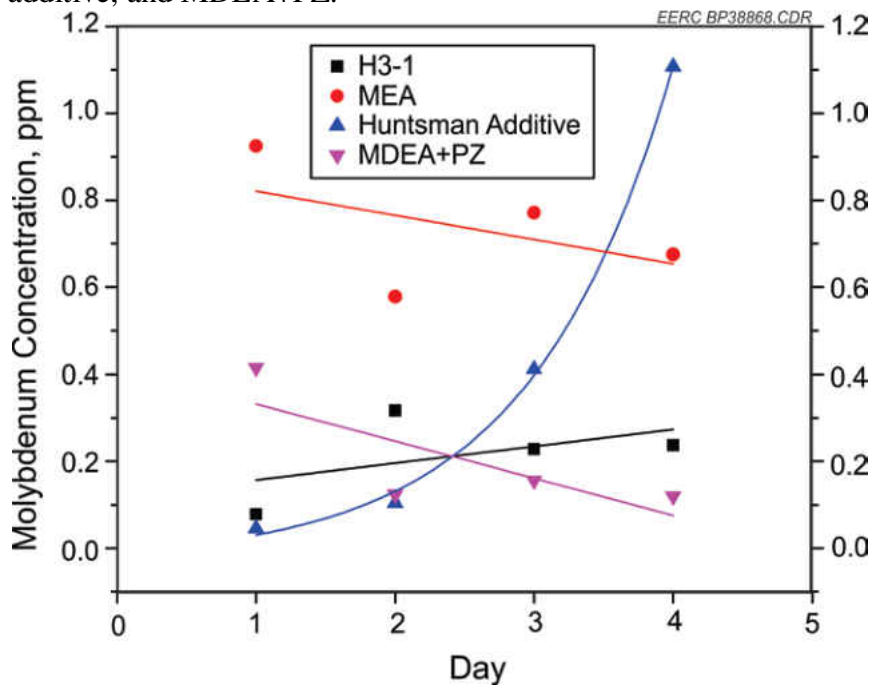


Figure 46. Comparative plot of molybdenum concentration for MEA, H3-1, Huntsman additive, and MDEA+PZ.

figures, Huntsman additive appears to yield the highest concentrations of all trace metals compared. All four solvents show an increasing trend of trace metal concentrations with time, with Huntsman additive's Ni trend rising sharply exponentially. The Cr and Fe concentrations decrease exponentially with time in MEA samples, while they increase with time in H3-1.

### *CO<sub>2</sub> Loading*

Huntsman additive samples. MDEA+PZ Fe concentration decreased linearly with time, and the Cr level was relatively steady throughout the duration of the test. The amounts of Mn and Mo in MEA samples exhibit an almost constant and a decreasing trend, respectively, while in H3-1 and Huntsman additive, the amounts show increasing trends. In MDEA+PZ, the amount of Mn is steady, while the amount of Mo decreases with time.

H3-1 solvent and MDEA+PZ have the lowest concentrations of all trace metals analyzed, typically less than 5 ppm; MEA has low- to midlevel amounts of trace metals; and Huntsman additive shows the highest amounts of the trace metals. The major difference in MEA test conditions compared to those of Huntsman additive is the amount of NO<sub>x</sub> and SO<sub>x</sub> added to the flue gas stream upstream to the absorber. Considering that MEA had the highest amount of sulfate HSS anions in solution samples, the high amount of trace metal contents in Huntsman additive samples is probably due to the injection of NO<sub>x</sub> into the system. The extent of corrosion as indicated by the amounts of trace metals found in the samples appears to correlate well with the trends and levels of HSSs observed for these solvents, except for MEA lean solutions where only the Ni trend correlates with that of the HSS.

CO<sub>2</sub> loadings were determined for all solvent technologies tested. The results of the individual solvents are plotted together in Figure 47, although not intended for direct comparison. These plots show that the CO<sub>2</sub> loading is roughly constant at about 0.26 mol CO<sub>2</sub> per mol amine for H3-1 solvent, although there appears to be an initial increasing trend during the first 4 days of testing. All other solvents show a decreasing trend, with the slope of the MEA curve being slightly steeper than that for Huntsman additive and MDEA+PZ. The downward trending of CO<sub>2</sub> loading for the solvents might be due to increased buildup of HSS and/or degradation. The HSS compounds would generally hold up some of the free amine in its bound form, thereby rendering it unavailable for CO<sub>2</sub>

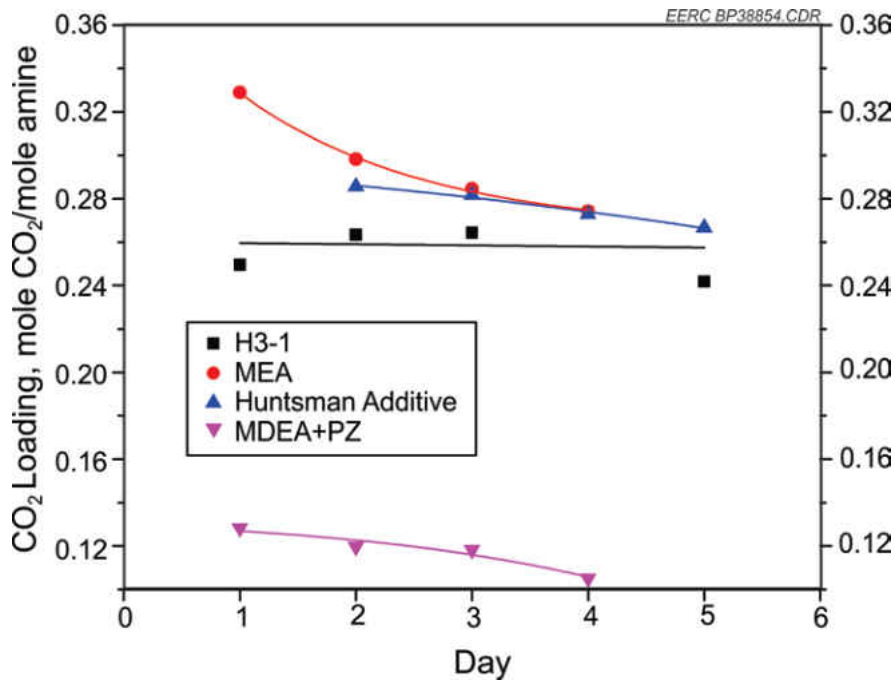


Figure 47. Plot of CO<sub>2</sub> loading for MEA, H3-1, Huntsman additive, and MDEA+PZ.

absorption. During the weeks of testing, several process conditions were varied which could lead to varying loading results. CO<sub>2</sub> loading is a function of several parameters, but one of the most important parameters is reboiler duty (the degree of regeneration). As process conditions changed during H3-1 solvent testing, an initial increasing trend in CO<sub>2</sub> loading was seen. This was most likely related to the changing reboiler duty of the column during testing of this solvent, which resulted in greater amounts of free amine regenerated in the stripper compared to other solvents. It is important to note that, generally, the CO<sub>2</sub> loading of any given amine solution is expected to decrease with time, which correlates with the increasing trend of HSS buildup in solution.

### Solvent Summary

Pilot-scale postcombustion CO<sub>2</sub> capture tests have been completed on four main amine solvent technologies during Phase I of the PCO<sub>2</sub>C project, including standard 30 wt% MEA used as the baseline solvent and H3-1, Huntsman additive, and MDEA+PZ supplied by commercial partners in the project. All tests were conducted for 5 days, running 24-hour cycles a day, unless interrupted by the need to troubleshoot and/or resolve a problem with process equipment. The effects of several parameters on the CO<sub>2</sub> capture performance were investigated during these tests, including solvent regeneration energy (reboiler duty), solvent flow rate, flue gas flow rate, stripper column static pressure, and absorber inlet temperature. Samples collected during testing were also analyzed at the EERC's ARL to determine the levels of free amine, HSS, trace metal corrosion products, major elements, and solvent CO<sub>2</sub> loading.

### *Overall CO<sub>2</sub> Capture Performance*

All solvents tested were able to reach the goal of 90% CO<sub>2</sub> capture during testing. A number of test parameters were manipulated to monitor CO<sub>2</sub> capture under varying conditions. Some test parameters had significant effects on the CO<sub>2</sub> capture rate, while others seemed to have little to no effect. Reboiler duty and liquid-to-gas ratio both had significant impacts on CO<sub>2</sub> capture, while other parameters such as SO<sub>2</sub> level and stripper column static pressure seemed to have less effect.

Data from the advanced solvents and MEA tests conducted suggest that for similar test conditions, MEA will require about 10%–40% more heat input to achieve 90% CO<sub>2</sub> capture than the advanced amine-based solvents. H3-1 required the lowest regeneration energy input (~1475 Btu/lb CO<sub>2</sub>); the reboiler duty for MDEA+PZ was ~1600 Btu/lb CO<sub>2</sub>. The regeneration energy requirement for MEA was estimated to be in the range 1775–1940 Btu/lb CO<sub>2</sub> captured. Thus the advanced solvents appear to be potentially less costly to run than a 30 wt% MEA solution.

Investigations of the effects of liquid-to-gas ratio showed that MEA solution required a higher solvent flow rate (about 30%–50%) than H3-1 to attain 90% CO<sub>2</sub> capture for a given amount of treated flue gas. Consequently, use of H3-1 for a large-scale process could lead to significant economic benefits over MEA. Conversely, tests on MDEA+PZ showed a solvent usage about 135% higher than MEA was needed to reach 90% capture, indicating that MEA could potentially be more effective in terms of solvent usage.

CO<sub>2</sub> capture at various stripper column static pressures was recorded for each solvent. Overall, the data showed that increases in stripper pressure typically resulted in

slightly better CO<sub>2</sub> capture for each solvent. Also, it appears that liquid-to-gas ratio also increases with stripper pressure, likely because the pressure in the column produces a higher head pressure on the lean solvent pump. System performance is as good or better for pressures in the stripper up to 12 psig as it is for lower pressures. This is a potential economic benefit for downstream CO<sub>2</sub> storage. Running at higher pressures in the stripper could result in lower total compression ratio needed to prepare the CO<sub>2</sub> stream for storage or EOR usage.

Based on this data two important factors were determined that will highly impact the CO<sub>2</sub> capture modeling effort. These factors are for the regeneration energy and the liquid to gas ratio. The liquid to gas ratio factor will be used to determine if the column height will need to be less than or more than that of the MEA system. The regeneration energy will be used to determine the amount of energy that can be reduced from the MEA base case model. An economic analysis will then put a cost to these factors in terms of increased or decreased capital and operating expenses. Table 12 summarizes the factors for each solvent.

#### *Overall Solvent Sample Analysis*

Measurements of the concentration of free amine in lean solvent solutions indicated that H3-1 had the highest amount, followed by Huntsman additive. The level of free amine in lean MEA solution was the least. Although the initial fresh amine concentrations were different for the different solvents, the free amine content in each solvent was decreasing



Table 12. Factors developed based on pilot scale data to modify the MEA based model.

Factor	MEA	H3-1	MDEA+PZ
L/G Ratio	1	0.65	2.3
Regeneration Energy	1	0.75	0.9
Solvent Make-up	1	0.3	0.1

roughly exponentially with time. MEA which had similar starting fresh amine concentrations as Huntsman additive showed lower free amine content in lean solutions than Huntsman additive.

In terms of HSS formation, the MEA solvent samples had the highest amounts of sulfate and thiosulfate salts, followed by H3-1; Huntsman additive had the least amounts of these salts. Nitrite and nitrate determinations showed insignificant amounts in all solvents tested, with less than 10 ppm of nitrite and/or nitrate detected only in cases where higher than baseline amounts of NO<sub>x</sub> were added to the flue gas upstream of the absorber (i.e., during Huntsman additive testing). Chloride concentrations were also highest in MEA samples, while moderate levels were detected in H3-1 and Huntsman additive solutions. The main organic HSSs analyzed in the samples were formate, acetate, and oxalate, which are oxidative degradation products of MEA-based solvents. It was observed that the amounts of these organic anions were higher in MEA samples than those of Huntsman additive. H3-1 is a different type of advanced amine that is not expected to bear these types of organic anions, and as such, analysis of H3-1 samples did not indicate any formate, acetate, or oxalate anions present.

The extent of corrosion of process equipment was also monitored during testing by analyzing the samples for trace metals such as Ni, Fe, Cr, Mn, and Mo, which are the basic components of stainless steels used to fabricate the columns and piping. Results indicate that Huntsman additive solutions had the highest amounts of corrosion products, particularly, Cr, Ni, and Fe with concentrations in the range 5–35 ppm, 3–27 ppm, and 11–16 ppm, respectively. MEA samples had midrange trace metal amounts in ranges of 3–5 ppm for Ni, 8–13 ppm for Cr, 4–9 ppm for Fe, and less than 2 ppm for Mn and Mo. In H3-1 solutions, the amounts of all five trace metals were below 5 ppm.

The results presented in this report are based on data obtained from 4 to 5 days of testing these technologies on the EERC's 75-lb/hr CTF pilot-scale unit. Longer-term tests would be useful in gathering extensive data that could provide better estimates of the parameters that were investigated in this study. However, it is expected that the data provided in this report will provide useful insights into the applicability of these solvents on real flue gas environments.

## CHAPTER VII

### SOLVENT SYSTEM MODELING AND ECONOMIC EVALUATION

#### Introduction

Software models developed by AspenTech are excellent tools for evaluating technologies from a technical and economical perspective. Aspen Plus is used to develop carbon capture process flow models, including detailed mass and energy balances around the entire power generation system. The information developed is then exported to APEA to size the equipment and determine the cost to run and build the system. The APEA software allows modelers to quickly generate equipment sizes and designs, calculate estimated capital and operating costs, and allow for rapid evaluation of process alternatives to compare profitability.

Aspen Plus was used to model a 500-MW power plant facility equipped with a solvent-based capture system utilizing the solvent evaluated during the PCO<sub>2</sub>C program. The model, which initially represented the pilot-scale coal combustion and amine-based CO<sub>2</sub> capture system, was scaled to fit a typical 500-MW power plant facility. In the model, coal feed rates were increased from 50 lb/hr to 6000 tons/day to simulate the production of heat and flue gas. The flue gas was cooled, filtered, and SO<sub>2</sub> scrubbed. The clean flue gas was sent to the CO<sub>2</sub> capture system, where an absorber tower removed 90% of the CO<sub>2</sub> from the flue gas with a generic MEA-based solvent. The CO<sub>2</sub>-rich solvent was heated and sent to a stripper tower, which removed the CO<sub>2</sub> from the solvent.

The lean solvent was recycled back to the absorber, and the CO<sub>2</sub> stream was compressed and liquefied for pipeline transport. The model attempted to simulate solvent degradation rates based on SO<sub>2</sub> concentration from the flue gas, and modifications were also made to the model to minimize solvent losses due to evaporation in the absorber.

An attempt was made to model an advanced amine-based solvent that was experimentally shown to significantly reduce solvent flow rate and steam consumption, but the effort was unsuccessful because of insufficient reaction chemistry data for the advanced solvent in Aspen databanks. To make economic comparisons in APEA between the advanced solvent and generic MEA solvent, experimental data were used to estimate equipment sizes and steam consumption rates, which showed a 35% reduction in solvent flow rate and 25% to 30% reduction in stripper reboiler duty.

The full-scale model developed in Aspen Plus was then exported into APEA to size the equipment and estimate costs for constructing a CO<sub>2</sub> capture facility to an existing coal-fired power plant. Because of limitations in the size of towers and other equipment, three independent CO<sub>2</sub> capture trains were required to process the volume of flue gas. APEA sized each component of the system and calculated the material and construction costs to build each unit. The total capital expenditure for the CO<sub>2</sub> capture and liquefaction system was estimated to be US\$237 million for MEA-based solvent and US\$220 million for the advanced solvent. User-specified costs for raw materials, utilities, and labor allowed the economic analyzer to estimate annual operating costs. The utility cost of steam had a very significant impact on operating costs, so factors such as solvent steam consumption rate and the efficiency of the power plant for converting steam to electricity were important in determining costs. The cost to produce electricity is also a

determining factor in the economics. A sensitivity analysis calculated a range of CO<sub>2</sub> capture costs from US\$24 to US\$66 per ton.

## Aspen Plus Model Description

### *Coal Combustion*

An Aspen Plus model was created to simulate the production of heat and flue gas from the combustion of coal (Figure 48). The model was originally designed to represent the EERC CTF, and pilot-scale data were used for model calibration. The primary inputs to the combustion model were coal, primary air, and secondary air. Coal was fed to the Decomp block, which was used to convert the nonconventional coal input stream into basic elements that can be used by Aspen and normalized the yields to maintain a mass balance. Coal input properties such as heat capacity and density were obtained through proximate, ultimate, and sulfur analyses. The primary air stream was heated, mixed with the decomposed coal stream CHN, and fed to the AF-CTF block.

The AF-CTF block simulated coal combustion with air using chemical and phase equilibrium calculations. A heat stream between the Decomp block and the AF-CTF block represented the change in enthalpy between the actual coal input to the system and the basic elements used in the equilibrium calculations. The Heat 2 stream simulated the amount of heat lost to the surrounding environment. The secondary air stream represented secondary air injection into the boiler and was adjusted to regulate the amount of oxygen present in the flue gas. The hot-gas stream represented the flue gas exiting the combustor and was the result of the chemical and phase equilibrium calculations. Based on pilot-scale data, its temperature was maintained at 2015°F and contained approximately 14% CO<sub>2</sub> (wet basis.)

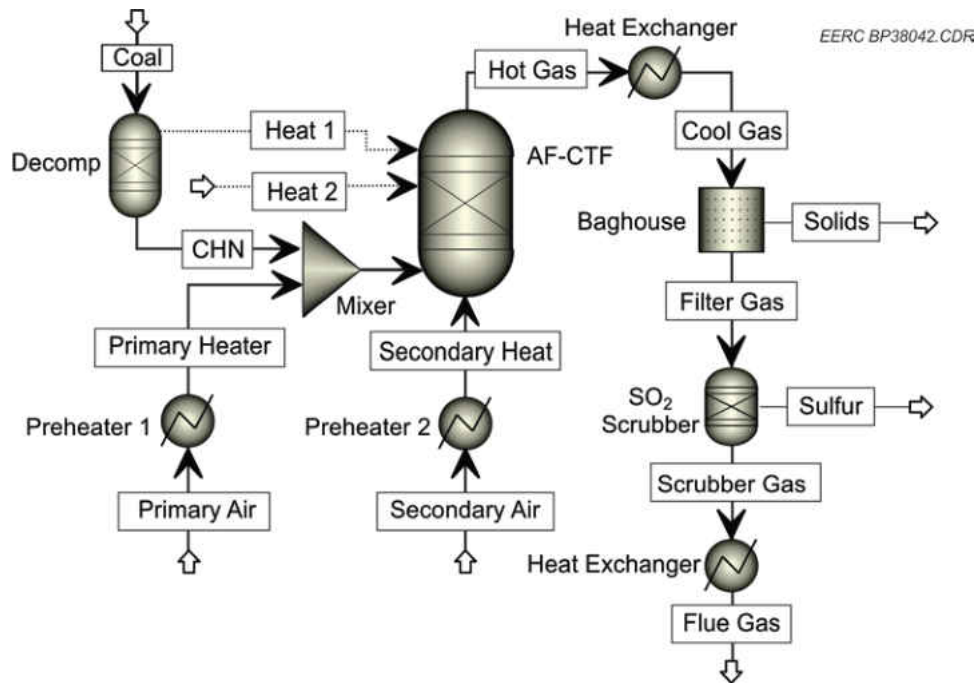


Figure 48. Aspen Plus process model for coal combustion and flue gas cleaning.

The hot-gas stream was cooled to 339°F by the heat exchanger. Then, the gas was sent to the baghouse where the simulation of the removal of particulate ash occurred. The filtered gas for this simulation contained about 300 ppm of sulfur compounds, which was reduced to less than 5 ppm by the SO<sub>2</sub> scrubber block. For the purposes of this simulation, the sulfur removal was a simple separator and was not rigorously modeled. A final heat exchanger reduced the temperature of the flue gas to 110°F. Approximately 58,000 tons a day of flue gas was produced by this model. With 14 mol% of CO<sub>2</sub>, 12,444 tons per day of CO<sub>2</sub> was emitted into the atmosphere without a CO<sub>2</sub> capture system.

### *CO<sub>2</sub> Capture*

The flue gas generated by the coal combustion model was sent to an MEA solvent-based CO<sub>2</sub> capture system (Figure 49). Since it was determined that three individual

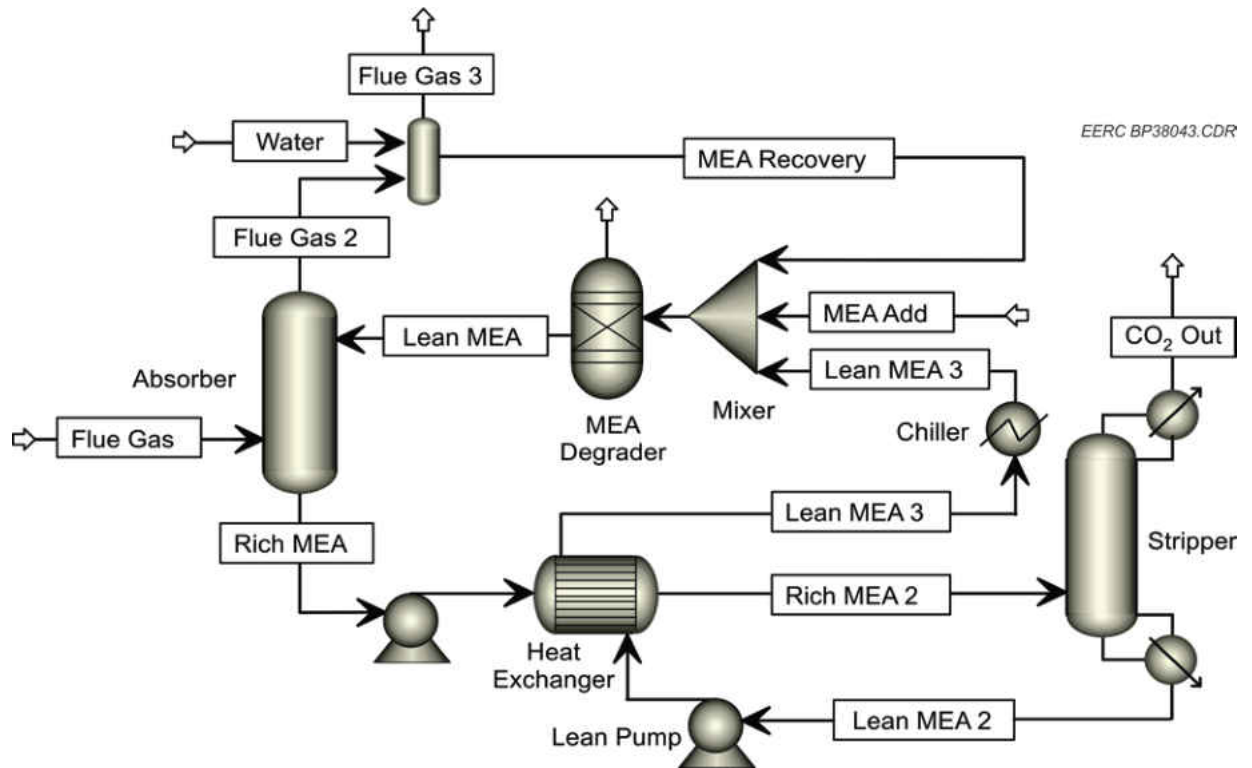


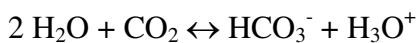
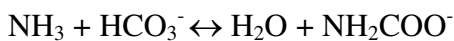
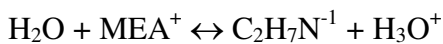
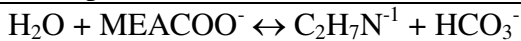
Figure 49. Aspen Plus process model for CO<sub>2</sub> capture system.

capture trains would be required, the mass flow rate of the flue gas stream was reduced to a third, and only one CO<sub>2</sub> capture train was modeled. Flue gas from the combustor system entered the bottom of the absorber tower, while the lean MEA solvent entered the top of the tower. The absorber tower contained 1-inch-diameter metal packing material to facilitate contact between the countercurrent flows of the flue gas and liquid solvent streams. CO<sub>2</sub> absorption is exothermic in nature, so the flue gas was heated to 148°F during absorption and exited the top of the absorber tower. The flow rate of lean MEA entering the top of the tower was adjusted so that 90% of the CO<sub>2</sub> in the flue gas was captured. The height and diameter of the tower were increased to improve CO<sub>2</sub> capture rates and minimize pressure drop.

A rate-based add-on package to Aspen Plus called RateSep was used to calculate the rate of CO<sub>2</sub> absorption and desorption in the towers. Aspen Plus is capable of generating the electrolyte reaction chemistry for CO<sub>2</sub> capture with MEA and has built-in rate constants. Table 13 lists the reactions used to determine the rate of absorption.

For the absorber model, the number of theoretical stages and height per stage were specified for the packed column. The mass balance, energy balance, reaction equilibrium, vapor liquid equilibrium, diffusion limitations, and reaction kinetics were all calculated using Aspen Plus and RateSep. The rate-based approach is critical for accurately predicting the size of columns because equilibrium calculations will severely undersize columns. The results were presented on a stage-by-stage basis, which enabled further optimization of the column.

Table 13. Chemical Equilibrium Reactions for General MEA Sorbent and CO<sub>2</sub> Absorption.





The CO<sub>2</sub>-rich MEA leaving the bottom of the absorber tower was pumped through a heat exchanger and sent to the top of the stripper tower. The heated column separated the absorbed CO<sub>2</sub> from the amine, and lean MEA exited through the bottom. The hotter, lean MEA stream was used to preheat the rich MEA solution. The CO<sub>2</sub> exited the top of the stripper tower and was sent to a gas compressor for liquefaction. A water-cooled condenser at the top of the tower, which was maintained at 120°F, minimized the amount of water and other liquids evaporating from the tower. A steam-driven reboiler at the bottom of the tower provided the heat necessary to drive off the CO<sub>2</sub> from the MEA. The temperature of the tower operated between 190° and 225°F. The height and diameter of the tower were adjusted to minimize pressure drop and to allow sufficient time for desorption of CO<sub>2</sub> to take place. After the hot, lean MEA solution passed through the heat exchanger, it was further cooled to 110°F in a chiller. The chiller block simply represented a heat exchanger, which used cooling water as a heat sink. The lean MEA eventually was recycled back to the top of the absorber tower.

In practice, 100% of the MEA is not able to be recycled. Some MEA is lost through evaporation in the absorber and stripper. MEA is also degraded from impurities in the flue gas such as sulfur compounds, chlorine, nitrogen oxides, and oxygen. An attempt was made to model these losses in Aspen Plus and quantify rate. The rate of MEA evaporation from the towers was a straightforward thermodynamic calculation. A very small fraction of MEA was lost in the stripper, but a rather significant amount, 800 lb/hr, was being evaporated through the absorber. In order to minimize these losses in large absorber towers, a freshwater scrubber was employed at the top of the tower. This scrubber was modeled in Aspen Plus as a separate, short tower, which was called wash

zone. The flue gas with evaporated MEA exiting from the absorber tower was sent to the bottom of the wash zone, while freshwater was added to the top of the wash zone. The amount of freshwater added to the system was equal to the amount that evaporated from the system. The water and absorbed MEA exited the bottom of the wash zone and was added back into the top of the absorber tower via the mixer block. The wash zone effectively cut the losses of MEA through evaporation by a factor of 10.

Modeling MEA losses by degradation from flue gas impurities proved to be much more challenging. A significant effort was devoted to developing chemical equilibrium reactions between flue gas impurities and HSSs from MEA. The Aspen Plus RateSep model is unable to process solids; therefore, any HSS modeling is very difficult if the salt concentration is near the precipitation point. Because of these difficulties, HSS formation was not modeled within Aspen. However, an estimate of the degradation rate could still be calculated based on commonly accepted molar ratios and from the pilot scale testing results. For instance, one mole of  $\text{SO}_2$ ,  $\text{SO}_3$ , or  $\text{NO}_2$  would degrade approximately two moles of MEA. Based on these ratios, a calculator block was set up in Aspen Plus to estimate the amount of MEA that would degrade based on the concentration of impurities on the flue gas. A separator block in the process model, MEADGRD, would pull out the calculated amount of degraded MEA. To make up for the lost MEA due to degradation, and evaporation as well, an MEAADD stream was created to add the appropriate amount of MEA.

### *CO<sub>2</sub> Compression and Liquefaction*

The  $\text{CO}_2$  exited the stripper column at 120°F and slightly above atmospheric pressure. It was saturated with water as well. The  $\text{CO}_2$  was then sent to a three-stage

centrifugal compressor, where it was compressed to 190 psi (Figure 50). Approximately 90% of the water condenses in the compressor. The remainder of the water must be removed to meet water specifications for pipeline transportation of CO<sub>2</sub>. A CO<sub>2</sub> dryer was employed to drop the concentration of water to near negligible levels. After the CO<sub>2</sub> was dry, a condenser was used to liquefy the CO<sub>2</sub> by dropping the temperature of the stream to -26°C. A pump is used to increase the pressure of the liquid CO<sub>2</sub> to 2000 psi.

### Aspen Process Economic Analyzer

After the Aspen Plus models had been built, analyzed, and optimized, they were imported into APEA to determine the capital and operating costs of a CO<sub>2</sub> capture system. Since the scope of the project is to build a CO<sub>2</sub> capture facility onto an existing coal combustion power plant, the Aspen Plus model as shown in Figure 48 was not included in the economic analysis. Only the CO<sub>2</sub> capture and liquefaction system as shown in Figures 49 and 50 were imported into the economic analyzer.

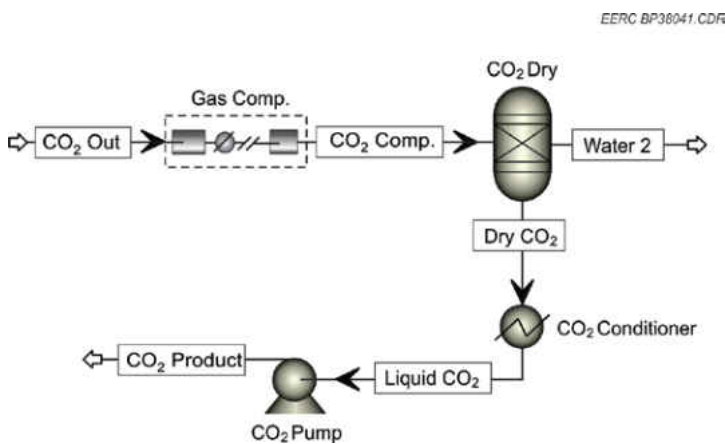


Figure 50. CO<sub>2</sub> compression and liquefaction.

After the process model was loaded, APEA assigned specific equipment types to each process block from a large database of various real-world components. For example, APEA assigned a floating head shell and tube heat exchanger for the main heat exchanger in the CO<sub>2</sub> capture model. APEA determined from its database of equipment that this was the most appropriate type based on flow rates, materials, and other factors. The user had the ability to manually assign a specific equipment type and materials of construction to a process block as well. Because of the corrosive nature of MEA, much of the equipment in this model was constructed of stainless steel instead of cheaper carbon steel.

An important aspect of evaluating the cost of a system was properly sizing the equipment used in a given process. APEA calculated the size of each piece of equipment used in the process and provided those calculations to the user for review. The user was able to revise sizes to fit needs or manually enter sizes for unsized equipment.

Operating costs are calculated by APEA, but the user can override certain APEA values to view the impact of various choices on investment analysis measures of profitability. For example, the user can assign cost rates to product and raw material streams. In the case of CO<sub>2</sub> capture modeling, the model took into account the cost of the MEA sorbent. APEA's detailed economics module allowed the user to perform interactive economic scenarios. APEA developed key economic measures, including payout time, interest rate of return, net present value, and income and expenses on changing any economic premise. APEA performed the economic evaluation over a specified time line of the project, from planning phases through the entire life of the process facility.

## Results

Aspen Plus and APEA were used to model six different scenarios, which varied solvent type and power plant efficiency/age. Aspen Plus was used to calculate mass and energy balances and to size the equipment for the MEA-based solvent. An unsuccessful attempt was made to model two other advanced amine-based solvents in Aspen Plus. The main components of the solvents were found in the databanks, but many of the solvent's physical and chemical properties were missing. Chemical reaction equilibrium constants were also not defined, so it was not possible to accurately calculate CO<sub>2</sub> absorption rates or determine equipment sizes or steam consumption rates. Therefore, experimental data were used to determine the economic effect that advanced solvents had because of differing flow rates and steam consumption.

Steam consumption is a large contributor to the additional cost of implementing a CO<sub>2</sub> capture system in power plants, so accurately estimating the true cost of steam is important for economic analysis. Low-pressure steam is taken for heating and regenerating solvent, so that less steam is available for conversion to electricity and revenue for the power plant is reduced. An equivalence factor has been estimated in other studies (59–63) to estimate the amount of electricity generation that is lost from the consumption of low-pressure steam. The equivalence factor for older, less efficient plants was estimated to be 20% of stripper reboiler duty, while that for newer, more efficient plants is approximately 10%.

A summary of the costs for each scenario is given in Table 14, which assumed the cost of electricity at a base rate of US\$0.08 per kilowatt-hour. The cost of electricity has a large effect on the economics of the system, and a sensitivity analysis is given later. The

Table 14. Summary of CO<sub>2</sub> Capture Costs, US\$

	MEA (old plant)	H3-1 (old plant)	MDEA + PZ (old plant)	MEA (new plant)	H3-1 (new plant)	MDEA + PZ (new plant)
Total	237,000,00	220,000,00	381,000,00	237,000,00	220,000,00	381,000,00
Capital Cost	0	0	0	0	0	0
Operating Cost	117,000,00	97,000,000	113,000,00	86,000,000	76,000,000	100,000,00
Utilities Cost	91,000,000	73,000,000	83,000,000	63,000,000	54,000,000	70,000,000
Annual Cost (total)	166,000,00	143,000,00	192,000,00	136,000,00	122,000,00	178,000,00
CO <sub>2</sub> Capture Cost, US\$, ton	46	40	53	38	34	49
CO <sub>2</sub>	67	52	74	48	41	65
Avoidanc e Cost, US\$, ton						
Rate Increase	0.058	0.046	0.065	0.042	0.036	0.057

column headings indicate the solvent and the plant efficiency of converting low pressure steam to electricity, which is denoted by the age of the plant. A more detailed breakdown of the costs for the MEA scenario and some of the parameters used for the economic analysis are given in Appendix C1. Appendix C2 is an APEA-generated report that contains itemized details for the direct costs of each piece of equipment. Appendix C3 is another APEA-generated report that specifies the materials, sizes, and vendor equipment costs for each unit.

The total capital costs vary between the solvent used for each scenario. The H3-1 solvent had a 35% reduction in flow when compared to the base MEA case, which

slightly reduced the size of the towers, pumps, and heat exchangers. Conversely, MDEA+PZ required over two times the flow rate of MEA to capture a comparable amount of carbon dioxide, and consequently the total capital costs are appreciably higher. Operating costs varied significantly between all scenarios, which were primarily due to the changes in steam consumption or cost of steam. Switching to a more advanced solvent reduced the consumption of steam, and improving the efficiency of the plant reduced the cost of steam. Utility costs were minimized in the case of solvent H3-1 in a new plant configuration because of low steam consumption and high plant efficiency. Additionally, with the lowest capital costs due to lower solvent flow rate, the minimal cost of capturing CO<sub>2</sub> was achieved with this scenario at US\$34 per ton. The cost of capturing CO<sub>2</sub> was highest at US\$53 per ton when the capital intensive MDEA+PZ scenario was used in an older, less efficient plant. The power plant must raise electricity rates to recover the cost of CO<sub>2</sub> capture. The total annualized cost was divided by the amount of energy produced in a year to determine the rate increase. Storage and handling expenses were not considered for the postcombustion economic modeling. These factors could increase the cost of capture by approximately US\$10 per ton of CO<sub>2</sub>.

The CO<sub>2</sub> capture costs take into account the dollars spent on capital and annual operating expenses, but it does not consider the revenue lost from electricity that is unable to be sold to customers because of parasitic load from the CO<sub>2</sub> capture process. A metric called CO<sub>2</sub> avoidance cost is used to reflect this lost revenue. The equation is defined below, and this value reflects the average cost in dollars per ton of reduced CO<sub>2</sub> emissions, while still providing the same amount of electricity to consumers. The reference case establishes CO<sub>2</sub> emissions and cost of electricity with no capture process:

$$Cost\ of\ CO_2\ Avoided = \frac{\left(\frac{\$}{kWh}\right)_{capture} - \left(\frac{\$}{kWh}\right)_{reference}}{\left(\frac{Tons\ CO_2}{kWh}\right)_{reference} - \left(\frac{Tons\ CO_2}{kWh}\right)_{capture}}$$

The breakdown of the annualized cost of CO<sub>2</sub> capture is given in Figure 51, which again assumed a base electricity cost of US\$0.08 per kilowatt-hour. Utilities such as steam and electricity were the highest contributors to the operating costs for the base case of MEA. Utility costs were effectively reduced when improving the efficiency of the plant and switching to the advanced solvent H3-1, which consumed less steam for stripper column reboiling. MDEA+PZ also had slightly lower utility costs than MEA, but capital recovery costs were significantly higher because of the additional equipment required to handle the larger solvent flow rate. For comparison purposes, the oxy-fired scenario was included. Utility costs are high in this case because of the considerable expense of operating an ASU. In order to compare this to other studies the cost of CO<sub>2</sub> avoided is shown in the same manner in Figure 52.

Figure 53 breaks down the contribution of various process units toward total capital costs. For the base MEA and H3-1 case, the capital costs were relatively similar. The absorber towers were the most expensive unit, followed by the heat exchangers. The absorber tower for the base case of MEA (35' D × 116' H) was a much larger vessel than the stripper tower (20' D × 107' H), which accounts for the significant difference in price. Because of the corrosive nature of the MEA solution, much of the equipment had to be constructed of stainless steel, which added considerably to the cost. The H3-1 solvent



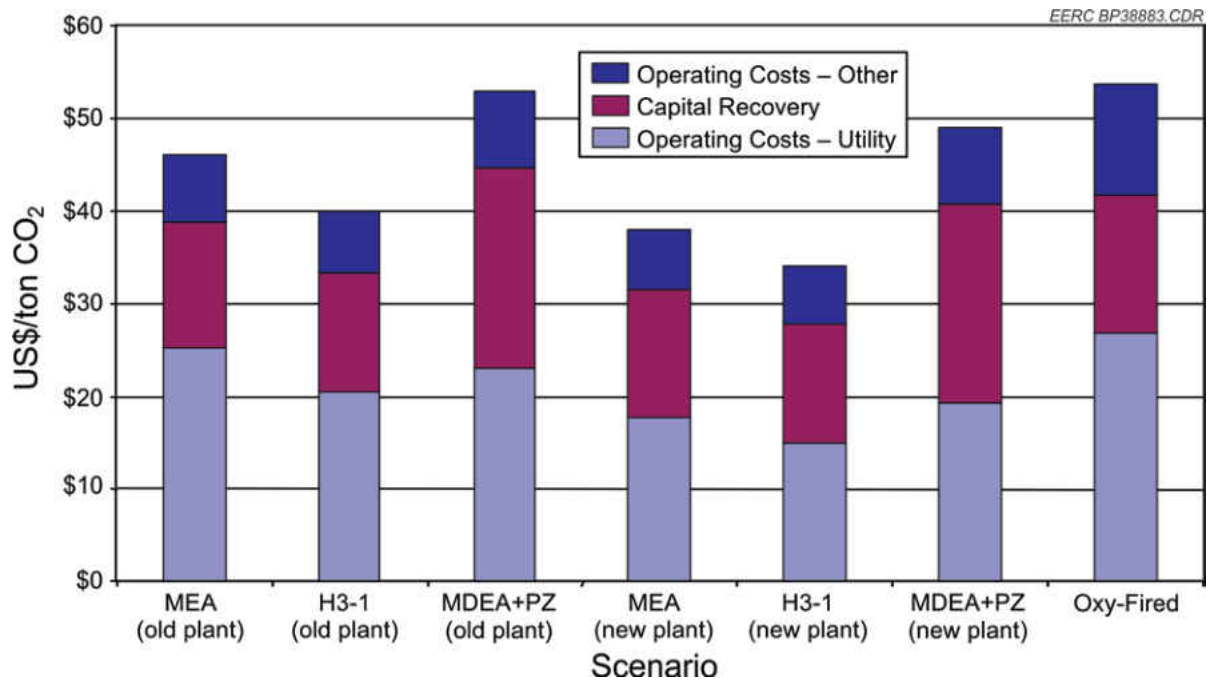


Figure 51. Breakdown of levelized capital and operating expenses per ton of CO<sub>2</sub> captured.

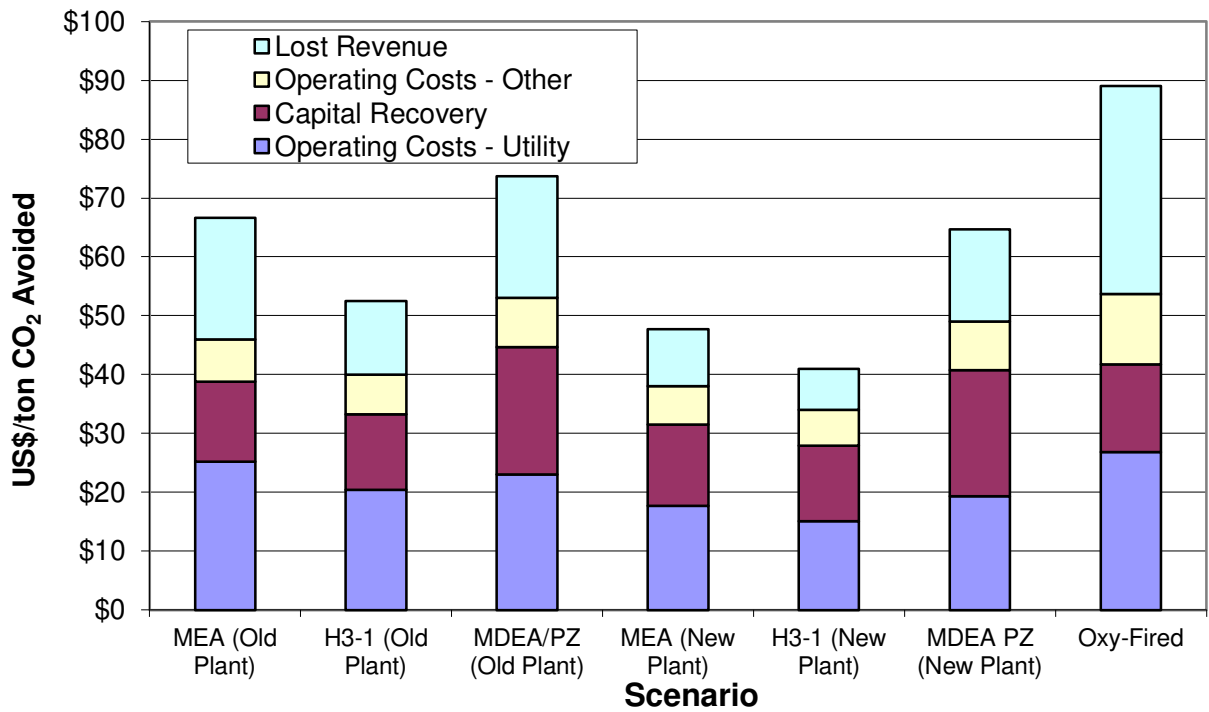


Figure 52. Breakdown of levelized capital and operating expenses per ton of CO<sub>2</sub> avoided.

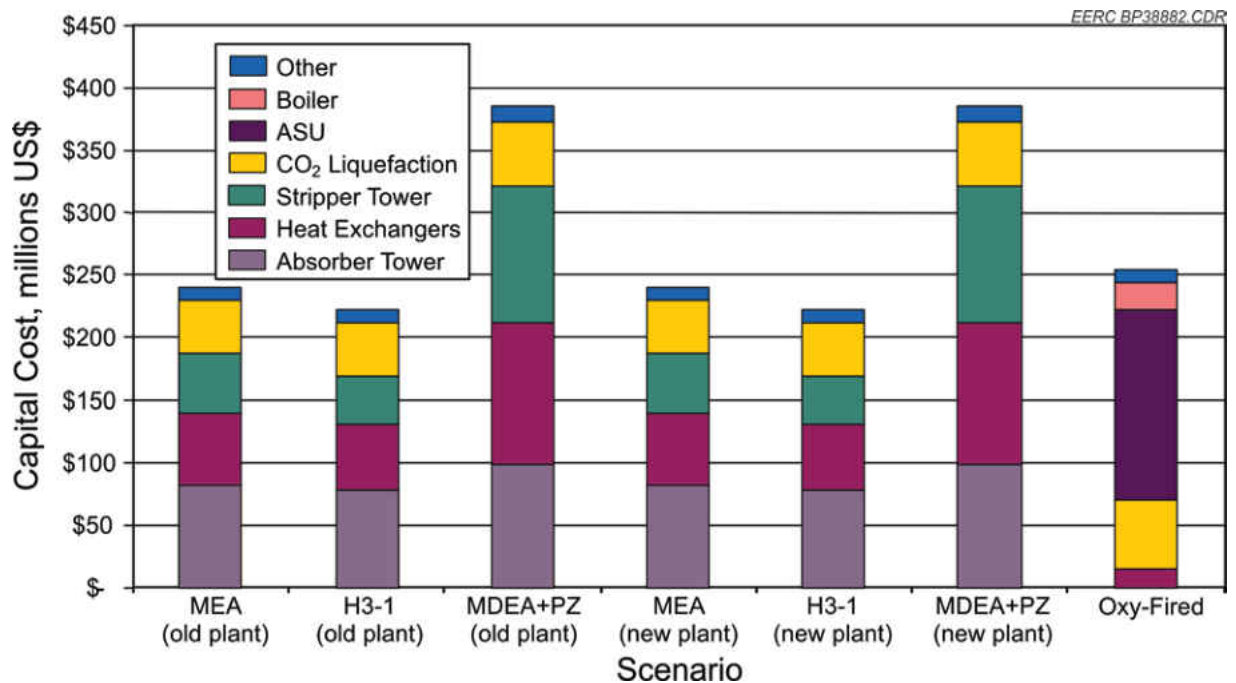


Figure 53. Breakdown of individual contributions for direct equipment costs.

reduced the flow rate required to absorb the same amount of CO<sub>2</sub>. While not dramatic, this reduction allowed for some process units to be sized smaller. In particular, the stripper tower diameter was reduced by 4 feet, and the solvent heat exchangers were also reduced in size and cost. Equipment costs could be more dramatically reduced if a less corrosive solvent were used. Expensive stainless steel was used for the construction of the components that are in contact with the amine-based solvents.

Capital costs for MDEA+PZ were dramatically higher because of a 2.3 factor increase in solvent flow rate. Four capture trains were required for this case instead of three, and two stripper columns were required for each train instead of one. The heat exchanger costs were much higher as well as the size of the main exchanger had to

essentially be doubled. For the oxy-fired scenario, the main contributor to capital costs was the ASU. The costs for this scenario were higher than MEA or H3-1, but not as extensive as MDEA+PZ.

The parasitic load, or energy penalty, for each scenario is given in Figure 54. Electricity was consumed by the capture process mainly from CO<sub>2</sub> liquefaction. The gas compressor and chiller unit required significant amounts of energy, and this value remained constant for all six scenarios because the same amount of CO<sub>2</sub> was captured and compressed for transport. The change in energy penalty was due to differing steam consumption rates and the efficiency of the plant for converting steam to electricity.

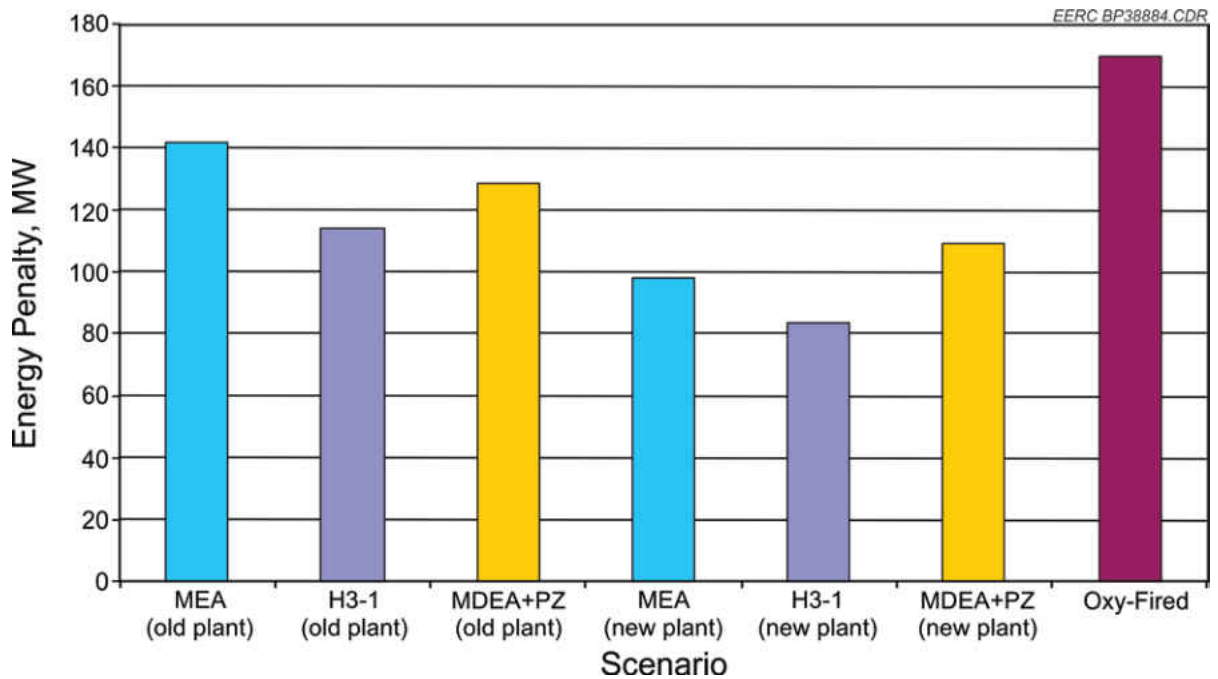


Figure 54. Energy penalty, or parasitic load.

Newer, more efficient plants lost less electricity for a given amount of steam that was consumed by the capture process, and more advanced solvents such as H3-1 and MDEA+PZ consumed less steam. The oxy-fired scenario had the greatest parasitic load, and this was due to the large amount of electricity required for the air separation unit. The cost to produce electricity had a dramatic effect on the economics of carbon dioxide capture systems, which is shown as sensitivity analyses in Figures 55–57. When electricity was produced relatively inexpensively, the electrical costs to operate the system were reduced significantly, and the revenue lost from parasitic steam consumption was not as great. In a best-case scenario where the cost to produce electricity was only US\$0.03 per kilowatt-hour, the CO<sub>2</sub> capture cost was reduced to a range of US\$24 to US\$36 per ton. On the other hand, if the cost to produce electricity was raised to US\$.14 per kilowatt-hour, the range of CO<sub>2</sub> capture costs increased to US\$46 to US\$76 per ton. In order to recoup the costs of operating the CO<sub>2</sub> capture system, the price of electricity that was sold to customers must be increased. This rate increase is shown in Figure 57, and the sensitivity analysis of CO<sub>2</sub> avoidance costs is shown in Figure 57.

### Summary

Aspen Plus was used to model a 500-MW coal combustion facility and an add-on MEA-based CO<sub>2</sub> capture and liquefaction facility. Rate-based chemical absorption rates and material and energy balances were modeled in Aspen Plus. The model was imported into APEA to determine total project construction costs and annual operating costs. Total capital expenditure was estimated to be in a range of US\$220M to US\$381M. The cost of steam was the highest contributor to the annualized cost of capturing CO<sub>2</sub> for the base case of MEA

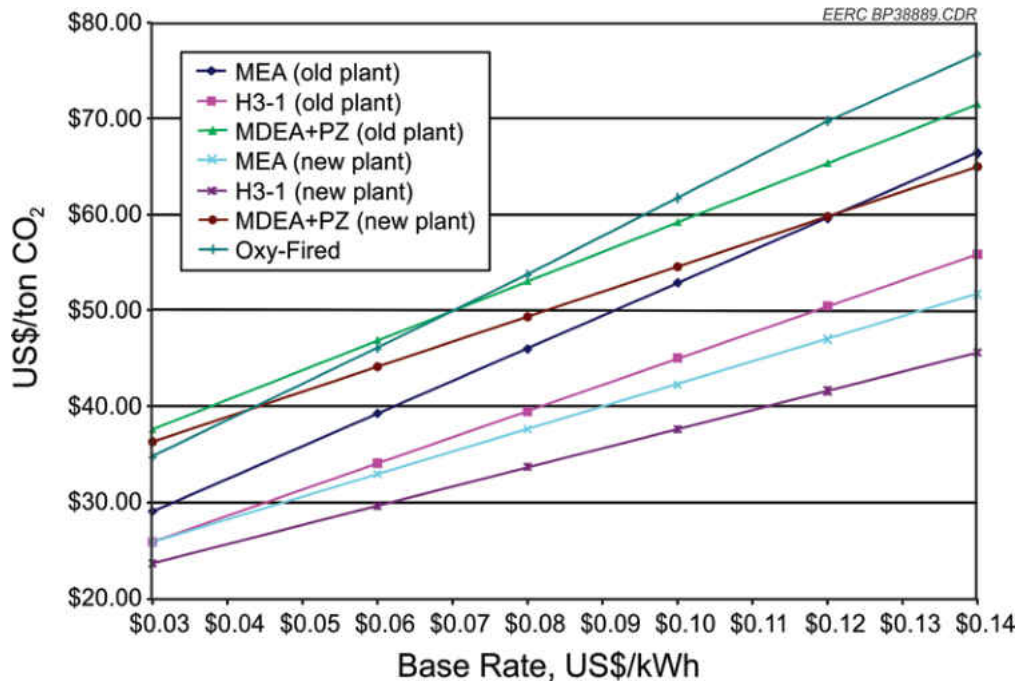


Figure 55. Sensitivity analysis of the cost to produce electricity on CO<sub>2</sub> capture costs.

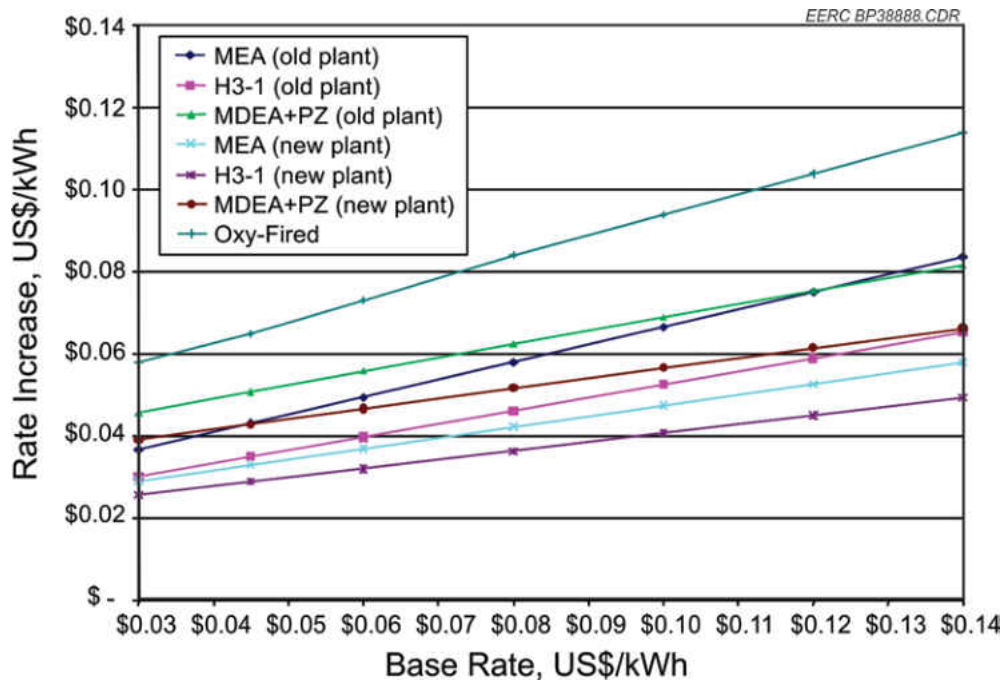


Figure 56. Sensitivity analysis of the cost to produce electricity on electricity rate increase.

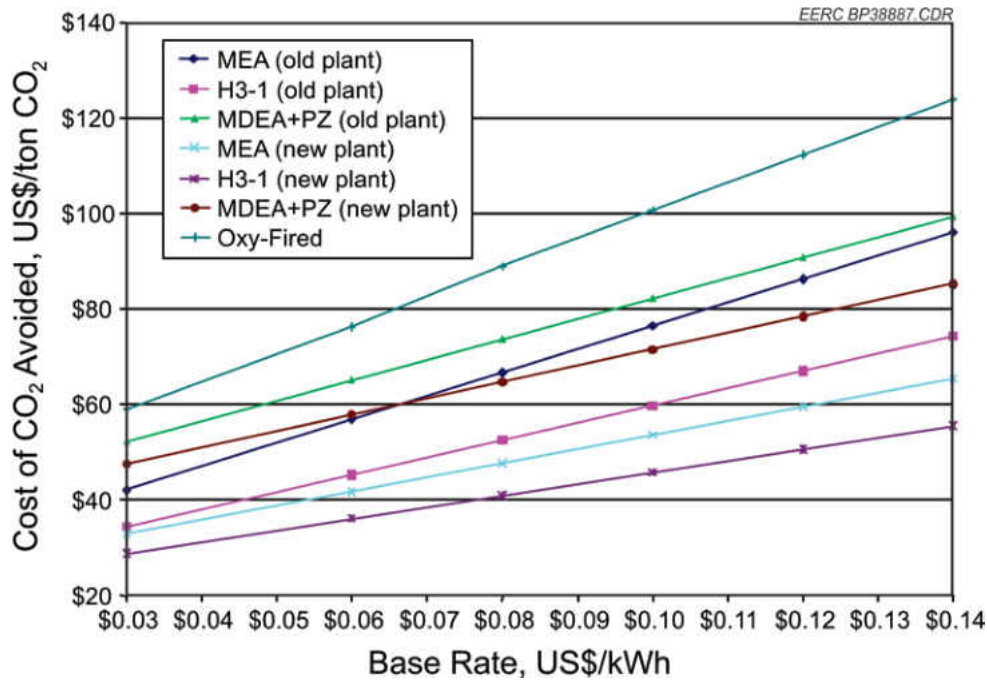


Figure 57. Sensitivity analysis of the cost of CO<sub>2</sub> avoidance on electricity rate increase.

solvent in a relatively inefficient power plant. Steam costs could be dramatically reduced by improving the efficiency of the power plant and switching to an advanced solvent. The cost of producing electricity had a dramatic effect on the cost of CO<sub>2</sub> capture as well. A sensitivity analysis showed that the cost can range from US\$41 to US\$74 per ton of CO<sub>2</sub> Avoided. Consequently, to make up for these additional costs, power plants may have to increase the electricity rates by US\$0.021 to US\$0.065 per kilowatt-hour.

## CHAPTER VIII

### CONCLUSIONS

It was determined that advanced solvents are the best available technology for implementing CO<sub>2</sub> capture at the large scale. Advanced solvents will be the technology that will make it to the market place sooner than other technologies due to the long time use of amine solvents in the oil and gas industry for their removal of CO<sub>2</sub>. For the case of postcombustion capture, the main conclusions are that 90% CO<sub>2</sub> capture can be met with MEA and advanced solvents. The EERC system was able to capture at least 90% of the CO<sub>2</sub> present in the flue gas for each advanced solvent and the baseline MEA. Results of the testing indicate that the use of advanced solvents, such as H3-1, can reduce the cost of capture considerably. The main way to make postcombustion capture more economical is through thermal management. This can be accomplished by improving solvents, as mentioned above, and through improving the equipment used for absorption and stripping.

Data from the advanced solvents and MEA tests conducted show that for similar test conditions, MEA required about 10–40% more regeneration energy input to achieve 90% CO<sub>2</sub> capture than the advanced amine-based solvents. H3-1 required the lowest heat input (~1475 Btu/lb CO<sub>2</sub>), and the reboiler duty for MDEA+PZ was ~1600 Btu/lb CO<sub>2</sub>.

The regeneration energy requirement for MEA was estimated to be in the range of 1775–1940 Btu/lb CO<sub>2</sub> captured.

The MEA case required a 30% to 50% higher solvent flow rate than H3-1 to attain 90% CO<sub>2</sub> capture for a given amount of treated flue gas. Conversely, tests on MDEA+PZ showed a solvent usage about 135% higher than MEA to reach 90% capture. Consequently, use of H3-1 for a large-scale process could lead to significant economic benefits over MEA and MDEA+PZ. Lower solvent flow rates require smaller pumps and less energy to pump the solvent through the columns.

Solvent samples from each test run were analyzed for corrosion and degradation product concentrations. MEA had the highest amounts of sulfate and thiosulfate, followed by H3-1; Huntsman additive had the least amount of these salts. The main organic salts found in the samples were formate, acetate, and oxalate, which are oxidative degradation products of amine-based solvents. Organic ion concentration was higher in MEA samples than Huntsman additive. H3-1 samples did not indicate any organic ions present. Solvents showing higher concentrations of degradation products would need a larger makeup stream when scaled up. Huntsman additive and H3-1 both represent potential cost savings over MEA in total solvent needs.

The extent of corrosion of process equipment was also monitored during testing by analyzing the samples for trace metals. Results indicate that Huntsman additive solutions had the highest amounts of corrosion products, particularly Cr, Ni, and Fe, with concentrations in the 3–35 ppm range. In H3-1 solutions, the amount of all five trace metals analyzed were below 5 ppm. No distinct benefits in using an advanced solvent over MEA were observed in the area of corrosion of the system's wetted parts. Overall,



corrosion product concentrations were very low for all solvents, and long-term testing would be needed to make firm conclusions on specific solvent corrosion rates.

Aspen Plus was used to model a 500-MW coal combustion facility and an add-on MEA-based CO<sub>2</sub> capture and liquefaction facility. Rate-based chemical absorption rates and material and energy balances were modeled in Aspen Plus. The model was imported into APEA to determine total project construction costs and annual operating costs. Total capital expenditure was estimated to be in a range of US\$220M to US\$381M. The cost of steam was the highest contributor to the annualized cost of capturing CO<sub>2</sub> for the base case of MEA solvent in a relatively inefficient power plant. Steam costs could be dramatically reduced by improving the efficiency of the power plant and switching to an advanced solvent. The cost of producing electricity had a dramatic effect on the cost of CO<sub>2</sub> capture as well. A sensitivity analysis showed that the cost can range from US\$41 to US\$74 per ton of CO<sub>2</sub> Avoided. Consequently, to make up for these additional costs, power plants may have to increase the electricity rates by US\$0.021 to US\$0.065 per kilowatt-hour.

Advanced solvents show promise, but improvements will still need to be made to reduce capital and operating costs to make the technology economically feasible for today's market. Advanced contactors and solvent promoters will be technologies that may enable these solvent to become more economically favorable. Larger scale and longer term testing is needed to determine the full potential of these systems. It is possible that costs can be reduced as scale-up occurs and the integration of the total process is achieved.

## APPENDICES

**APPENDIX A**

**POSTCOMBUSTION SOLVENT-BASED  
CAPTURE**

## **APPENDIX A1 ANALYTICAL METHODS**

### **STANDARDIZATION OF FRESH AMINE SOLVENTS**

#### **Equipment**

The method used to standardize the initial amine solvents was potentiometric titration using a Fischer Scientific Accumet<sup>®</sup> 950 pH meter employing a glass electrode; a magnetic stirrer was used to continuously stir the solution. The meter was precalibrated to pH 7 and 4 in order to more accurately determine endpoints that lie in the base and acid regions, respectively.

#### **Procedure**

The procedure for standardizing these amine solutions involved taking portions of the solutions (about 1 mL), titrating with standardized aqueous HCl solution, and using a pH meter to monitor the endpoint. The same method and procedure was adopted to determine the concentrations of free and “bound” amine in samples of lean amine solutions for the different amines that were tested. However, while the free amine was determined using the acid titration, the bound amine was quantified using a base titration with standard aqueous sodium hydroxide solution as the titrant.

### **DETERMINATION OF INORGANIC ANION CONCENTRATIONS**

#### **Equipment**

The inorganic anions were detected and quantified using a Dionex 2120i ion chromatograph equipped with an injection valve, 10- $\mu$ L sample loop, AS4A sample

column, AS4G guard column, an anion self-regenerating suppresser, a conductivity detector, and a software system (PeakNet version 4.3) for data collection.

### **Procedure**

The samples were analyzed as-received, i.e., without prefiltration, and the solid particles were settled in the bottom of the sample bottles. The solutions retained their coloration, which was pale yellow in some and reddish in others. A small portion (about 2 mL) of the sample was taken and diluted by factors of 10 and/or 50 using deionized water; the extent of dilution is actually determined by whether or not the column was overloaded at a given concentration. About 1 mL of the diluted samples were then injected into the column and analyzed. The data and chromatographs generated were used for further data reduction and interpretation of the results.

## **DETERMINATION OF METAL CONCENTRATIONS**

### **Equipment**

Metals present in the sample solutions were determined using inductively coupled plasma atomic emission spectroscopy (ICP–AES). Specifically, a Leeman Labs PS1000 Sequential ICP-AES, with an argon gas supply and equipped with borosilicate or polypropylene autosampler tubes was employed.

### **Procedure**

The standard procedures used at the Energy & Environmental Research Center (EERC) Analytical Research Laboratory (ARL) were adopted in these analyses. The steps include rigorous calibration processes, stabilization of the plasma, and determining the peak optics and source. After these steps are completed, the samples are then analyzed.

After the analysis, the data are further reduced to take into account the appropriate units and/or the various dilution factors, if any were necessary.

### **Determination of Free and Bound Amine Concentrations**

The free and bound amine concentrations were determined using an acid-base titration technique. This method is not very accurate because of interferences from other basic ionic species in lean amine solution, including  $\text{OH}^-$  and weak acid anions such as acetate. This limitation can be improved by using a different property of the solution that has less interference to determine the endpoint. For example, measuring the conductance of the solution during titration may produce better results. Cummings et al. (65) have found this technique to be much better than regular acid-base titration using a pH meter.

Potentiometric titrations were used to obtain an initial idea about the trends of these quantities in the solution samples collected during testing. The same procedure used to standardize the fresh amine samples was used to determine the concentrations of free and bound amine in the lean solutions, with acid titration used to quantify the free amine and base titration used to obtain the bound amine content. In Phase II of the project, the approach by Cummings et al. (65), which measures the conductance of the solution as opposed to pH, will be adopted and/or further developed to make more accurate determinations of these quantities.

Locating the endpoint in these titrations is extremely difficult because the base, in this case free amine, is a weak base, and its corresponding acid is also a weak acid. Thus titration of the weak base with HCl and the weak acid with NaOH does not give a sharp endpoint for the lean solutions. However, the acid endpoints for determining the

concentration of fresh amine solutions (which are basically all free amine) are very sharp and unmistakable. Hence, in order to determine the concentration of free and bound amine in lean amine solutions, acid and base titration curves were determined for representative sample solutions. From these titration curves, a reasonable pH was determined where equivalent amounts of acid (base) react with the free (bound) amine in lean amine solutions. These pHs were then used as reference guides for performing titrations of all lean amine solutions to determine the concentrations of free and bound amine. These curves are shown in Figures 58 through 59.

As seen in Figures 58 and 59, the acid titrations show two endpoints: one for the free amine at a higher pH and the other probably for weak acid anions in solution, which occurs at a lower pH. The first endpoint for lean monoethanolamine (MEA) solution was determined to be about pH 6.87, and the second was at about pH 3.88; the first and second endpoints for lean Solvent A solution were found to be around pH 7.5 and pH 4.0, respectively. Also, the endpoint in the case of Solvent A was a little sharper than that for MEA samples. According to previous studies by Cummings et al, the second endpoint corresponds to the titration of weak acid anions in solution such as formate and acetate and excess  $\text{OH}^-$  ions. However, in our samples there is no  $\text{OH}^-$  used in the pilot plant scrubbing process, and so there is no expectation that there are any  $\text{OH}^-$  ions involved in the second endpoint in this case. Pending further analysis on the samples, we expect this second endpoint to be a result of weak organic anions and/or the carbonate and bicarbonate ions in solution. The reference pH for the other lean amine solutions was determined in a similar way, prior to carrying out complete titrations for free and bound amine determinations.

Figures 60 and 61 show the base titration curves. As mentioned earlier and shown in these figures, the base endpoints were more difficult to discern than the acid endpoints. That notwithstanding, the endpoint was estimated to be about pH 11.5, and this was used as a reference pH to determine the concentrations of the bound amine in lean amine solutions.

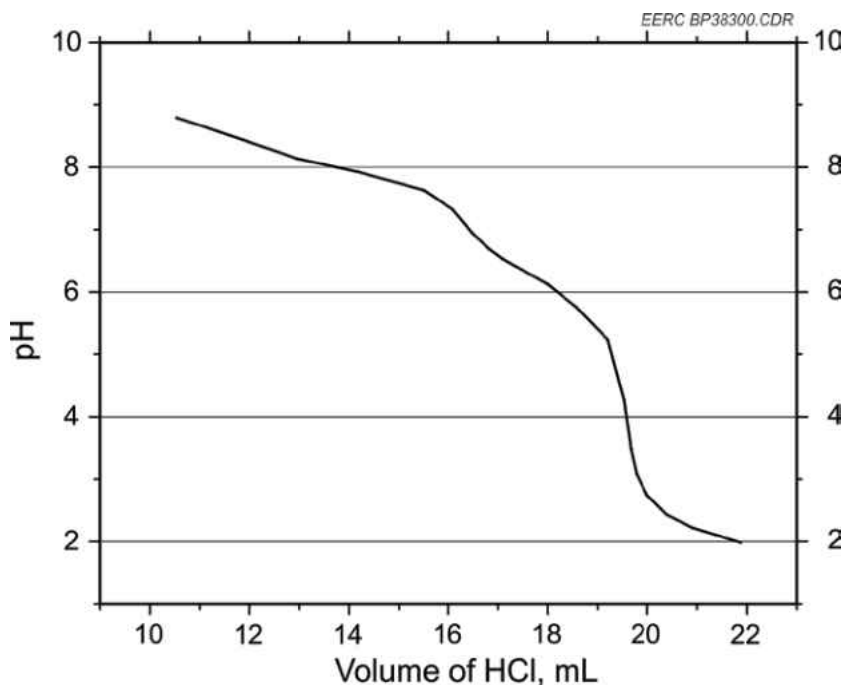


Figure 58. Acid titration curve of MEA Sample No. 95.

### Determination of CO<sub>2</sub> Loading

Carbon dioxide loading in the amine solutions was derived from total organic carbon (TOC) analysis performed at the University of North Dakota's Environmental Analytical Research Laboratory (EARL) at the School of Engineering & Mines. However, the amount of amine in solution for each sample was determined separately



and combined with TOC data to get the reported CO<sub>2</sub> loading, expressed as ratios of moles of CO<sub>2</sub> to that of amine in a given sample.

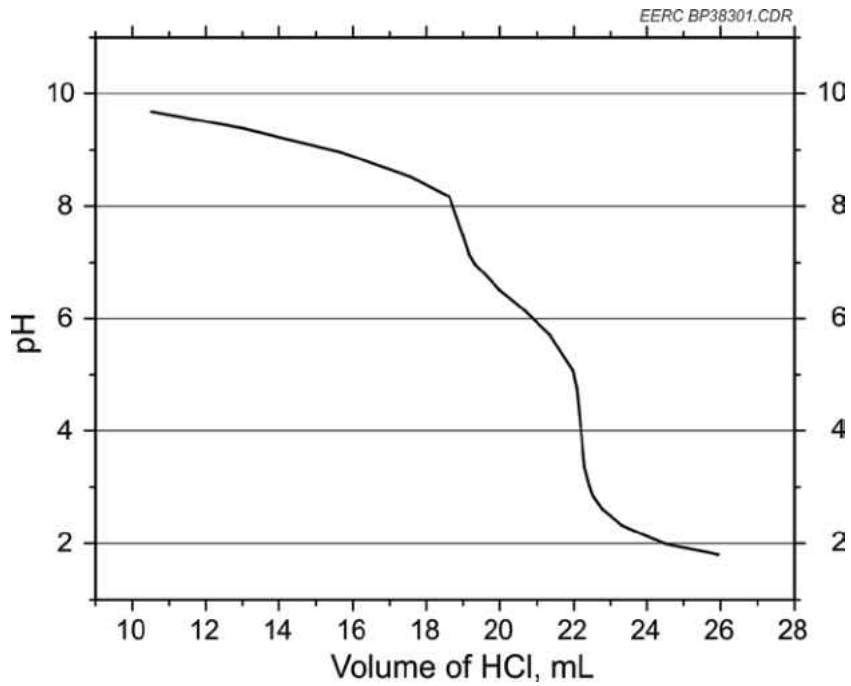


Figure 59. Acid titration curve of Solvent A Sample No. 48.

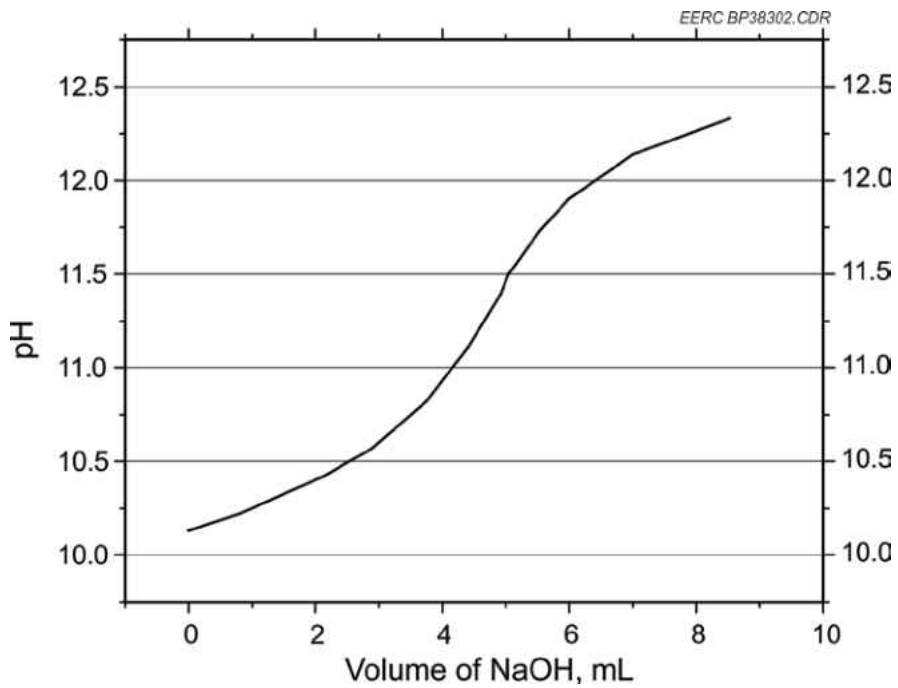


Figure 60. Base titration curve of MEA Sample No. 95.

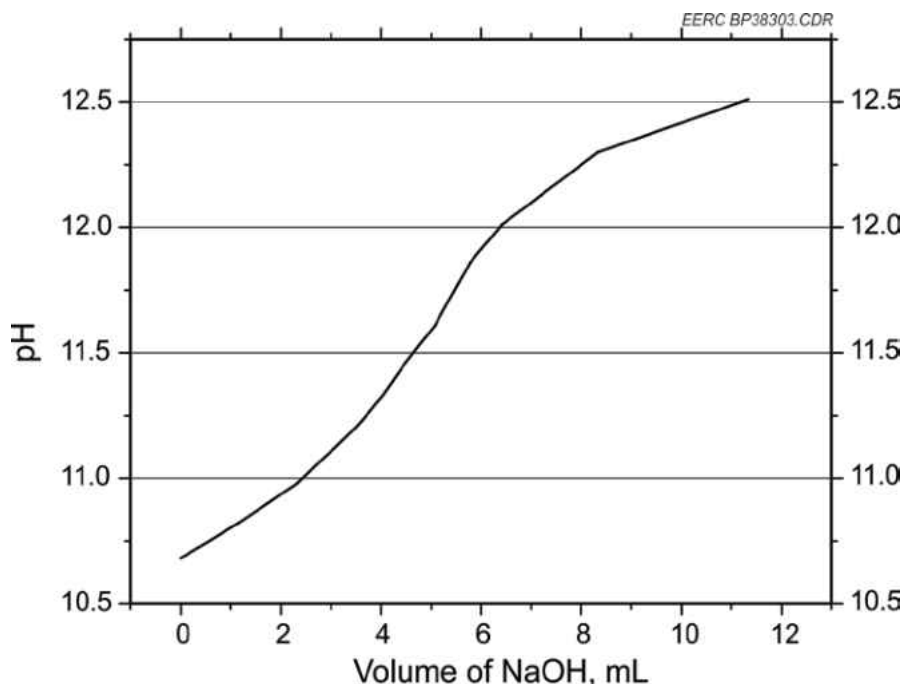


Figure 61. Base titration curve of Solvent A Sample No. 48.

### Equipment

The CO<sub>2</sub> loading in lean amine solutions was determined as the total inorganic carbon content of the solution using a TOC analyzer. The specific model of the TOC analyzer used is TOC-VCSH, which is manufactured by Shimadzu Corporation.

### Procedure

The standard procedure for TOC analysis at EARL involves the following steps:

- Standards preparation. Two stock solutions, about 1000 ppm each, were made for TOC and inorganic carbon analysis. The TOC stock solution was made by dissolving anhydrous potassium biphthalate in deionized water, and the inorganic carbon stock solution was made up of anhydrous sodium bicarbonate and sodium carbonate dissolved in deionized water. A set of

working standard solutions for calibration were then derived from the stock solutions by further dilution as needed.

- Sample preparation. Turbid samples were filtered through a 0.45- $\mu\text{m}$  filter; otherwise, they were simply diluted (if needed) to required concentration and loaded into the equipment in small vials for analysis.

## **DETERMINATION OF ORGANIC ANION CONCENTRATIONS**

### **Equipment**

Organic anions including formate, acetate and oxalate, and select inorganic anions were also determined using a Dionex ICS 3000 ion chromatography (IC) system. This system uses a gradient-based separation method to separate the analytes and is equipped with complete eluent generation and conductivity detection capabilities.

### **Procedure**

Standard IC analysis procedures adopted at the EERC's ARL were used. A gradient method was utilized in order to separate and elute weak retaining analytes such as the organic anions and minimize the elution time of strong interacting analytes such as thiocyanate. Table 15 displays the general operating parameters, and Table 16 shows the gradient method used for the standard and unknown samples. The samples were diluted by a factor of 100 prior to analysis.

Availability of good analyte standards is an important component of IC analysis. Figure 62 represents a chromatogram from a 10 ppm standard solution of the different analytes that were determined. Fluoride, acetate, formate, chloride, nitrite, bromide, nitrate, sulfate, oxalate, phosphate, thiosulfate, and thiocyanate were all separated and

detected in the chromatogram. The method provides sufficient resolution for all of the analytes and has a run time of 44 minutes.

Table 15. Operating Parameters of the ICS 3000 System

---

Trap Column	ATC-3
Sample Volume	25 $\mu$ L
Column	Ion Pac AS11-HC and AG11-HC (guard)
Eluent Generator	KOH
Eluent 1	Deionized water
Eluent 2	Deionized water
Eluent 3	Deionized water
Eluent 4	Deionized water
Eluent Flow Rate	1.5 mL/min
Operating Temperature	30°C
SRS Suppressor	Anion self-regenerating suppressor
Background Conductivity	$\leq 3.5 \mu$ S
Typical Operating Back Pressure	2100–2700 psi

---

Table 16. Gradient Conditions Used for Standards and Samples

Time, min	KOH Eluent Concentration,	
	mM	Comments
0	1	
9	1	End isocratic analysis
17	15	Gradient analysis
25	30	
33	65	
38	65	
38.1	1	Equilibration for next run
44	1	

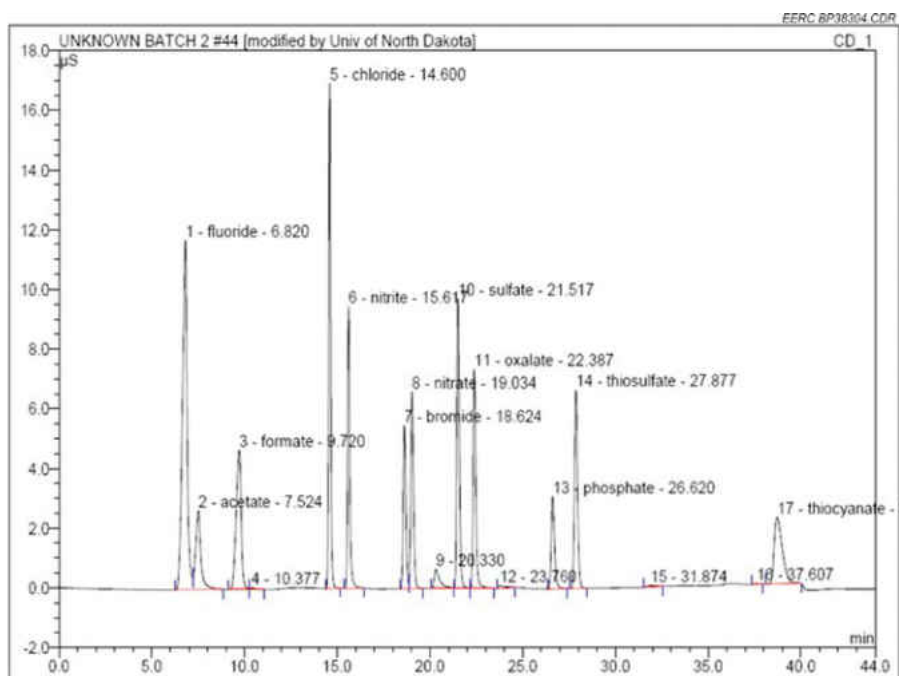


Figure 62. Chromatogram of 10 ppm analyte standard solutions.

## APPENDIX A2 CALCULATIONS

### CALCULATING CO<sub>2</sub> CAPTURE

One key result for each test condition was CO<sub>2</sub> capture across the absorber column. Analyzers monitoring the unit provide CO<sub>2</sub> concentration as a percentage of the total gas flow. Analyzers used to calculate CO<sub>2</sub> capture were the furnace exit analyzer, the absorber inlet/outlet analyzer, and the dedicated stack analyzer. The basic formula for calculating percent CO<sub>2</sub> capture used in reducing the data is given in Equation A2-1 (basic CO<sub>2</sub> capture equation). When analyzer data were not available directly at the absorber outlet, CO<sub>2</sub> values at the stack were substituted as a close approximation.

$$\%CO_2 capture = \frac{Q_{in} * CO_2 in - Q_{out} * CO_2 out}{Q_{in} * CO_2 in} * 100 \quad [Eq. A2-1]$$

Where

$Q_{in}$  = Absorber inlet flow rate (scfm\*)

$Q_{out}$  = Absorber outlet flow rate (scfm\*)

$CO_{2 in}$  = CO<sub>2</sub> percentage of total inlet flow rate (%)

$CO_{2 out}$  = CO<sub>2</sub> percentage of total outlet flow rate (%)

\*Standard conditions for flow rate calculations are 68°F and 1 atm.

A more accurate representation of CO<sub>2</sub> removal is obtained by correcting for air inleakage across the absorber and by correcting for a standard O<sub>2</sub> level at each analysis point. Air inleakage between the furnace and the postcombustion system was determined

by noting the O<sub>2</sub> levels at the furnace exit and the absorber inlet. Because the analyzer for the absorber inlet was normally positioned to read the absorber outlet, a constant air inleakage value was determined by averaging the inlet O<sub>2</sub> levels taken occasionally through the test and comparing them with the constant O<sub>2</sub> level at the furnace exit. This inleakage value was assumed to be constant throughout the test and consisting of 21% O<sub>2</sub> and 79% N<sub>2</sub>. CO<sub>2</sub> and O<sub>2</sub> levels at the absorber inlet were then corrected according to this air inleakage number using Equation A2-2 (calculating the air inleakage as a flow rate) and Equation A2-3 (correcting absorber inlet values for air inleakage).

$$Q_{leak} = O_{2\ leak} * Q_{in} + \frac{79}{21} * O_{2\ leak} * Q_{in} \quad [\text{Eq. A2-2}]$$

$$CO_{2in}^* = \frac{CO_{2\ furnace} * (Q_{in} - Q_{leak})}{Q_{in}} \quad [\text{Eq. A2-3}]$$

Where

$Q_{leak}$  = Amount of air leaking in upstream of the absorber (scfm)

$O_{2\ leak}$  = O<sub>2</sub> leaking into the system as a percentage of absorber inlet flow (%)

$CO_{2\ furnace}$  = CO<sub>2</sub> developed during combustion at the furnace exit (%)

The data were also inspected to find if there was any air inleakage across the absorption column which could possibly bias the analyzer data at the outlet. No significant inleakage was observed across the absorption column after comparing O<sub>2</sub>

levels at the inlet and outlet to the column. The air leakage across the absorber is assumed to be zero for all calculations in this report. On a larger scale, this assumption may not hold, and air leakage across the absorber column should be quantified before calculating CO<sub>2</sub> capture.

Once the corrected numbers for CO<sub>2</sub> and O<sub>2</sub> were found, the CO<sub>2</sub> values used in the calculation were corrected to a standard O<sub>2</sub> level using Equation A2-4 (correcting to 3% oxygen). For the data, 3% O<sub>2</sub> was chosen as a standard value, with an assumed standard concentration of 21% O<sub>2</sub> in air.

$$CO_{2\ in} = CO_{2\ in}^* * \frac{21-3}{21-O_{2\ in}} \quad [\text{Eq. A2-4}]$$

Where  $O_{2\ in}$  = percentage of O<sub>2</sub> at the inlet, corrected for air leakage (%).

With the corrected value for the percentage of CO<sub>2</sub> at the inlet to the absorber, Equation A2-1 was used to calculate the percentage of the CO<sub>2</sub> in the flue gas that is absorbed by the solvent before the absorber outlet.

In addition to calculating the CO<sub>2</sub> removal rate, it was of interest to know the mass of CO<sub>2</sub> removed. Knowing both the mass removal rate and the volumetric removal rate helps the end user to come to a more informed conclusion on the performance of the system or solvent being tested. CO<sub>2</sub> mass removal rate was calculated for monoethanolamine (MEA) in terms of g CO<sub>2</sub> per minute. Equation A2-5 (CO<sub>2</sub> mass entering the absorber) was used to calculate the mass of CO<sub>2</sub> entering the absorber



column. It assumes the flue gas behaves as an ideal gas. Pressure at the absorber was near ambient throughout the test, so  $P_{in}$  is assumed to be atmospheric pressure, or 1 atm.

$$mCO_{2\ in} = \frac{Q_{in} * CO_{2\ in} * P_{in}}{T_{in} * R} \quad [\text{Eq. A2-5}]$$

Where

$mCO_{2\ in}$  = Mass flow rate of  $CO_2$  entering the absorber (g  $CO_2$ /min)

R = Ideal gas constant (3.659E-5 ft<sup>3</sup>\*atm/°R\*g)

Similarly, the  $CO_2$  in the flue gas leaving the absorber is calculated by substituting absorber outlet values for inlet values, as in Equation A2-6 ( $CO_2$  mass leaving the absorber).

$$mCO_{2\ out} = \frac{Q_{out} * CO_{2\ out} * P_{in}}{T_{out} * R} \quad [\text{Eq. A2-6}]$$

Where  $mCO_{2\ out}$  = Mass flow rate of  $CO_2$  leaving the absorber (g  $CO_2$ /min).

After calculating the  $CO_2$  mass entering and exiting the absorber with the flue gas, we can do a mass balance to find how much is being absorbed by the solvent and carried over to the stripper column. Equation A2-7 ( $CO_2$  mass capture rate across the absorber) shows the mass balance equation used to find  $CO_2$  capture rate across the absorption column.

$$mCO_{2\text{ capture}} = mCO_{2\text{ in}} - mCO_{2\text{ out}} \quad [\text{Eq. A2-7}]$$

Where  $mCO_{2\text{ capture}} = CO_2$  mass absorption rate of the solvent (g/min).

Knowing the  $CO_2$  capture from the flue gas across the absorber in terms of both percentage and mass allows for a better understanding of the system performance when comparing to other variables such as reboiler duty rate and inlet flow rate.

### **CALCULATING REBOILER DUTY RATE**

One of the key performance metrics of the postcombustion system is the reboiler duty. Reboiler duty tells a prospective investor how much steam must be used to regenerate the solvent by driving off the  $CO_2$  that was collected in the absorption column. For the EERC's pilot-scale system, data were collected by the data acquisition system for steam flow rate, steam temperature and condensate temperature. Manual recordings of steam pressure at the reboiler inlet were made periodically. Pressures were used as a check on the assumption that the steam coming in was saturated. The condensate leaving the reboiler was assumed to be a saturated liquid. Knowing the temperatures of both of these streams, enthalpy values were looked up in a steam table to find the heat of vaporization. The enthalpy difference between the steam and condensate streams was multiplied by the steam flow rate to produce a value for the reboiler duty. This calculation is shown in Equation A2-8. A similar calculation was performed for the condenser heat exchanger. The condenser duty data, however, were not able to be accurately reduced because the control valve for the water flow through the condenser

was sized such that a representative flow rate through the condenser was not easily calculated.

$$\dot{H}_{reboiler} = \dot{m}_{steam} * (h_{vap} - h_{cond}) \quad [\text{Eq. A2-8}]$$

Where

$H_{reboiler}$  = Reboiler duty (Btu/hr)

$m_{steam}$  = Mass flow rate of steam into reboiler (lb/hr)

$h_{vap}$  = Enthalpy of saturated steam at reboiler inlet temperature (Btu/lb)

$h_{cond}$  = Enthalpy of saturated liquid at reboiler condensate stream (Btu/lb)

One important performance metric of CO<sub>2</sub> capture systems is energy use per pound of CO<sub>2</sub> captured. Steam consumption in the reboiler heat exchanger makes up a significant portion of the energy used to capture CO<sub>2</sub> in a typical CCS application. The value is commonly reported in the literature as Btu/lb CO<sub>2</sub> captured. Reboiler steam use in Btu/lb CO<sub>2</sub> for the pilot demonstration system is calculated by combining Equations A2-7 and A2-8, and then converting the applicable units. This calculation is shown in Equation A2-9:

$$SteamUse = \frac{\dot{H}_{reboiler}}{m_{CO_2 capture}} * \frac{hr}{60 min} * \frac{g}{2.2E-3 lb} \quad [\text{Eq. A2-9}]$$

Where SteamUse = Steam heat used to release CO<sub>2</sub> from solution (Btu/lb CO<sub>2</sub> captured).

## APPENDIX B

### DETAILED SOLVENT RESULTS

Table 17. Proximate/Ulimate Analysis of Antelope Coal used for testing.

	As-Det.	As-Recd.	Dry	Dry/Ash Free
Proximate Analysis, wt%				
Moisture	11.38	24.41	N/A	N/A
Volatile Matter	34.07	29.06	38.44	40.63
Fixed Carbon, ind.	49.77	42.45	56.16	59.37
Ash	4.79	4.08	5.40	N/A
Ultimate Analysis, wt%				
Hydrogen	5.44	6.28	4.70	4.97
Carbon	61.63	52.57	69.54	73.51
Nitrogen	4.79	4.08	5.40	5.71
Sulfur	0.35	0.30	0.39	0.42
Oxygen, ind.	23.01	32.69	14.57	15.40
Ash	4.79	4.08	5.40	N/A
Heating Value, Btu/lb	10,340	8820	11,668	12,334

As-received hydrogen not including hydrogen from moisture 3.55%.

As-received oxygen not including oxygen from moisture 11.01%.

Table 18. Typical flue gas composition from the combustion of coal.

Component	Combustor Outlet	Absorber Inlet
CO <sub>2</sub> , %	12 - 15	12 - 14
SO <sub>2</sub> , ppm	350 - 400	0 - 50
O <sub>2</sub> , %	3 - 4	5 - 7
NO <sub>x</sub> , ppm	100 - 200	0 - 50
CO, ppm	5 - 10	5 - 10

## APPENDIX B-1

### H3-1 TEST RESULTS

H3-1 solvent was tested continuously on the CTF for about a week, from February 8 to 16, 2010. The fuel used for this test was Antelope PRB subbituminous coal, and the CTF was operated at a FEGT of around 2000°F. The solvent was used as-received with an amine concentration of 40–50 wt%. The goal of H3-1 testing was to explore its CO<sub>2</sub> capture efficiency under multiple test conditions, including varying stripper column static pressure, varying reboiler duty, and varying flue gas inlet flow rates. During testing, samples were periodically drawn from the absorber and titrated to determine the concentration of free amine in the column so as to decide whether solvent and/or water makeup was necessary. If the amine concentration appeared to be rising, more deionized water was added, and if the solution was becoming more dilute, fresh amine was added.

When the data collected during the test run were corrected for oxygen and air leakage, CO<sub>2</sub> capture efficiencies of 90% or greater were achieved, with some periods where the performance was as high as 96%. For the first 2 days of the test, levels of 90% were attained consistently. Near the end of the second day of testing, with an inlet flue gas flow rate of approximately 100 scfm, the static pressure on the stripper column was increased to 8 psig, then to 12 psig, and CO<sub>2</sub> removal of >90% was achieved. On a separate occasion with the stripper pressure at 12 psig and flue gas flow rate of 75 scfm, about 95% CO<sub>2</sub> capture was achieved. Test periods using the same parameters as the baseline case were run for H3-1. Several variables including solvent flow rate, reboiler

duty, stripper pressure, and flue gas flow rate were changed during the test to determine correlations between variables.

## **System Performance**

### *Test Parameter Analysis*

Testing for H3-1 was designed to be a direct comparison against the baseline solvent base. In general, increased regeneration energy corresponded to increased CO<sub>2</sub> capture levels. Increases in CO<sub>2</sub> capture also appeared to correlate directly with increases in solvent flow rate. Like MEA, solvent temperatures throughout the system were important to keep within an acceptable performance window, but when pushed outside that window, CO<sub>2</sub> capture did not drop off as sharply as in MEA.

Behavior of the solvent for each inlet flue gas flow is presented in Figure 63. CO<sub>2</sub> capture is presented as a function of solvent pumping rate for three different flow rate cases. The 75 scfm flow rate test case required much lower solvent flow than the 100 scfm case to reach the 90% capture goal. The system captured 90% CO<sub>2</sub> using about 57% less solvent when treating 75 scfm of flue gas compared to 100 scfm. Data from the 60 scfm case were not as complete as the two higher flow cases, so a performance curve for the data could not be constructed.

Figure 64 presents CO<sub>2</sub> capture rate for H3-1 as a function of regeneration energy input for test periods at solvent flow rates between 4 and 6 gpm. CO<sub>2</sub> capture for the cases with the stripper operating at 12 psig static pressure reached 90% at a regeneration energy input of about 1475 Btu/lb CO<sub>2</sub>. For the test periods at 4 psig, regeneration energy

required for 90% CO<sub>2</sub> capture was almost 16% lower than the 12 psig case with a value of about 1240 Btu/lb. Both of these cases were run at similar lean solvent flow rates of about 4 gpm. A second 12 psig case is shown in Figure 64 at a slightly higher solvent flow rate. CO<sub>2</sub> capture rates for the high flow case are much higher than the lower solvent flow cases for similar regeneration energy levels.

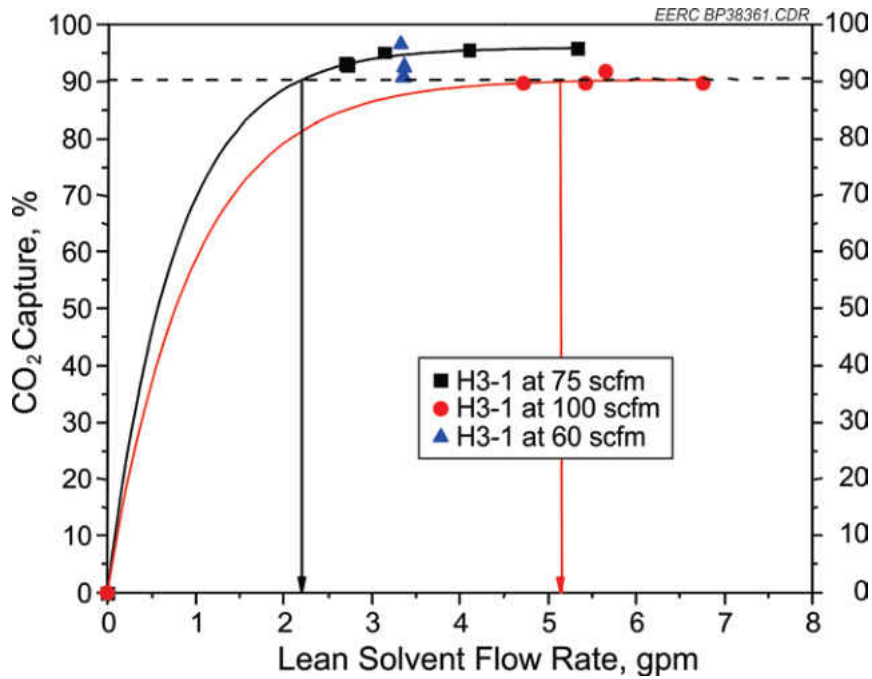


Figure 63. CO<sub>2</sub> capture for various inlet flows using H3-1.

***Stripper Pressure***

To demonstrate the impact of stripper column pressure, Figure 65 shows CO<sub>2</sub> capture and liquid-to-gas ratio for a series of test periods as a function of stripper static pressure.

### Solvent Temperature Effects

One of the key operational concerns in running tests on the postcombustion system was maintaining consistent temperatures at key points in the solvent loop. Figure 66 shows a sharp decrease in CO<sub>2</sub> capture rate as the inlet solvent temperature approaches a level that is unsustainable in the system. For a solvent flow rate of 4 gpm, CO<sub>2</sub> capture rate decreased sharply once the gas outlet temperature rose above 115°F. It was assumed that the solvent entering the absorber through the spray nozzle at the top of the column quickly reached the temperature of the gas leaving the column.

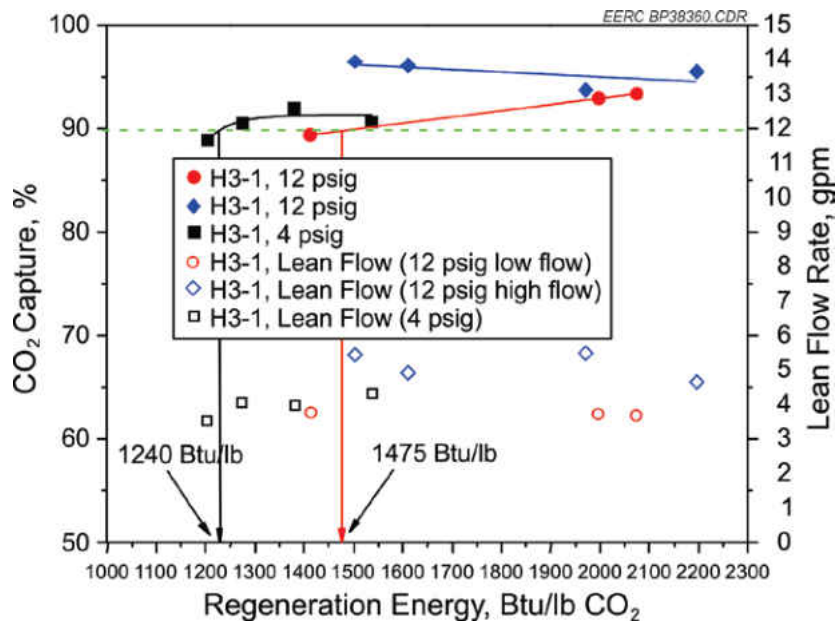


Figure 64. Comparison of H3-1 reboiler duty at varying conditions.



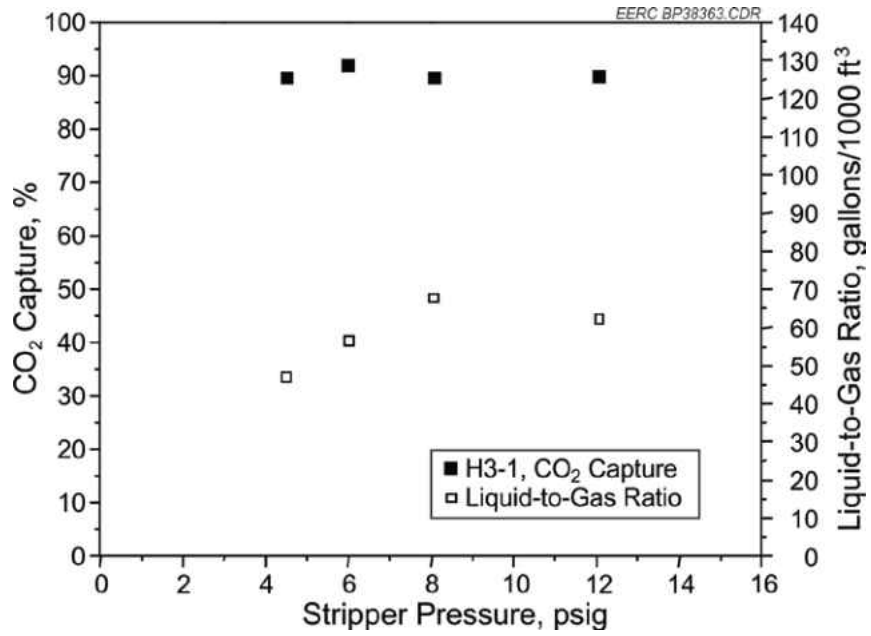


Figure 65. Effect of stripper pressure on H3-1 performance.

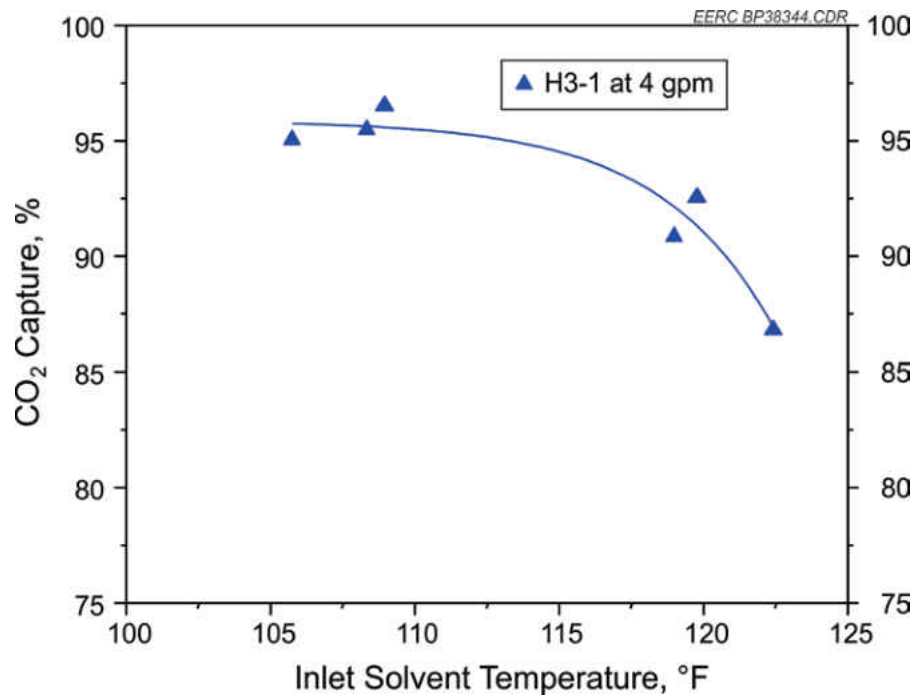


Figure 66. Effect of absorber inlet solvent temperature on CO<sub>2</sub> capture for H3-1.

### Liquid-to-Gas Ratio

Figure 67 shows the effect of liquid-to-gas ratio on CO<sub>2</sub> capture rate for a series of test periods. As liquid-to-gas ratio increased, CO<sub>2</sub> capture rate increased. For a liquid-to-gas ratio increase from 32 to 39, CO<sub>2</sub> capture increased from about 90% to 95%. However, the rate of increase dropped off dramatically at 39 gal/1000 ft<sup>3</sup>. An additional increase of 16 gal/1000 ft<sup>3</sup> led to an increase of only about 1% in CO<sub>2</sub> capture. The data show that a point of diminishing returns in CO<sub>2</sub> capture rate occurred at a treated flue gas level of 75 scfm with a liquid-to-gas ratio of about 39.

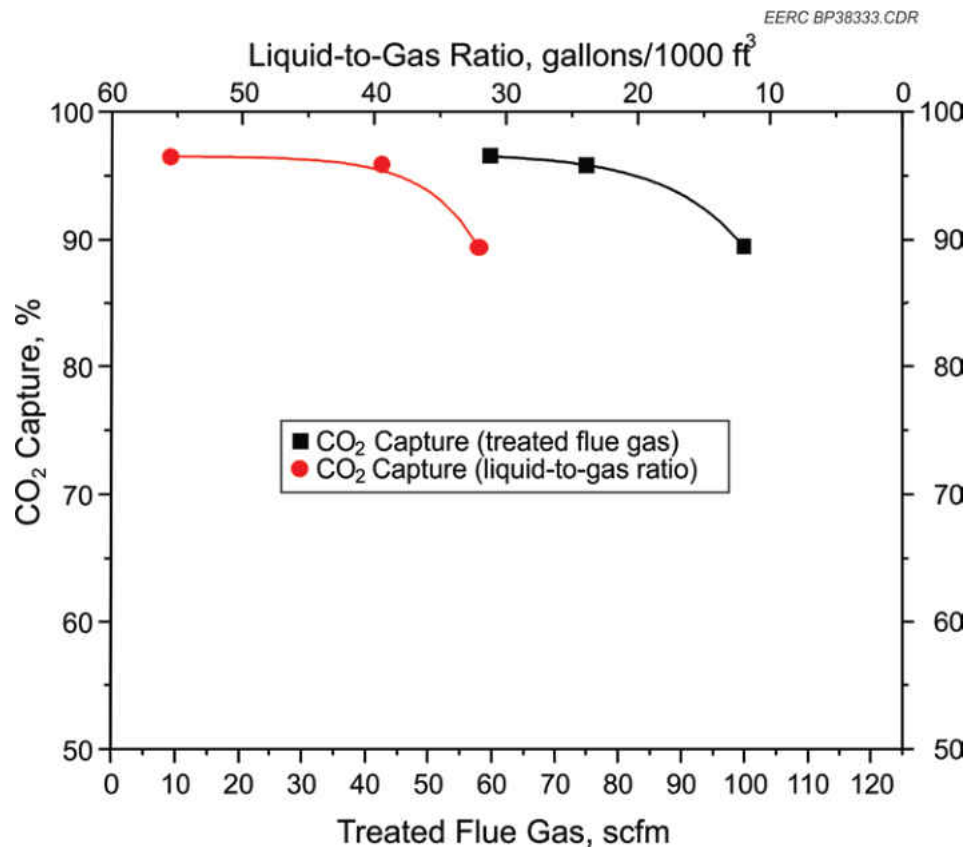


Figure 67. Gas flow rate and liquid-to-gas ratio effects on CO<sub>2</sub> capture.

### H3-1 Sample Analysis

### *Free Amine in Lean H3-1 Solutions*

The concentration of free amine in lean H3-1 solutions was determined by titration using aqueous HCl as titrant. A summary of the results is shown in Figure 68 for the absorber and stripper. The results show that the concentration of free amine in the absorber was in the range of about 29–36 wt% and that in the stripper ranged from about 34 to 43 wt%, and the concentration of the initial amine solution loaded in the absorber was determined to be about 48 wt%. The sharp drop between the initial amine concentration and Day 1 of the test is due to the fact that fresh amine solvent without any flue gas exposure contains no absorbed CO<sub>2</sub> and other compounds, but after Day 1, the solution becomes lean (i.e., loaded with CO<sub>2</sub>), and so the concentration of free amine in lean solution is much lower than for fresh amine solution. Similar to the case of MEA, the results indicate that our titration protocol for this solvent was reasonable given that similar approaches reported previously (20) have shown overestimates of over 100% for free amine in lean amine solution samples.

Unlike the case of MEA, the endpoint in the titration was relatively sharper for H3-1 samples. In this case, the first endpoint corresponds to the free amine in lean H3-1 solutions, while the second endpoint at lower pH corresponds to acid consumption by weak carboxylic acid anions (if present) and/or carbonates and bicarbonates. Because these possible acid anions and/or carbonates and bicarbonates are weaker bases than free amine, they have a lower endpoint than the free amine; hence, the two endpoints can be detected separately. The plots in Figure 68 also show that the free amine concentrations in the absorber and stripper decrease exponentially with time. These trends correlate well

with the increasing trends of HSS buildup in solution, which take up some of the free amine. For the same reason as in the case of MEA (i.e., free amine is regenerated in the stripper), the concentration of free amine in the absorber was lower than that in the stripper.

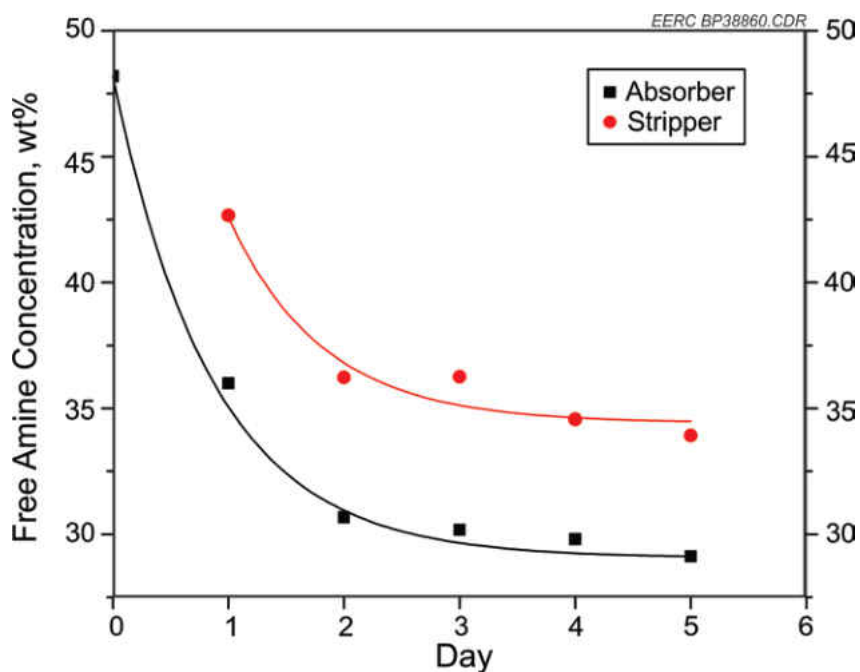


Figure 68. Concentration of free amine in lean H3-1 solutions.

### ***Bound Amine in Lean H3-1 Solutions***

The concentration of bound amine in lean H3-1 solutions was determined also by titration using aqueous NaOH solution as the titrant. The endpoints in these base titrations were difficult to detect because they were not sharp; hence pH curves were used to obtain the reference pH at the endpoint of 11.5. Using this reference pH to mark the endpoint,

the concentrations of bound amine in the sample solutions were determined. Because the titration quantifies all amine cation species in solution, the amount of amine cation obtained for the first day of the test was used as baseline and subtracted from values of subsequent days to obtain what is truly bound and not regenerable. The results are summarized in Table 19 for the absorber and stripper.

The concentration of bound amine in the absorber ranged from about 0 to 1.32 wt% in the course of the 5 days of testing; the range seen for stripper samples was about 0–2.38 wt%. In both the stripper and absorber, the concentration of bound amine tends to increase linearly and is consistent with the total HSS concentration seen from the IC data.

Table 19. Bound Amine in Lean H3-1

Day	Absorber Bound Amine, wt%	Stripper Bound Amine, wt%
1	0.00	0.00
2	0.15	1.08
3	0.31	0.38
4	1.32	2.38
5	-0.19	1.14

### ***Inorganic Anions in Lean H3-1 Solvent Solutions***

Over the 5-day test period, inorganic anions were observed to accumulate in the scrubbing system. The results are displayed in Figure 69. The sulfate concentration was the highest, ranging from about 400 ppm at the beginning of testing to about 2250 ppm at the end of the test. The sulfate and thiosulfate levels are much higher toward the end of the test because of injection of 10, 20, and 50 ppm of SO<sub>2</sub> on Day 3 of testing. The NO<sub>x</sub> levels were maintained at baseline, i.e., less than 10 ppm, which is the reason for the

negligible amounts of nitrites and nitrates observed in these samples. The chloride ion level was not directly measured in the flue gas entering the absorber, but chloride levels can be compared with coal chlorine level, which was about 2353 ppm for the Antelope PRB subbituminous coal used in this test. The amount of chloride ion in solution was near zero for the first 2 days of testing, but showed significant amounts that were seen to increase with time from Day 3 to Day 5 because of buildup. Comparison between the absorber and stripper indicated that the concentrations of these anions were similar for both the absorber and stripper.

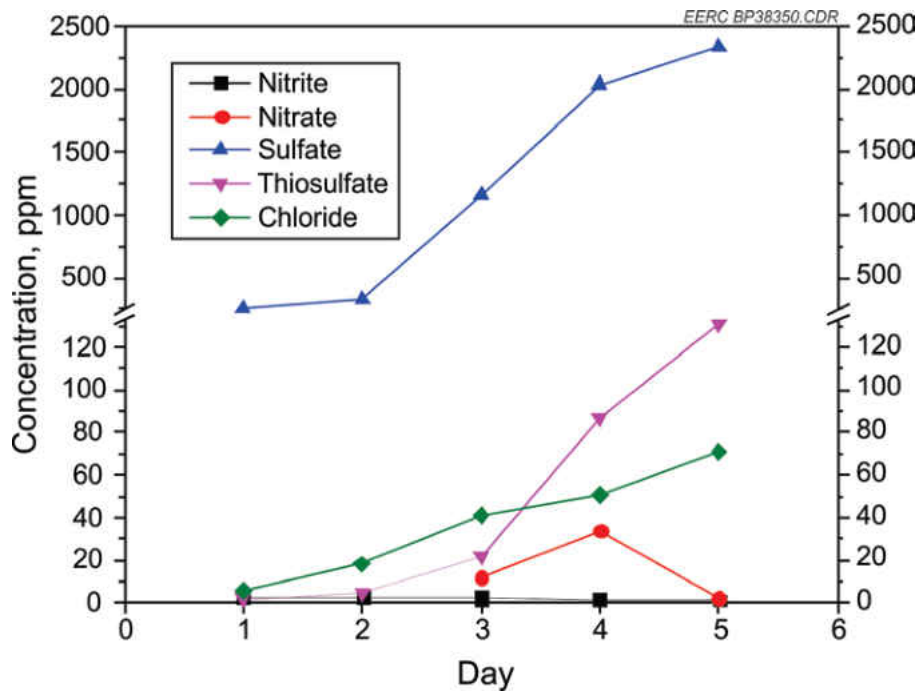


Figure 69. Concentration of inorganic anions in lean H3-1 solutions.

### ***Organic Anions in Lean H3-1 Solutions***

The major organic anions that were tested in solution samples for all the solvents were formate, acetate, and oxalate, which are some of the major organic anion degradation products of MEA. In H3-1 solutions, we do not expect these to be present since the amine is different from MEA and will degrade in the presence of oxygen via different oxidative degradation mechanisms. In order to make any predictions on plausible organic anion degradation products, the mechanisms of degradation need to be determined prior to analysis. An analysis of the samples for formate, acetate, and oxalate yielded zero concentrations for these anions in lean H3-1 solution samples, which confirms that different mechanisms are involved.

### ***Trace Metals in Lean H3-1 Solutions***

Trace metal concentrations observed in lean H3-1 solutions were generally low. These results are presented in Figure 70. The same trace metals that were analyzed in MEA samples (Ni, Cr, Fe, Mn, and Mo) were analyzed in H3-1 samples. Unlike in MEA samples where Cr and Fe had slightly higher concentrations, Ni and Fe have slightly higher concentrations in H3-1 samples. As seen in plots, these levels are significantly lower than those seen in MEA samples. Another difference between H3-1 samples and MEA samples is that all trace metals show an increasing trend with time; in MEA samples, the amount of Cr and Fe decreased exponentially with time. Increasing trends in the amount of these trace metals is expected and correlates well with the buildup of HSS in solution. The very low levels of corrosion components in H3-1 samples could possibly reflect the relatively short testing time and, hence, the low amounts of corrosive HSS in

solution. The low amounts of HSS observed are also due to the fact that the flue gas composition had relatively low amounts of  $\text{NO}_x$  ( $< 10$  ppm) and  $\text{SO}_x$  at the beginning of the test, except on Day 3 when additional  $\text{SO}_2$  was injected into the system. Mn and Mo concentrations are well below 1 ppm and appear to remain relatively constant throughout the test period. These concentrations are similar to those seen in the case of MEA and reflect the fact that Mn and Mo are only minor components of stainless steel used in fabricating the process equipment for this study.

### ***Major Elements in Lean H3-1 Solutions***

The results of major element screening in H3-1 samples are presented in Figure 71. Unlike MEA solutions, H3-1 samples had much lower concentrations of these elements. Sodium concentration is the highest in H3-1 samples, similar to what was observed in MEA samples. All other major elements had insignificant levels, except for Al with a concentration in the range of about 10–35 ppm. The results also indicate that the concentration of Na and Al increase with time, while those of Ca, K and Mg are relatively constant.

The impact of such major elements which are mainly constituents of coal minerals (particulates) on the integrity of amine solvent technologies has yet to be investigated. This will constitute an important part of the studies envisioned within the  $\text{PCO}_2\text{C}$  project. With the very low levels of these major elements in the tested samples, it is not possible to draw any definitive conclusions about their effects on amine solvents in  $\text{CO}_2$  scrubbing systems. Therefore, prolonged testing to allow for significant accumulation of these elements is necessary to be able to see the effects on solvent scrubbing systems.



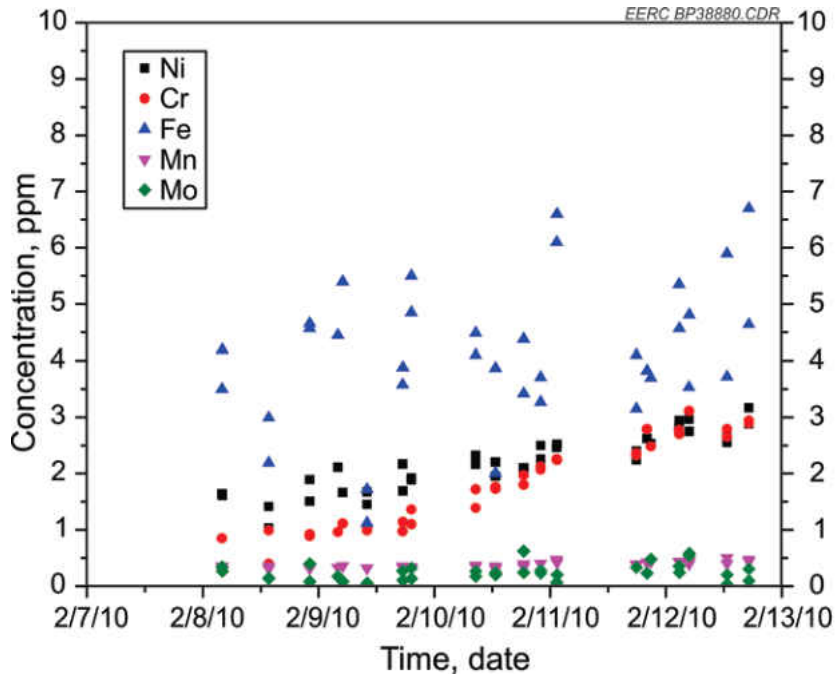


Figure 70. Concentration of trace metals in lean H3-1 solutions.

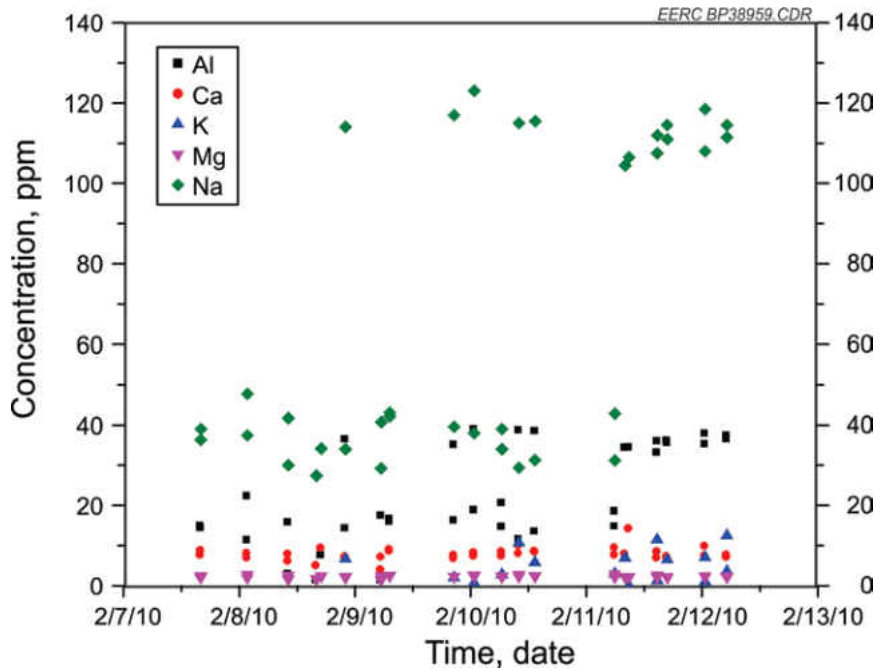


Figure 71. Concentration of major elements in lean H3-1 solutions.

### CO<sub>2</sub> Loading in Lean H3-1 Solutions

The results of CO<sub>2</sub> loading in lean H3-1 solutions are presented in Figure 72 for samples collected from the absorber and stripper during the test period. These results were obtained by determining the total amine and the total dissolved CO<sub>2</sub> in solution samples; the CO<sub>2</sub> loading is then expressed as a ratio of moles of CO<sub>2</sub> to moles of amine. The CO<sub>2</sub> loading in the absorber ranged from about 0.25 to 0.27 during the test period and that for the stripper ranged from about 0.13 to 0.17. The results are consistent with the fact that CO<sub>2</sub> is absorbed by the solution in the absorber and released from solution in the stripper. The trend observed in Figure 72 is an increase in CO<sub>2</sub> loading with time during the first 4 days of testing, but dropped on the last day, which is different from a decreasing trend observed in MEA samples. The average loading in the absorber was determined to be about 0.26, which is represented by the roughly linear trend line for the absorber data, including the fifth day of testing. The upward trend observed for the data is possibly related to the higher reboiler duty used during testing of H3-1, which regenerates more free amine in this test than was the case with other solvents.

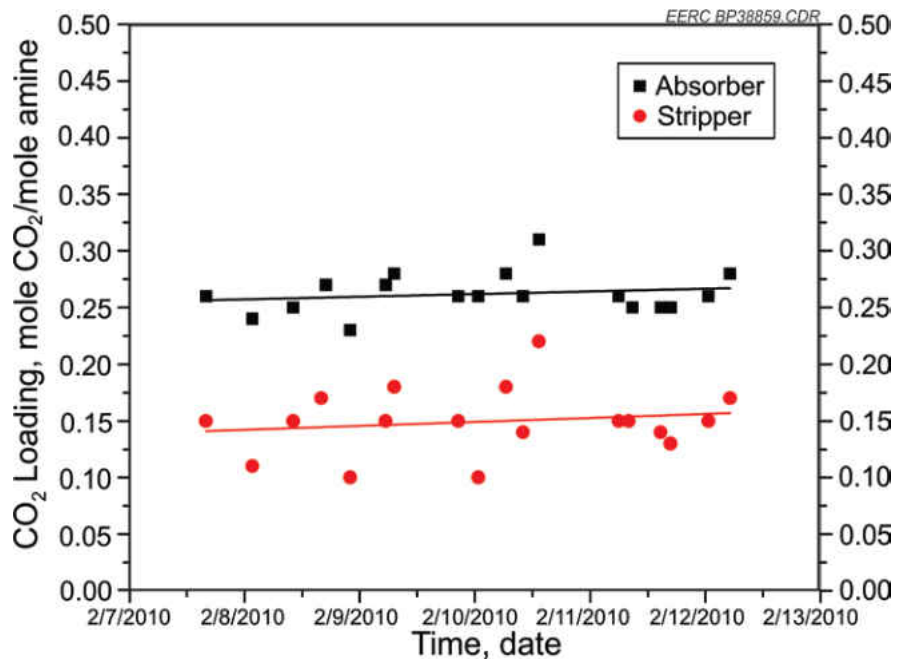


Figure 72. CO<sub>2</sub> loading in lean H3-1 solutions.

## APPENDIX B-2

### HUNTSMAN ADDITIVE TEST RESULTS

Huntsman additive was supplied by Huntsman Petrochemical Corporation and the final mixing was performed at the EERC prior to testing on May 10–14, 2010. The goals for these tests were twofold: 1) to investigate its CO<sub>2</sub> capture performance for varying system variables similar to MEA and H3-1 tests and 2) to investigate how well it can resist degradation because of flue gas components like O<sub>2</sub>, SO<sub>x</sub>, and NO<sub>x</sub>. During tests with varying system parameters, conditions that achieve 90% CO<sub>2</sub> capture were established. In order to determine the impact of HSS buildup in solution, these parameters were maintained relatively steady as the amount of NO<sub>x</sub> and SO<sub>x</sub>, in turn, were varied. The results of these tests are presented below.

#### **System Performance**

Huntsman additive solvent was run through a series of test conditions for the first day of testing and thereafter was set to a test condition that would meet 90% CO<sub>2</sub> capture. Four of the 5 days of testing were run at that test condition, with interruptions only for system maintenance. Huntsman additive captured CO<sub>2</sub> from the flue gas stream at a consistent 88%–91% level for the entire test period. The addition of SO<sub>2</sub> and NO<sub>x</sub> levels to the flue gas stream entering the absorber did not have a noticeable effect on the CO<sub>2</sub> capture levels over the 4 days of testing. A conclusion on solvent performance over a longer duration with acid gas levels used during the test cannot be made without further testing.

With parametric testing for Huntsman additive lasting less than one full day, there were not enough test periods to form conclusions on the effects of reboiler duty rate, stripper column pressure, solvent flow rate, or flue gas flow rate. The long-term test was run at 75 scfm flue gas flow rate with a stripper column static pressure of 12 psig. Flue gas inlet temperature was around 108°F, and the system was run with a lean solvent flow rate of about 5.8 gpm.

### ***Comparing Degradation Product Levels from SO<sub>2</sub> and NO<sub>x</sub>***

Huntsman additive was tested to evaluate degradation product buildup for SO<sub>2</sub> and NO<sub>x</sub> levels above those tested during baseline. The solvent employed an additive designed to protect against HSS formation compared to the baseline MEA solvent. Figure 73 presents sulfur-based HSS concentrations in relation to the SO<sub>2</sub> input from the flue gas for Huntsman additive. Sulfate levels reached about 650 ppm after the first 4 days of testing. For the majority of the week of baseline testing, SO<sub>2</sub> levels were near zero or 1 ppm, with an increase in total SO<sub>2</sub> beginning near the end of the test. The higher SO<sub>2</sub> values for Day 1 are a result of the wet scrubber being brought online to the proper removal rate. Sulfate levels found in the solvent samples were about 90% lower in Huntsman additive compared to MEA following a week of testing for each solvent. The comparison suggests that the additive tested in Huntsman additive had a significant impact on the creation of sulfur-based HSS formation.

Nitrogen-based HSS concentrations were examined, and Figure 74 presents nitrogen-based HSSs nitrite and nitrate for the Huntsman additive. During testing of Huntsman additive, NO<sub>x</sub> levels were increased throughout the test to assess the ability of

the advanced solvent to protect against salt formation.  $\text{NO}_x$  input was plotted to give context to the analysis results. Both nitrite and nitrate levels increased throughout the test, with final concentrations of 4 and 7 ppm, respectively. These values are slightly higher than the MEA data where inlet  $\text{NO}_x$  levels were 0–1 ppm.

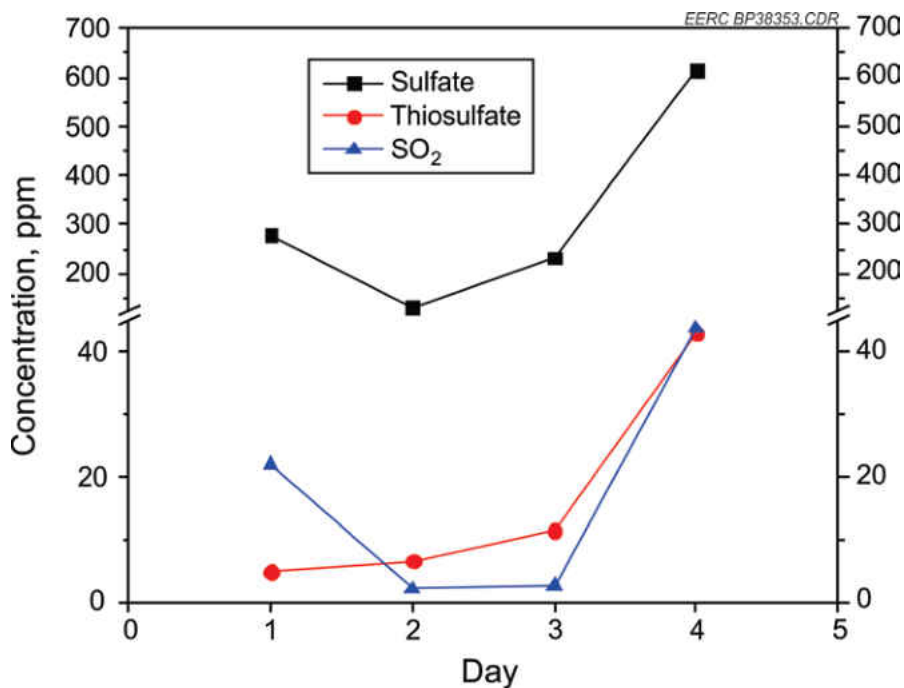


Figure 73. Concentration of sulfate and thiosulfate salts in lean Huntsman additive solutions during  $\text{SO}_2$  injection tests.

### ***Solvent Degradation Product Effect Comparison Summary***

Of the three advanced solvents tested during the scope of the project, Huntsman additive was specifically tested to characterize the performance of an additive designed to limit HSS formation. For sulfur-based HSSs, Huntsman additive analysis samples showed concentration levels nearly 90% less than those found in the baseline MEA case.

However, the same performance characteristic was not evident when oxygen-based HSS compounds were compared. For oxalate and formate, the advanced solvent produced nearly the same results as 30 wt% MEA.

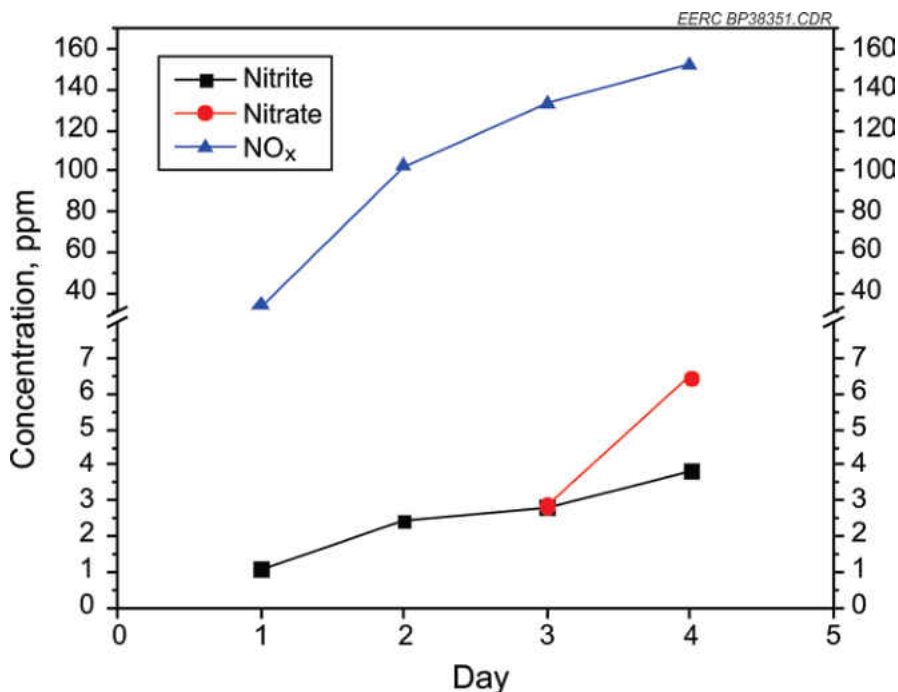


Figure 74. Concentration of nitrite and nitrate salts in lean Huntsman additive solutions during NO<sub>x</sub> injection tests.

## Huntsman additive Sample Analysis

### *Free Amine in Lean Huntsman Additive Solutions*

The free amine concentrations determined in samples collected during testing of Huntsman additive are shown graphically in Figure 75. The concentration of free amine ranged from about 23 to 25 wt% in the absorber and 25.5 to 29 wt% in the stripper, with the initial amine concentration determined to be 31.7 wt%. The sharp drop between the

initial amine concentration and Day 1 of the test is due to the fact that fresh amine solvent without any flue gas exposure contains no absorbed CO<sub>2</sub> and other compounds, but after Day 1, the solution becomes lean (i.e., loaded with CO<sub>2</sub>), and so the concentration of free amine in lean solution is much lower than for fresh amine solution. In general, these concentrations were observed to decrease linearly with time, much like what was observed for MEA and H3-1 solvent. The endpoint in the titration of these samples was more difficult to detect. Given that Huntsman additive was a mixture of amines, the solution chemistry becomes more complex, and there are likely more interferences with the endpoint in the titrations. As a result, different approaches will be investigated in Phase II of the project to improve on the detection of the endpoint and, hence, the quantification of the free amine in lean Huntsman additive solutions.

#### ***Bound Amine in Lean Huntsman Additive Solutions***

The bound amine concentrations observed in lean solution samples of Huntsman additive are summarized in Table 20. Note that because the titration quantifies all amine cation species in solution, the amount of amine cation obtained for the first day of the test was used as baseline and subtracted from values of subsequent days to obtain what is truly bound and not regenerable. The bound amine concentration seen in these samples ranged from about 0 to 0.3 wt% in the absorber and about 0–0.87 wt% in stripper. The bound amine values in the stripper are consistent with the IC HSS data.

#### ***Inorganic Anions in Lean Huntsman Additive Solutions***

The concentrations of inorganic anions in samples collected during testing of Huntsman additive are shown in Figure 76. The sulfate concentration was the highest,



ranging from about 350 to about 600 ppm during the test period. Chloride, nitrite, nitrate, and thiosulfate ions were present in smaller amounts. The sulfate and thiosulfate content rose sharply on the fourth day of testing because of higher levels of SO<sub>2</sub> (about 10–50 ppm) injected into the flue gas upstream of the absorber. In general, the concentrations appear to increase with time.

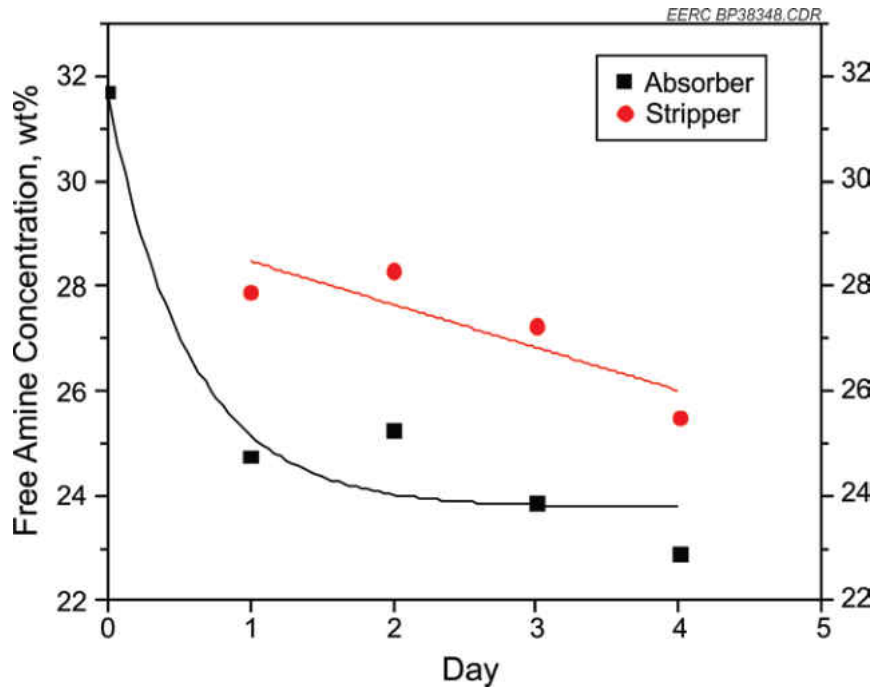


Figure 75. Concentration of free amine in lean Huntsman additive solutions.

Table 20. Bound Amine in Lean Huntsman Additive

Day	Absorber Bound Amine, wt%	Stripper Bound Amine, wt%
1	0.00	0.00
2	0.29	0.85
3	-0.54	0.87
4	-0.79	-0.26

### *Organic Anions in Lean Huntsman Additive Solutions*

Figure 77 displays the results obtained for organic anions, mainly, formate and oxalate. Formate ions were present in larger quantities than oxalate; no acetate ions were found in the analyzed samples. Both concentrations of formate and oxalate increase with time, with a much sharper increase on the last day of testing, which corresponds to the rise in O<sub>2</sub> concentration following a decreasing trend in the previous test days.

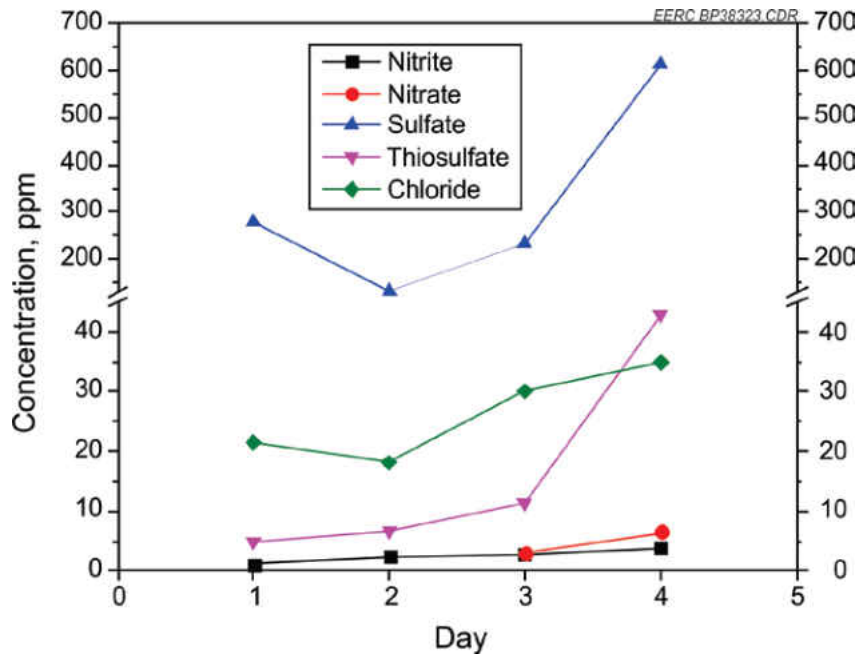


Figure 76. Concentration of inorganic anions in lean Huntsman additive solutions.

### *Trace Metals in Lean Huntsman Additive Solutions*

Concentrations of trace metals found in samples collected during testing of Huntsman additive are presented in Figure 78. These results indicate that the trace metal concentrations increase exponentially with time. Cr appears to have the largest concentration, followed by iron and then nickel. These trends in trace metal

concentrations for Huntsman additive are similar to those seen for H3-1 samples and correlate with increasing trends observed for HSS. The amounts of Cr and Ni increase to higher values in Huntsman additive samples than those seen for MEA or H3-1 solvent. This may be a reflection of the higher levels of SO<sub>x</sub> and NO<sub>x</sub> that were added to the flue gas entering the absorber. Although there was a much greater sulfate content in MEA samples (up to 7000 ppm), there was less corrosion observed in MEA samples compared to Huntsman additive samples. The major difference between MEA test samples and Huntsman additive test samples is that higher levels of NO<sub>x</sub> were administered during Huntsman additive testing. This seems to suggest that higher NO<sub>x</sub> levels could lead to greater corrosion of process equipment.

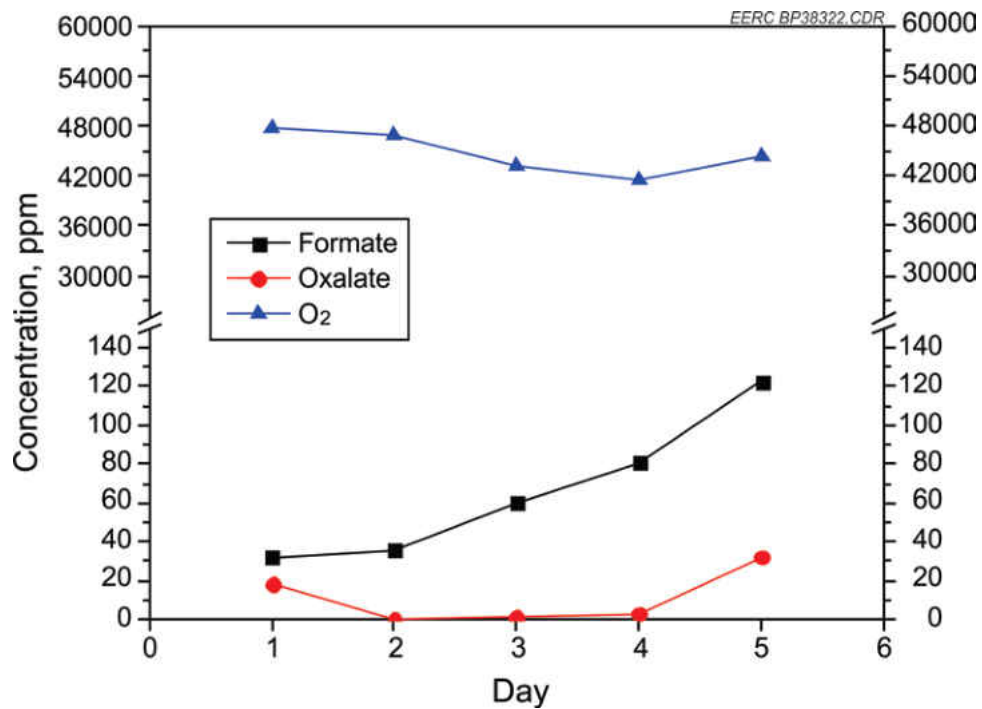


Figure 77. Concentration of organic anions in lean Huntsman additive solutions.

### Major Elements in Lean Huntsman Additive Solutions

The concentrations of the major elements detected in samples of Huntsman additive during the test period are shown in Figure 79. It was also observed that the amounts of the major elements in these samples were lower than those seen in the standard MEA test samples. An important distinction in this case is the amount of K, which increases sharply in the last 2 days of the test. The Na content shows an increase with time, and the Al level somewhat shows an increase with time. Because these concentrations are so small, it is difficult to make firm conclusions with these data. Hence, additional and longer-term tests are required to confirm these trends.

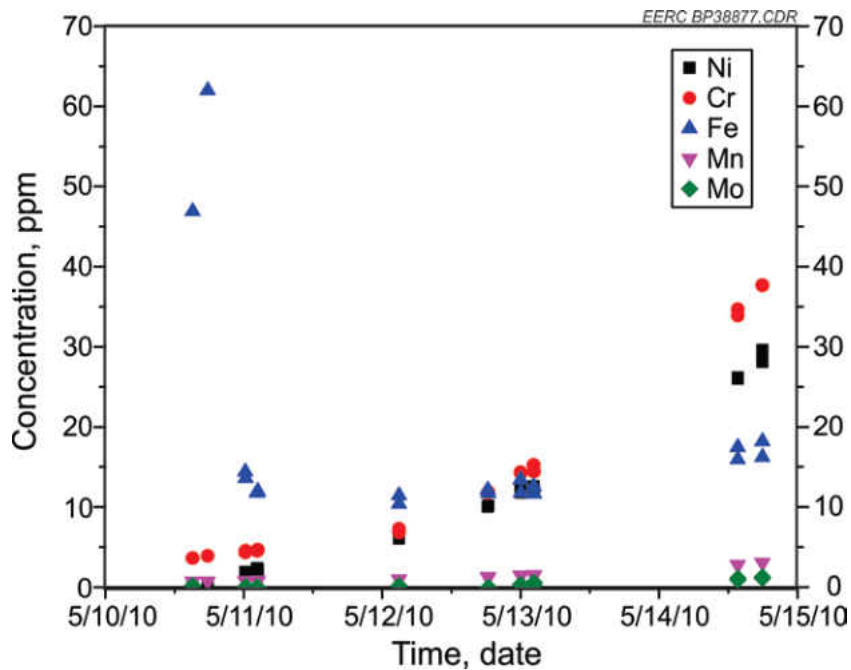


Figure 78. Concentration of trace metals in lean Huntsman additive solutions.

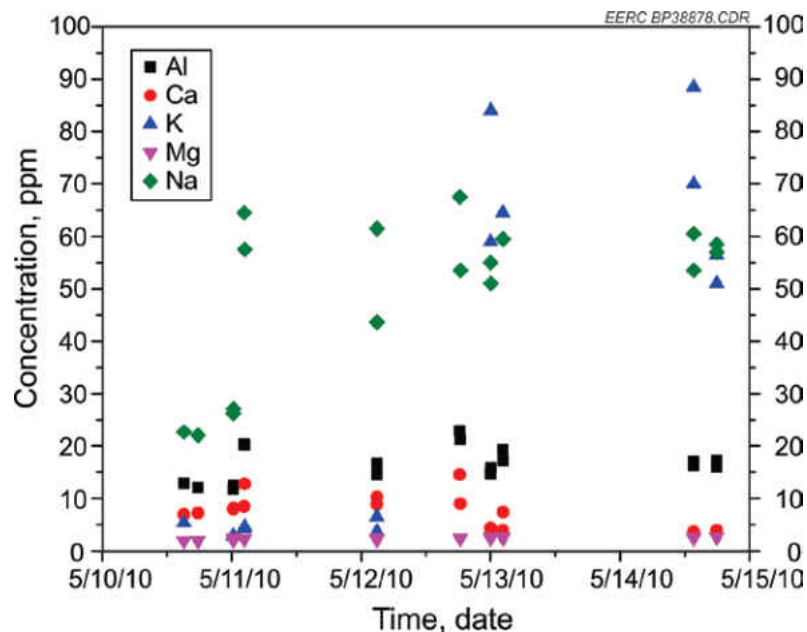


Figure 79. Concentration of major elements in lean Huntsman additive solutions.

### ***CO<sub>2</sub> Loading in Lean Huntsman Additive Solutions***

The CO<sub>2</sub> loading determined in samples of Huntsman additive are displayed in Figure 80 for the absorber and stripper. The absorber CO<sub>2</sub> loading ranges from about 0.29 to about 0.30 mole CO<sub>2</sub> per mole amine and that of the stripper is in the range of about 0.21–0.23. For both columns, the CO<sub>2</sub> loading decreases linearly with time. This is similar to the trend observed in MEA samples, but different from that seen in H3-1 solvent samples. A decreasing trend is expected because of an increasing trend in HSSs in solutions. The HSSs convert some of the free amine that absorbs CO<sub>2</sub> into its bound form and, thus, make it unavailable for further CO<sub>2</sub> absorption.

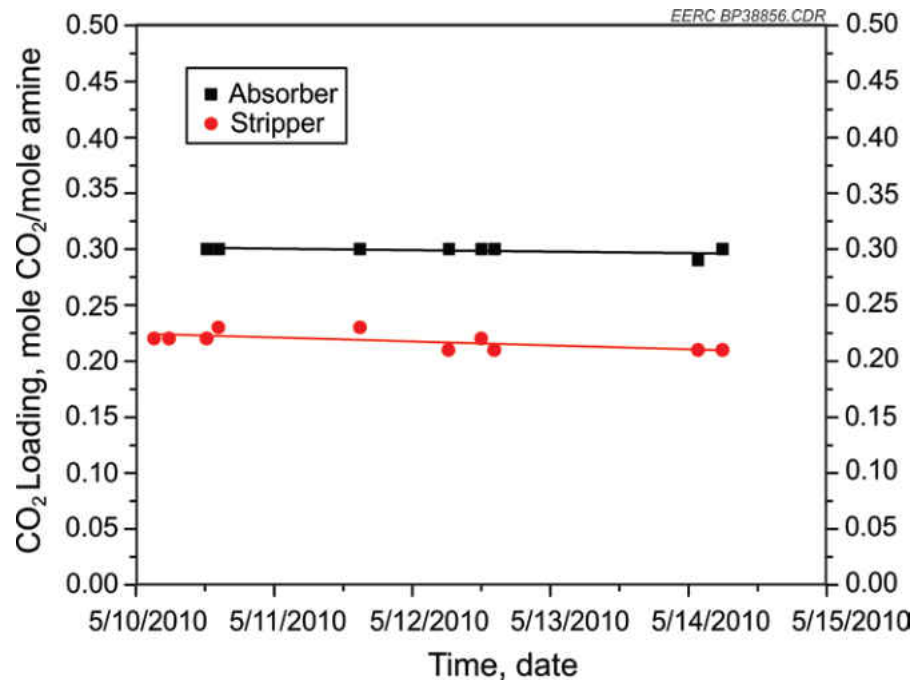


Figure 80. CO<sub>2</sub> loading in lean solutions of Huntsman additive.

## APPENDIX B-3

### MDEA+PZ TESTING RESULTS

The final advanced solvent tested for Phase I was MDEA+PZ. The test was run continuously, pausing daily for necessary system maintenance. Beginning June 14, 2010, the PCO<sub>2</sub>C postcombustion system was loaded with MDEA+PZ to begin a weeklong test. The fuel used for this test was Antelope PRB coal, the same as all previous runs, and the CTF was again operated at a FEGT of around 2000°F. The goal of the MDEA+PZ test run was to explore the removal efficiency of the media under multiple test conditions, including various static pressure levels in the stripper column, various reboiler duty rates, and various flue gas inlet flow rates. SO<sub>2</sub> was allowed to the column during the MDEA+PZ test at levels of 10–20 ppm throughout the test.

CO<sub>2</sub> capture rates were much lower for MDEA+PZ than with the other advanced solvents for the mid- and high-level flue gas flow rates. CO<sub>2</sub> capture rates of 90% and greater were only reached during test periods of 60 scfm flue gas. The first 2 days of testing with the higher flow rates saw capture rates of about 70% and 80%, respectively. For the final 2 days of testing, SO<sub>2</sub> was increased by reducing the effectiveness of the wet scrubber. SO<sub>2</sub> was increased in increments of 10 ppm every few hours up to about 80 ppm.

Test periods using the same parameters as the baseline case were run for MDEA+PZ. Absorber inlet flow rate, lean solvent flow rate, stripper static pressure, and reboiler duty were all manipulated during the MDEA+PZ test to determine correlations between the variables.

The MDEA+PZ test run had some challenges not seen in previous test runs. Because it was run during summer, the cooling water was warmer than previous test runs, which made it difficult to maintain some of the critical temperatures. Also, house steam pressure was more variable because of low usage across the entire service area. These changes provided a good test of the system with variations out of the control of the operational staff. Issues with these changes allowed operational engineers to identify fixes to better control the system while accounting for such variables. The CO<sub>2</sub> capture performance was determined for the same system parameters that were investigated for other solvents, including reboiler duty, flue gas flow rate, solvent flow rate, and absorber inlet temperature. The results from these tests are presented below.

### **System Performance**

The postcombustion capture system loaded with MDEA+PZ captured 90% of the incoming CO<sub>2</sub> for extended durations of time. Capture rates were dependent upon system parameters such as liquid-to-gas ratio, reboiler duty, and solvent flow rate. As with the base case and other advanced solvents, CO<sub>2</sub> capture rate generally increased with an increase in reboiler duty. Increases in liquid-to-gas ratio typically led to increases in CO<sub>2</sub> capture rate for MDEA+PZ.

### ***CO<sub>2</sub> Capture Performance***

Unlike previous solvents tested, MDEA+PZ was not able to absorb significantly more than 90% of the incoming CO<sub>2</sub>. Figure 81 shows the CO<sub>2</sub> capture rate as a function of both flue gas flow and liquid-to-gas ratio. Test periods plotted to show the effect of flue gas flow rate are all at about the same solvent flow rate, 6.5 gpm. 90% CO<sub>2</sub> capture



was reached at 60 scfm flue gas flow rate and a liquid-to-gas ratio of about 110. Generally, as the liquid-to-gas ratio decreased, CO<sub>2</sub> capture rate decreased for MDEA+PZ.

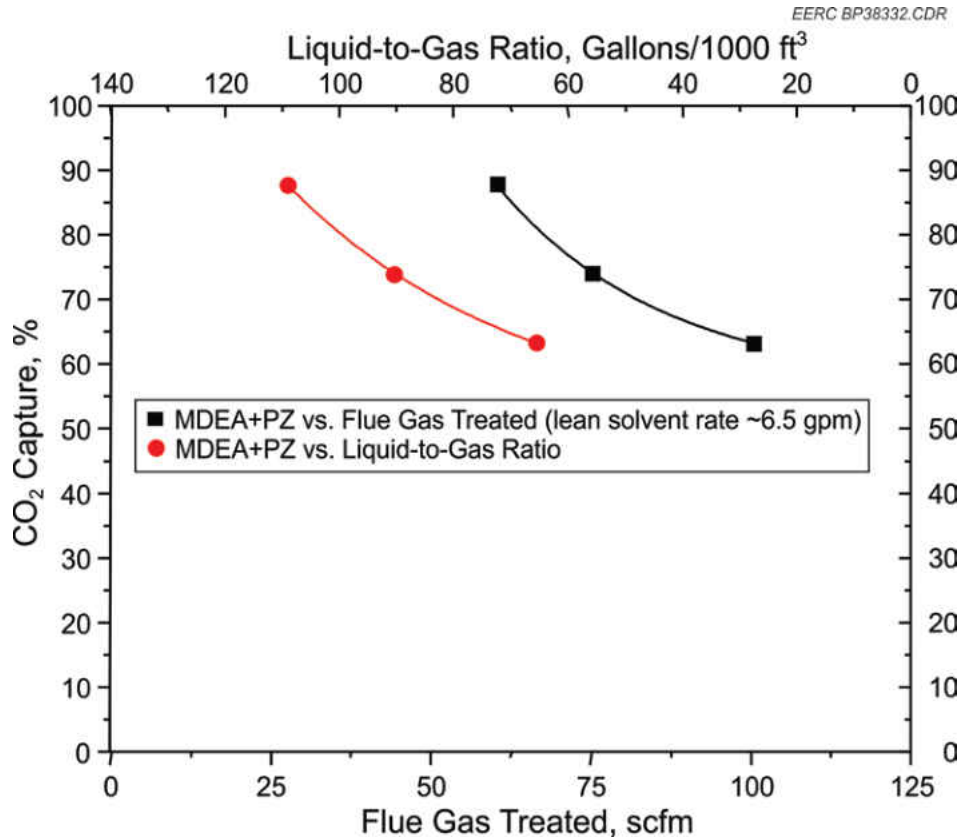


Figure 81. MDEA+PZ solvent performance based on flue gas flow rate and liquid-to-gas ratio.

### ***Impact of Stripper Pressure***

Another test parameter that had an effect on CO<sub>2</sub> capture for MDEA+PZ was stripper pressure. Figure 82 presents CO<sub>2</sub> capture and liquid-to-gas ratios for a series of stripper pressure values. At a stripper pressure of 4 psig, CO<sub>2</sub> capture for MDEA+PZ averaged around 85%. For the 12 psig test periods shown, CO<sub>2</sub> capture averaged about

90%. One of the benefits of increased stripper column pressure was a higher head pressure on the lean solvent pump. This reduced the amount of energy needed to run the pump as it had a higher head pressure. Test periods run at higher stripper column pressures typically had a higher liquid-to-gas ratio and resulted in a higher CO<sub>2</sub> capture rate.

Increasing stripper column pressure has the added benefit of potentially reducing the amount of compression needed at the CO<sub>2</sub> storage phase. This, in turn, could lead to lower total cost as smaller equipment for compression would be needed during the transport and storage phase.

### ***Flow Rate Effects***

Figure 83 shows CO<sub>2</sub> capture as a function of lean solvent flow rate for each flue gas flow rate tested. For each gas flow rate case, an increase in solvent flow was related to an increase in CO<sub>2</sub> capture rate. Capture rate also increased as total flue gas flow rate decreased. The tests run on MDEA+PZ did not reach 90% capture at any time for 75 or 100 scfm. Only when 60 scfm was treated in the absorber column did the capture rate reach 90%.

### ***Solvent Regeneration Energy Requirement***

Figure 84 shows the effect of regeneration energy input on CO<sub>2</sub> capture rate. The test periods compared were all run at the same stripper column pressure with a solvent flow rate of about 7.5 gpm. Two CO<sub>2</sub> capture curves were developed from the data: one as a linear fit and another as a polynomial fit. Data used to develop the curves were between

83% and 89% capture. Extrapolating the data to the 90% capture level with the two curves produced a range of regeneration energy input levels required to meet 90% CO<sub>2</sub> capture.

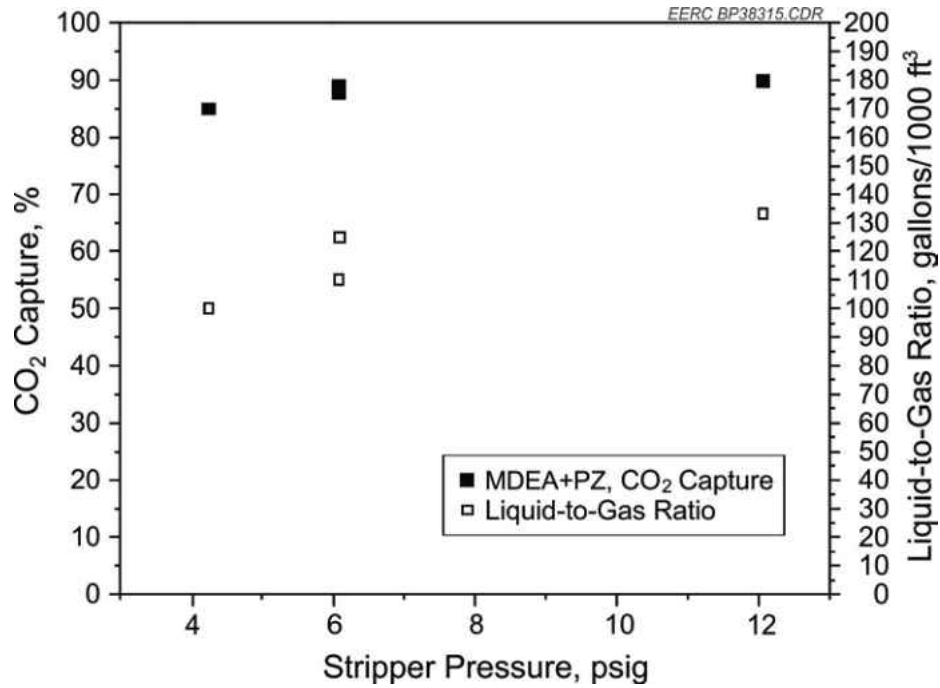


Figure 82. Effect of stripper pressure on CO<sub>2</sub> capture for MDEA+PZ.

Figure 85 displays the concentration of free amine determined in samples collected during testing of MDEA+PZ. Performing titrations for MDEA+PZ solutions was much more difficult because the endpoints between MDEA and PZ are not distinct. Nonetheless, an approach was developed to determine the amounts of MDEA and PZ in solution. The results show that the concentration of free amine was relatively steady at about 46.5 wt% in the absorber and about 50 wt% in the stripper, with the initial amine concentration determined to be about 56 wt%.

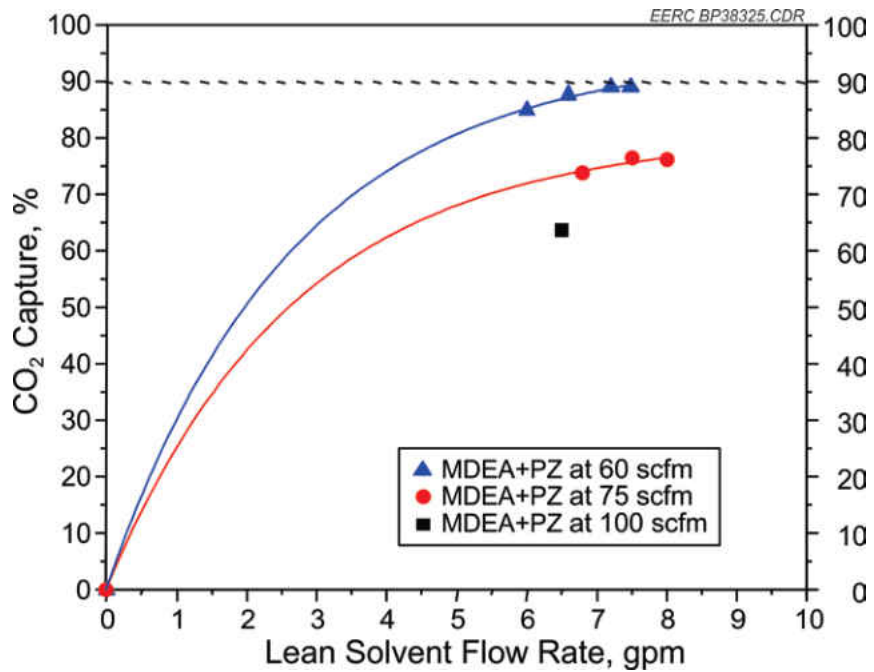


Figure 83. CO<sub>2</sub> capture for various inlet gas flows for MDEA+PZ.

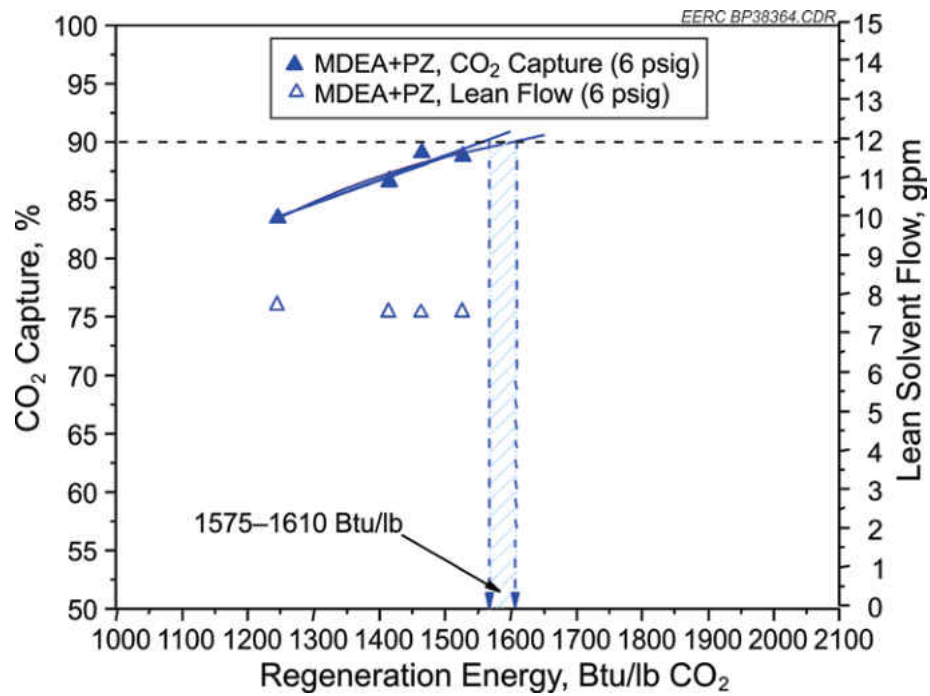


Figure 84. MDEA+PZ solvent regeneration energy requirements.

### Free Amine in Lean MDEA+PZ Solutions

Although the curves appear to show a somewhat slight increasing trend with time, this trend can only be confirmed if better methods are developed for performing the titrations. The sharp drop between the initial amine concentration and Day 1 of the test is a reflection of the fact that fresh amine solvent without any flue gas exposure contains no absorbed CO<sub>2</sub> and other compounds, but after Day 1, the solution becomes lean (i.e., loaded with CO<sub>2</sub>), and so the concentration of free amine in lean solution is much lower than for fresh amine solution. The trend observed in this case is different from that seen for MEA, H3-1, and Huntsman additive solvents, which decreased roughly linearly with time.

The endpoint in the titration of these samples was more difficult to detect, as was the case with Huntsman additive samples. Given that MDEA+PZ, like Huntsman additive, was a mixture of amines, the solution chemistry becomes more complex, and there are likely more interferences with the endpoint in the titrations especially when their pK<sub>a</sub> values are very close. As a result, different approaches will be investigated in Phase II of the project to improve on the detection of the endpoint and, hence, the quantification of the free amine in lean MDEA+PZ solution samples.

### Bound Amine in Lean MDEA+PZ Solutions

The bound amine concentrations observed in lean solution samples of MDEA+PZ are summarized in Table 21. As in the case of the other solvents, the amount of amine cation obtained for the first day of the test was used as baseline and subtracted from values of subsequent days to obtain what is truly bound and not regenerable. This was

necessary because the titration process quantifies all amine cation species in solution. The bound amine concentration seen in these samples ranged from 2–3 wt% in stripper. The absorber data appear to exhibit a linearly decreasing trend, while the stripper data are relatively steady and simply fluctuate around an average value of about 2.5 wt%.

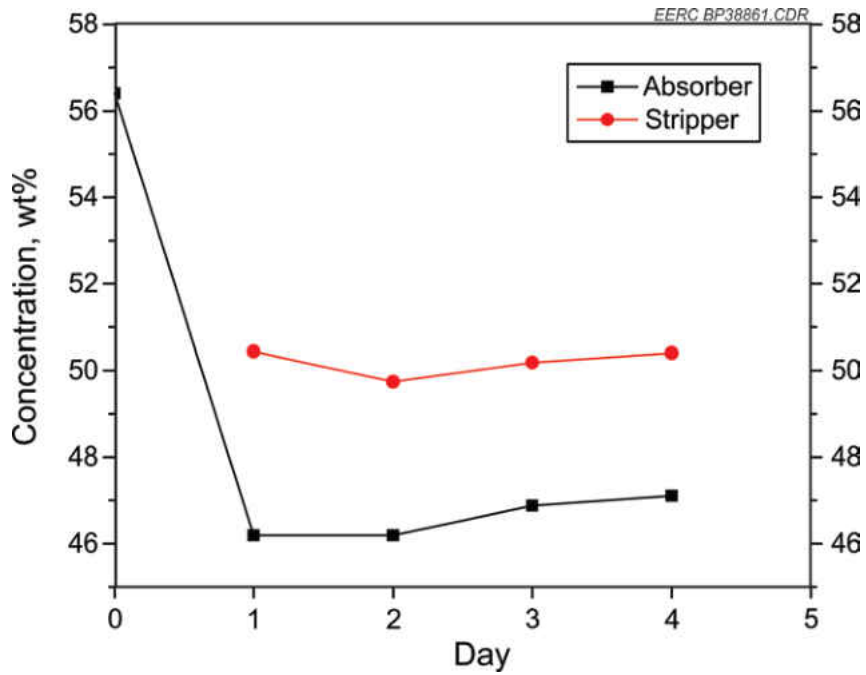


Figure 85. Concentration of free amine in lean MDEA+PZ solutions.

Table 21. Bound Amine in Lean MDEA+PZ

Day	Absorber Bound Amine, wt%	Stripper Bound Amine, wt%
1	0.00	0.00
2	-0.11	-0.18
3	-0.09	0.51
4	-0.75	-0.19

### Organic and Inorganic Anions in Lean MDEA+PZ Solutions

The concentration of inorganic anions in samples collected during testing of MDEA+PZ is displayed in Figure 86. As in the case of the other solvents, the sulfate concentration was the highest ranging from about 225 to about 475 ppm during the test period. Chloride, nitrate, and thiosulfate ions were present in smaller amounts. No nitrite ions were observed. In general, the concentrations appear to increase with time as would be expected because of accumulation in the system and extended effects on the solvent. Samples of MDEA+PZ solutions were also analyzed for the three organic anions tested in the other solvents, i.e., formate, acetate, and oxalate. In this case, only formate ions were detected, and the results are also shown in Figure 86. As seen in the plot, the amount of formate ions increased with time, similar to the inorganic ions. The absence of oxalate and acetate is not surprising in MDEA+PZ samples, since acetate and oxalate are typical degradation products of MEA because of extended oxygen exposure.

### Trace Metals in Lean MDEA+PZ Solutions

The concentration of trace metals found in samples collected during testing of MDEA+PZ are presented in Figure 87. These results indicate that trace metal concentrations were generally low in MDEA+PZ solutions, with the highest concentration being less than 10 ppm. While the Ni and Cr levels appear to increase with time, the Fe content shows a slight decreasing trend. Mo and Mn were barely detectable, with concentration levels that are very close to zero throughout the test. The results for MDEA+PZ are similar to those seen for the other solvents, where Fe, Cr, and Ni appear to be the most vulnerable metal species to corrosion by amine solutions. However,

because the levels are generally low, longer-term tests are needed to further determine the impact of these amine solutions on process equipment because of corrosion.

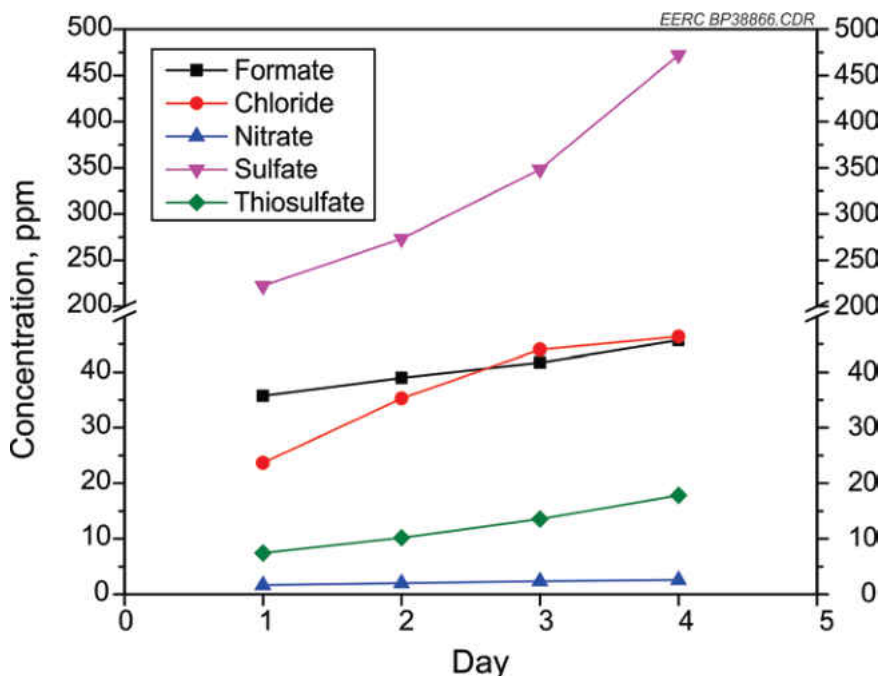


Figure 86. Concentration of organic and inorganic anions in lean MDEA+PZ solution samples.

#### Major Elements in Lean MDEA+PZ Solutions

The concentration of the major elements detected in samples of MDEA+PZ during the test period are shown in Figure 88. Unlike the other solvents tested, the overall trend in all major elements detected was decreasing, except for Ca and Mg that show a somewhat steady trend. Sodium levels were also slightly higher in the other solvents than in MDEA+PZ samples. In general, levels of all major elements were low, with Na that appeared in the highest concentration in all solvents having less than 150 ppm levels and all other elements were present in less than 100 ppm. However, perhaps because of the



relatively short test period, levels of major elements did not accumulate in amounts large enough to cause noticeable effects on the amine solvents. Hence, longer-term studies will be needed to determine the impact of major elements on alkanolamine solvents.

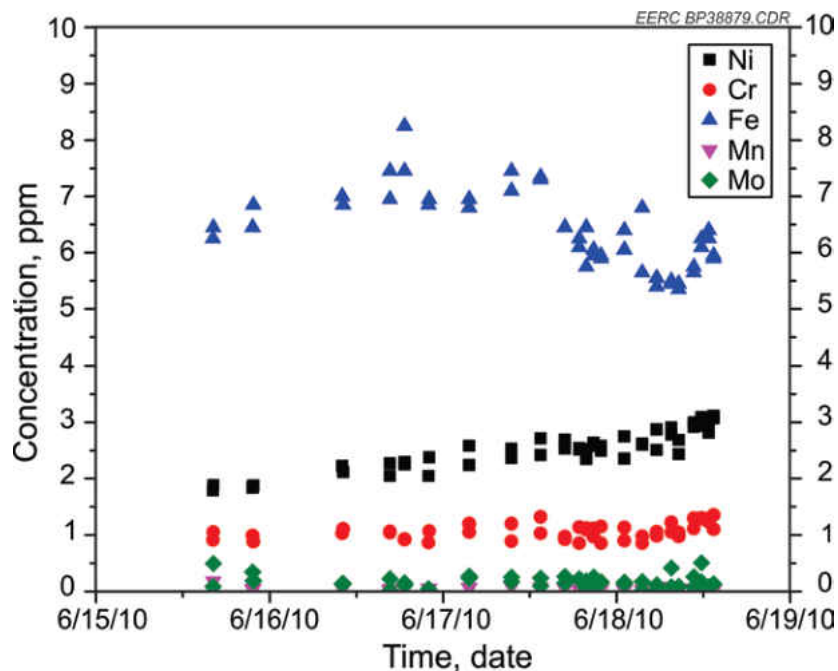


Figure 87. Concentration of trace metals in lean MDEA+PZ solution samples.

### *CO<sub>2</sub> Loading in Lean MDEA+PZ Solutions*

The CO<sub>2</sub> loading determined in samples of MDEA+PZ is displayed in Figure 89 for the absorber and stripper. The absorber CO<sub>2</sub> loading ranges from about 0.11 to about 0.130 mole CO<sub>2</sub> per mole amine, and that of the stripper was around 0.04. For the absorber column, the CO<sub>2</sub> loading decreases linearly with time; the decreasing trend for the stripper loading is more gradual. This is similar to the trend observed in MEA samples, but different from that seen in H3-1 solvent samples. A decreasing trend is

expected because of an increasing trend in HSSs in solutions, which convert some of the free amine that absorbs CO<sub>2</sub> into its bound form and, thus, make it unavailable for further CO<sub>2</sub> absorption.

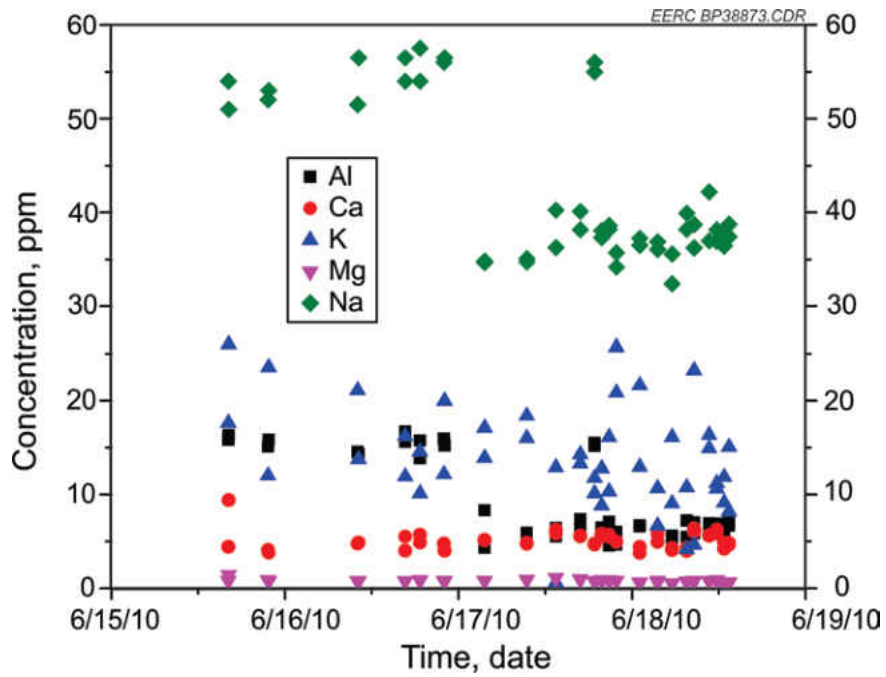


Figure 88. Concentration of major elements in lean MDEA+PZ solution samples.

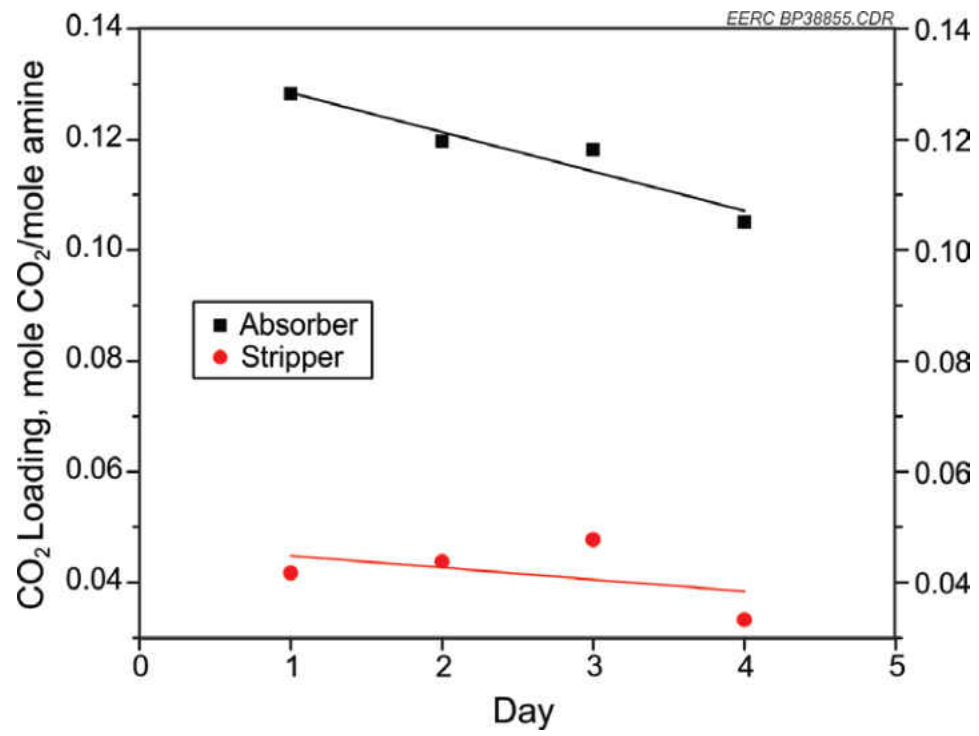


Figure 89. CO<sub>2</sub> loading in lean solutions of MDEA+PZ.

## APPENDIX C

### APEA COST EVALUATION PARAMETERS AND COST RESULTS FOR SINGLE TRAIN OF BASE CASE MEA

ITEM	UNITS	VALUE
<b>CAPITAL COST EVALUATION BASIS</b>		
Project Type		Plant addition adjacent to existing plant
Plant Location		North America
User Currency Name		Dollars
<b>TIME PERIOD</b>		
Period Description		Year
Operating Hours per Period	Hours/period	8000
Number of Weeks per Period	Weeks/period	52
Number of Periods for Analysis	Period	20
<b>SCHEDULE</b>		
Duration of EPC Phase	Weeks	79
Length of Start-Up Period	Weeks	20
Duration of Construction Phase	Weeks	44
<b>CAPITAL COST PARAMETERS</b>		
Working Capital Percentage	Percent/period	5
<b>OPERATING COST PARAMETERS</b>		
Operating Supplies (lump sum)	Cost/period	0
Laboratory Charges (lump sum)	Cost/period	0
User Entered Operating Charges (as percentage)	Percent/period	25
Operating Charges(percent of operating labor costs)	Percent/period	25
Plant Overhead (percent of operating labor and maintenance costs)	Percent/period	50
General and Administrative Expenses (percent of subtotal operating costs)	Percent/period	8
<b>GENERAL INVESTMENT PARAMETERS</b>		
Tax Rate	Percent/period	40
Interest Rate	Percent/period	20
Economic Life of Project	Period	10
Salvage Value (Fraction of Initial Capital Cost)	Percent	20
Depreciation Method		Straight line
<b>ESCALATION</b>		
Project Capital Escalation	Percent/period	5
Products Escalation	Percent/period	5
Raw Material Escalation	Percent/period	3.5
Operating and Maintenance Labor Escalation	Percent/period	3
Utilities Escalation	Percent/period	3

ITEM	UNITS	VALUE
<b>PROJECT RESULTS SUMMARY</b>		
Total Project Capital Cost	Cost	\$79,024,500.00
Total Raw Materials Cost	Cost/period	\$1,177,570.00
Total Operating Labor and Maintenance Cost	Cost/period	\$2,920,000.00
Total Utilities Cost	Cost/period	\$47,168,000.00
Total Operating Cost	Cost/period	\$57,192,000.00
Operating Labor Cost	Cost/period	\$920,000.00
Maintenance Cost	Cost/period	\$2,000,000.00
Operating Charges	Cost/period	\$230,000.00
Plant Overhead	Cost/period	\$1,460,000.00
Subtotal Operating Cost	Cost/period	\$52,955,500.00
G and A Cost		\$4,236,440.00
<b>PROJECT CAPITAL SUMMARY</b>		
		Total Cost
Purchased Equipment	Cost	\$31,203,500.00
Equipment Setting	Cost	\$269,735.00
Piping	Cost	\$11,102,600.00
Civil	Cost	\$867,959.00
Steel	Cost	\$214,358.00
Instrumentation	Cost	\$851,032.00
Electrical	Cost	\$625,169.00
Insulation	Cost	\$664,669.00
Paint	Cost	\$67,195.50
Other	Cost	\$12,325,000.00
G and A Overheads	Cost	\$1,647,220.00
Contract Fee	Cost	\$1,741,300.00
Escalation	Cost	\$0.30
Contingencies	Cost	\$11,084,300.00
Total Project Cost	Cost	\$72,664,100.00
Adjusted Total Project Cost	Cost	\$71,775,700.00
<b>ENGINEERING SUMMARY</b>		
		Cost
Basic Engineering		\$877,600.00
Detail Engineering		\$1,542,900.00
Material Procurement		\$447,500.00
Home Office		\$415,800.00
Total Design, Engineer, Procurement Cost		\$3,283,800.00
<b>RAW MATERIAL COSTS AND PRODUCTS SALES</b>		
Raw Materials Cost per hour	Cost/hour	\$147.20
Total Raw Materials Cost	Cost/period	\$1,177,570.00

<b>ITEM</b>	<b>UNITS</b>	<b>VALUE</b>
<b>OPERATING LABOR AND MAINTENANCE COSTS</b>		
Operating Labor		
Operators per Shift		3
Unit Cost	Cost/operator/hour	\$20.00
Total Operating Labor Cost	Cost/period	\$640,000.00
Maintenance		
Cost/8000 Hours		\$2,000,000.00
Total Maintenance Cost	Cost/period	\$2,000,000.00
Supervision		
Supervisors per Shift		1
Unit Cost	Cost/supervisor/hour	\$35.00
Total Supervision Cost	Cost/period	\$280,000.00
<b>UTILITIES COSTS</b>		
Electricity		
Rate	kW	\$17,930.90
Unit Cost	Cost/kWh	0.0775
Total Electricity Cost	Cost/period	\$11,117,200.00
Steam		
Rate	Klb/hour	562.37
Unit Cost	Cost/Klb	\$8.00
Total Steam Cost	Cost/period	\$35,992,009.86
Cooling Water		
Rate	MMgal	2.077
Unit Cost	Cost/MMgal	\$120.00
Total Fuel Cost	Cost/period	\$58,790.40

\*Aspen process economic analyzes and monoethanalamine.

## REFERENCES

1. Metz, B.; Davidson, O.; Coninik, H.; Loos, M.; Meyer, L. *IPCC Special Report Carbon Dioxide Capture and Storage Technical Summary*; ISBN 92-9169-119-4 (accessed June 15, 2006).
2. Chen, S.G.; Lu, Y.; Rostam-Abadi, M. *Carbon Dioxide Capture and Transportation Options in the Illinois Basin*; U.S. DOE Contract: DE-FC26-03NT41994 October 1, 2003–September 30, 2004.
3. U.S. Environmental Protection Agency (U.S. EPA, 2004). Greenhouse Gas Inventory Sector Analysis. [www.yosemite.epa.gov](http://www.yosemite.epa.gov) (accessed June 15, 2006).
4. Dagobert G. Kessel, “Global warming — facts, assessment, countermeasures”, *Journal of Petroleum Science and Engineering, Volume 26, Issues 1-4, May 2000, Pages 157-168*, <http://www.sciencedirect.com>, accessed October 2009.
5. Georgios A. Florides, Paul Christodoulides, “Global warming and carbon dioxide through sciences” *Environment International, Volume 35, Issue 2, February 2009, Pages 390-401*, <http://www.sciencedirect.com>, accessed October 2009.
6. Hadley Centre. 2007. Data from Hadley Centre of the UK Met Office. <http://www.cru.uea.ac.uk/cru/data/temperature/#datdown>.

7. American Clean Energy and Security Act, H.R. 2454, 2009, Available at:  
<http://markey.house.gov/index.php?option=content&task=view&id=3583&Itemid=125>
8. American Power Act, 2010, Available at:  
<http://lieberman.senate.gov/index.cfm/news-events/news/2010/5/kerry-lieberman-american-power-act-bill-will-secure-americas-energy-climate-future>
9. Energy Tax Prevention Act, H.R. 910, S. 482, 2011, Available at:  
<http://thomas.loc.gov/cgi-bin/query/z?c112:H.R.910>:
10. Defending America's Affordable Energy and Jobs Act, S. 228, 2010, Available at: <http://thomas.loc.gov/cgi-bin/query/z?c112:S.228>:
11. Environmental Protection Agency, Greenhouse Gas Rulemaking Webpage, Accessed 12/6/11, Available at:  
<http://www.epa.gov/climatechange/emissions/ghgrulemaking.html>
12. Pew Center for Climate and Energy Solutions, EPA Update, Accessed 12/6/11, Available at: <http://www.c2es.org/federal/executive/epa>
13. Environmental Protection Agency, Endangerment Finding Webpage, Accessed 12/6/11, Available at: <http://www.epa.gov/climatechange/endangerment.html>
14. Environmental Protection Agency, Greenhouse Gas Regulations Webpage, Accessed 12/6/11, Available at: <http://epa.gov/otaq/climate/regulations.htm>
15. Environmental Protection Agency, Greenhouse Gas Tailoring Rule Fact Sheet, Accessed 12/6/11, Available at:  
<http://www.epa.gov/NSR/documents/20100413fs.pdf>



16. Regional Greenhouse Gas Initiative Website, Accessed 12/6/11, Available at:  
<http://www.rggi.org/>
17. Western Climate Initiative Website, Accessed 12/6/11, Available at:  
<http://www.westernclimateinitiative.org/>
18. Pew Center for Climate and Energy Solutions, Midwest Greenhouse Gas Reduction Accord Update, Accessed 12/6/11, Available at:  
<http://www.pewclimate.org/states/news/2009/06/midwestern-greenhouse-gas-reduction-accord-releases-recommendations>
19. Midwestern Energy Summit Fact Sheet, Accessed 12/6/11, Available at:  
<http://www.midwesterngovernors.org/energysummit.htm>
20. Pew Center for Climate and Energy Solutions, State and Regional Climate Action, Accessed 12/6/11, Available at: <http://www.c2es.org/states-regions>
21. Minnesota Public Radio, ND sues Minnesota over coal power restrictions, Accessed 12/6/11, Available at:  
<http://minnesota.publicradio.org/display/web/2011/11/02/nd-sues-minnesota-over-coal-power-restrictions/>
22. Australian Government Climate Change Website, Accessed 12/6/11, Available at: <http://www.climatechange.gov.au/government/national-targets.aspx>
23. Australian Government Carbon Pricing Website, Accessed 12/6/11, Available at: <http://www.climatechange.gov.au/en/government/reduce/carbon-pricing.aspx>

24. Australian Government Clean Energy Plan Website, Accessed 12/6/11,  
Available at: <http://www.climatechange.gov.au/en/government/clean-energy-future.aspx>
25. Environment Canada News Release, Accessed 12/6/11, Available at:  
<http://www.ec.gc.ca/default.asp?lang=En&n=714D9AAE-1&news=2E5D45F6-E0A4-45C4-A49D-A3514E740296>
26. Chinese Government Press Release, Accessed 12/6/11, Available at:  
[http://english.gov.cn/2009-11/26/content\\_1474008.htm](http://english.gov.cn/2009-11/26/content_1474008.htm)
27. Pew Center for Climate and Energy Solutions, EU Fact Sheet, Accessed  
12/6/11, Available at: <http://www.c2es.org/docUploads/eu-fact-sheet-12-05-09.pdf>
28. Speech by Prime Minister Yukio Hatoyama of Japan to the U.N. Summit on  
Climate Change, September 22, 2009, Accessed: 12/6/11, Available at:  
[http://www.kantei.go.jp/foreign/hatoyama/statement/200909/ehat\\_0922\\_e.html](http://www.kantei.go.jp/foreign/hatoyama/statement/200909/ehat_0922_e.html)
29. Japan's Vision and Actions toward Low-Carbon Growth and a Climate-  
Resilient World, Japanese Ministry of Foreign Affairs, November 29, 2011,  
Accessed: 12/6/11, Available at:  
[http://www.mofa.go.jp/policy/environment/warm/cop/lowcarbongrowth\\_vision\\_1111.html](http://www.mofa.go.jp/policy/environment/warm/cop/lowcarbongrowth_vision_1111.html)
30. Nichols, C. *Coal-Fired Power Plants in the United States: Examination of the  
Costs of Retrofitting with CO<sub>2</sub> Capture Technology*; U.S. Department of  
Energy National Energy Technology Laboratory Technical Report;  
DOE/NETL-402/102309, Jan 2011.

31. U.S. Environmental Protection Agency eGrid Database, [www.epa.gov/cleanenergy/energy-resources/egrid/index.html](http://www.epa.gov/cleanenergy/energy-resources/egrid/index.html) (accessed July 29, 2011).
32. Rao, A.; Rubin, E. A Technical, Economic, and Environmental Assessment of Amine-Based CO<sub>2</sub> Capture Technology for Power Plant Greenhouse Gas Control. *Environ. Sci. Technol.* **2002**, *36*, 4467–4475.
33. Gijlswijk, R.; Feron, P.; Oonk, H.; Brouwer, J. *Environmental Impact of Solvent Scrubbing of CO<sub>2</sub>*; IEA GHG Programme Technical Study; Report No.: 2006/14; Oct 2006.
34. “Ethanolamine is Serious Short of Supply,” China Chemical Reporter, [http://goliath.ecnext.com/coms2/gi\\_0199-5760508/ethanolamine-is-serious-short-of.html](http://goliath.ecnext.com/coms2/gi_0199-5760508/ethanolamine-is-serious-short-of.html) (accessed August 2, 2011).
35. Pavlish, B.M.; Fiala, N.J.; Downs, J.G.; Tolbert, S.G.; Kay, J.P.; Stanislawski, J.J.; Laumb, J.D.; Curran, T.J.; Snyder, A.C.; Azenkeng, A.; Lentz, N.B. *Partnership for CO<sub>2</sub> Capture Phase I*; Final Report for U.S. Department of Energy National Energy Technology Laboratory Cooperative Agreement No. DE-FC26-08NT43291, North Dakota Industrial Commission Agreement No. FY08-LXIV-164, ATCO Power Canada Ltd., Baker Petrolite Agreement No. 016-49154, Black & Veatch Corporation, C-Quest Technologies, Constellation Energy, Hitachi Power Systems America Ltd., Huntsman Corporation, Lignite Energy Council, Metso Power, Midwest Generation EME LLC, Minnesota Power, Nebraska Public Power District, PPL Montana, Saskatchewan Power,

and TransAlta Corporation; EERC Publication 2010-EERC-09-01; Energy & Environmental Research Center, Grand Forks, ND, Sept 2010.

36. Chapel, D.; Ernst, J.; Martz, C. Recovery of CO<sub>2</sub> from Flue Gases: Commercial Trends. Presented at the Canadian Society of Chemical Engineers Annual Meeting, Saskatoon, Saskatchewan, Canada, Oct 4–6, 1999; Paper No. 340.
37. Kaplan, L.J. Cost-Saving Process Recovers CO<sub>2</sub> from Power Plant Flue Gas. *Chem. Eng.* **1982**, *80* (24), 30–31.
38. Pauley, C.R.; Simiskey, P.L.; Haigh, S. N-Ren Recovers CO<sub>2</sub> from Flue Gas Economically. *Oil Gas J.* **1984**, *82* (20), 87–92.
39. Al-Baghil, N.A.; Pruess, S.A. A Rate-Based Model for the Design of Gas Absorbers for the Removal of CO<sub>2</sub> and H<sub>2</sub>S Using Aqueous Solutions of MEA and DEA. *Fluid Phase Equilibria* **2001**, *185*, 31–43.
40. Summerfield, I.; Goldthorpe, S.; Sheikh, K.; Williams, N.; Ball, P. The Full Fuel Cycle of CO<sub>2</sub> Capture and Disposal. *Energy Convers. Mgmt.* **1995**, *36*, 849–852.
41. Stewart, E.J.; Lanning, R.A. Reduce Amine Plant Solvent Losses (Part 1). *Hydrocarbon Process.* **1994**, *May*, 67–81.
42. Stewart, E.J.; Lanning, R.A. Reduce Amine Plant Solvent Losses (Part 2). *Hydrocarbon Process.* **1994**, *June*, 51–54.
43. Yagi, T.; Shibuya, H.; Sasaki, T. Application of Chemical Absorption Process to CO<sub>2</sub> Recovery from Flue Gas Generated in Power Plants. *Energy Convers. Manage.* **1992**, *33* (5–8), 349–355.

44. Barchas, R.; Davis, R. The Kerr-McGee/ABB Lummus Crest Technology for the Recovery of CO<sub>2</sub> from Stack Gases. *Energy Convers. Manage.* **1992**, *33* (5–8), 333–340.
45. Strazisar, B.R.; Anderson, R.R.; White, C.M. Degradation Pathways for Monoethanolamine in a CO<sub>2</sub> Capture Facility. *Energy Fuels* **2003**, *17* (4), 1034–1039.
46. Rao, A.B.; Rubin, E.S.; Berkenpas, M.B. *An Integrated Modeling Framework for Carbon Management Technologies: Volumes 1 & 2*; Final Report for U.S. Department of Energy National Technology Laboratory Contract DE-FC26-00BNT40935; Carnegie Mellon University, Pittsburgh, PA, March 2004.
47. Fluor Corporation, [www.fluor.com](http://www.fluor.com) (accessed 1/06/09).
48. Booras, G. Updated Evaluation of Advanced Coal Technologies with CO<sub>2</sub> Capture. EPRI, Palo Alto, CA: 2005, 1010229.
49. KM-CDR Process<sup>®</sup> [www.mhi.co.jp/mcec/product/recov\\_CO2/index.html](http://www.mhi.co.jp/mcec/product/recov_CO2/index.html) (accessed 11/6/2008).
50. Mimura, T.; Matsumoto, K.; Iijima, M.; Mitsuoka, S. Development and Application of Flue Gas Carbon Dioxide Recovery Technology [PDF/290KB], Mitsubishi Heavy Industries, Ltd., [http://www.mhi.co.jp/mcec/product/recov\\_CO2/download/index.html](http://www.mhi.co.jp/mcec/product/recov_CO2/download/index.html) (accessed 11/6/2008)
51. Yagi, Y.; Mimura, T.; Yonekawa, T.; Yoshiyama, R. Development and Improvement of CO<sub>2</sub>-Capture system [PDF/1.11MB], Mitsubishi Heavy

- Industries, Ltd. [www.mhi.co.jp/mcec/product/recov\\_CO2/download/index.html](http://www.mhi.co.jp/mcec/product/recov_CO2/download/index.html) (accessed 11/6/2008).
52. Barchas, R.; Davis, R. The Kerr-McGee/ABB Lummus Crest Technology for the Recovery of CO<sub>2</sub> from Stack Gases. *Energy Convers. Manage.* **1992**, *33* (5–8), 333–340.
  53. Alstom Power Systems. Chilled Ammonia Process for CO<sub>2</sub> Capture. Presentation: 01/01/2007, Alstom, 2007, [www.alstom.com](http://www.alstom.com).
  54. IEA Greenhouse Gas R&D Program. International Test Network for CO<sub>2</sub> Capture; Report No. PH4/11 on Third Workshop, Apeldoorn, Netherlands, May 16–17); IEA: United Kingdom, 2002.
  55. Brandon M. Pavlish and Michael Jones, The CO<sub>2</sub> Capture Workshop, Presented at Air Quality 7 October 2009, Arlington, Virginia
  56. National Institute of Standards and Technology (NIST). Phase change data for Carbon dioxide.  
<http://webbook.nist.gov/cgi/cbook.cgi?ID=C124389&Units=SI&Mask=4#Thermo-Phase> (accessed 7/27/2009).
  57. HTC Pureenergy, CO<sub>2</sub> Capture Management Solutions.  
[www.htcenergy.com/CO2.html](http://www.htcenergy.com/CO2.html) (accessed 11/10/2008).
  58. Idem, R.; Wilson, M.; Tontiwachwuthikul, P.; Chakma, A.; Veawab, A.; Aroonwilas, A.; Gelowitz, D. Pilot Plant Studies of the CO<sub>2</sub> Capture Performance of Aqueous MEA and Mixed MEA/MDEA Solvents at the University of Regina CO<sub>2</sub> Capture Technology Development Plant and the

- Boundary Dam CO<sub>2</sub> Capture Demonstration Plant. *Ind. Eng. Chem. Res.* **2006**, *45*, 2414-2420.
59. Smelser, S.C.; Stock, R.M.; McCleary, G.J. *Engineering and Economic Evaluation of CO<sub>2</sub> Removal from Fossil-Fuel-Fired Power Plants*; EPRI IE-7365, Vol. 2, Project 2999-10, Prepared by Fluor Daniel Inc., for EPRI and IEA; EPRI: Palo Alto, CA, 1991.
60. Hendriks, C. *Carbon Dioxide Removal from Coal-Fired Power Plants*; Kluwer Academic Publishers: The Netherlands, 1994; pp 14-223.
61. Mimura, T.; Simoyoshi, H. Development of Energy Saving Technology for Flue Gas Carbon Dioxide Recovery in Power Plants by Chemical Absorption Method and Steam System. *Energy Conversion and Management* 1997, **38**, 57–S62.
62. Bolland, O.; Undrum, H. Removal of CO from Gas 2 Turbine Power Plants: Evaluation of Pre- and Postcombustion Methods. In *Proceedings of the Fourth International Conference on Greenhouse Gas Control Technologies*; Interlaken, Switzerland, 1998.
63. Marion, J.; Nsakala, N. Engineering Feasibility of CO<sub>2</sub> Capture on an Existing U.S. Coal-Fired Power Plant. In *Proceedings of the Twenty-Sixth International Conference on Coal Utilization and Fuel Systems*; Clearwater, FL, USA, March 5–8, 2001.